

UPV/EHU
FACULTAD DE CIENCIA Y TECNOLOGÍA
DEPARTAMENTO DE QUÍMICA ORGÁNICA
E INORGÁNICA

***Catalytic Enantioselective Transannular Reactions
towards C-B and C-C Bond Formation***

MEMORIA PRESENTADA POR

Jana Sendra Viscarro

PARA OPTAR AL GRADO DE DOCTOR
CON MENCIÓN “DOCTOR INTERNACIONAL”

Leioa, 2023

Quiero expresar mi agradecimiento a los Profesores Dr. José L. Vicario y Dra. Elena Fernández por la dirección y supervisión de este trabajo, así como por la ayuda y confianza depositadas en mí. Igualmente agradezco a los Profesores Dra. M^a Luisa Carrillo, Dr. Efraím Reyes, Dra. Uxue Uria y Dr. Liher Prieto, así como a los actuales y antiguos integrantes de ambos grupos de investigación por su continuo apoyo durante el desarrollo de esta tesis doctoral. También me gustaría agradecer a mis amigos que con su respaldo han contribuido de una forma u otra a la realización de este trabajo. Per descomptat, agraeixo infinitament a la meva família que sense el seu suport i la seva comprensió no hagués estat possible.

I would also like to thank Prof. Varinder K Aggarwal for the opportunity I was given to work in his group at the University of Bristol.

Asimismo, agradezco al Spanish Ministerio de Ciencia, Innovación y Universidades (MCIU) por la concesión de una “beca predoctoral de formación de personal investigador no doctor” (FPI) y por la financiación otorgada (PID2019-104090RB-100, PID2019-109674GB-I00 and FEDER-PID2020-118422GB-I00) así como por la subvención a grupos de investigación IT908-16. Finalmente agradecer también el apoyo técnico y humano de los SGIker de la UPV/EHU y al Servei de Recursos Científics y Tècnics de la URV.

Summary

Transannular reactions have proven to be an extremely efficient synthetic tool for the preparation of complex polycyclic molecules. This reactivity is favored by the strain release produced during the process and it requires, by definition, the employment of cyclic precursors, which are characterized by the inherent ring strain of the structure. The resulting conformational rigidity can be employed to control the stereochemistry of the reaction. In that context, the present manuscript encompasses the study and development of novel transannular reactions relying on the use of asymmetric catalytic organoboron chemistry and organocatalysis as efficient systems to promote these transformations and induce enantiocontrol.

Thus, on the one hand, the feasibility of medium-sized cyclic keto-enones to undergo copper-catalyzed conjugate borylation and subsequent transannular aldol reaction has been studied. The relative configuration of three adjacent stereocenters is controlled, giving access to a single diastereoisomer for a wide range of substrates tested. The reaction could also be carried out in a highly enantioselective fashion through the incorporation of a chiral ligand in the catalytic system.

On the other hand, the suitability of cycloalkenone hydrazones to undergo enantioselective transannular (3+2) cycloaddition reaction was explored under chiral Brønsted acid catalysis. This reaction afforded stereodefined polycyclic scaffolds, with a bridged pyrazolidine ring, which could be further transformed to synthetically challenging *cis*-1,3-diamines.

Finally, the results obtained for the switchable behaviour of cyclooctatetraene oxide to undergo single or double ring contraction process, under Brønsted acid catalysis, are disclosed in this manuscript. This process is modulated through the pK_a of the catalyst and could be coupled to an allylation reaction that enabled the synthesis of homoallylic alcohols. A complete mechanistic picture of the reaction and a rationale behind the influence of the catalyst is provided based on both experimental and computational data.

Resumen

Las reacciones transanulares han demostrado ser una herramienta sintética eficiente para la preparación de moléculas policíclicas complejas. Esta reactividad se ve favorecida por la liberación de tensión que se produce durante el proceso y requiere, por definición, el empleo de precursores cíclicos, que se caracterizan por la tensión de anillo inherente en la estructura. La rigidez conformacional resultante se puede emplear para controlar la estereoquímica de la reacción. En este contexto, el presente manuscrito abarca el estudio y desarrollo de nuevas reacciones transanulares basadas en el uso de la organocatálisis y la catálisis asimétrica de boro como sistemas eficientes para promover estas transformaciones e inducir enantiocontrol.

Así, por un lado, se ha estudiado la viabilidad de reacciones en cascada borilación conjugada/aldólica transanular en ceto-enonas cíclicas de tamaño medio. El control de la configuración relativa de los tres estereocentros adyacentes da acceso a la formación de un solo diastereoisómero para una amplia gama de sustratos. La reacción enantioselectiva se pudo llevar a cabo mediante la incorporación de un ligando quiral en el sistema catalítico.

Por otro lado, se estudió la capacidad de las hidrazonas de cicloalquenona para participar en reacciones de cicloadición (3+2) transanulares bajo catálisis ácida de Brønsted quiral. Esta reacción proporcionó productos policíclicos estereodefinidos, con un anillo puente de pirazolidina, que pudieron ser posteriormente transformados para la obtención de distintas *cis*-1,3-diaminas.

Finalmente, los resultados obtenidos para el comportamiento conmutable del óxido de ciclooctatetraeno al sufrir un proceso de contracción de anillo simple o doble, bajo catálisis ácida, se describen en este manuscrito. Este proceso es modulado a través del pK_a del catalizador y puede acoplarse a una reacción de alilación, permitiendo la síntesis de alcoholes homoalílicos. Asimismo, también se proporciona el mecanismo de la reacción y una justificación de la influencia del catalizador basado en datos experimentales y computacionales.

Laburpena

Erreakzio transanularrak molekula polizikliko konplexuak prestatzeko baliabide sintetiko eraginkorrak direla ikusi da. Erreaktibitate hau erreakzioaren baitan gertatzen diren tentsio askapenaren eraginez faboratua dago eta definizioz, aurrekari ziklikoen erabilera, egituraren berezko eraztun-tentsioak ezaugarritzen dituena, beharrezkoa da. Sortutako konformazio zurruntasuna erreakzioaren estereokimika kontrolatzeko erabili daiteke. Testuinguru honetan, idazki honek, organokatalisiaren eta boroaren katalisi asimetrikoaren erabileran, erreakzioak sustatzeko eta enantiokontrola eragiteko eran, oinarritutako erreakzio transanularren ikerketa eta garapena barneratzen ditu.

Alde batetik, tamaina ertaineko zeto-enona ziklikoen borilazio konjokatu/aldolika transanularren kaskada erreakzioen bateragarritasuna ikertu da. Hiru ondoko estereozentroen konfigurazioa erlatiboan kontrolak, substratu sorta handi batean, diastereoisomero bakarra eratzea ahalbidetu du. Sistema katalitikoan ligando kiral bat eransteak, erreakzioa enantioselektiboa izatea ahalbidetu duelarik.

Beste alde batetik, Brønsted kiral bidezko katalisi azidoen (3+2) zikloadizio erreakzio transanularretan zikloalkenonen hidrazonen esku-hartze gaitasuna ikertu da. Erreakzio honek, esterikoki definitutako eta pirazolidina eraztun-zubidun produktuen sorrera ahalbidetu du, ostean *cis*-1,3-diamina desberdinak sortzeko eralda zitezkeenak.

Azkenik, katalisi azidopean, eraztun sinple edo bikoitzaren uzurtze prozesuaren eraginez ziklooktatetraeno oxidoak jasandako jokaera aldagarrien emaitzak ondoko idatzi honetan deskribatzen dira. Prozesu hau katalizatzearen pK_a -ren bitartez modulatzeko da eta alilazio erreakzio batekin akoplatu daiteke, alkohol homoalilikoaren sintesia ahalbidetuz. Era horretan, erreakzioaren mekanismoa eskaintzen da eta katalizatzailearen eragina arrazoitzen da, datu esperimental eta konputazionalen oinarrituz.

Index

CHAPTER 1 - Introduction

1. TRANSANNULAR REACTIONS.....	5
2. TRANSANNULAR REACTIONS IN STEREOSELECTIVE SYNTHESIS.....	13
3. PRECEDENTS OF THE RESEARCH GROUPS	22
3.1. Transannular reactivity: UPV/EHU research group	22
3.2. Organoboron chemistry: URV research group.....	27
4. GENERAL OBJECTIVES.....	32

CHAPTER 2 - Catalytic Stereoselective Borylative Transannular Reactions

1. INTRODUCTION.....	39
1.1. Nucleophilic organoboron chemistry.....	39
1.2. Stereoselective borylative ring closing of functionalized alkenes	48
2. SPECIFIC OBJECTIVES AND WORK PLAN.....	54
3. RESULTS AND DISCUSSION	57
3.1. Proof of concept.....	57
3.2. Optimization of the reaction conditions	58
3.3. Scope of the diastereoselective Cu/dppf borylative transannular reaction	61
3.4. Enantioselective Cu(I)-catalyzed borylative transannular reaction	68
4. CONCLUSIONS.....	74

CHAPTER 3 - Transannular Enantioselective (3+2) Cycloaddition of Cycloalkenone Hydrazones under Brønsted Acid Catalysis

1. INTRODUCTION.....	79
1.1. Asymmetric organocatalysis	79
1.2. Hydrazones in (3+2) cycloaddition reactions: Synthesis of pyrazolidines	89
2. SPECIFIC OBJECTIVES AND WORK PLAN.....	98
3. RESULTS AND DISCUSSION	102
3.1. Proof of concept	102
3.2. Optimization of the reaction conditions	104
3.3. Scope of the enantioselective transannular (3+2) cycloaddition reaction.....	108
3.4. Transformation of the adducts: Synthesis of enantioenriched 1,3-diamines	117
3.5. Mechanistic insights and stereochemistry of the reaction	119
4. CONCLUSIONS.....	124

CHAPTER 4 - Switchable Brønsted Acid-Catalyzed Ring Contraction/Enantioselective Allylation of Cyclooctatetraene Oxide

1. INTRODUCTION.....	129
1.1. Electrocyclic reactions.....	129
1.2. Cyclooctatetraene systems: structure and reactivity	137
2. SPECIFIC OBJECTIVES AND WORK PLAN.....	141
3. RESULTS AND DISCUSSION	144
3.1. Proof of concept	144
3.2. Mechanistic and computational studies	148
3.3. Enantioselective ring contraction/allylation process	166
4. CONCLUSIONS.....	174

CHAPTER 5 - Final Conclusions**FINAL CONCLUSIONS 179****CHAPTER 6 - Experimental**

1. GENERAL METHODS AND MATERIALS.....	187
2. CATALYTIC STEREOSELECTIVE BORYLATIVE TRANSANNULAR REACTIONS	191
2.1. Synthesis of the starting materials	191
2.2. Cu/dppf catalyzed transannular conjugated borylation/aldol cyclization	194
2.3. Cu/Josiphos catalyzed transannular conjugated borylation/aldol cyclization	204
2.4. Oxidation procedures	210
3. TRANSANNULAR ENANTIOSELECTIVE (3+2) CYCLOADDITION OF CYCLOALKENONE HYDRAZONES	212
3.1. Synthesis of the starting materials	212
3.2. Enantioselective transannular (3+2) cycloaddition	221
3.3. Derivatization procedures for the cycloaddition adducts	231
3.4. Reductive cleavage for the synthesis of enantioenriched 1,3-diamines.....	240
4. SWITCHABLE BRØNSTED ACID-CATALYZED RING CONTRACTION/ENANTIOSELECTIVE ALLYLATION	245
4.1. Synthesis of the starting materials	245
4.2. Enantioselective ring contraction/allylation reaction	246

CHAPTER 7 - Scientific Collaborations

1. PROJECTS IN COLLABORATION	263
1.1. Transition-metal-free stereoselective borylation of allenamides.....	263
1.2. Synthesis of carbocyclic boronic esters <i>via</i> intramolecular lithiation-borylation and ring contraction	267

Appendix

Abbreviations, acronyms and symbols	259
Resumen extendido	259
Papers	263

Supplementary information

Full document, NMR-spectra, HPLC traces, Crystallographic data	USB
--	-----

The numbering of references, figures, schemes and tables has been restarted at the beginning of each chapter.

1

1

Introduction

1. TRANSANNULAR REACTIONS	5
2. TRANSANNULAR REACTIONS IN STEREOSELECTIVE SYNTHESIS ..	13
3. PRECEDENTS OF THE RESEARCH GROUPS	22
3.1. Transannular reactivity: UPV/EHU research group	22
3.2. Organoboron chemistry: URV research group	27
4. GENERAL OBJECTIVES	32

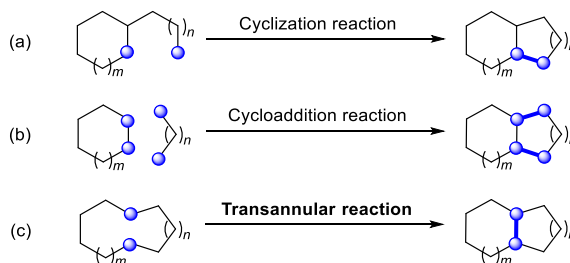
1. TRANSANNULAR REACTIONS

The main purpose of synthetic organic chemists has relayed on the development of novel strategies in order to obtain new compounds, which could have interesting properties and thereby showing an important impact on human life. Since most pharmaceutical and biologically active compounds are constituted by highly complex scaffolds,^{1,2} these approaches are often not easy to achieve and a good design of the synthetic plan is required in order to obtain the final target in the minimum number of steps. Therefore, important efforts have recently been directed towards the development of methodologies that could solve more than one synthetic difficulty at a time, also reducing the number of organic transformations such as protection/deprotection steps. This fact would allow the possibility to accomplish challenging synthetic frameworks in a very concise and efficient manner.

From a synthetic point of view, most of these compounds with potential interest are constituted by polycyclic architectures. Up to date, several approaches are already described in order to obtain the mentioned molecular complexity and can be classified according to three general reaction types (Scheme 1.1). The first type refers to *cyclization reactions*, in which a functionalized side chain reacts with other functionality present in a pre-existing cyclic structure in the molecule (Scheme 1.1a). The second scenario, *cycloaddition reactions*, encompasses those cases where two C-C or C-heteroatom bonds are formed through the intermolecular reaction between two components, one of them having a ring in its structure (Scheme 1.1b).³ On the other hand, the third scenario is a scarcely developed

-
- ¹ For selected reviews for the synthesis of carbo- and heterocycles: (a) Maier, M. E. *Angew. Chem. Int. Ed.* **2000**, *39*, 2073. (b) Balme, G.; Bouyssi, D.; Monteiro, N. *Pure Appl. Chem.* **2006**, *78*, 231. (c) Mondal, S.; Santhivardhana, R. Y.; Mukherjee, S.; Biju, A. T. *Acc. Chem. Res.* **2019**, *52*, 425. (d) Sajid, M. A.; Khan, Z. A.; Shahzad, S. A.; Naqvi, S. A. R.; Usman, M. *Mol. Divers.* **2020**, *24*, 295.
- ² (a) Bhat, S. V.; Nagasampagi, B. A.; Sivakumar, M. (2005). *Chemistry of Natural Products*; Springer: Berlin. (b) Andrushko, V. (2013). *Stereoselective Synthesis of Drugs and Natural Products*; Wiley: Karlsruhe. (c) García-Castro, M.; Zimmermann, S.; Sankar, M. G.; Kumar, K. *Angew. Chem. Int. Ed.* **2016**, *55*, 7586.
- ³ For selected reviews on cyclization and cycloaddition reactions, see: (a) Gulías, M.; López, F.; Mascareñas, J. L. *Pure Appl. Chem.* **2011**, *83*, 495. (b) Ylijoki, K. E. O.; Stryker, J. M. *Chem. Rev.*

synthetic tool which involves the use of *transannular reactions*. In this particular case, both reacting sites are present within a unique starting material (Scheme 1.1c).⁴



Scheme 1.1. General synthetic strategies to achieve polycyclic architectures.

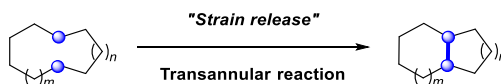
Due to the closer relationship with the research presented in this manuscript, special attention will be dedicated to transannular reactions. As it has been mentioned above, in this type of transformations the two reacting sites are present in the same cyclic substrate and the formation of the new C-C or C-heteroatom covalent bond occurs through the ring, leading to the preparation of two or more smaller cycles with multiple stereocenters in many cases. The relative proximity of the two reactive moieties provides an additional entropic advantage, allowing transannular reactions to occur in such sterically congested structures for which analogous intermolecular and intramolecular acyclic systems would be unreactive. Nevertheless, transannular reactions have received less attention and up to date, a reduced number of reactions have been developed mostly due to the inherent difficulty when preparing the corresponding cyclic precursors. The advances achieved on the development of new strategies for the synthesis of medium and large rings have allowed to overcome this limitation and transannular reactions have arisen as a useful tool for accessing complex polycyclic structures and

2013, 113, 2244. (c) Held, F. E.; Grau, D.; Tsogoeva, S. B. *Molecules*, **2015**, 20, 16103. (d) Klier, L.; Tur, F.; Poulsen, P. H.; Jørgensen, K. A. *Chem. Soc. Rev.* **2017**, 46, 1080. (e) Albano, G.; Aronica, L. A. *Synthesis*, **2018**, 50, 1209. (f) Barrett, A. G. M.; Ma, T.-K.; Mies, T. *Synthesis*, **2018**, 50, 1209.

⁴ For selected reviews, see: (a) Reyes, E.; Uria, U.; Carrillo, L.; Vicario, J. L. *Tetrahedron*, **2014**, 70, 9461. (b) Reyes, E.; Prieto, L.; Carrillo, L.; Uria, U.; Vicario, J. L. *Synthesis* **2022**, 54, 4167.

therefore, resulting in very straightforward methodologies for the synthesis of natural products.⁵

In order to better understand the course of transannular reactions from a thermodynamic point of view, it is necessary to know the structural and energetic factors inherent to the cyclic precursor and the polycyclic product formed, since these will be the ones that determine the enthalpy and entropy changes of the overall process and therefore, the feasibility of the reaction. In that sense, the outcome of the transannular reaction will be highly dependent on the thermodynamic variations involved in the transformation and thus, strongly related with the macrocyclic environment. Therefore, the size of the ring would determine the chemical and physical properties of the cyclic compounds and the most studied parameter is the inherent ring strain energy variation present in the described systems.⁶ The release of ring strain during a transannular process can be a key driving force for a transannular reaction to be thermodynamically favoured (Scheme 1.2).



Scheme 1.2. Transannular bond formation through the strain release.

In fact, the existence of certain strain is an aspect that characterizes most of the cyclic compounds described and this is due to the existing interactions originated by their three-dimensional conformation. Hence, the resulting strain is the consequence of the combination of three independent factors. The first one is the *angular strain* (Figure 1.1a), associated to the angle deviation in comparison with the theoretical values determined for the hybridization of the corresponding atoms, which lead to the efficient overlapping between the molecular orbitals. The second

⁵ (a) Roxburgh, C. J. *Tetrahedron*, **1995**, *51*, 9767. (b) Clarke, P. A.; Reeder, A. T.; Winn, J. *Synthesis*, **2009**, 691. (c) Peterson, M. L. (2015). *The synthesis of macrocycles for drug discovery. Macrocycles in Drug Discovery*; Levin, J. I., Eds.; RSC: Cambridge, pp 398-465.

⁶ Yang, L.; Xie, L.; Wei, Y.; Devi, M.; Huang, W. (2017). *Steric Strain in molecular organics*. In *Encyclopedia of Physical Organic Chemistry*; Wang, Z.; Eds.; John Wiley & Sons, Inc.: USA.

component is the *torsional strain* (Figure 1.1b), as a result of the eclipsing interactions between adjacent linked atoms and the third one is the *transannular strain* (Figure 1.1c), involving those possible unfavored repulsive interactions between non-adjacent atoms that are spatially close to each other in the ring structure. The most common methodology in order to determine the strain energies of different cycloalkanes is through the difference in heat of combustion between the cyclic molecule and the analogous open chain compound as the reference.⁷ Those values are illustrated in the following Figure 1.1, showing the variation of the strain energy (kcal/mol) depending on the ring size of the cyclic precursor.⁶

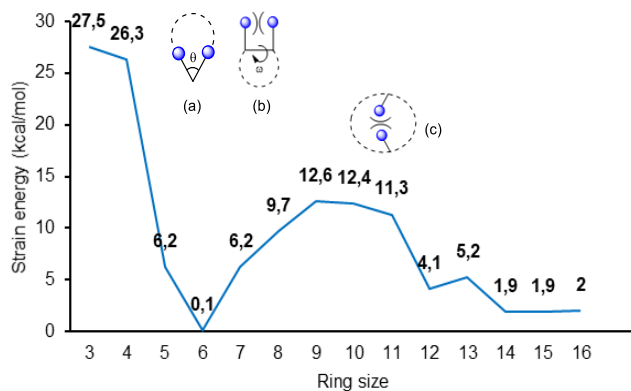


Figure 1.1. Strain energies for cycloalkanes.

The data shown in Figure 1.1 indicates that small cycles have extremely high strain energy values (27.5-26.3 kcal/mol) and therefore, explaining their instability and reactivity. Regarding medium-sized rings, higher energy values are observed (9.7-12.6 kcal/mol) compared to those measured for 5, 6 and 7 membered cycloalkanes (0.1-6.2 kcal/mol), whereas larger rings were supposed to be almost ring strain free. For medium size cyclic systems the transannular component becomes the major contributor of the overall strain. These rings show a tendency to minimize the repulsive interactions by adopting low energy conformations and

⁷ McMurry, J. E. *Stability of cycloalkanes: ring strain*. (2012). *Organic Chemistry*; Eds.; Brooks Cole: Mexico, pp 114-115.

the inherent conformational rigidity facilitates the stereochemical control of the overall process when new stereocenters are generated. Furthermore, it is known that in larger systems the mentioned strain becomes even weaker due to the higher flexibility. This fact increases the number of energetically similar conformations leading to a more complex scenario that up to date, it has been more scarcely examined than in the case of small cycles.⁸

For example, conformational studies have reported up to 11 possible conformations for the case of cyclooctane. In particular, the boat-chair (BC) conformer has been found to be the most energetically favoured. As for the other medium-sized cycles such as cyclononane and cyclodecane the twist boat-chair (TBC) and the boat-chair-boat (BCB) were the preferred ones respectively (Figure 1.2).⁹

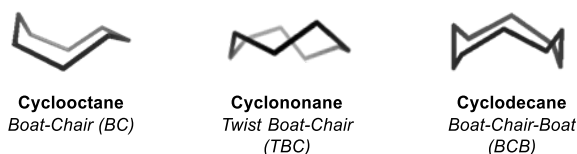


Figure 1.2. Energetically favoured conformations for medium sized cycloalkanes.

For the analogous eleven membered cycloalkane, ¹³C-NMR studies demonstrated that it could exist as a mixture of two energetically favoured conformations at low temperatures (Figure 1.3) whereas at high temperatures, the number of possible conformations in equilibrium increases significantly.¹⁰

⁸ (a) Nasipuri, D. (2005). *Stereochemistry of organic compounds. Principles and applications*: New Age International Publishers; New Dehli. (b) Dragojlovic, V. *ChemTexts* **2015**, 1, 14.

⁹ (a) Hendrickson, J. B. *J. Am. Chem. Soc.* **1964**, 86, 4854. (b) Still, W. C.; Galynker, I. *Tetrahedron*, **1981**, 37, 3981. (c) Kolossvary, I.; Guida, W. C. *J. Am. Chem. Soc.* **1993**, 115, 2107. (d) Wiberg, K. B. *J. Org. Chem.* **2003**, 68, 9322.

¹⁰ Pawar, D. M.; Brown, J.; Chen, K.-H.; Allinger, N. L.; Noe, E. A. *J. Org. Chem.* **2006**, 71, 6512.

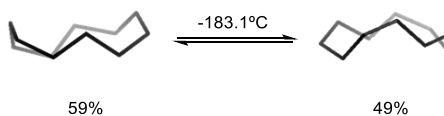


Figure 1.3. Energetically favoured conformations for cycloundecane.

On the other hand, the energetic and conformational study of functionalized cycloalkanes is more complicated, since the substituents or functionalities incorporated into the cyclic structure would determine the adopted molecular geometry and consequently would affect their physical and chemical properties. In this sense, the size and the nature of the substituents would establish the energy of the present interactions as well as the conformations acquired to minimize the repulsions generated and the kinetic barriers that separate them. Besides, the incorporation of an insaturation in the cyclic structure would notably decrease the conformational flexibility, leading to a scenario in which a planar chirality could even be observed in certain cycloalkenes, whose stereochemical stability is highly dependent on the size of the ring and the substituents present in it.¹¹ As it can be seen in Figure 1.4, a representative example of the mentioned case above would be the *trans*-cyclooctene. At room temperature, the enantiomeric conformers are stable and no interconversion of both species is observed due to the high activation energy inherent in the rotation of the double bond with respect to the rest of the molecule.¹² This activation energy barrier is due to the transannular strain present in the planar conformation that the molecule adopts in order to interconvert from one enantiomer to the other.

¹¹ For a selected review of planar chirality in medium-sized cycles: Nubbemeyer, U. *Eur. J. Org. Chem.* **2001**, 1801.

¹² (a) Cope, A. C.; Mehta, A. S. *J. Am. Chem. Soc.* **1964**, *86*, 5626. (b) Cope, A. C.; Pawson, B. A. *J. Am. Chem. Soc.* **1965**, *87*, 3649.

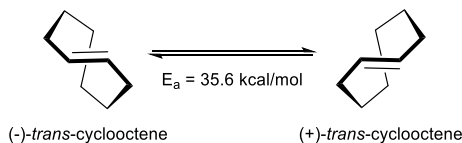


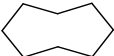
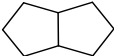
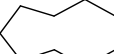
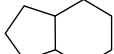
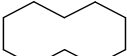
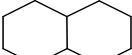
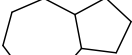
Figure 1.4. Interconversion of the enantiomeric conformers for the *trans*-cyclooctene.

As mentioned, from a thermodynamic point of view, the enthalpy variations involved on the course of the transannular reaction should be a key aspect to take into account in order to study whereas a process would be energetically favoured and therefore, predict the viability of the chemical reaction. In this context, a transannular reaction would be thermodynamically favoured when the energy of the polycyclic product is lower than the energy of the corresponding cyclic precursor, being the strain release the driving force of the transformation.¹³ It has to be highlighted that all cyclic compounds, with the exception of three-membered rings, can undergo transannular reactions. However, the greatest synthetic application has found to be with medium or large rings.

As it can be seen in the following Table 1.1, in general the [6,6] ring fusion would be the most stable arrangement followed by the [6,5], [5,5] and [5,7]. Moreover, the stability for the same type of bicyclic structure is influenced by the relative configuration of the atoms involved in the formation of the transannular bond therefore, the *cis/trans* fusion of the corresponding products would not be equally favoured. For the specific case of the cyclooctane ($n = 8$), the transannular reaction would not be highly favoured since the strain energy corresponding to the bicyclic product is higher than the one from the precursor. Regarding cyclononane ($n = 9$) and cyclodecane ($n = 10$), the transannular reaction would be favoured thermodynamically, in general, considering the strain release associated to the formation of the bicyclic products and in particular, favouring the formation of the *trans* fusion.

¹³ (a) Chang, S.-J.; McNally, D.; Shary-Tehrany, S.; Hickey, M. J.; Boyd, R. H. *J. Am. Chem. Soc.* **1970**, *92*, 3109. (b) Engler, E. M.; Andose, J. D.; Schleyer, P. V. R. *J. Am. Chem. Soc.* **1973**, *95*, 8005.

Table 1.1. Strain energies for different cycloalkanes.

n	Cycloalkane	Strain energy (Kcal/mol)	Product	Strain energy (Kcal/mol)
8		11.9		<i>cis</i> : 12.0 <i>trans</i> : 18.4
9		15.5		<i>cis</i> : 8.9 <i>trans</i> : 7.9
10		16.4		<i>cis</i> : 4.1 <i>trans</i> : 1.0
				<i>cis</i> : 13.4 <i>trans</i> : 13.1

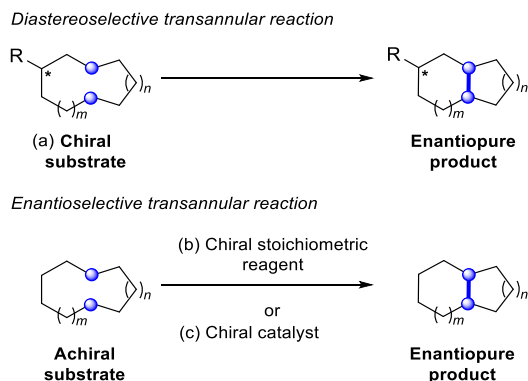
This trend reflected in the table are not necessarily extrapolated to all cycloalkanes since, as previously mentioned, the properties of the studied molecules are significantly influenced by the presence of a functionality. Moreover, the probability of a certain transannular reaction to occur would be determined by the size of the cycles and the hybridization of the carbon involved in the reaction (Baldwin's rules)¹⁴ and in any case, the energy barriers could be overcome under specific experimental conditions.

¹⁴ (a) Baldwin, J. E. *J. Chem. Soc., Chem. Commun.* **1976**, 12, 734. (b) Baldwin, J. E.; Kruse, L. I. *J. Chem. Soc., Chem. Commun.* **1977**, 13, 233. (c) Baldwin, J. E.; Lusch, M. J. *Tetrahedron* **1982**, 38, 2939.

2. TRANSANNULAR REACTIONS IN STEREOSELECTIVE SYNTHESIS

As it has been described in the previous section, the intrinsic conformational constraints associated to the structure of cyclic systems, converts transannular reactions to be a suitable synthetic tool for the development of stereoselective methodologies giving access to enantiopure targets, containing multiple stereogenic centers.^{4,5,15} Up to date, numerous examples of stereocontrolled transannular reactions have been already reported, demonstrating the utility of this approach. These can be classified into three main categories depending on the strategy employed for achieving stereocontrol. The first is based on using the internal asymmetric induction exerted by the macrocycle itself due to inherent conformational properties. In that sense, the introduction of chiral elements at the cyclic precursor would determine the stereochemistry of the final product through the conformational restrictions and the minimization of the repulsive interactions present because of the introduced elements. Therefore, the stereocontrol is induced by the use of a chiral substrate leading to a *substrate-directed diastereoselective transannular reaction* (Scheme 1.3a). The second one relies on the use of chiral stoichiometric reagents (Scheme 1.3b) and the third one is based on asymmetric catalysis (Scheme 1.3c). Both make use of an achiral cyclic starting material resulting in an overall *enantioselective transannular process*.

¹⁵ Yang, J.; Xue, H. (2013). *Transannular cyclization in natural product total synthesis*. In *Stereoselective Synthesis of Drugs and Natural Products*; Andrushko, V.; Ndrushko, N., Eds.; John Wiley & Sons Inc.: Karlsruhe, pp 551-579.

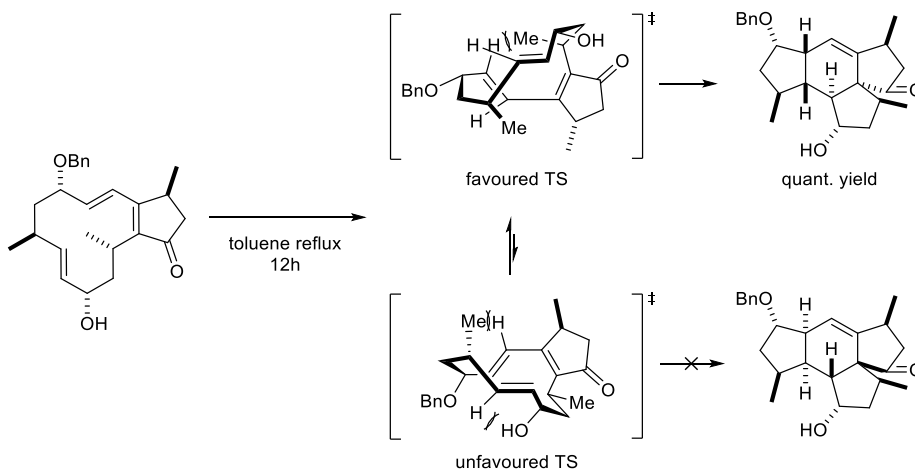


Scheme 1.3. General synthetic strategies for stereoselective transannular reactions.

Among the wide number of examples reported for the construction of enantiopure products with a relatively complex scaffold through transannular reactions,¹⁶ most of them involve diastereoselective processes in which a chiral substrate is used. The following example depicted in Scheme 1.4 clearly shows that the stereocenters present in the precursor have a significantly influence on the reaction outcome in terms of stereoselectivity. Uemura and co-workers demonstrated in 2004 that the minimization of transannular repulsive interactions, present on the conformations acquired by the macrocyclic environment in the different transition states, could favour the selective formation of enantiopure spirotricycles through the diastereoselective transannular Diels-Alder (TADA) reaction of the specified cyclic starting material.¹⁷

¹⁶ For recent examples on transannular reactions in stereoselective synthesis of enantiopure compounds not involving natural product synthesis, see: (a) Felzmann, W.; Arion, V. B.; Miesusset, J.-L.; Mulzer, J. *Org. Lett.* **2006**, *8*, 3849. (b) Surprenant, S.; Lubell, W. D. *Org. Lett.* **2006**, *8*, 2851. (c) Franklin, A. I.; Bensa, D.; Adams, H.; Coldham, I. *Org. Biomol. Chem.* **2011**, *9*, 1901. (d) Atmuri, N. D. P.; Lubell, W. D. *J. Org. Chem.* **2015**, *80*, 4904. (e) Kamimura, A.; Moriyama, T.; Ito, Y.; Kawamoto, T.; Uno, H. *J. Org. Chem.* **2016**, *81*, 4664. (f) Atmuri, N. D. P.; Reilley, D. J.; Lubell, W. D. *Org. Lett.* **2017**, *19*, 5066. (g) Chan, D.; Chen, Y.; Low, K.-H.; Chiu, P. *Chem. Eur. J.* **2018**, *24*, 2375. (h) Maiga-Wandiam, B.; Corbu, A.; Maissot, G.; Sautel, F.; Yu, P.; Lin, B. W.-Y.; Houk, K. N.; Coss, J. *J. Org. Chem.* **2018**, *83*, 5975.

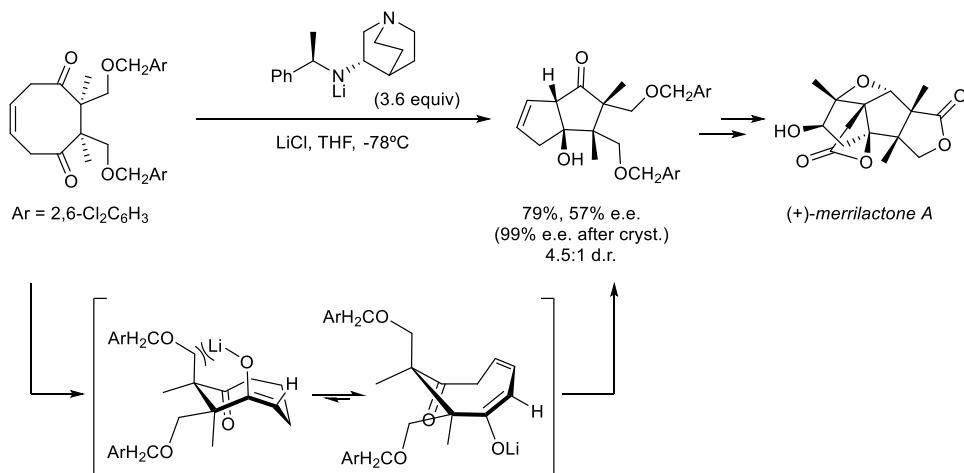
¹⁷ Araki, K.; Saito, K.; Arimoto, H.; Uemura, D. *Angew. Chem. Int. Ed.* **2004**, *43*, 81.



Scheme 1.4. Substrate-controlled diastereoselective TADA reaction.

On the other hand, there are some limited examples regarding the use of chiral stoichiometric reagents as the stereocontrolling element. The reported examples are based on the desymmetrization of *meso* compounds, such as the desymmetrization of different cyclic 1,4-diketones developed by Inoue and co-workers as illustrated in Scheme 1.5.¹⁸ This approach was based on a transannular aldol reaction, employing stoichiometric amounts of a chiral base, in particular, the lithium anilide, in order to promote the enantioselective deprotonation step in the α -position of one of the two carbonyl moieties. The resulting *E*-enolate further reacted with the pending ketone in a diastereoselective fashion, forming the transannular C-C bond with total stereocontrol due to the acquired conformation of the cyclic intermediate, minimizing the repulsive interactions between the bulky 2,6-dichlorophenyl substituent and the C-O bond of the enolate. The authors could also demonstrate the utility of the methodology by employing it as the key step in the enantioselective total synthesis of (+)-merrilactone A.

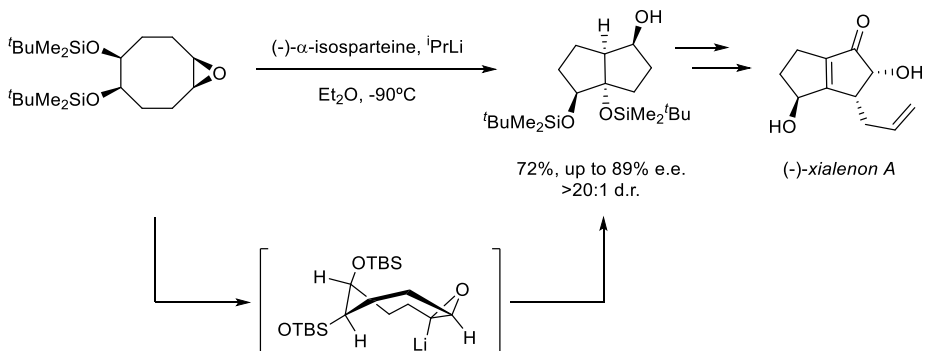
¹⁸ Inoue, M.; Lee, N.; Kasuya, S.; Sato, T.; Hiram, M.; Moriyama, M.; Fukuyama, Y. *J. Org. Chem.* **2007**, *72*, 3065.



Scheme 1.5. Enantioselective transannular aldol reaction for the synthesis of (+)-merrilactone A.

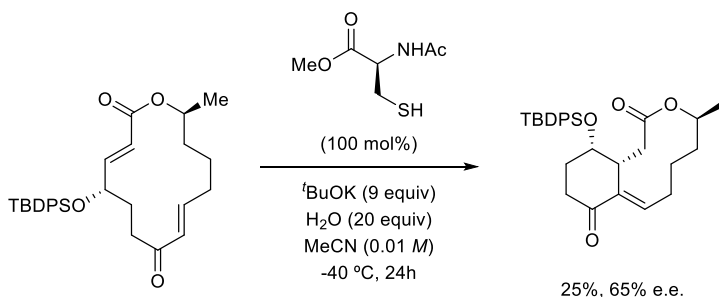
Inspired by the work of Inoue, the group of Hodgson reported a related example for the desymmetrization of *meso*-epoxides as depicted in Scheme 1.6.¹⁹ The stereoselectivity of the reaction was controlled during the enantioselective deprotonation step at the α -position of the oxirane through the use of an *in situ* formed chiral base, leading to the formation of a chiral intermediate that underwent subsequent transannular C-H insertion. This transformation gave access to functionalized bicyclic alcohols with good yields and enantioselectivity and it could be further used for the synthesis of (-)-xialenon A.

¹⁹ Hodgson, D. M.; Cameron, I. D.; Christlieb, M.; Green, R.; Lee, G. P.; Robinson, L. A. *J. Chem. Soc. Perkin Trans. 1*, **2001**, 2161.



Scheme 1.6. Enantioselective transannular epoxide ring-opening employing chiral reagents.

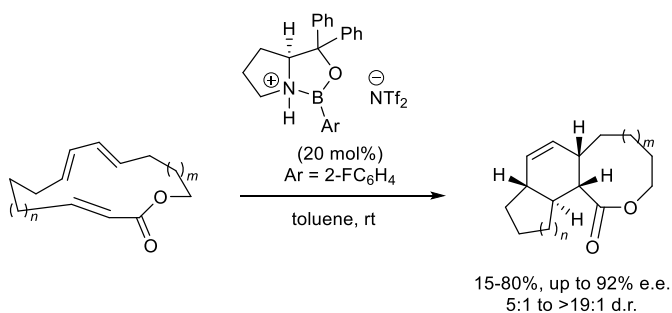
In 2011, the group of Miller demonstrated that an enantioselective transannular Rauhut-Currier ring contraction reaction was occurring when stereodefined 14-membered macrocycles, as the one shown in Scheme 1.7, were reacted with a chiral amino acid-based catalyst such as cysteine, obtaining the final product with rather low yield and moderate enantioselectivity.²⁰ These synthetic studies allowed preparation of an expanded set of Sch-642305-based compounds, which can show inhibitory activities towards the HIV life cycle.



Scheme 1.7. Enantioselective cysteine-catalyzed Rauhut-Currier transannular ring contraction.

²⁰ Dermenci, A.; Selig, P. S.; Domoaal, R. A.; Spasov, K. A.; Anderson, K. S.; Miller, S. J. *Chem. Sci.* **2011**, *2*, 1568.

In addition to these three limited cases of enantioselective transannular reactions using stoichiometric chiral reagents, several examples also exist in which asymmetric catalysis is employed as the methodological tool to achieve enantiocontrol. The first catalytic and enantioselective transannular reaction was reported by Jacobsen and co-workers in 2007. In this seminal report, the authors described a novel Lewis acid-catalyzed transannular Diels-Alder (TADA) transformation of macrolactones by the use of a chiral oxazaborolidine catalyst (Scheme 1.8).²¹ This methodology enabled the synthesis of enantioenriched polycyclic products, showing to be remarkably general across a broad range of macrocyclic substrates, including α,β -unsaturated ketones and esters. In all cases the reaction provided the endo products in moderate to good yields and excellent enantioselectivity.



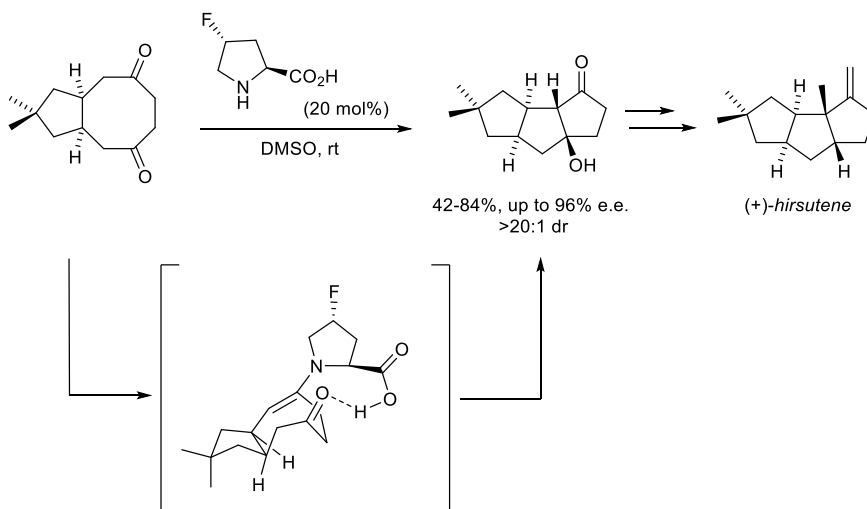
Scheme 1.8. Organocatalytic and enantioselective TADA reaction reported by Jacobsen.

In 2008, List and co-workers reported the first organocatalytic transannular aldol reaction of cyclic diketones using a proline derivative as the chiral catalyst.²² As it can be seen in Scheme 1.9, this reaction would proceed through the formation of an enamine intermediate and the stereochemistry would be governed by the specific H-bond interactions established in the transition structure. Besides, the authors attributed the obtained *cis* conformation of the ring fusion to the *E* geometry of the enamine intermediate. With this approach, different tricyclo[6.3.0]undecane

²¹ Balskus, E. P.; Jacobsen, E. N. *Science* **2007**, *317*, 1736.

²² Chandler, C. L.; List, B. *J. Am. Chem. Soc.* **2008**, *130*, 6737.

type cores could be prepared with good yields and enantioselectivity and it could be further used for the synthesis of different biologically active precursors such as (+)-hirsutene.

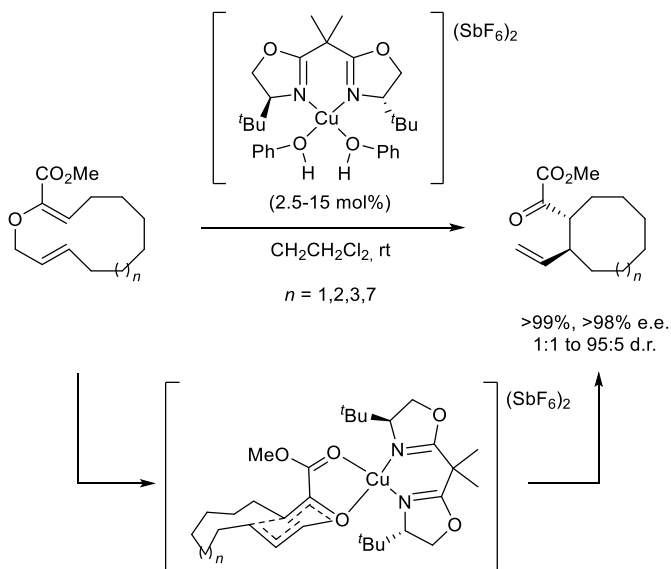


Scheme 1.9. Organocatalyzed enantioselective transannular aldol reaction.

A new challenge was achieved some years later within the field of the transition metal catalysis. The first Cu(II)-bis-oxazoline-catalyzed transannular Gosteli-Claisen rearrangement of cyclic 2-alkoxycarbonyl substituted allyl vinyl ethers was reported by Hiersemann co-workers (Scheme 1.10),²³ proposing that the high efficiency and stereoselectivity of this methodology was due to the structure of the catalyst, the ring size of the cyclic precursor and the configuration of the insaturation. In that sense, the authors observed that the best results were obtained with those substrates in which a 6-membered cyclic transition state was favoured, leading to the straightforward generation, in a single step and total control, of the two critical stereogenic centers and the nine-membered carbon scaffold.²⁴

²³ Jaschinski, T.; Hiersemann, M. *Org. Lett.* **2012**, *14*, 4114.

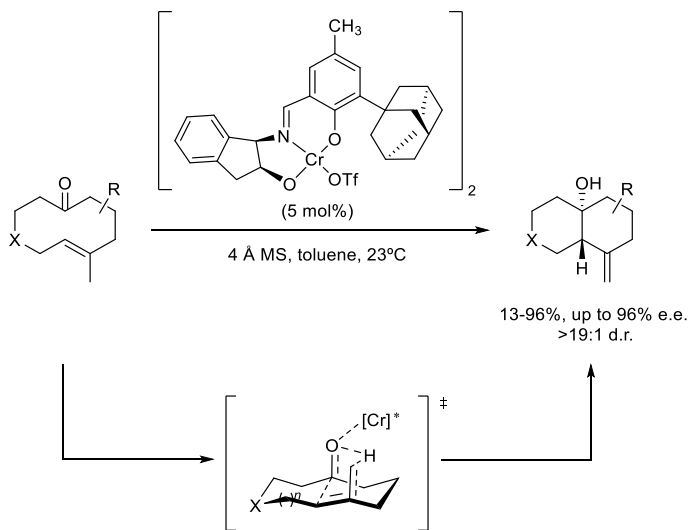
²⁴ Pollex, A.; Hiersemann, M. *Org. Lett.* **2005**, *7*, 5705.



Scheme 1.10. Cu (II)-catalyzed enantioselective {1,6}- transannular Gosteli-Claisen.

Soon afterwards, the group of Jacobsen described a highly enantio- and diastereoselective transannular ene-type reaction using a chiral Lewis acid as catalyst, specifically a chromium (III) complex with a chiral tridentate azomethine ligand as shown in Scheme 1.11.²⁵ This methodology was tested using unactivated 9- and 10- membered cyclic keto-olefins, including different substituents or heteroatoms within the structure of the starting material, leading to the diastereo- and enantioselective synthesis of decalinol-based scaffolds, which is a common skeleton present in many biologically active compounds and natural products.

²⁵ Rajapaksa, N. S.; Jacobsen, E. N. *Org. Lett.* **2013**, *15*, 4238.



Scheme 1.11. Cr(III)-catalyzed enantioselective transannular ene-type reaction.

Finally, our group has also contributed to the field by developing several catalytic enantioselective transannular transformations of different cyclic substrates and these examples will be disclosed in detail in the next section.

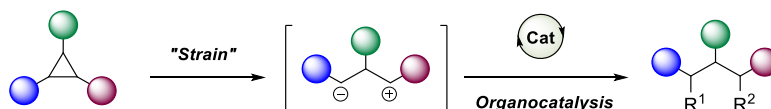
3. PRECEDENTS OF THE RESEARCH GROUPS

Due to the co-direction of the present work, two complementary fields of expertise have guided me in this thesis, and the next section highlights the conceptual skills from both fields.

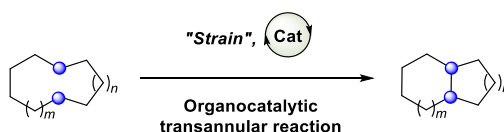
3.1. Transannular reactivity: UPV/EHU research group

Taking advantage of the experience in organocatalysis gathered by the group in previous years, during the last decade the main research line has been pivoted on the development of enantioselective transformations through the ring strain release inherent into different sized cyclic starting materials. In this sense, on the one hand, the ring strain present in small-sized carbo- and heterocycles makes them susceptible to suffer ring opening leading to the formation of a polyfunctionalized intermediate, capable of undergoing a subsequent chemical transformation in the presence of other reagents (Scheme 1.12a). On the other hand, for the case of medium-sized cyclic substrates, the existing inherent strain allows to trigger highly efficient transannular processes (Scheme 1.12b).

(a) *Small-sized cycles*



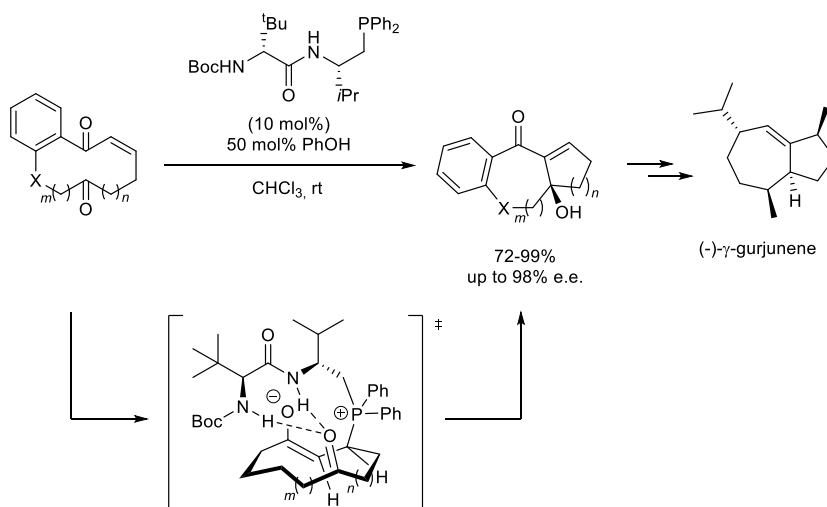
(b) *Medium-sized cycles*



Scheme 1.12. Principal research interests of the group.

Regarding the second type of processes mentioned above, the group has recently developed several transannular reactions⁴ in an enantioselective fashion. The first report involved the design and use of a catalytic and enantioselective Morita-Baylis-Hillman reaction catalyzed by a chiral enantiopure bifunctional

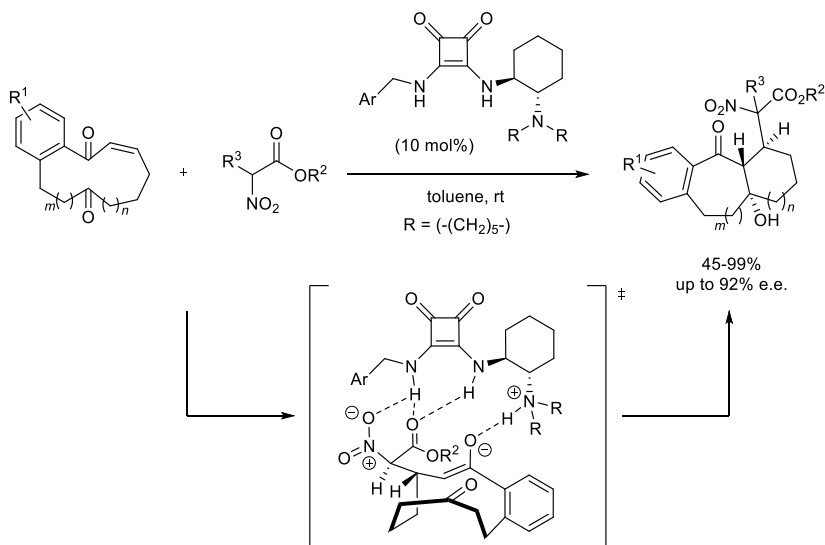
phosphine (Scheme 1.13).²⁶ This methodology opens a new pathway for the preparation of polycyclic carbo- and heterocycles containing fused rings of different sizes with excellent yields and excellent control on the stereochemical outcome of the generation of the newly formed stereogenic tertiary alcohol placed at the ring junction. In this sense, the selection of the bifunctional phosphine is crucial in order to obtain good levels of enantioinduction since the catalyst is both activating the substrate, through the phosphine moiety, and establishing H-bonding interactions between the NH moieties and the electrophilic ketone during the aldol addition step. Moreover, the potential of this transformation could also be demonstrated by developing the first enantioselective total synthesis of (-)- γ -gurjunene.



Scheme 1.13. Catalytic enantioselective transannular Morita-Baylis-Hillman reaction.

²⁶ (a) Mato, R.; Manzano, R.; Reyes, E.; Carrillo, L.; Uria, U.; Vicario, J. L. *J. Am. Chem. Soc.* **2019**, *141*, 9495. (b) Mato, R.; Manzano, R.; Reyes, E.; Prieto, L.; Uria, U.; Carrillo, L.; Vicario, J. L. *Catalysts* **2022**, *12*, 67.

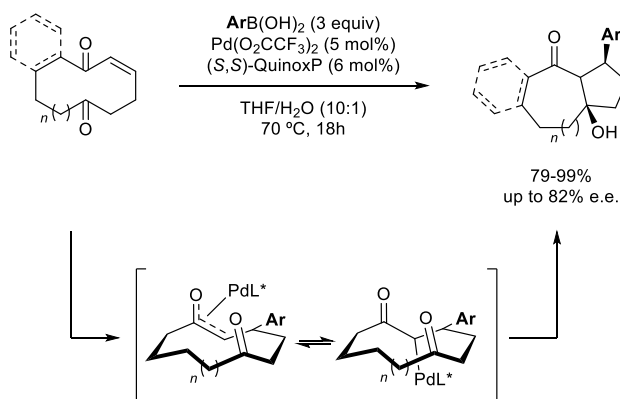
One year later, the same cyclic substrates were used on a catalytic enantioselective domino Michael/transannular aldol reaction under the use of bifunctional tertiary amine/squaramide catalysis (Scheme 1.14).²⁷ This cascade process leads to densely substituted bicyclo[5.4.0]undecane structures with three contiguous stereogenic centers and total control on the stereochemistry in a single step. In this case, the role of the bifunctional tertiary amine/squaramide catalyst is to ensure that the initial conjugate addition step of the sequence proceeds with excellent enantiocontrol and therefore, it is subsequently transferred to the transannular aldol step. The structural constrain of this particular substrates, and thus the *Z*-configured medium-sized cyclic *Z*-enolate intermediate would explain the diastereoselectivity observed for the overall cascade process.



Scheme 1.14. Catalytic enantioselective domino Michael/transannular aldol reaction.

²⁷ Mato, R.; Reyes, E.; Carrillo, L.; Uria, U.; Prieto, L.; Manzano, R.; Vicario, J. L. *Chem. Commun.* **2020**, 56, 13149.

A recent collaboration of the group with the “Instituto de Investigaciones Químicas” (IIQ-CSIC), from Sevilla, showed the potential of the previously used medium-sized cyclic ketoenones to undergo a palladium-catalyzed asymmetric conjugate addition of aryl boronic acids and subsequent transannular aldol trapping reaction (Scheme 1.15).²⁸ The use of the *in situ* generated [Pd/(QuinoxP*)] as the catalytic active species enabled the synthesis of several arylbicyclic scaffolds with good isolated yields, diastereomeric ratios and enantiocontrol. The reaction also showed to be tolerant within a wide range of cyclic substrates and functionalized aryl boronic acids, including heterocyclic compounds.



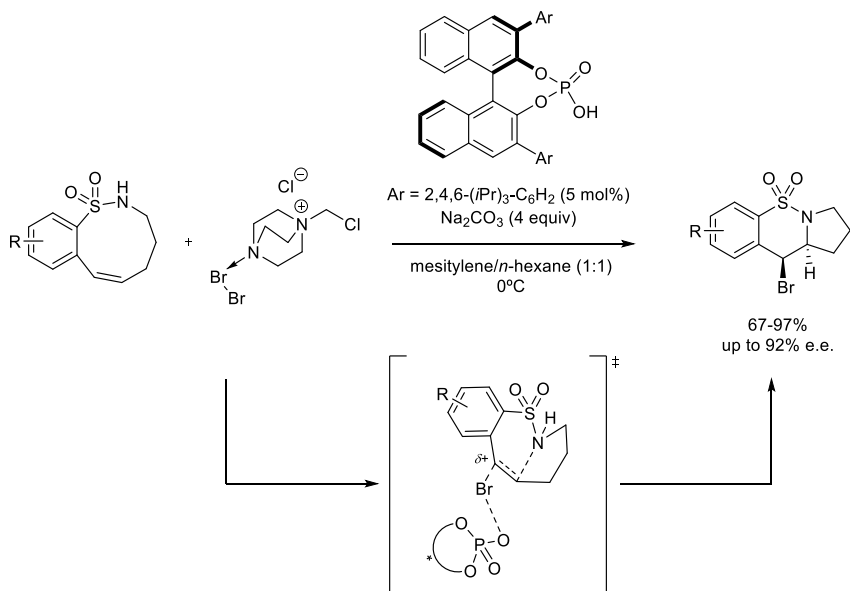
Scheme 1.15. Enantioselective Pd(II)-catalyzed conjugate addition/transannular aldol reaction.

Finally, a more recent example reported the catalytic and enantioselective version of a transannular aminobromination of enebenzosultams (Scheme 1.16).²⁹ The authors demonstrated that chiral phosphoric acids are suitable catalysts under phase transfer catalysis (PTC) conditions, leading to different polycyclic benzosulfonamides with good to excellent yields and enantioselectivities. Calculations suggested that the reaction followed a concerted mechanism and proposed a transition structure in which an intramolecular attack of the nitrogen to the homobenzylic position occurs completing the transannular cyclization. The

²⁸ Prieto, L.; Rodríguez, V.; Vicario, J. L.; Reyes, E.; Hornillos, V. *Chem. Commun.* **2022**, 58, 6514.

²⁹ Luis-Barrera, J.; Rodríguez, S.; Uria, U.; Reyes, E.; Prieto, L.; Carrillo, L.; Pedrón, M.; Tejero, T.; Merino, P.; Vicario, J. L. *Chem. Eur. J.* **2022**, 28, e2022022.

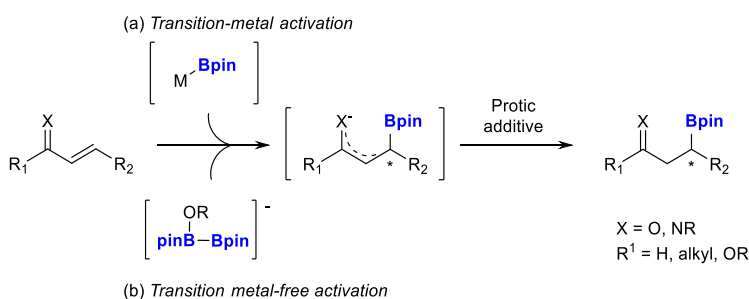
observed regioselectivity of the *anti*-Markonikov addition could be rationalized due to the formation of the more stable [6,5] arrangement at the final product rather than the [5,6] ring fusion.



Scheme 1.16. Enantioselective transannular phase-transfer catalyzed aminobromination.

3.2. Organoboron chemistry: URV research group

The group of Prof. Elena Fernández has directed the interest towards the development of atom-efficient processes for the synthesis of high added value organoboranes. Our efforts have been focused on the study of catalytic boron addition reactions to unsaturated substrates using inexpensive transition metals or even with transition metal-free methodologies. Moreover, significant efforts have been focused on the asymmetric version of the catalytic boron-addition reactions, in order to afford chiral organoboron compounds, which have shown to be of special interest on the scientific and industrial scenarios for their utility both in pharmaceuticals and material sciences. In 2009, the group aimed to obtain β -borylated compounds through conjugate borylation of different α,β -unsaturated acceptors (Scheme 1.17). The project was conducted through two strategies depending on the activation mode employed for the generation of the nucleophilic boryl moiety. The first scenario set *transition-metal complexes* (Scheme 1.17a) as the selected catalysts for the B-B bond cleavage. The second strategy involves a more challenging alternative developed by the group. This approach launched the use of Lewis bases, such as alkoxides,³⁰ for the polarization of the corresponding B-B bond and the formation of an *acid-base Lewis adduct* (Scheme 1.17b) that eventually reacts with the conjugated substrate.



Scheme 1.17. Strategies for the conjugate borylation of α,β -unsaturated acceptors.

³⁰ For a recent review of alkoxide activation of diboranes for C-B formation, see: Carbó, J. J.; Fernández, E. *Chem. Commun.* **2021**, 57, 11935.

In this context, the group has been able to develop many protocols and a selection of them is summarized in the following Scheme 1.18. Thus, regarding the first classification, palladium and nickel (a)³¹ have been used for the catalytic β -borylation of ketones and esters, together with the first example of an iron-mediated β -borylation of α,β -unsaturated carbonyl substrates (b).³² Moreover, it has been also successfully expanded the mentioned Cu(I)-catalytic approaches (c)³³ for the stereoselective β -borylation of different conjugated ketones and imines using, in all cases, symmetrical diboranes such as B₂pin₂.

In parallel it was launched the transition metal-free β -borylation of α,β -unsaturated carbonyl substrates using catalytic amounts of base to activate the symmetrical (d)³⁴ and unsymmetrical diboranes (e, f).³⁵ This pioneer strategy implemented by the group opened a new pathway towards the selective preparation of selective organoboron compounds. The protocol was extended to the use of pinB-X (X=SPh, SePh) reagents facilitating the C-heteroatom bonds

³¹ (a) Lillo, V.; Geier, M. J.; Westcott, S. A.; Fernández, E. *Org. Biomol. Chem.* **2009**, *7*, 4674. (b) Bonet, A.; Gulyás, H.; Koshevoy, I. O.; Estevan, F.; Sanaú, M.; Ubeda, M. A.; Fernández, E. *Chem. Eur. J.* **2010**, *16*, 6382. (c) Pubill-Ulldemolins, C.; Bonet, A.; Bo, C.; Gulyás, H.; Fernández, E. *Org. Biomol. Chem.* **2010**, *8*, 2667.

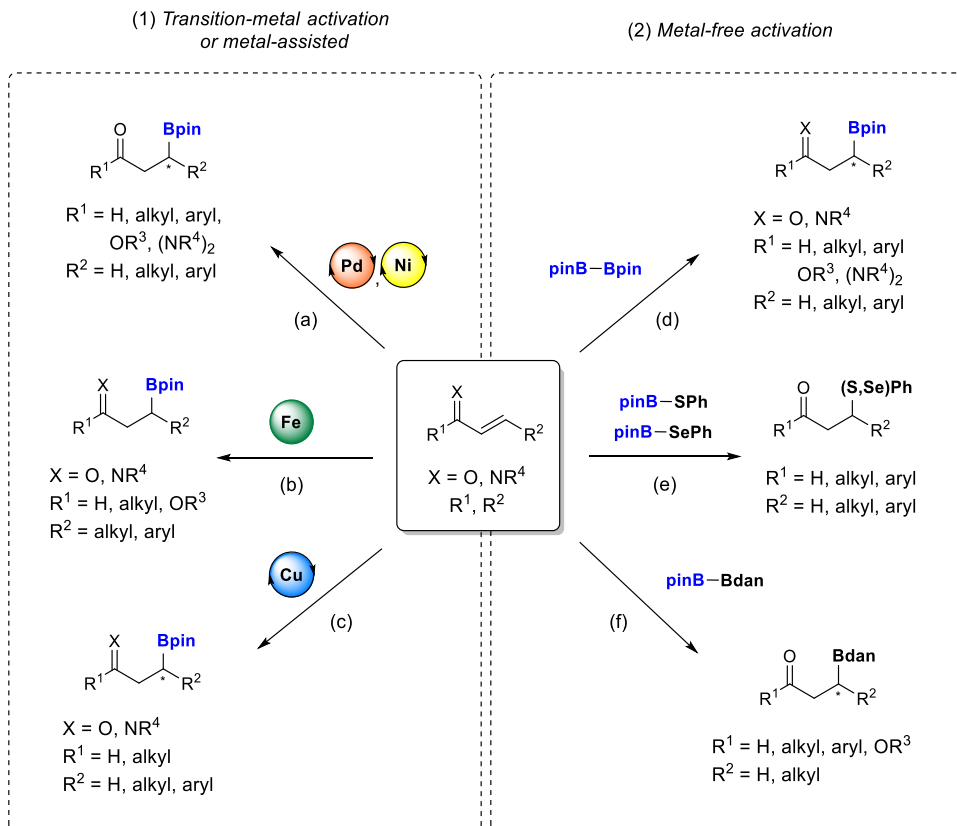
³² Bonet, A.; Solé, C.; Gulyás, H.; Fernández, E. *Chem. Asian. J.* **2011**, *6*, 1011.

³³ Selected examples: (a) Lillo, V.; Prieto, A.; Bonet, A.; Díaz-Requejo, M. M.; Ramírez, J.; Pérez, P. J.; Fernández, E. *Organometallics*, **2009**, *28*, 659. (b) Bonet, A.; Lillo, V.; Ramírez, J.; Díaz-Requejo, M. M.; Fernández, E. *Org. Biomol. Chem.* **2009**, *7*, 1533. (c) Solé, C.; Fernández, E. *Chem. Asian. J.* **2009**, *4*, 1790. (d) Solé, C.; Whiting, A.; Gulyás, H.; Fernández, E. *Adv. Synth. Catal.* **2011**, *353*, 376. (e) Solé, C.; Bonet, A.; De Vries, H. M.; De Vries, J. G.; Lefort, L.; Gulyás, H.; Fernández, E. *Organometallics* **2012**, *31*, 7855. (f) Calow, A. D. J.; Batsanov, A. S.; Fernández, E.; Solé, C.; Whiting, A. *Chem. Commun.* **2012**, *48*, 11401. (g) Calow, A. D. J.; Solé, C.; Whiting, A.; Fernández, E. *ChemCatChem* **2013**, *8*, 2233. (h) Calow, A. D. J.; Batsanov, A. S.; Pujol, A.; Solé, C.; Fernández, E.; Whiting, A. *Org. Lett.* **2013**, *15*, 4810.

³⁴ Selected examples: (a) Bonet, A.; Gulyás, H.; Fernández, E. *Angew. Chem. Int. Ed.* **2010**, *49*, 5130. (b) Pubill-Ulldemolins, C.; Bonet, A.; Bo, C.; Gulyás, H.; Fernández, E. *Chem. Eur. J.* **2012**, *18*, 1121. (c) Pubill-Ulldemolins, C.; Bonet, A.; Gulyás, H.; Bo, C.; Fernández, E. *Org. Biomol. Chem.* **2012**, *10*, 9677. (d) Calow, A. D. J.; Carbó, J. J.; Cid, J.; Fernández, E.; Whiting, A. *J. Org. Chem.* **2014**, *79*, 5163. (e) La Cascia, E.; Sanz, X.; Bo, C.; Whiting, A.; Fernández, E. *Org. Biomol. Chem.* **2015**, *13*, 1328.

³⁵ Selected examples: (a) Cid, J.; Carbó, J. J.; Fernández, E. *Chem. Eur. J.* **2014**, *20*, 3616. (b) Sanz, X.; Vogels, C. M.; Decken, A.; Bo, C.; Westcott, S. A.; Fernández, E. *Chem. Commun.* **2014**, *50*, 8420. (c) Civit, M. G.; Sanz, X.; Vogels, C. M.; Webb, J. D.; Geier, S. J.; Decken, A.; Bo, C.; Westcott, S. A.; Fernández, E. *J. Org. Chem.* **2015**, *80*, 2148.

formation in under milder reaction conditions and without the use of any transition-metal complexes.

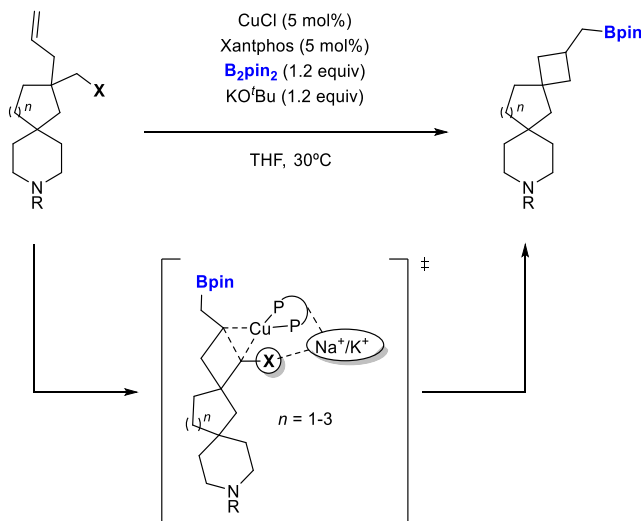


Scheme 1.18. Examples of conjugated borylations developed by Fernández's research group.

More recently, the group moved the interest towards the stereoselective borylative cyclization of different functionalized alkenes. The first example describes a Cu(I)-catalyzed borylative ring closing via C-C coupling of *O*- or *N*-containing polycyclic alkenyl halides (Scheme 1.19).³⁶ This strategy allows the direct preparation of [*m,n*]-spiroheterocyclic scaffolds (*m,n* = 3-5) with a pendant methylene boronate fragment that can be further functionalized giving access to

³⁶ Royes, J.; Ni, S.; Farré, A.; La Cascia, E.; Carbó, J. J.; Cuenca, A. B.; Fernández, E. *ACS Catal.* **2018**, *8*, 2833.

dispirocyclic molecular architectures, which are present in many biologically active compounds towards dementia or Alzheimer's disease.³⁷

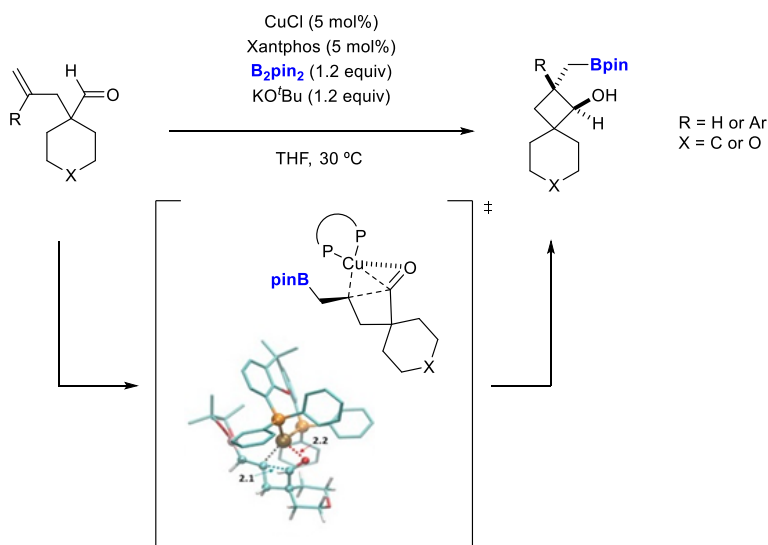


Scheme 1.19. Borylative ring closing of alkenyl halides.

Finally, as an extension of the previously mentioned method it has been demonstrated that γ -alkenyl aldehydes are suitable substrates to undergo consecutive borylcupration/C-C coupling reaction.³⁸ As it is shown in Scheme 1.20, chemo- and regioselective addition of Cu-B to the alkene occurs and engages a concomitant intramolecular 1,2-addition of the aldehyde functional group rendering the corresponding 2-(borylmethyl)cycloalkenols. In order to demonstrate the diastereoselectivity of the reaction, computational studies determined that during the intramolecular C-C coupling step, the aldehyde adopts an *anti*-disposition with respect to the borylmethyl unit as it is depicted in Scheme 1.20.

³⁷ (a) Voss, F.; Schunk, S.; Steinhagen, H. *RSC Drug Discov. Ser.* **2016**, 439. (b) Hügel, H. M.; De Silva, N. H.; Siddiqui, A.; Blanch, E.; Lingham, A. *Bioorg. Med. Chem.* **2021**, 43, 116270.

³⁸ Maza, R. J.; Royes, J.; Carbó, J. J.; Fernández, E. *Chem. Commun.* **2020**, 56, 5973.



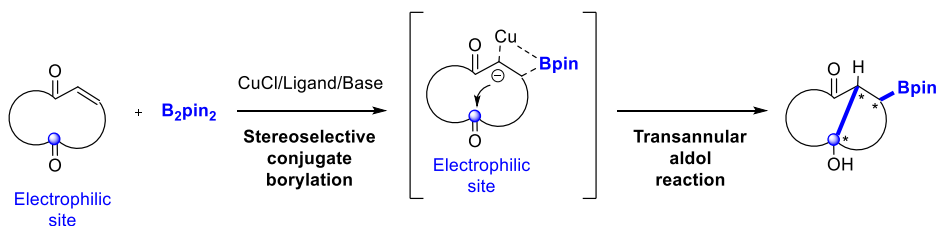
Scheme 1.20. Borylative ring closing of γ -alkenyl aldehydes.

Considering that copper catalysis has become one of the most powerful methods to stereoselectively install boron across diverse π -systems, the group believes that, this protocol also affords tremendous versatility enabled through difunctionalization of the π -system by the addition of an electrophile. There is still room to discover electrophiles to intercept catalytic intermediates in borylative difunctionalization strategies to open new synthetic approaches towards target compounds.

4. GENERAL OBJECTIVES

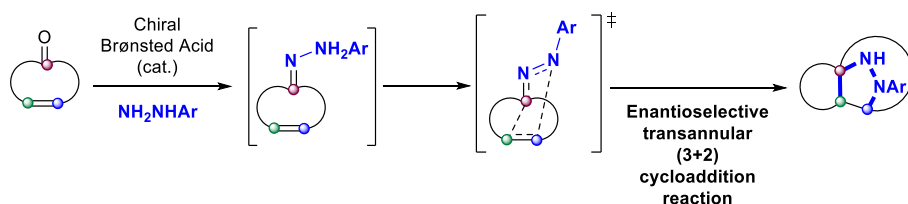
The aim of this work pretends to find synergies between the expertises of both participating research groups, by combining transannular reactivity with organoboron chemistry. In that sense, we focused our research on the development of *novel asymmetric catalytic transannular transformations* involving organoboron compounds for the stereoselective synthesis of complex structures in an operationally simple and environmentally friendly manner. The research was divided in three parts as follows:

In the first part of this work, we envisioned to survey the reactivity of cyclic ketoenones as suitable substrates to react with nucleophilic organoboron reagents. The key point of the reaction will be the formation of a copper enolate prompted by the initial conjugate addition of the boron-based nucleophile to the conjugated double bond. This particular scenario will favour the subsequent transannular aldol step in which the formed enolate will be trapped by the pendant electrophilic ketone through the incorporation of a chiral ligand on the Cu(I) centre and the overall process would result into a **pioneer stereoselective transannular borylative ring closing reaction** (Scheme 1.21). This methodology will allow the preparation of enantioenriched polycyclic organoboranes.



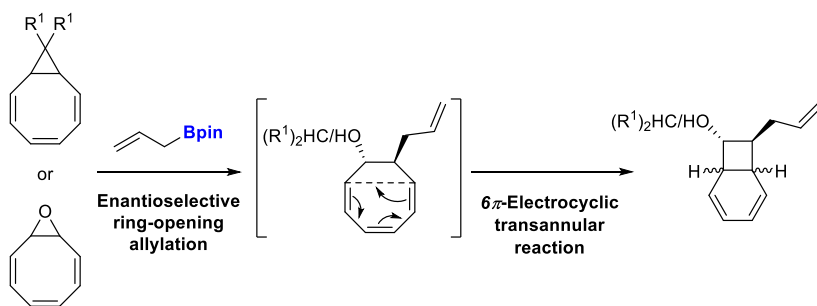
Scheme 1.21. Envisioned conjugate borylation/transannular aldol reaction.

In the second part, chiral Brønsted acid catalysis will be employed in order to promote an **enantioselective transannular (3+2) cycloaddition reaction between cycloalkenone hydrazones**. We propose the *in situ* generation of the hydrazone intermediate enabling the further formation of the corresponding 1,3-dipole in the presence of a chiral Brønsted acid catalyst that will react with the pending alkene moiety. This transformation would give access to enantioenriched polycyclic adducts with a bridged pyrazolidine skeleton (Scheme 1.22).



Scheme 1.22. Envisioned organocatalytic transannular (3+2) cycloaddition reaction of hydrazones.

Finally, in the third part of the presented research work we will be focused on studying the reactivity of strained cyclooctatetraene-derived epoxides or cyclopropanes as electrophiles with potential to undergo ring-opening with allylborane nucleophiles under Brønsted acid catalysis. We propose that initially an **enantioselective ring-opening through allylboration** would occur, taking place together with a desymmetrization process. Subsequently, the cyclooctatetraene scaffold is expected to undergo a **subsequent transannular 6 π -electrocyclic reaction** to afford enantioenriched functionalized bicyclo[4.2.0]octa-2,4-diene scaffolds (Scheme 1.23).



Scheme 1.23. Envisioned organocatalytic ring-opening allylation/transannular 6 π -electrocyclization.

2

2

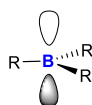
Catalytic Stereoselective Borylative Transannular Reactions

1. INTRODUCTION	39
1.1. Nucleophilic organoboron chemistry.....	39
1.2. Stereoselective borylative ring closing of functionalized alkenes	48
2. SPECIFIC OBJECTIVES AND WORK PLAN	54
3. RESULTS AND DISCUSSION	57
3.1. Proof of concept.....	57
3.2. Optimization of the reaction conditions.....	58
3.3. Scope of the diastereoselective Cu/dppf borylative transannular reaction	61
3.4. Enantioselective Cu(I)-catalyzed borylative transannular reaction.....	68
4. CONCLUSIONS	74

1. INTRODUCTION

1.1. Nucleophilic organoboron chemistry

The particular electronic structure of B in organoboron compounds justifies the electrophilic character of trivalent organoboron compounds which have been traditionally considered to act as Lewis acids (Figure 2.1). For this reason, their reactivity is based on interacting with electron-rich organic molecules generating neutral or anionic tetravalent organoboron compounds, which can behave as nucleophiles.¹



Trivalent organoboron compound
(BR₃)

Figure 2.1. Structure of organoboronboron compounds.

In the last century, organoboron chemistry has gained interest in the organic synthetic field, being illustrated by two Nobel prizes: Brown (1979, together with Wittig) and Suzuki (2010, with Heck and Negishi). Both, Brown and Suzuki, contributed to the development of organoboron compounds as versatile building blocks in organic chemistry.^{2,3} In that context, the innovation on synthetic methodologies to generate C-B bonds is of major concern because it represents an important and interesting source of functionality as they can be further transformed into new C-O, C-N, C-X and C-C bonds in a selective way.⁴ One of the earliest attempts to prepare organoboranes, from diboron reagents, was originally

¹ (a) Suginome, M. *J. Synth. Org. Chem. Jpn.* **2007**, 65, 11, 1048. (b) Cid, J.; Gulyás, H.; Carbó, J. J.; Fernández, E. *Chem. Soc. Rev.* **2012**, 41, 3558.

² (a) Miyaura, N.; Suzuki, A. *Chem. Rev.* **1995**, 95, 2457. (b) Suzuki, A. *Chem. Commun.* **2005**, 4759. (c) Miyaura, N. (2008). *Metal-Catalyzed Cross-Coupling Reactions of Organoboron Compounds with Organic Halides*, Meijere, A.; Diederich, F.; 2nd edition, Eds.; Wiley-VCH, pp. 41-123. (d) Lennox, J. J.; Lloyd-Jones, G. C. *Chem. Soc. Rev.* **2014**, 43, 412.

³ Carreras, J.; Caballero, A.; Pérez, P. J. *Chem. Asian. J.* **2019**, 14, 329.

⁴ (a) Neeve, E. C.; Geier, S. J.; Mkhaid, I. A. I.; Westcott, S. A.; Marder, T. B. *Chem. Rev.* **2016**, 16, 9091. (b) Cuenca, A. B.; Shishido, R.; Ito, H.; Fernández, E. *Chem. Soc. Rev.* **2017**, 46, 415.

done by the group of Schlesinger and co-workers through the direct addition of a tetra(halo)diboron reagent to alkenes (Figure 2.2a).⁵ Despite the fact that the reaction took place efficiently without any catalyst, the inherent instability of the tetra(halo)diboranes implied the development of tetra(alkoxy)diboranes and tetra(amino)diboron reagents (Figure 2.2b).

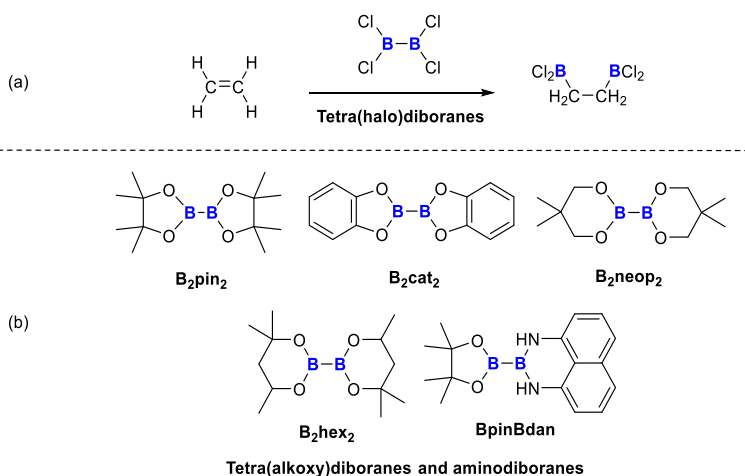


Figure 2.2. Diboron reagents scope.

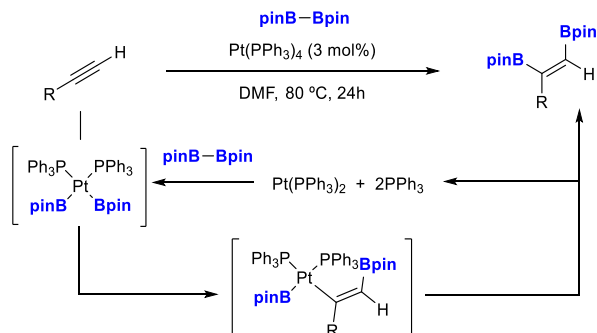
However, these diboron reagents are less reactive than the corresponding tetra(halo)diboranes, since there is a subtle π donation from the lone pair of O and N substituents to the empty p -orbital of the boron,¹ diminishing its Lewis acidity and thus, making its direct addition to unsaturated substrates less efficient. For that reason, an external activation of the reagent is needed in order to weak the B-B bond strength and perform the straightforward catalytic borylation reaction.

In that sense, transition metal complexes were postulated to potentially activate the B-B bond. Miyaura and co-workers⁶ reported the first example in which they postulated the cleavage of the B-B bond in bis(pinacolato)diboron (B_2pin_2) by

⁵ (a) Urry, G.; Wartik, T.; Moore, R. E.; Schlesinger, H. I. *J. Am. Chem. Soc.* **1954**, *76*, 5299. (b) Pubill-Ulldemolins, C.; Fernández, E.; Bo, C.; Brown, J. M. *Org. Biomol. Chem.* **2015**, *13*, 9619.

⁶ (a) Ishiyama, T.; Matsuda, N.; Miyaura, N.; Suzuki, A. *J. Am. Chem. Soc.* **1993**, *115*, 11018. (b) Ishiyama, T.; Matsuda, N.; Murata, N.; Ozawa, F.; Suzuki, A.; Miyaura, N. *Organometallics*, **1996**, *15*, 713.

oxidative addition to a Pt complex, generating the catalytic species B-Pt-B, which was then added to a terminal alkyne, resulting to be the first transition-metal-catalyzed 1,2-diboration reaction (Scheme 2.1). In this particular case, the B-B bond activation has been suggested to occur through the homolytic B-B bond cleavage, due to the easy oxidative addition on metals with low oxidation states. The coordination and insertion of the alkyne to B-Pt-B species generates an alkenyl-platinum intermediate that follows a reductive elimination, affording the desired 1,2-diborated species and regenerating the Pt complex (Scheme 2.1). The catalytic systems are normally modified with basic ligands, such as PPh_3 , to become efficient catalytic systems towards diboration of alkenes, allenes and dienes giving the corresponding diborated products via *syn*-addition pathway.⁷

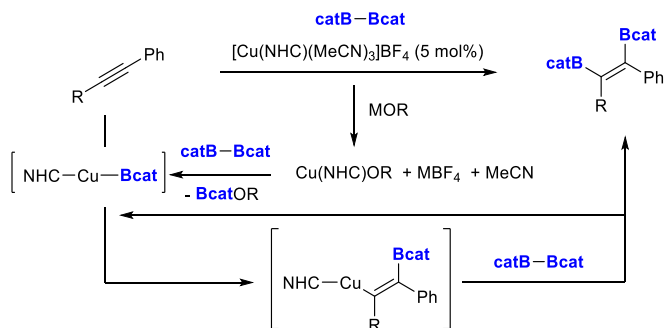


Scheme 2.1. Catalytic cycle for the Pt-catalyzed diboration of alkynes.

Alternative transition metals, such as Cu(I) complexes, do not involve a change on the oxidation state of the metal center during the activation of the diborane. Instead, a σ -bond metathesis step is considered to take place resulting in a heterolytic cleavage of the B-B bond, as it is shown in Scheme 2.2 for bis(catecholato)diboron (B_2cat_2). This situation generates the Cu-Bcat moiety and B-OR as byproduct, becoming the driving force of the reaction. The newly formed Cu-B unit interacts with unsaturated substrates, such as alkynes, promoting the 1,2-addition, and a second σ -bond metathesis is needed to release the desired

⁷ Lesley, G.; Nguyen, P.; Taylor, N. J.; Marder, T. B.; Scott, A. J.; Clegg, W.; Norman, N. C. *Organometallics* **1996**, *15*, 5137.

product and regenerate the key active species.⁸ The catalytic systems are normally modified with basic ligands, such as N-heterocyclic carbenes (NHC), giving the corresponding diborated products as a result of a *syn*-addition pathway.



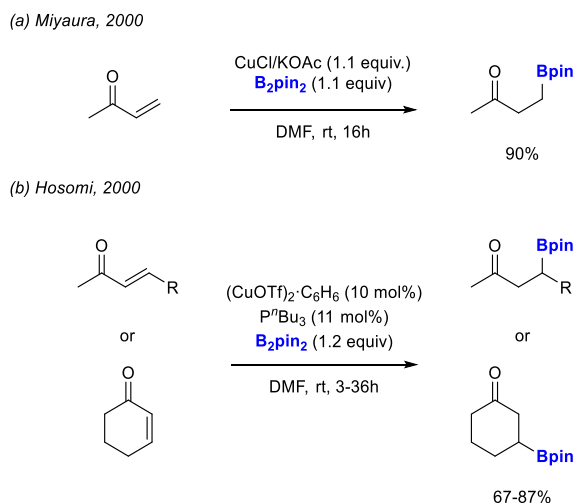
Scheme 2.2. Catalytic cycle for the Cu-catalyzed diboration of alkynes.

Nevertheless, if we move from non-activated unsaturated substrates to electron poor unsaturated substrates, such as α,β -unsaturated carbonyl compounds, the 1,4-addition of the Cu-B moiety is preferred. This methodology gives access to β -borylated carbonyl compounds,⁹ which have shown to be valuable building blocks for synthetic chemistry since they can be direct precursors to obtain the corresponding β -hydroxyl carbonyl compounds, which are difficult to prepare selectively through the direct conjugate addition of water or alcohols.

⁸ (a) Westcott, S.A. & Fernández, E. (2015). *Singular Metal Activation of Diboron Compounds. Advances in Organic Chemistry*; Academic Press: Cambridge. (b) Laitar, D. S.; Mueller, P.; Sadighi, J. P. *J. Am. Chem. Soc.* **2005**, *127*, 17196. (c) Laitar, D. S.; Tsui, E. Y.; Sadighi, J. P. *J. Am. Chem. Soc.* **2006**, *128*, 11036. (d) Lillo, V.; Fructos, M. R.; Ramírez, J.; Braga, A. A. C.; Maseras, F.; Díaz-Requejo, M. M.; Perez, P. J.; Fernández, E. *Chem. Eur. J.* **2007**, *13*, 2614.

⁹ (a) Lillo, V.; Bonet, A.; Fernández, E. *Dalton Trans.* **2009**, 2899. (b) Schiffner, J. A.; Müther, K.; Oestreich, M. *Angew. Chem. Int. Ed.* **2010**, *49*, 1194. (c) Hartmann, E.; Devendra, J. V.; Oestreich, M. *Chem. Commun.* **2011**, 47, 7917. (d) Hu, J.; Ferger, M.; Shi, Z.; Marder, T. B. *Chem. Soc. Rev.* **2021**, *50*, 13129. (e) Bose, S. K.; Mao, L.; Kuehn, L.; Radius, U.; Nekvinda, J.; Santos, W. L.; Westcott, S. A.; Steel, P. G.; Marder, T. B. *Chem. Rev.* **2021**, *121*, 13238. (f) Das, K. K.; Mahato, S.; Hazra, S.; Panda, S. *Chem. Rec.* **2022**, *22*, e202100290.

The basic concepts for the Cu(I)-catalyzed conjugate borylation reactions were established after the seminal reports by Miyaura¹⁰ and Hosomi¹¹ in 2000 (Scheme 2.3). Miyaura's approach proposed that the σ -bond metathesis step from B₂pin₂ to Cu(I) salts was the key step for the reaction (Scheme 2.3a) whereas the Hosomi's approach was able to demonstrate that the metal salt itself does not consume the diborane, in the absence of the α,β -unsaturated substrate, contrarily to the aforementioned Pt(0)-catalyzed activation strategy (Scheme 2.3b). Therefore, the coordination of a diphosphine ligand to the copper might accelerate the reaction, preventing the aggregation of the metal salt forming Cu(I) clusters, and affording the corresponding 1,4-addition products efficiently.



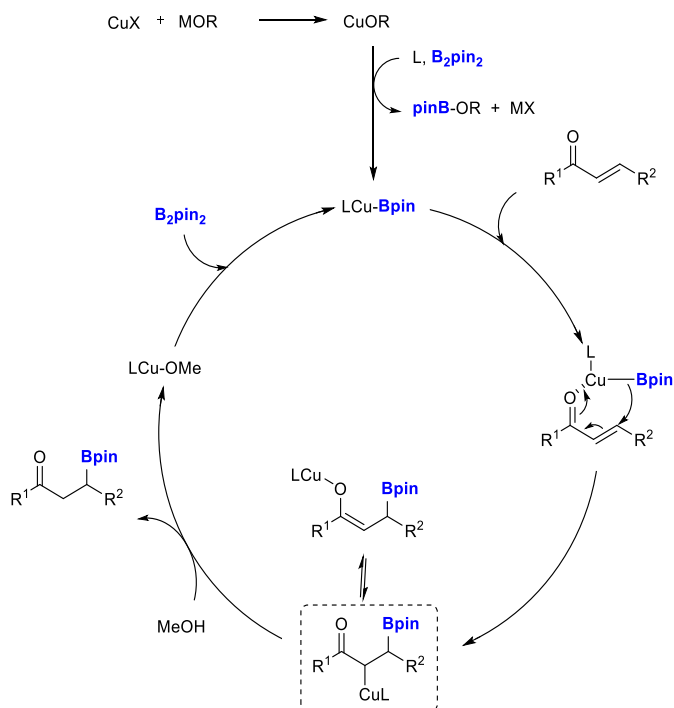
Scheme 2.3. Early examples of Cu(I)-catalyzed conjugate borylation reactions of enones, by complementary works by Miyaura and Hosomi.

Some years later, Yun and co-workers also contributed significantly to the development of the field by disclosing the effect of alcohol additives to the reaction outcome. They could observe that reaction rates were dramatically accelerated by the addition of MeOH, which was supposed to react with the organocopper species,

¹⁰ (a) Takahashi, K.; Isiyama, T.; Miyaura, N. *Chem. Lett.* **2000**, 982. (b) Takahashi, K.; Isiyama, T.; Miyaura, N. *J. Organomet. Chem.* **2001**, 625, 47.

¹¹ Ito, H.; Yamanaka, H.; Tateiwa, J.-I.; Hosomi, A. *Tetrahedron Lett.* **2000**, 41, 6821.

affording the protonated product and the corresponding copper methoxide (Cu-OMe), which after σ -bond metathesis with the diborane, eventually regenerates the active catalytic species (Scheme 2.4).¹²



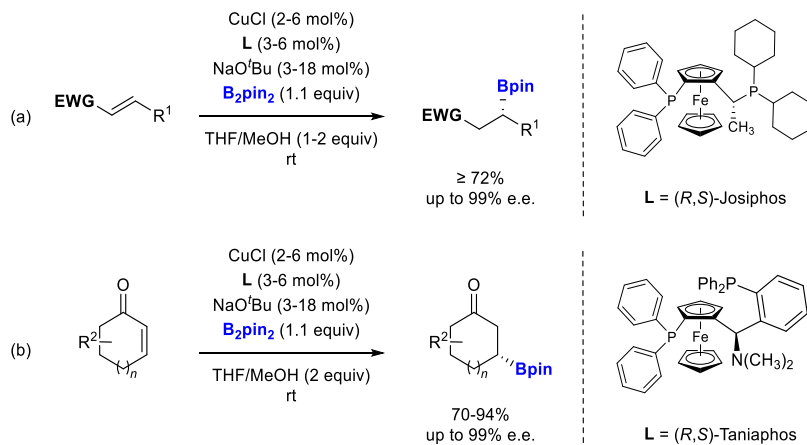
Scheme 2.4. Catalytic cycle for the Cu(I)-catalyzed conjugate borylation of α,β -unsaturated ketones.

The same research group also developed the asymmetric β -boration of different α,β -unsaturated compounds (Scheme 2.5). In all cases, the stereochemistry of the reaction was controlled using chiral Josiphos-type ligand, which showed to be the optimal one for the enantioselective conjugated borylation of nitriles^{13a}, esters^{13a}, ketones^{13b} and amides^{13c} (Scheme 2.5a). The reaction also tolerated cyclic α,β -

¹² (a) Mun, S.; Lee, J.-E.; Yun, J. *Org. Lett.* **2006**, *8*, 21, 4887. (b) DFT-calculations for the mechanistic understanding: Dang, L.; Lin, Z.; Marder, T. B. *Organometallics* **2008**, *27*, 4443.

¹³ (a) Lee, J.-E.; Yun, J. *Angew. Chem. Int. Ed.* **2008**, *47*, 145. (b) Sim, H.-S.; Feng, X.; Yun, J. *Chem. Eur. J.* **2009**, *15*, 1939. (c) Chea, H.; Sim, H.-S.; Yun, J. *Adv. Synth. Catal.* **2009**, *351*, 855.

unsaturated carbonyl compounds as starting materials (Scheme 2.5b). However, the previously mentioned chiral ligand was not as efficient in terms of enantiocontrol and Cu(I)-(*R,S*)Taniaphos catalytic system was used instead.¹⁴

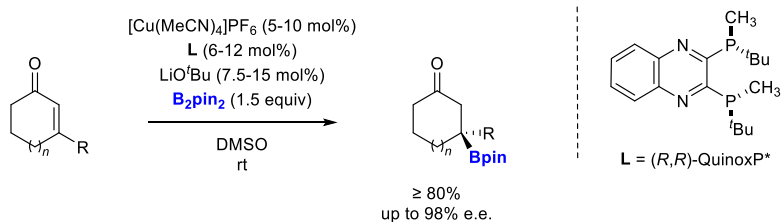


Scheme 2.5. Cu(I)-catalyzed enantioselective borylation of α,β -unsaturated carbonyl substrates.

The next challenge was accomplished by Shibasaki and co-workers after developing an efficient catalytic system for the enantioselective conjugate borylation of β -substituted cyclic enones (Scheme 2.6).¹⁵ Shibasaki's approach used $[\text{Cu}(\text{MeCN})_4]\text{PF}_6$ as precursor of catalyst and LiO^tBu as base, in the absence of MeOH and contrarily to Yun's catalytic system, they proposed that the *in situ* formation of LiPF_6 was the driving force of the reaction justifying the lack of protic solvents used.

¹⁴ Feng, X.; Yun, J. *Chem. Commun.* **2009**, 6577.

¹⁵ Chen, I.-H.; Yin, L.; Itano, W.; Kanai, M.; Shibasaki, M. *J. Am. Chem. Soc.* **2009**, *131*, 11664.



Scheme 2.6. Cu(I)-catalyzed enantioselective conjugate borylation by Shibasaki.

In 2009, Fernández and co-workers¹⁶ extended the library of suitable chiral ligands¹⁷ by demonstrating the potential of *N*-heterocyclic carbenes (NHCs) in copper-catalyzed asymmetric β -borylation of α,β -unsaturated carbonyl compounds.^{18,19} As it is shown in Scheme 2.7, the β -borylation of different esters and aldehydes takes place regioselectively at the β -position originating therefore a stereogenic center with the appropriate chiral copper catalytic system.

One year later, and inspired by the pioneer work of Fernández and co-workers, Hoveyda²⁰ reported the first example of catalytic enantioselective conjugate borylation to trisubstituted alkenes of acyclic α,β -carboxylic esters using C_1 -symmetric Cu-based *N*-heterocyclic carbene complex depicted in Scheme 2.7. Different alkyl and aryl substituted esters were efficiently borylated with high yields and enantioselectivities generating a B-substituted quaternary carbon.

¹⁶ Lillo, V.; Prieto, A.; Bonet, A.; Díaz-Requejo, M. M.; Ramírez, J.; Pérez, P. J.; Fernández, E. *Organometallics*, **2009**, *28*, 659.

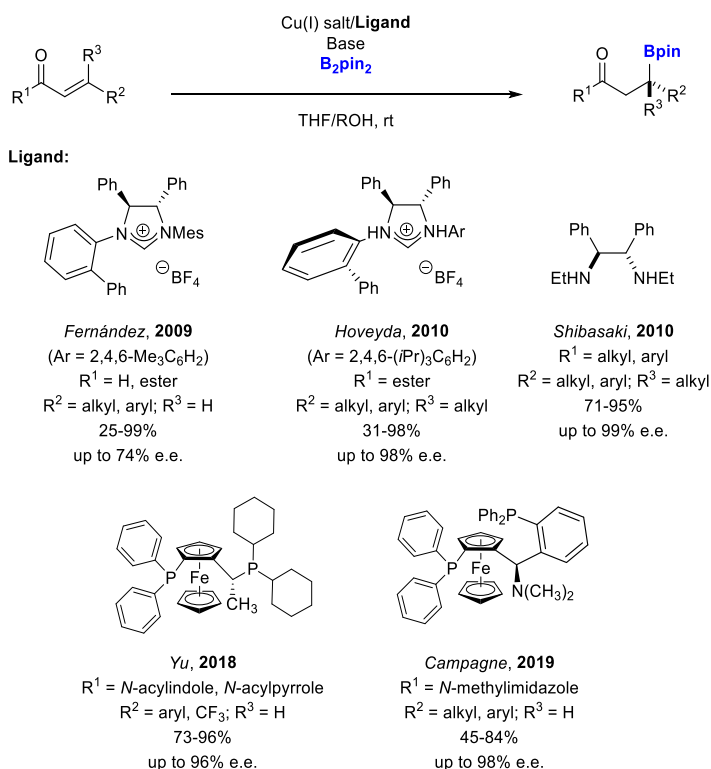
¹⁷ For other reported examples using phosphorous- and nitrogen-containing ligand: (a) Fleming, W. J.; Müller-Bunz, H.; Lillo, V.; Fernández, E.; Guiry, P. J. *Org. Biomol. Chem.* **2009**, *7*, 2520. (b) Chen, I.-H.; Kanai, M.; Shibasaki, M. *Org. Lett.* **2010**, *12*, 4098.

¹⁸ For others examples reported later using NHCs: (a) Hirsch-Weil, D.; Abboud, K. A.; Hong, S. *Chem. Commun.* **2010**, *46*, 7525. (b) Park, J. K.; Lackey, H. H.; Rexford, M. D.; Kovnir, K.; Shatruk, M.; McQuade, D. T. *Org. Lett.* **2010**, *12*, 5008.

¹⁹ A selected review about NHC-Copper complexes in enantioselective synthesis of C-C, C-B, C-H and C-Si bonds: Hoveyda, A. H.; Zhou, Y.; Shi, Y.; Brown, K.; Wu, H.; Torker, S. *Angew. Chem. Int. Ed.* **2020**, *59*, 21304

²⁰ (a) Lee, K.-S.; Zhugralin, A. R.; Hoveyda, A. H. *J. Am. Chem. Soc.* **2009**, *131*, 7253. (Correction: *J. Am. Chem. Soc.* **2010**, *132*, 12766). (b) O'Brien, J. M.; Lee, K.-S.; Hoveyda, A. H. *J. Am. Chem. Soc.* **2010**, *132*, 10630.

More recent examples have been reported reinforcing the capability of ferrocenyl-type ligands, such as Josiphos and Taniaphos, for the efficient control on the enantioselectivity of these type of transformations. As it is summarized in Scheme 2.7, Yu²¹ and Campagne²² proposed different type of Michael acceptors as suitable starting materials for the asymmetric Cu(I)-catalyzed β -borylation reaction obtaining in all cases chiral organoboranes with good to excellent yields and total stereocontrol.



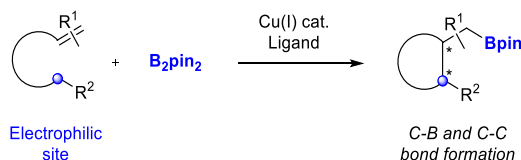
Scheme 2.7. Library of suitable ligands for the Cu-catalyzed asymmetric conjugate borylation reactions.

²¹ (a) Jiang, Q.; Guo, T.; Yu, Z. *J. Org. Chem.* **2017**, *82*, 1951. (b) Jiang, Q.; Guo, T.; Gao, R.; Wang, Q.; Lou, J.; Yu, Z. *J. Org. Chem.* **2018**, *83*, 7981.

²² Lauberteaux, J.; Crévisy, C.; Baslé, O.; Marcia de Figueiredo, R.; Mauduit, M.; Campagne, J.-M. *Org. Lett.* **2019**, *21*, 6, 1872.

1.2. Stereoselective borylative ring closing of functionalized alkenes

Borylative ring closing reactions of functionalized alkenes bearing an internal electrophile are complementary strategies to efficiently obtain carbocyclic architectures. There are many examples in the literature involving borylative cyclizations using transition-metal catalysis such as Pd, Au, Rh or Ni.²³ However, copper-catalysis has been less studied. As it is shown in Scheme 2.8, most of the reported reactions take place through borylcupration of the alkene, followed by intramolecular C-C coupling, contributing essentially to the 1,2-carboboration sequence. The nature of the electrophilic site for the intramolecular cyclization are mainly carbonyl-based functionality, imine or alkylhalides.²⁴



Scheme 2.8. Stereoselective intramolecular 1,2-carboboration.

After some relevant precedents on conjugate borylation and subsequent intermolecular aldol sequence, involving cyclic and acyclic α,β -unsaturated carbonyl compounds,²⁵ the first enantioselective copper-catalyzed intramolecular version was published by Lam and co-workers in 2012.²⁶ In this work, the group described the straightforward formation of four contiguous stereocenters, two of them became tetrasubstituted, by the direct enantioselective domino conjugate borylation/aldol cyclization sequence. When the corresponding enone dione shown in Scheme 2.9 reacts with bis(pinacolato)diboron under the specified chiral Cu(I)

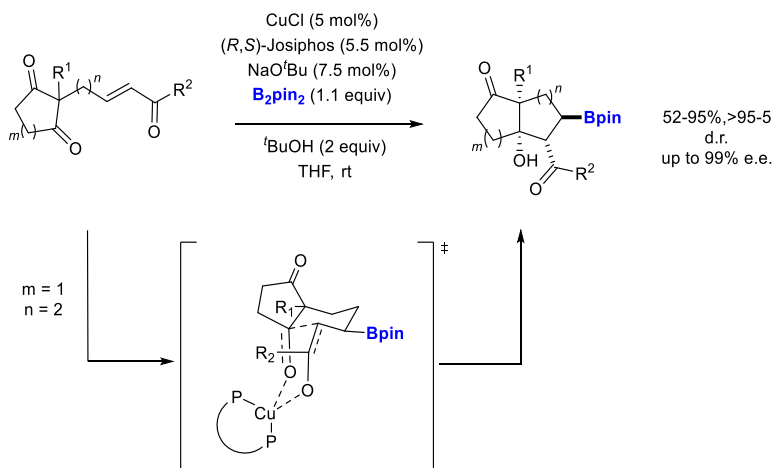
²³ For a review on this concept see: Buñuel, E.; Cárdenas, D. *J. Chem. Eur. J.* **2016**, *22*, 5446.

²⁴ For a review, see: Kubota, K.; Iwamoto, H.; Ito, H. *Org. Biomol. Chem.* **2017**, *15*, 285. For some examples, see: (a) Ito, H.; Toyoda, T.; Sawamura, M. *J. Am. Chem. Soc.* **2010**, *132*, 5990. (b) Kubota, K.; Yamamoto, E.; Ito, H. *J. Am. Chem. Soc.* **2013**, *135*, 2635. (c) Zuo, Y.-J.; Chang, X.-T.; Hao, Z.-M.; Zhong, C.-M. *Org. Biomol. Chem.* **2017**, *15*, 6323. (d) Royes, J.; Ni, S.; Farré, A.; La Cascia, E.; Carbó, J. J.; Cuenca, A. B.; Fernández, E. *ACS Catal.* **2018**, *8*, 2833.

²⁵ (a) Bocknack, B. M.; Wang, L.-C.; Krische, M. J. *Proc. Natl. Acad. Sci. USA* **2004**, *101*, 5421. (b) Welle, A.; Cirriez, V.; Riant, O. *Tetrahedron* **2012**, *68*, 3435.

²⁶ Burns, A. R.; González, J. S.; Lam, H. W. *Angew. Chem. Int. Ed.* **2012**, *51*, 10827.

catalytic system, the regioselective formation of the new C-B bond occurs at the β -position of the conjugated system, generating the first stereogenic center. Once the stereoselectivity has been determined, the resulting copper enolate is then trapped by the pendant ketone to deliver the bicyclic final product containing the multiple stereocenters with high yields, diastereo- and enantioselectivities. The diastereoselectivity of the reaction is rationalized by the suggested formation of a (*Z*)-enolate in the chairlike Zimmerman-Traxler-type transition-state.²⁷



Scheme 2.9. Enantioselective Cu(I)-catalyzed borylative aldol cyclization.

Inspired by the previous examples reported by Ito and Brown,²⁸ the group of Lautens²⁹ reported a diastereo- and enantioselective borylcupration to synthesize enantioenriched cyclobutanols, whose synthesis still remains largely unexplored and the known approaches to prepare them still relies mainly on desymmetrization strategies.³⁰ As an alternative to the limited synthetic scenario, Lautens and co-workers launched the use of γ - δ unsaturated ketones, as model systems, for the enantioselective copper-catalyzed borylation. The optimal catalytic system for the

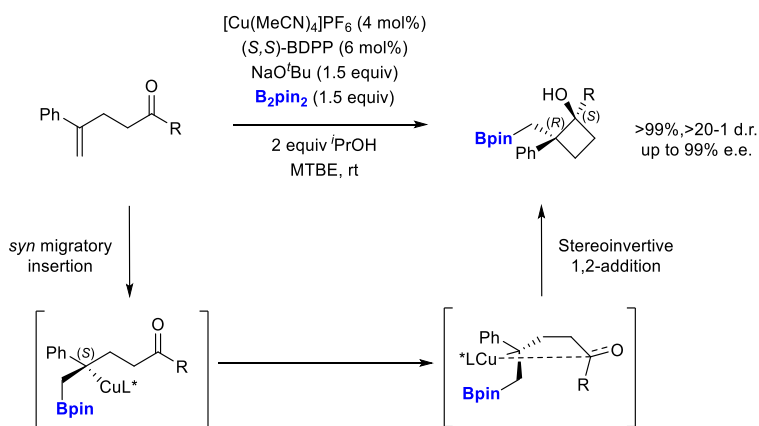
²⁷ Zimmerman, H. E.; Traxler, M. D. *J. Am. Chem. Soc.* **1957**, *79*, 1920.

²⁸ (a) Yamamoto, E.; Kojima, R.; Kubota, K.; Ito, H. *Synlett* **2015**, *26*, 272. (b) Huang, Y.; Smith, K. B.; Brown, M. K. *Angew. Chem. Int. Ed.* **2017**, *56*, 13314.

²⁹ Whyte, A.; Mirabi, B.; Torelli, A.; Prieto, L.; Bajohr, J.; Lautens, M. *ACS Catal.* **2019**, *9*, 9253.

³⁰ Guisán-Ceinos, M.; Parra, A.; Martín-Heras, V.; Tortosa, M. *Angew. Chem. Int. Ed.* **2016**, *55*, 6969.

asymmetric borylcupration of 1,1-disubstituted styrenes, required (*S,S*)-BDPP, as the chiral ligand. In this context, the first step consists in an enantioselective *syn*-migratory insertion of the copper boryl species with the styrene moiety to give the chiral benzylic copper species (Scheme 2.10). Authors suggest that the new (*S*)-benzylic stereocenter undergoes a stereoinvertive 1,2-addition to the proximally tethered ketone. Regarding the diastereoselectivity of the process, the authors suggested that it might be determined in the cyclization step by adopting preferentially the conformation where steric interactions are reduced.

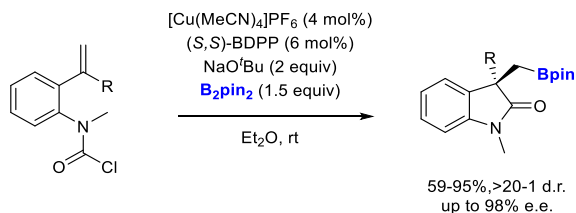


Scheme 2.10. Enantioselective synthesis of boryl-functionalized cyclobutanols.

This reactivity is not limited to ketones as internal electrophilic sites. The same research group developed an enantioselective copper-catalyzed intramolecular borylacylation to obtain chiral borylated 3,3-disubstituted oxindoles using carbamoyl halides as internal electrophiles.³¹ As it is depicted in Scheme 2.11, the reaction takes place through an initial stereocontrolled borylcupration of styrene using (*S,S*)-BDPP as chiral ligand and leading to the generation of a benzylic organocopper species. This intermediate is further trapped by the tethered carbamoyl chloride giving access to highly valuable chiral 3,3-disubstituted

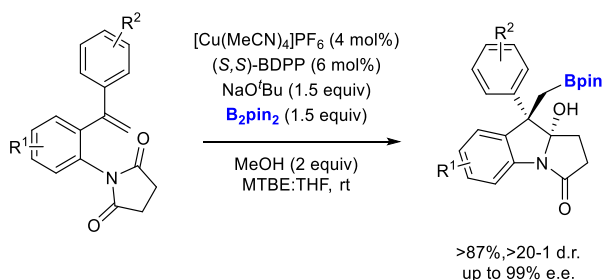
³¹ Whyte, A.; Burton, K. I.; Zhang, J.; Lautens, M. *Angew. Chem. Int. Ed.* **2018**, *57*, 13927.

oxindole scaffolds with good yields, diastereoselectivity and high levels of enantioinduction.



Scheme 2.11. Enantioselective intramolecular copper-catalyzed borylacylation.

The same group extended this methodology to the cyclization with other carbonyl-based electrophilic moieties, such as cyclic imides.³² The work demonstrates the utility of these substrates to give a direct access to polycyclic boron-containing indolines, via enantioselective borylcupration/1,2-imide addition cascade reaction (Scheme 2.12).³³

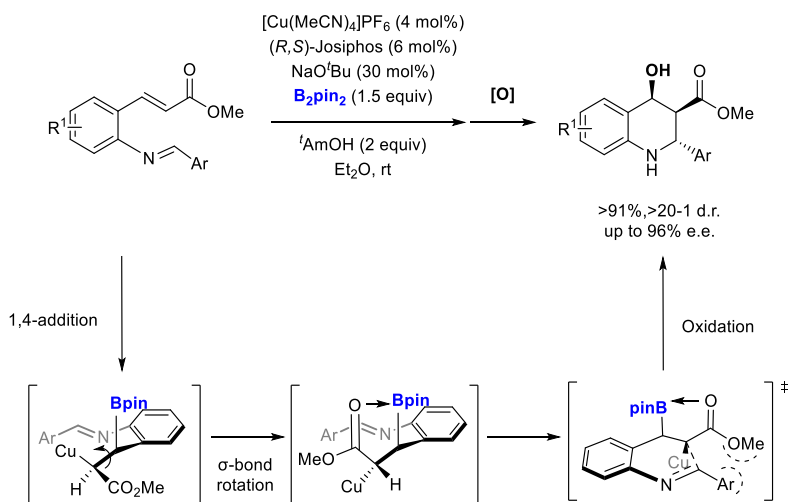


Scheme 2.12. Enantioselective copper-catalyzed borylative cyclization of imides.

³² For previous non enantioselective examples of imide cyclizations, see: (a) Lee, J.; Ha, J. D.; Cha, J. K. *J. Am. Chem. Soc.* **1997**, *119*, 8127. (b) Santra, S.; Masalov, N.; Epstein, O. L.; Cha, J. K. *Org. Lett.* **2005**, *7*, 5901. (c) Hoyer, T. R.; Dvornikovs, V.; Sizova, E. *Org. Lett.* **2006**, *8*, 5191. (d) Shi, S.; Szostak, M. *Org. Lett.* **2015**, *17*, 5144. (e) Shi, S.; Lalancette, R.; Szostak, M. *Synthesis*, **2016**, *48*, 1825.

³³ Whyte, A.; Torelli, A.; Mirabi, B.; Lautens, M. *Org. Lett.* **2019**, *21*, 8373.

Finally, it has been recently demonstrated that in addition to carbonyl-based moieties, imines can also act as internal electrophiles in an efficient way. In this particular work, Lautens and co-workers applied the use of different Michael acceptors, such as the one depicted below in Scheme 2.13, as suitable precursors for the synthesis of chiral tetrahydroquinolines containing four contiguous stereocenters.³⁴ It is noteworthy to mention, however, that in this case a chiral Josiphos-type ligand is selected as the optimal ligand to modify the copper catalytic system, in order to perform the conjugated borylation with high control of the stereochemistry. Therefore, both the copper reactive species and the boryl moiety are added towards the same face of the conjugated double bond and a later rotation occurs around the corresponding sigma bond. This is favoured due to the oxophilic nature of the boron atom leading to the formation of a five-membered cycle that stabilizes the formed enolate. At that point, the authors suggested that the high diastereoselectivity of the transformation could arise from possible interactions between the present aryl group on the imine and the pendant copper, which is still bounded to the substrate.



Scheme 2.13. Enantioselective copper-catalyzed borylation/Mannich cyclization of imines.

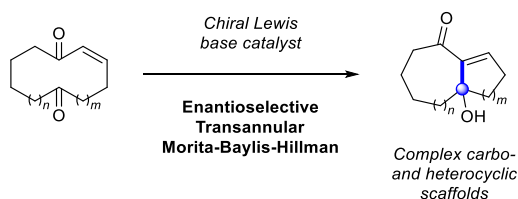
³⁴ Larin, E. M.; Loup, J.; Polishchuk, I.; Ross, R. J.; Whyte, A.; Lautens, M. *Chem. Sci.* **2020**, *11*, 5716.

In summary, the selected examples illustrate the potential of borylative cyclizations for the preparation of stereodefined polycyclic organoboranes. Nevertheless, this field is still under development and several reports have appeared afterwards demonstrating the synthetic applicability of the envisioned tandem borylcupration-cyclizations pathways.³⁵

³⁵ Recent examples of borylative cyclizations: (a) Zhang, G.; Cang, A.; Wang, Y.; Li, Y.; Xu, G.; Zhang, Q.; Xiong, T.; Zhang, Q. *Org. Lett.* **2018**, *20*, 1798. (b) Zheng, P.; Han, X.; Hu, J.; Zhao, X.; Xu, T. *Org. Lett.* **2019**, *21*, 6040. (c) Liu, B.; Qiu, H.; Chen, X.; Li, W.; Zhang, J. *Org. Chem. Front.* **2020**, *7*, 2492. (d) Dherbassy, Q.; Manna, S.; Shi, C.; Prasitwatcharakorn, W.; Crisenza, G. E. M.; Perry, G. J. P.; Procter, D. J. *Angew. Chem. Int. Ed.* **2021**, *60*, 14355. (e) De Jesús Cruz, P.; Crawford, E. T.; Liu, S.; Johnson, J. S. *J. Am. Chem. Soc.* **2021**, *143*, 16264. (f) Jadhav, S. B.; Dash, S. R.; Maurya, S.; Nanubolu, J. B.; Vanka, K.; Chegondi, R. *Nat. Commun.* **2022**, *13*, 854. (g) Khalse, L. D.; Gorad, S. S.; Ghorai, P. *Org. Lett.* **2022**, *24*, 7566.

2. SPECIFIC OBJECTIVES AND WORK PLAN

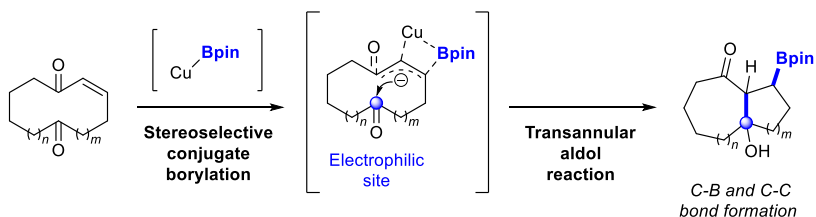
Borylative ring closing reaction of activated alkenes, bearing an internal electrophilic site, stands as an efficient strategy for the synthesis of carbocycles. Besides, transannular reactivity has appeared as an unconventional strategy to directly obtain polycyclic carbo- and heterocyclic architectures for the generation of molecular complexity. In fact, the Vicario's research group has been able to develop an efficient and straightforward methodology to access bicyclic carbo- and heterocyclic scaffolds through a transannular Morita-Baylis-Hillman reaction in an enantioselective fashion (Scheme 2.14).³⁶



Scheme 2.14. Previous precedents of the group.

In this sense, and combining the previously mentioned concepts on nucleophilic boron chemistry, we encouraged to survey medium and large cyclic ketoenones as potential substrates to undergo a **Cu-catalyzed stereoselective transannular borylative reaction**. Our proposal is based on the captivating feature of using simple diboron reagents, that would be catalytically activated by a Cu(I) salt, to generate the Cu-Bpin catalytic system where Bpin has a nucleophilic character. This species would further react with the conjugated olefin of the ketoenone cyclic substrate by the formation of a copper enolate. Finally, as it is well-established by enolate chemistry, the alkylcuprate intermediate would be able to react with the pendant electrophilic ketone resulting into a pioneer transannular borylative ring closing reaction (Scheme 2.15).

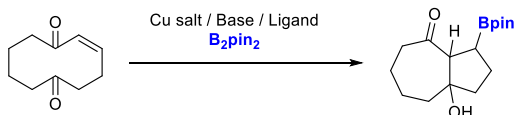
³⁶ Mato, R.; Manzano, R.; Reyes, E.; Carrillo, L.; Uria, U.; Vicario, J. L. *J. Am. Chem. Soc.* **2019**, *141*, 9495.



Scheme 2.15. Specific objective of the project.

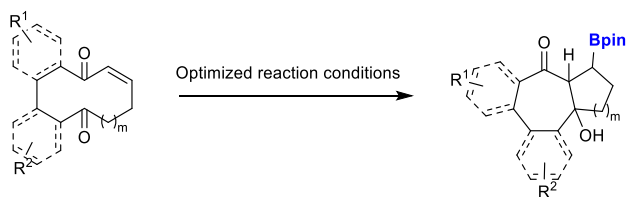
In order to achieve the stated objective, the following work plan was designed:

1. *Proof of concept and optimization of the reaction:* Evaluation of the reaction viability under the catalytic system based on Cu/ligand/base to promote both the activation of the diboron reagent and efficiently execute the borylcupration/cyclization steps in a model substrate (Scheme 2.16). A screening of different bases, ligands and copper sources were taken into consideration to explore their influence to obtain the final desired borylated adduct in high chemical yields and total stereocontrol.



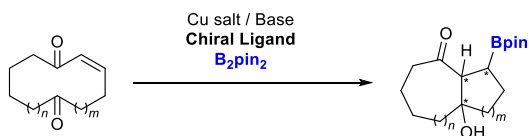
Scheme 2.16. Envisioned model reaction.

2. *Scope of the reaction:* Once the optimal reaction conditions have been established, substrates with different ring sizes are considered to be tested in order to determine the substrate scope of the transannular approach. Different substituents attached to the ketones were also studied to establish how their electronic and/or steric properties influence the reaction outcome (Scheme 2.17).



Scheme 2.17. Scope of the reaction.

3. *Enantioselective version of the reaction:* Incorporation of chiral ligands to the copper catalyst system is explored to evaluate the feasibility of developing the enantioselective borylative transannular approach. A library of different chiral ligands with different structural symmetric nature are tested for the preparation of highly enantioenriched polycyclic organoboranes (Scheme 2.18).



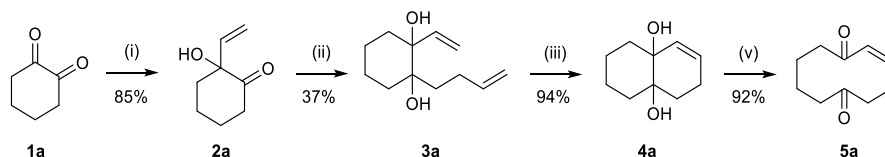
Scheme 2.18. Studied enantioselective version of the reaction.

3. RESULTS AND DISCUSSION

On account of the described precedents on this topic and after establishing the specific objectives of the chapter, we describe here the discussion of the most representative results obtained on this part of the research work.

3.1. Proof of concept

As previously mentioned, bibliographic examples highlighted the importance of the structure of the substrate in any approach to develop an intramolecular version of borylative ring closing of activated alkenes. The key point to achieve the desired reactivity relies on the need to carefully design the disposition of the two reacting functionalities that are placed in the same precursor. Therefore, we focused our initial efforts on evaluating the viability of the envisaged consecutive conjugated borylation-transannular aldol reaction using (*Z*)-cyclodec-2-ene-1,6-dione (**5a**) as model substrate. The synthesis of **5a** was previously developed in the group following the synthetic strategy summarized in Scheme 2.19.³⁶

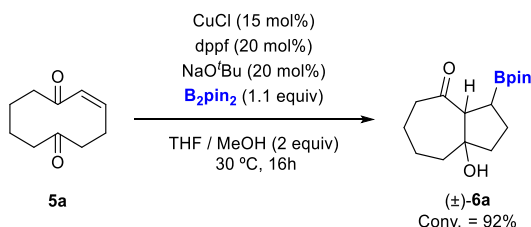


- (i) $\text{CH}_2=\text{CHMgBr}$ (2 equiv), THF (0.1 M), 0 °C to rt, 16h
(ii) $\text{CH}_2=\text{CHCH}_2\text{CH}_2\text{MgBr}$ (3.8 equiv), THF (0.5 M), 0 °C to 40 °C, 2h
(iii) Grubbs 2nd gen. (2.5 mol%), CH_2Cl_2 (33 mM), reflux
(iv) $\text{Pb}(\text{OAc})_4$ (1 equiv), CH_2Cl_2 (0.4 M), rt, 30 min

Scheme 2.19. Synthetic strategy for the preparation of the model cyclic substrate **5a**.

The next step was to select a suitable catalytic system in order to favour the first envisaged conjugated borylation of the corresponding enone moiety. Taking into account the described precedents for this type of transformation, we decided to use a catalytic system based on a copper salt, such as CuCl , and an alkoxide base in order to promote the B-B bond activation of bis(pinacolato)diboron through a σ -

bond metathesis step.^{1b} To our delight, when this reaction was performed in THF and with the addition of MeOH at 30 °C for 16h, we could observe the formation of the desired bicyclic organoborane with high values of conversion, calculated as the consumption of substrate **5a**, in ¹H-NMR, using naphthalene as internal standard. As it is shown in Scheme 2.20, the reaction took place regioselectively to the β-carbon of the conjugated enone and only one diastereoisomer was observed, presumably generated along the diastereoselective transannular aldol step.



Scheme 2.20. Proof of concept reaction.

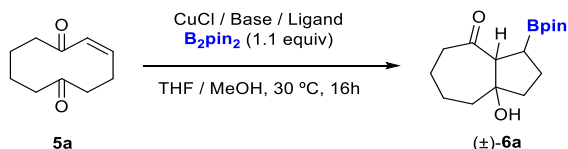
3.2. Optimization of the reaction conditions

In view of the positive outcome observed in the proof of concept and considering the previous results as an evidence of the feasibility of the reaction, we next planned to study the influence of bases and ligands in the borylated product formation.

As it is summarized in Table 2.1, we first tested different bases such as KO^tBu and NaOMe, at 20 mol% loading, to be compared with the use of NaOtBu. In the first case, the transannular reaction took place with moderate conversion (Entry 2) whereas no reaction occurred when NaOMe was used as the base of choice (Entry 3). At this point and since NaOtBu resulted to be the most efficient base towards the explored reaction, we next studied the influence of introducing different mono- and diphosphines as ligands. We modified the CuCl with PPh₃, PCy₃, P(nBu)₃, di(phenylphosphino)ethane (dppe) and di(phenylphosphino)ferrocene (dppf), at 15 mol% loading. Interestingly, high conversions and isolated yields were achieved for all the cases, providing the borylated bicyclo[5.3.0]decane product (±)-**2**, as a single diastereoisomer (Entries 4-8).

Different copper(I) sources, such as CuI and $[\text{Cu}(\text{CH}_3\text{CN})_4]\text{OTf}$, were tested using dppf as the ligand and NaO^tBu as the base, however, they were found to be less efficient (Entries 9-10). Moreover, no product formation was detected using Cu(II), as CuO, or in absence of the copper catalyst (Entries 11-12). Interestingly, for those mentioned cases where the desired product was isolated, the bicyclic borylated adduct (\pm)-**6a** was obtained with total control on the regioselectivity and in any case, the corresponding product resulting only from the conjugate borylation was observed. On the other hand, for those cases where the reaction did not occur, the starting material (**5a**) was recovered unreacted.

Table 2.1. Cu-catalyzed diastereoselective borylative transannular reaction of model substrate **5a**.^[a]

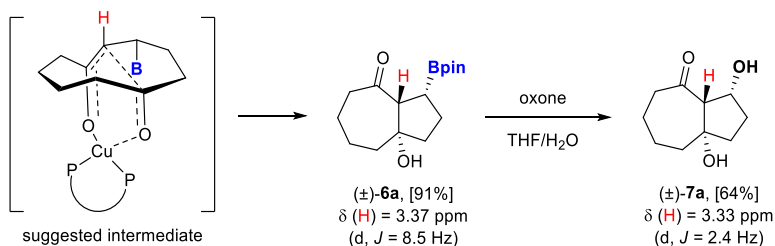


Entry	Cu catalyst	Base	Ligand	Conv.(%), ^[b] [IY%] ^[c]
1	CuCl	NaO^tBu	-	92
2	CuCl	KO^tBu	-	63
3	CuCl	NaOMe	-	0
4	CuCl	NaO^tBu	PPh_3	99
5	CuCl	NaO^tBu	PCy_3	82
6	CuCl	NaO^tBu	$\text{P}^t(\text{Bu})_3$	99, [91]
7	CuCl	NaO^tBu	dppe	99
8	CuCl	NaO^tBu	dppf	99, [86]
9	CuI	NaO^tBu	dppf	45
10	$[\text{Cu}(\text{CH}_3\text{CN})_4]\text{OTf}$	NaO^tBu	dppf	91
11	CuO	NaO^tBu	dppf	0
12	-	NaO^tBu	dppf	0

[a] Reactions were performed with 0.1 mmol of substrate **5a**, Cu catalyst (15 mol%), ligand (15 mol%), base (20 mol%), B_2pin_2 (1.1 equiv), THF (6 mL), MeOH (2 equiv), at 30 °C, 16h. [b] Conversion calculated as consumption of starting material by $^1\text{H-NMR}$ using naphthalene as internal standard. [c] IY: isolated yields of pure product after column chromatography.

The relative stereochemistry of the product was assigned by comparison of the ^1H NMR spectra with similar compounds. As it is depicted in Scheme 2.21, the product (\pm)-**6a** shows a characteristic doublet at 3.37 ppm for the proton in alpha to the ketone, with a coupling constant value $J = 8.5$ Hz. This value could be indicative of a conformation *cis*-axial/equatorial to the adjacent proton in the beta position. These values are in contrast with the reported *trans*-diaxial coupling constants for related products.³⁷ Moreover, when the product (\pm)-**6a** was oxidized with oxone, the corresponding diol (\pm)-**7a** showed a doublet at 3.33 ppm, with coupling constant values of $J = 2.4$ Hz (Scheme 2.21). Since oxidation of C-B takes place with retention of the stereochemistry, we suggested that the two studied protons could be in a quasi-coplanar disposition due to the possible repulsion of the two *cis* diol moieties present in compound (\pm)-**7a**.

On the other hand, in order to rationalize the high diastereoselectivity observed, we have suggested the formation of a favoured chelated (*Z*)-configured cyclic copper enolate intermediate (Scheme 2.21), since the hydroxyl group and the Bpin moiety are settled on the same face of the bicyclic (\pm)-**6a**.



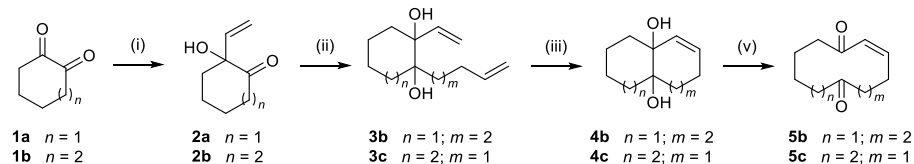
Scheme 2.21. Proposed stereochemical model for observed diastereoselective.

³⁷ Agapiou, K.; Cauble, D. F.; Krische, M J. *J. Am. Chem. Soc.* **2004**, *126*, 4528.

3.2. Scope of the diastereoselective Cu/dppf borylative transannular reaction

Once the proof of concept was verified under optimized reaction conditions, we next proceed to establish the general behaviour of the diastereoselective conjugated borylation-transannular aldol reaction. For this purpose, a series of substrates with different ring sizes were synthesized following the synthetic procedure shown in Table 2.2.

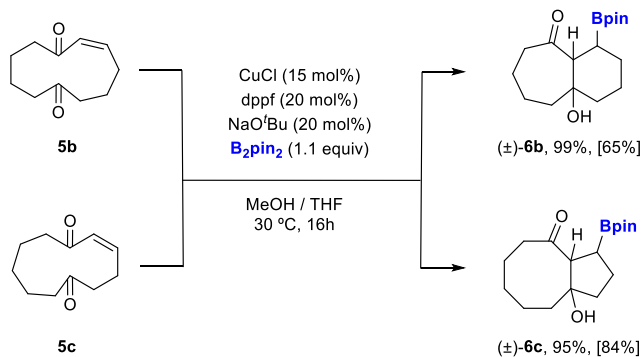
Table 2.2. Synthetic protocol of substrates **5b** and **5c**.³⁶



- (i) $\text{CH}_2=\text{CHMgBr}$ (2 equiv), THF (0.1 M), 0 °C to rt, 16h
(ii) $\text{CH}_2=\text{CHCH}_2(\text{CH}_2)_m\text{MgBr}$ (3.8 equiv), THF (0.5 M), 0 °C to 40 °C, 2h
(iii) Grubbs 2nd gen. (2.5 mol%), CH_2Cl_2 (33 mM), reflux
(iv) $\text{Pb}(\text{OAc})_4$ (1 equiv), CH_2Cl_2 (0.4 M), rt, 30 min

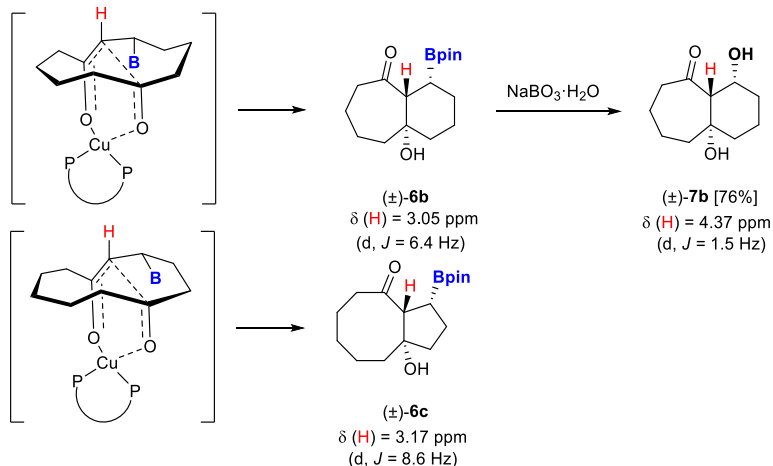
(i)		(ii)		(iii)		(iv)	
2	Yield (%)	3	Yield (%)	4	Yield (%)	5	Yield (%)
2b	85	3b	30	4b	94	5b	78
2c	32	3c	60	4c	50	5c	84

We next tested substrates (*Z*)-cycloundec-7-ene-1,6-dione (**5b**) and (*Z*)-cycloundec-2-ene-1,6-dione (**5c**) under the standard reaction conditions. Similarly to the model system, we were able to convert both substrates into the corresponding bicyclo[5.4.0]undecane structure (\pm)-**6b** and bicyclo[6.3.0]undecane core (\pm)-**6c**, respectively, as a single diastereoisomer in moderate to good yields (Scheme 2.22).



Scheme 2.22. Diastereoselective borylative transannular reaction of substrates **5b** and **5c**.

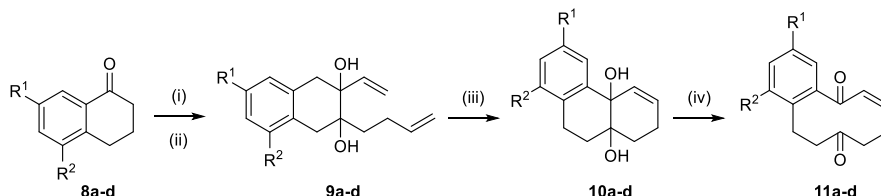
In order to confirm the relative stereochemistry of compounds (±)-**6b** and (±)-**6c**, we studied by 1H -NMR the proton in alpha to the ketone, and we found a similar configuration as for (±)-**6a**. As depicted in Scheme 2.23, both compounds show in the spectra a doublet at 3.05 ppm (for (±)-**6b**) and 3.17 ppm (for (±)-**6c**), with coupling constant values of $J = 6.4$ Hz, $J = 8.6$ Hz, respectively. Product (±)-**6b** was oxidized with $NaBO_3 \cdot H_2O$ and the corresponding diol (±)-**7b** showed a doublet at 4.37 ppm, with coupling constant value $J = 1.5$ Hz.



Scheme 2.23. Proposed stereochemical models.

Encouraged by these promising results, we pursued the next challenge by evaluating the influence of introducing fused aromatic systems, with different substitution patterns, along the carbon-based cyclic scaffold of the already tested ketoenones. Therefore, we first introduced a fused arene at the contiguous carbon of the enone moiety, leading to different cyclodec-2-en-1,6-dione structures (**11a-d**). These substrates were prepared following the slightly modified synthetic protocol used for the preparation of the previous substrates (Table 2.3).

Table 2.3. Synthetic protocol of substrates **11a-d**.³⁶



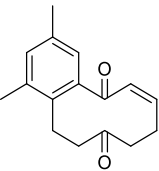
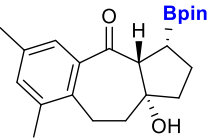
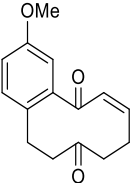
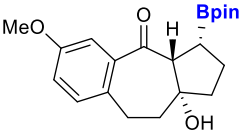
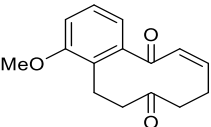
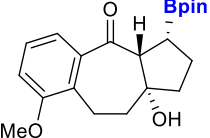
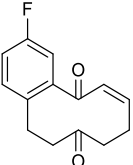
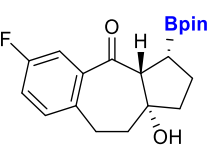
- (i) 1. PIDA (1.1 equiv), KOH (3 equiv), MeOH, 12h, then HCl, EtOH
2. $\text{CH}_2=\text{CHMgBr}$ (2 equiv), THF (0.1 M), 0 °C to rt, 16h
3. IBX (3 equiv), EtOAc (0.5 M), reflux, 16h
- (ii) $\text{CH}_2=\text{CHCH}_2\text{CH}_2\text{MgBr}$ (3.8 equiv), THF (0.5 M), 0 °C to 40 °C, 2h
- (iii) Grubbs 2nd gen. (2.5 mol%), CH_2Cl_2 (33 mM), reflux
- (iv) $\text{Pb}(\text{OAc})_4$ (1 equiv), CH_2Cl_2 (0.4 M), rt, 30 min

8	R¹	R²	(i)+(ii)		(iii)		(iv)	
			9	Yield (%)	10	Yield (%)	11	Yield (%)
8a	Me	Me	9a	26	10a	96	11a	79
8b	OMe	H	9b	16	10b	85	11b	64
8c	H	OMe	9c	25	10c	98	11c	46
8d	F	H	9d	-	10d	-	11d	70

Next, the obtained cyclic substrates were subjected to the optimized catalytic borylative transannular reaction conditions and it was observed that the reaction conversion was strongly dependant on the nature of the substituents present on the aryl core (Table 2.4). When 1,3-dimethyl- and 3-fluorosubstituted substrates (**11a**, **11d**) were tested, full conversion was achieved in both cases towards the borylated tricyclic products (\pm)-**12a** and (\pm)-**12d**, (Entries 1 and 4) In addition, the electronic nature and the position of the substituent seems to have an influence on the reaction outcome. For 1-methoxysubstituted substrate (**11c**) (Entry 3) the

reaction showed slightly better conversion than 3-methoxysubstituted macrocycle (**11b**) (Entry 2). However, in all cases the corresponding borylated adducts were isolated in good to moderate yields.

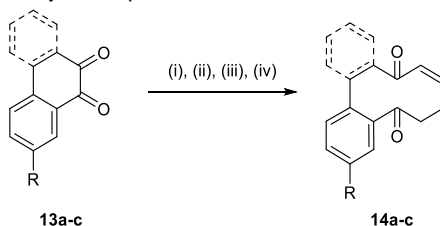
Table 2.4. Scope of diastereoselective Cu/dppf catalyzed borylative transannular reaction.^[a]

Entry	Substrate	Product	Conv.(%), ^[b] [Y%] ^[c]
1	 11a	 (±)-12a	99, [86]
2	 11b	 (±)-12b	90, [31]
3	 11c	 (±)-12c	96, [47]
4	 11d	 (±)-12d	99, [46]

[a] Reactions were performed with 0.2 mmol of substrate, CuCl (15 mol%), dppf (15 mol%), NaO^tBu (20 mol%), B₂pin₂ (1.1 equiv), THF (6 mL), MeOH (2 equiv), at 30 °C, 16h. [b] Conversion calculated as consumption of starting material by ¹H-NMR using naphthalene as internal standard. [c] IY: isolated yields of pure product after column chromatography.

We also studied the possibility of introducing one fused aromatic moiety next to the electrophilic ketone group as well as two fused aromatic systems. Table 2.5 collects the experimental procedure and yields for the preparation of substrates **14a-c** adapting the synthetic protocol of the previous substrates in this work.

Table 2.5. Synthetic protocol of substrates **14a-c**.

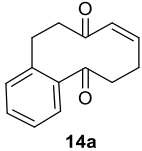
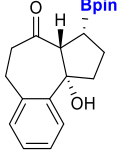
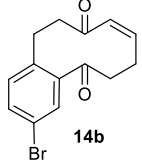
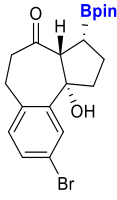
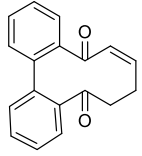
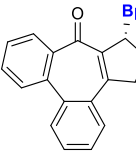


- (i) $\text{CH}_2=\text{CHMgBr}$ (2 equiv), THF (0.1 M), 0 °C to rt, 16h
(ii) $\text{CH}_2=\text{CHCH}_2\text{CH}_2\text{MgBr}$ (3.8 equiv), THF (0.5 M), 0 °C to 40 °C, 2h
(iii) Grubbs 2nd gen. (2.5 mol%), CH_2Cl_2 (33 mM), reflux
(iv) $\text{Pb}(\text{OAc})_4$ (1 equiv), CH_2Cl_2 (0.4 M), rt, 30 min

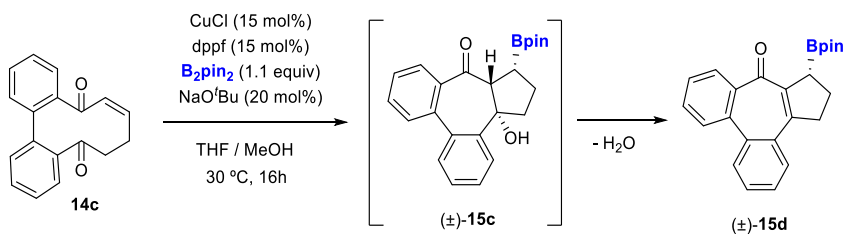
		(i)+(ii)+(iii)+(iv)		
13	R	No. Fused Ar ring	14	Yield (%)
13a	H	1	14a	65
13b	Br	1	14b	70
13c	H	2	14c	29

In this sense, when cyclic ketoenones **14a** and **14b** were tested in the copper catalyzed borylative transannular reaction, similar results were obtained (Table 2.6, Entries 1 and 2). The reaction proceeded efficiently affording the expected borylated products (\pm)-**15a** and (\pm)-**15b** in excellent conversions and good isolated yields. Nevertheless, the presence of two aromatic fused groups, one next to the enone and the other next to the ketone in substrate **14c**, had a detrimental influence on the reaction outcome since only moderate yield of the tetracyclic borylated product (\pm)-**15d** was observed (Entry 3). Remarkably, (\pm)-**15d** was isolated as a conjugated α,β -unsaturated ketone, suggesting that a dehydration process might be intrinsically favoured due to the highly conjugated nature of the resulting borylated adduct (Scheme 2.24).

Table 2.6. Scope of diastereoselective Cu/dppf catalyzed borylative transannular reaction.^[a]

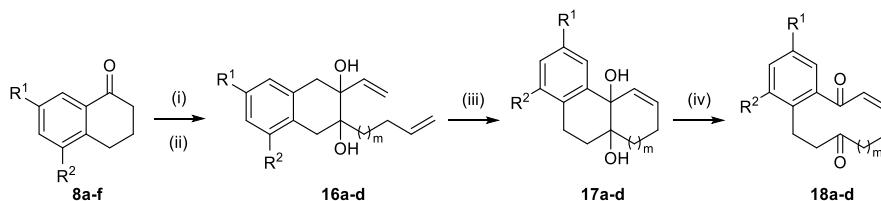
Entry	Substrate	Product	Conv.(%), ^[b] [IY%] ^[c]
1	 14a	 (±)- 15a	95, [60]
2	 14b	 (±)- 15b	99, [71]
3	 14c	 (±)- 15d	99, [58]

[a] Reactions were performed with 0.2 mmol of substrate, with CuCl (15 mol%), dppf (15 mol%), NaO^tBu (20 mol%), B₂pin₂ (1.1 equiv), THF (6 mL), MeOH (2 equiv), at 30 °C, 16h. [b] Conversion calculated as consumption of starting material by ¹H-NMR using naphthalene as internal standard. [c] IY: isolated yields of pure product after column chromatography.

**Scheme 2.24.** Copper catalyzed borylative transannular reaction of **14c** with intrinsic postulated dehydration pathway.

In order to complete the substrate scope, different cycloundec-2-en-1,7-dione substrates (**18a-d**) were analogously prepared, containing a fused aryl moiety with different substitution patterns (Table 2.7).

Table 2.7. Synthetic protocol of substrates **18a-d**.³⁶

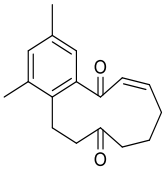
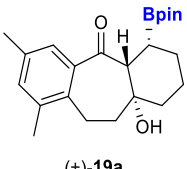
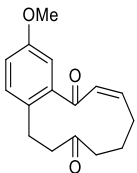
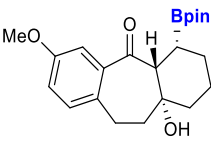
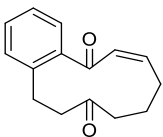
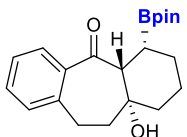
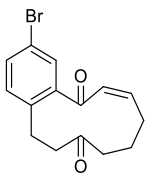
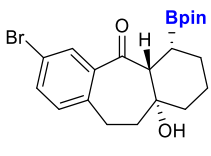


- (i) 1. PIDA (1.1 equiv), KOH (3 equiv), MeOH, 12h, then HCl, EtOH
2. $\text{CH}_2=\text{CHMgBr}$ (2 equiv), THF (0.1 M), 0 °C to rt, 16h
3. IBX (3 equiv), EtOAc (0.5 M), reflux, 16h
- (ii) $\text{CH}_2=\text{CHCH}_2(\text{CH}_2)_m\text{MgBr}$ (3.8 equiv) ($m = 2$), THF (0.5 M), 0 °C to 40 °C, 2h
- (iii) Grubbs 2nd gen. (2.5 mol%), CH_2Cl_2 (33 mM), reflux
- (iv) $\text{Pb}(\text{OAc})_4$ (1 equiv), CH_2Cl_2 (0.4 M), rt, 30 min

			(i)+(ii)		(iii)		(iv)	
8	R¹	R²	16	Yield (%)	17	Yield (%)	18	Yield (%)
8a	Me	Me	16a	32	17a	79	18a	90
8b	OMe	H	16b	24	17b	86	18b	78
8e	H	H	16c	24	17c	91	18c	95
8f	Br	H	16d	32	17d	89	18d	83

The same optimized Cu/dppf catalyzed borylative transannular reaction conditions were applied to the cyclic ketoenones **18a-d** towards the diastereoselective formation of bicyclo[5.4.0]undecane scaffolds (Table 2.8). In this particular case, when no substituents were present in the aromatic ring, the reaction afforded the corresponding tricyclic organoborane (\pm)-**19c** with moderate yield (Entry 1). When either two methyl groups or an halogen were incorporated to the fused ring, the corresponding adducts (\pm)-**19a** and (\pm)-**19d**, were obtained as single diastereoisomers but in a rather low yield, respectively (Entries 2 and 3). Contrarily, substitution with a 3-methoxy group at the phenyl system favoured the reaction outcome leading to the formation of the tricyclic product (\pm)-**19b** in good yield (Entry 4). Furthermore, in all cases the reaction maintained the same regio- and diastereoselectivity as the one observed with the model system.

Table 2.8. Scope of diastereoselective Cu/dppf catalyzed borylative transannular reaction.^[a]

Entry	Substrate	Product	[Y%] ^[b]
1	 18a	 (±)-19a	64
2	 18b	 (±)-19b	22
3	 18c	 (±)-19c	32
4	 18d	 (±)-19d	70

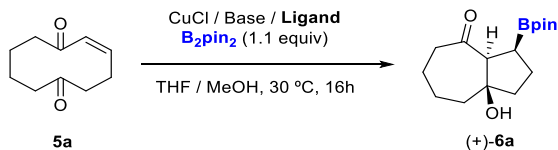
[a] Reactions were performed with 0.2 mmol of substrate, with CuCl (15 mol%), dppf (15 mol%), NaO^tBu (20 mol%), B₂pin₂ (1.1 equiv), THF (6 mL), MeOH (2 equiv), at 30 °C, 16h. [b] IY: isolated yields of pure product after column chromatography.

3.3. Enantioselective Cu(I)-catalyzed borylative transannular reaction

Once the scope of the racemic variant was established, we pursued the next challenge by evaluating the feasibility of developing an enantioselective version of the studied transannular conjugated borylation/aldol cyclization. With the optimized reaction conditions in mind, substrate **5a** was tested using different commercial phosphorous- containing chiral ligands (Table 2.9, **L1-L5**).

When C_2 -symmetrical chiral bisphosphines, such as BINAP (**L1**) or QuinoxP* (**L2**) were tested the reaction performed with excellent conversions but showing rather low levels of asymmetric induction (Entries 1 and 2). On the other hand, (*R*)-propane-1,2-diylbis(diphenylphosphine) (**L4**) was also tested but without any improvement in terms of enantioselectivity (Entry 4). We then moved to C_1 -symmetric ferrocene diphosphorous ligands such as Taniaphos (**L3**) and Josiphos (**L5**). As it has been already seen during the description of the existing precedents, this type of chiral ligands have shown to be optimal for the enantioselective β -borylation reaction of conjugated substrates. This could be rationalized due to the exhibited planar chirality as well as the steric bulkiness and rigidity, which are important features in order to provide an appropriate chiral environment. In this framework, although Taniaphos type ligand (**L3**) did not provide any improvements from the previous attempts (Entry 3), when Josiphos (**L5**) was screened, excellent values of conversion and enantioselectivity were obtained (Entry 5).

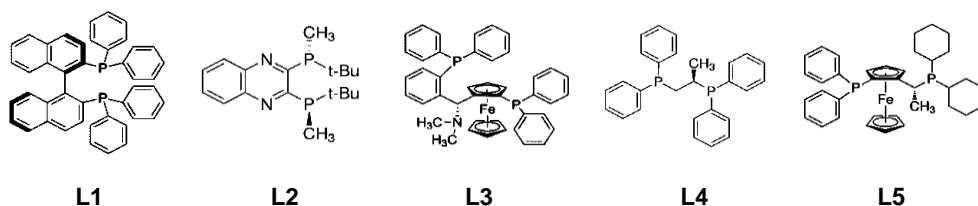
Table 2.9. Chiral ligand screening for the enantioselective borylative transannular reaction of model substrate **5a**.^[a]



Entry	Cu catalyst	Base	Ligand	Conv.(%) ^[b]	e.e.(%) ^[c]
1	CuCl	NaO ^t Bu	L1	99	22
2	CuCl	NaO ^t Bu	L2	84	30
3	CuCl	NaO ^t Bu	L3	79	14
4	CuCl	NaO ^t Bu	L4	91	8
5	CuCl	NaO ^t Bu	L5	99	92

[a] Reactions were performed with 0.1 mmol of substrate **5a**, with CuCl (15 mol%), ligand (15 mol%), NaO^tBu (20 mol%), B₂pin₂ (1.1 equiv), THF (6 mL), MeOH (2 equiv), at 30 °C, 16h. [b] Conversion calculated as consumption of starting material by ¹H-NMR using naphthalene as internal standard.

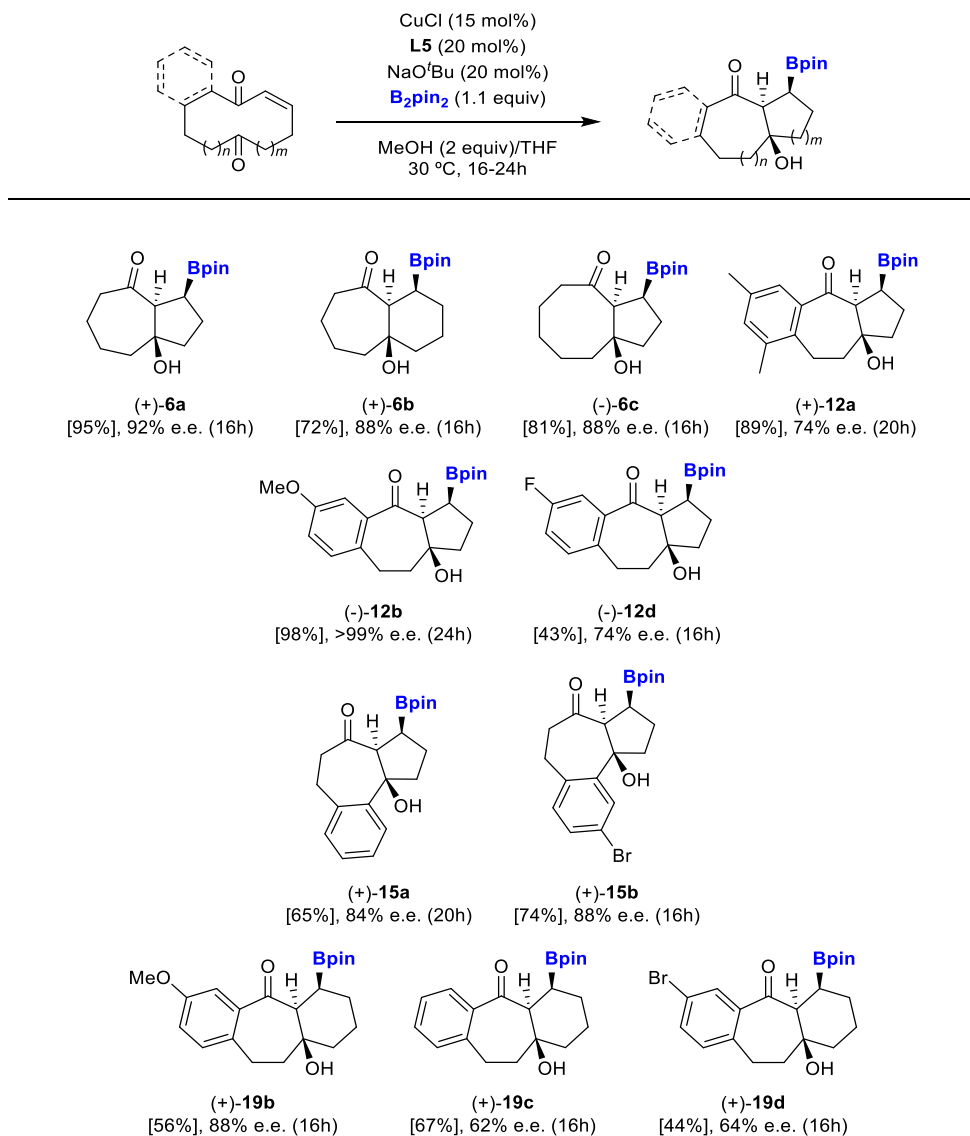
[c] e.e. was calculated by HPLC on chiral stationary phase.



With the optimal chiral ligand in hand, we address the next goal by extending the developed enantioselective Cu(I)-catalyzed borylative transannular reaction for the synthesis of complex polycyclic chiral organoboron compounds. Thereby, the previously mentioned ketoenones were subjected to the optimal reaction conditions and results are illustrated in Table 2.10.

For the first family of carbon-based skeleton (*Z*)-cyclodec-2-ene-1,6-dione (**5a**), (*Z*)-cycloundec-2-ene-1,6-dione (**5b**) and (*Z*)-cycloundec-7-ene-1,6-dione (**5c**) the reaction resulted efficient yielding the corresponding borylated adducts (+)-**6a**, (+)-**6b** and (-)-**6c**, respectively, with good to excellent yields and enantioselectivities after 16h (Scheme 2.10). Secondly, in the case of (*Z*)-cyclodec-2-ene-1,6-dione scaffolds, where a fused aromatic ring was incorporated, either next to the enone or the electrophilic ketone, the corresponding borylated tricyclic adducts were obtained in moderate to excellent yields and high levels of asymmetric induction (compounds (+)-**12a**, (-)-**12b**, (+)-**15a** and (+)-**15b**), with the only exception of fluorine containing compound (-)-**12d**. It has to be highlighted that different reaction times were needed in order to achieve full conversions. Slightly poorer results were obtained in the case of compounds (+)-**19c**, (+)-**19d** and (+)-**19b**, obtaining the corresponding substituted octahydro-1*H*-dibenzo[*a,d*][7]annulene core in moderate yields and moderate to good enantiomeric excesses.

In summary, we have been able to obtain the chiral borylated products with moderate to excellent yields and high enantiomeric excesses as well as a total control on the regio- and diastereoselectivity of the transformation.

Table 2.10. Scope of enantioselective Cu(I)-catalyzed borylative transannular reaction.^[a]

[a] Reactions were performed with 0.2 mmol of substrate, with CuCl (15 mol%), **L5** (15 mol%), NaO^tBu (20 mol%), **B₂pin₂** (1.1 equiv), THF (6 mL), MeOH (2 equiv), at 30 °C, 16-24h. Enantiomeric excess (e.e.) were calculated by HPLC on chiral stationary phase.

An enantiopure sample of compound (+)-**15a** could be recrystallized, determining the absolute configuration by single X-ray diffraction analysis (Figure 2.3). As it is depicted on the bottom, the pinacolborane moiety and the generated hydroxyl group are pointing towards the same face of the molecule whereas the third stereogenic centre is pointing towards the opposite face. This fact could match with the previous mentioned hypothesis of a possible formation of a (*Z*)-configured cyclic copper enolate intermediate, which would lead to the disposition of both groups in the same face.

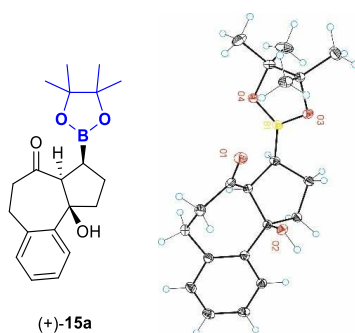
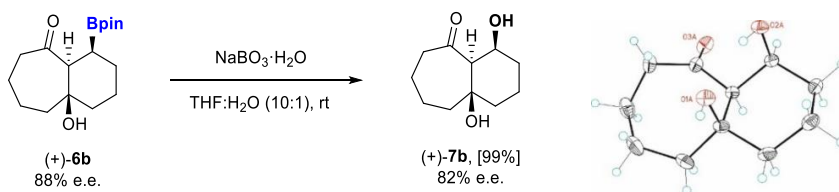


Figure 2.3. X-Ray diffraction analysis of compound (+)-**15a**.

Finally, having established an efficient strategy for the construction of borylated bi- and tricyclic complex scaffolds with high diastereo- and enantioselectivity, we next explored the possibility for the new alkyl boronate unit to undergo stereospecific transformations. In particular, compound (+)-**6b** was oxidized using sodium perborate in a mixture of THF:H₂O (10:1) as the solvent (Scheme 2.25).



Scheme 2.25. Stereospecific oxidation of C-B bond in compound (+)-**6b**.

The oxidation reaction took place with complete stereochemical retention from the C-B to the new C-OH bond giving a direct access to the formation of enantioenriched diols. Compound (+)-**7b** could be also recrystallized and analyzed by single X-ray diffraction, proving the absolute configuration of the final product.

4. CONCLUSIONS

The following conclusions can be highlighted for this chapter:

1. The proposed cyclic ketoenone systems can display a pioneer copper(I)-catalyzed conjugate borylation and subsequent aldol transannular reactivity as direct alternative to access polycyclic scaffolds.
2. An efficient catalytic system based on a CuCl, ligand (dppf) and a base (NaO^tBu), enables the activation of bis(pinacolato)diboron and its further regioselective addition to the enone moiety with subsequent diastereoselective transannular addition to the electrophilic ketone.
3. The described methodology provides excellent results with high yields and diastereoselectivities, with a wide substrate scope, including different ring sizes of the substrates as well as the incorporation of fused aromatic rings with different bulkiness and electronic properties.
4. The incorporation of a chiral Josiphos type ligand allowed to carry out the asymmetric version in a highly enantioselective fashion, expanding therefore the utility of the transformation, facilitating the construction of complex enantioenriched borylated bi- and tricyclic scaffolds. In addition, the reaction showed to be tolerant with a wide range of macrocyclic substrates, which contain fused aromatic rings with different substitution patterns.

3

3

Transannular Enantioselective (3+2) Cycloaddition of Cycloalkenone Hydrazones under Brønsted Acid Catalysis

1. INTRODUCTION	79
1.1. Asymmetric organocatalysis	79
1.2. Hydrazones in (3+2) cycloaddition reactions: Synthesis of pyrazolidines ...	89
2. SPECIFIC OBJECTIVES AND WORK PLAN	98
3. RESULTS AND DISCUSSION	102
3.1. Proof of concept.....	102
3.2. Optimization of the reaction conditions.....	104
3.3. Scope of the enantioselective transannular (3+2) cycloaddition reaction	108
3.4. Transformation of the adducts: Synthesis of enantioenriched 1,3-diamines	117
3.5. Mechanistic insights and stereochemistry of the reaction	119
4. CONCLUSIONS	124

1. INTRODUCTION

1.1. Asymmetric organocatalysis

The stereocontrolled preparation of chiral carbo- and heterocycles has arisen as one of the most important topics within the fields of medicinal and organic chemistry. Up to date, many efficient and straightforward methodologies have been reported for their enantioselective synthesis, mainly through the use of asymmetric catalysis with enzymes¹ or catalytic metal complexes². Nevertheless, during the last decades a more economically attractive way of inducing stereocontrol into a molecule has arisen by incorporating a small chiral organic molecule which is used in catalytic amounts to promote a given transformation. This field, known as organocatalysis,^{3,4} has been well-established as the “third pillar” in asymmetric catalysis⁵ and in 2021, the importance of this area was recognized by awarding the

-
- ¹ For enzymatic catalysis, see: (a) Tao, J.; Zhao, L.; Ran, N. *Org. Process Res. Dev.* **2007**, *11*, 259. (b) Moniruzzaman, M.; Kamiya, N.; Goto, M. *Org. Biomol. Chem.* **2010**, *8*, 2887. (c) Drauz, K.; Gröger, H.; May, O. (2012). *Enzyme Catalysis in Organic Chemistry*; 3rd edition; Wiley-VCH: Weinheim. (d) Callender, R.; Dyer, B. *Acc. Chem. Res.* **2015**, *48*, 407.
- ² For metal catalysis, see: (a) Beller, M.; Bolm, C. (2004). *Transition Metals for Organic Synthesis*; 3rd edition; Wiley-VCH: Weinheim. (b) Ojima, I. (2010). *Catalytic Asymmetric Synthesis*; 2nd edition; Wiley-VCH: New York. (c) Duka, G. (2012). *Homogeneous Catalysis with Metal Complexes*; Springer: Berlin. (d) Dixneuf, P.; Cadierno, V. (2013). *Metal Catalyzed Reactions in Water*; Wiley-VCH: Weinheim.
- ³ For the first use of the term “organic catalyst”, see: (a) Langebeck, W. *Angew. Chem.* **1928**, *41*, 740. (b) Langebeck, W. *Angew. Chem.* **1932**, *45*, 97. (c) Langebeck, W. (1949). *Die Organische Katalysatoren und ihre Beziehungen zu den Fermenten*; Springer-Verlag: Berlin.
- ⁴ First examples of organocatalytic reactions: (a) Marckwald, W. *Ber. Dtsch. Chem. Ges.* **1904**, *37*, 349. (b) Bredig, G.; Fiske, P. S. *Chem-Ztg.* **1912**, *35*, 324. (c) Bredig, G.; Fiske, P. S. *Biochem. Z.* **1913**, *46*, 7. (d) Pracejus, H. *Justus Liebigs Ann. Chem.* **1960**, *634*, 9. (e) Eder, U.; Sauer, G.; Wiechert, R. *Angew. Chem. Int. Ed. Engl.* **1971**, *10*, 496. (f) Hajos, Z. G.; Parrish, D. R. *J. Org. Chem.* **1974**, *39*, 1615.
- ⁵ Representative reviews and articles on organocatalysis: (a) Dalko, P. I.; Moisan, L. *Angew. Chem. Int. Ed.* **2001**, *40*, 3726. (b) Seayad, J.; List, B. *Org. Biomol. Chem.* **2005**, *3*, 719. (c) Yang, J. W.; List, B. *Science* **2006**, *313*, 1584. (d) List, B. *Chem. Rev.* **2007**, *107*, 5413. (e) MacMillan, D. W. C. *Nature* **2008**, *455*, 304. (f) Bertelsen, S.; Jørgensen, K. A. *Chem. Soc. Rev.* **2009**, *38*, 2178. (g) Marqués-López, E.; Herrera, R. P.; Christmann, M. *Nat. Prod. Rep.* **2010**, *27*, 1138. (h) Jacobsen, E. N.; MacMillan, D. W. C. *Proc. Natl. Acad. Sci. USA* **2010**, *107*, 20618. (i) Marson, C. M. *Chem. Rev.* **2012**, *41*, 7712. (j) Flanigan, D. M.; Romanov-Michailidis, F.; White, N. A.; Rovis, T. *Chem. Rev.* **2015**, *115*, 9307. (k) Akiyama, T.; Mori, K. *Chem. Rev.* **2015**, *115*, 9277. (l) Donslund, B. S.; Johansen, T. K.; Poulsen, P. H.; Halskov, K. S.; Jørgensen, K. A. *Angew. Chem. Int. Ed.* **2015**, *54*, 13860. (m) Silvi, M.; Melchiorre, P. *Nature* **2018**, *554*, 41. (n) Van Der Helm, M. P.; Klemm, B.; Eelkema, R. *Nat. Rev. Chem.* **2019**, *3*, 491. (o) Lassaletta, J. M. *Nat. Commun.* **2020**, *11*, 3787. (p)

Nobel Prize in Chemistry to Benjamin List and David McMillan for their groundbreaking work on developing this new synthetic tool.⁶

The principal factor that governs the stereoselectivity of an organocatalytic transformation is the ability of the small organic molecule to activate the reagents and also to transfer the chiral information by establishing interactions that allow the formation of a well-organized transition state. According to the nature of this substrate-catalyst interaction, the different modes for the substrate activation can be classified in two different groups (Figure 3.1). The first group, named *covalent organocatalysis*, is the one that includes all the corresponding activation modes in which the catalyst binds the substrate through covalent interactions. As it is depicted above in the examples found in Figure 3.1, there are many types of covalent organocatalysts such as aminocatalysts (via azomethine-type intermediates, Figure 3.1a) or *N*-heterocyclic carbenes (via Breslow-type intermediates, Figure 3.1b)⁷. The second group, *non-covalent organocatalysis*, gathers those situations where the interactions between the substrate and the catalyst are weaker. These interactions are non-covalent and they are commonly attributed to either hydrogen bonding or protonation (Figure 3.1d)⁸, electrostatic

Xiang, S.-H.; Tan, B. *Nat. Commun.* **2020**, *11*, 3786. (q) Han, B.; He, X.-H.; Liu, Y.-Q.; He, G.; Peng, C.; Li, J.-L. *Chem. Soc. Rev.* **2021**, *50*, 1522. (r) Garcia-Mancheño, O.; Waser, M. *Eur. J. Org. Chem.* **2022**, e202200950.

⁶ (a) List, B.; Lerner, R. A.; Barbas, C. F. *J. Am. Chem. Soc.* **2000**, *122*, 2395. (b) Ahrendt, K. A.; Borths, C. J.; MacMillan, D. W. C. *J. Am. Chem. Soc.* **2000**, *122*, 4243.

⁷ For selected reviews and articles on the use of NHC as organocatalysts, see: (a) Enders, D.; Niemeier, O.; Henseler, A. *Chem. Rev.* **2007**, *107*, 5606. (b) Marion, N.; Díez-González, S.; Nolan, S. P. *Angew. Chem. Int. Ed.* **2007**, *46*, 2988. (c) Phillips, E. M.; Chan, A.; Scheidt, K. A. *Aldrichim. Acta* **2009**, *42*, 55. (d) Biju, A. K.; Kuhl, N.; Glorius, F. *Acc. Chem. Res.* **2011**, *44*, 1182. (e) Bugaut, X.; Glorius, F. *Chem. Soc. Rev.* **2012**, *41*, 3511. (f) Chen, X. Y.; Ye, S. *Org. Biomol. Chem.* **2013**, *11*, 7991. (g) Ryan, S. J.; Candish, L.; Lupton, D. W. *Chem. Soc. Rev.* **2013**, *42*, 4906. (h) Walden, D. M.; Ogba, O. M.; Johnston, R. C.; Cheong, P. H. *Acc. Chem. Res.* **2016**, *49*, 1279. (i) Wang, M. H.; Scheidt, K. A. *Angew. Chem. Int. Ed.* **2016**, *55*, 14912.

⁸ For selected reviews and articles on H-bonding catalysis, see: (a) Schreiner, P. R. *Chem. Soc. Rev.* **2003**, *32*, 289. (b) Taylor, M. S.; Jacobsen, E. N. *Angew. Chem. Int. Ed.* **2006**, *45*, 1520. (c) Doyle, A. G.; Jacobsen, E. N. *Chem. Rev.* **2007**, *107*, 5713. (d) Yu, X.; Wang, W. *Chem. Asian J.* **2008**, *3*, 516. (e) Pihko, P. M. (2009). *Hydrogen Bonding in Organic Synthesis*; Wiley-VCH: Weinheim.

(phase-transfer catalysis, Figure 3.1e)⁹ or chiral Brønsted base catalysis (Figure 3.1f),¹⁰ among several others.

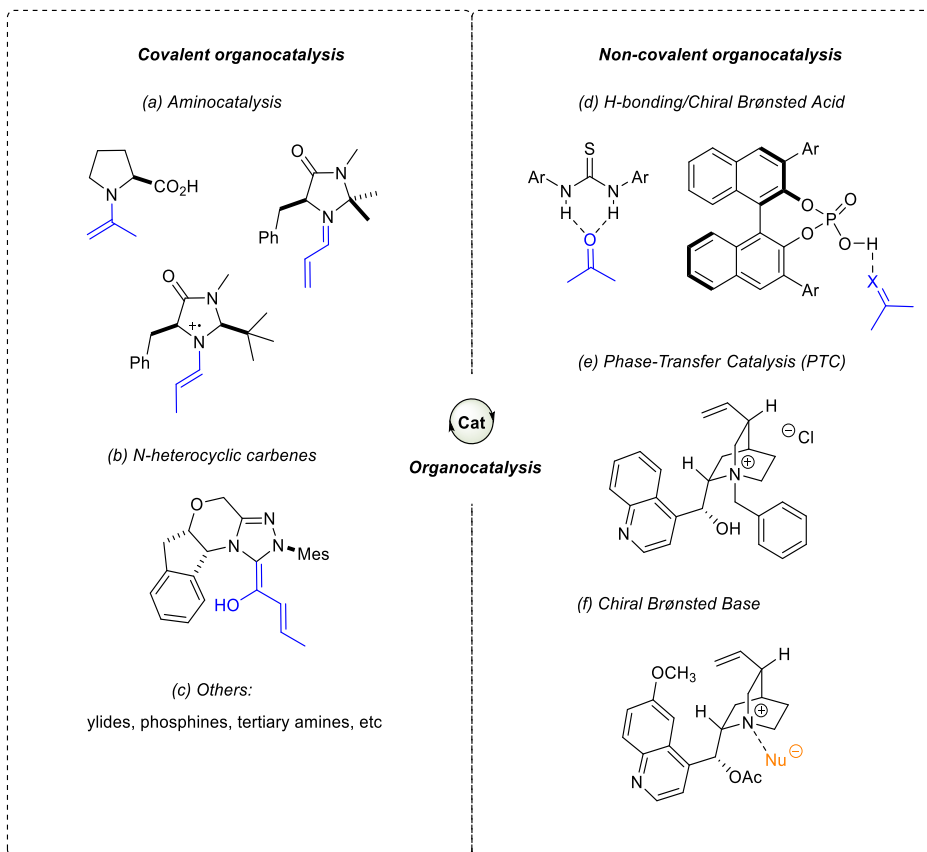


Figure 3.1. Organocatalytic activation modes.

Due to the closer relationship with the research presented in this chapter, special attention will be dedicated to non-covalent organocatalysis, in particular to chiral Brønsted acid catalysis. During the last years, the field of Brønsted acid

⁹ For selected reviews on chiral phase-transfer catalysis, see: (a) Ooi, T.; Maruoka, K. *Angew. Chem. Int. Ed.* **2007**, *46*, 4222. (b) Jew, S.; Park, H. *Chem. Commun.* **2009**, 7090. (c) Shirakawa, S.; Maruoka, K. *Angew. Chem. Int. Ed.* **2013**, *52*, 4312. (d) Kaneko, S.; Kumatabara, Y.; Shirakawa, S. *Org. Biomol. Chem.* **2016**, *14*, 5367.

¹⁰ For a review on Brønsted base catalysis: Palomo, C.; Oiarbide, M.; López, R. *Chem. Soc. Rev.* **2009**, *38*, 632.

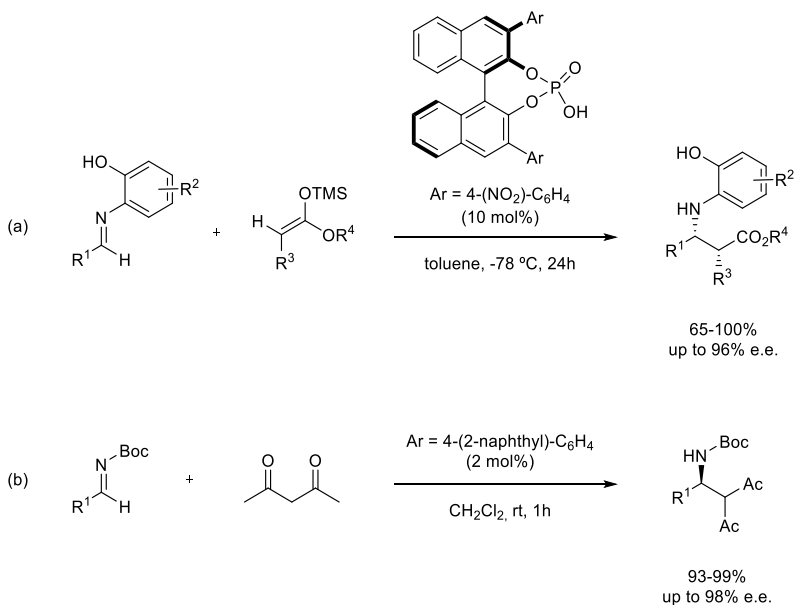
catalysis has been mainly governed by chiral BINOL-derived phosphoric acids as the selected organocatalysts, which are able to protonate an electrophilic substrate becoming activated towards a reaction with a nucleophile, also providing a chiral environment for the reaction to proceed stereoselectively.¹¹ This type of molecules were originally employed as resolving agents for chiral amines¹² until the pioneering work of Akiyama and co-workers also demonstrated the ability of these compounds to act as chiral catalysts in the first asymmetric Brønsted acid-catalyzed Mannich reaction (Scheme 3.1a).¹³ This reaction involved the activation of a *N*-(*o*-hydroxyphenyl)aldimine by the catalyst and subsequent reaction with a silyl enol ether nucleophile. Simultaneously, the group of Terada reported a more direct Mannich reaction between 1,3-diketones and *N*-Boc aldimines under the same type of BINOL-based chiral Brønsted acid catalysis (Scheme 3.1b).¹⁴ Contrarily to Akiyama, in this work the authors proposed that tuning the bulkiness of the catalyst, through the incorporation of substituents at the 3,3'-positions of the BINOL core would have a bigger impact in the stereochemical outcome of the reaction rather than the electronics of the catalysts itself.

¹¹ For selected reviews of this topic, see: (a) Parmar, D.; Sugiono, E.; Raja, S.; Rueping, M. *Chem. Rev.* **2014**, *114*, 9047. (b) Del Corte, X.; Martínez de Marigorta, E.; Palacios, F.; Vicario, J.; Maestro, A. *Org. Chem. Front.* **2022**, *9*, 6331.

¹² For examples of chiral resolution of amines, see: (a) Jacques, J.; Fouquey, C.; Viterbo, R. *Tetrahedron Lett.* **1971**, 4617. (b) Arnold, W.; Daly, J. J.; Imhof, R.; Kyburz, E. *Tetrahedron Lett.* **1983**, *24*, 343. (c) Wilen, S. H.; Qi, J. Z.; Williard, P. G. *J. Org. Chem.* **1991**, *56*, 485. (d) Fujii, I.; Hirayama, N. *Helv. Chim. Acta* **2002**, *85*, 2946. (e) Aikawa, K.; Kojima, M.; Mikami, K. *Angew. Chem. Int. Ed.* **2009**, *48*, 6073. (f) Verkuijl, B. J. V.; de Vries, J. G.; Feringa, B. L. *Chirality*, **2011**, *23*, 34. (g) Schuur, B.; Verkuijl, B. J. V.; Bokhove, J.; Minnaard, A. J.; de Vries, J. G.; Heeres, H. J.; Feringa, B. L. *Tetrahedron* **2011**, *67*, 462. (h) Eelkema, R.; Feringa, B. L. *Org. Lett.* **2006**, *8*, 1331.

¹³ Akiyama, T.; Itoh, J.; Yokota, K.; Fuchibe, K. *Angew. Chem. Int. Ed.* **2004**, *43*, 1566. For theoretical calculations, see: Yamanaka, M.; Itoh, J.; Fuchibe, K.; Akiyama, T. *J. Am. Chem. Soc.* **2007**, *129*, 6756.

¹⁴ Uraguchi, D.; Terada, M. *J. Am. Chem. Soc.* **2004**, *126*, 5356. For theoretical calculations, see: Gridnev, I. D.; Kouchi, M.; Sorimachi, K.; Terada, M. *Tetrahedron Lett.* **2007**, *48*, 497.



Scheme 3.1. Mannich-type reaction by Akiyama and Terada, respectively.

The key featuring behind the design of this type of highly efficient chiral Brønsted acid catalysis relies on the presence of a highly acidic proton on the phosphate functionality that can interact with the electrophile and influence conformational preferences in the transition states, forming rigid three-dimensional structures and stabilizing possible reactive intermediates inside the congested chiral pocket (Figure 3.2). Depending on the degree of the corresponding proton transfer, we can refer to hydrogen-bonding activation catalysis, when the acidic proton is still bound to the catalyst, whereas for the case of Brønsted acid activation a complete proton transfer occurs from the catalyst to the substrate.¹⁵

¹⁵ (a) Reisman, S. E.; Doyle, A. G.; Jacobsen, E. N. *J. Am. Chem. Soc.* **2008**, *130*, 7198. (b) Mita, T.; Jacobsen, E. N. *Synlett* **2009**, 1680. (c) Brown, A. R.; Kuo, W.-H.; Jacobsen, E. N. *J. Am. Chem. Soc.* **2010**, *132*, 9286. (d) Moyano, A.; Rios, R. *Chem. Rev.* **2011**, *111*, 4703.

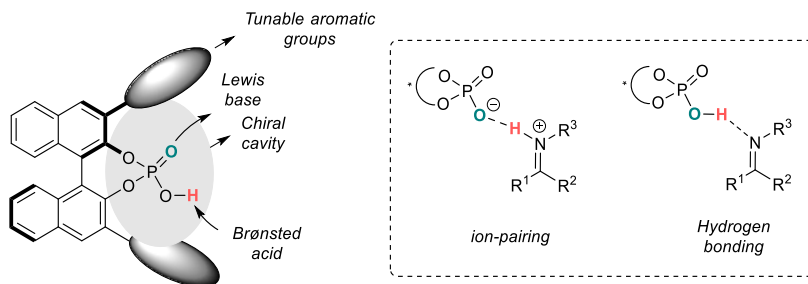
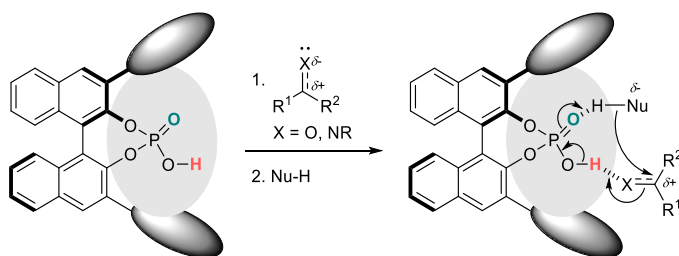


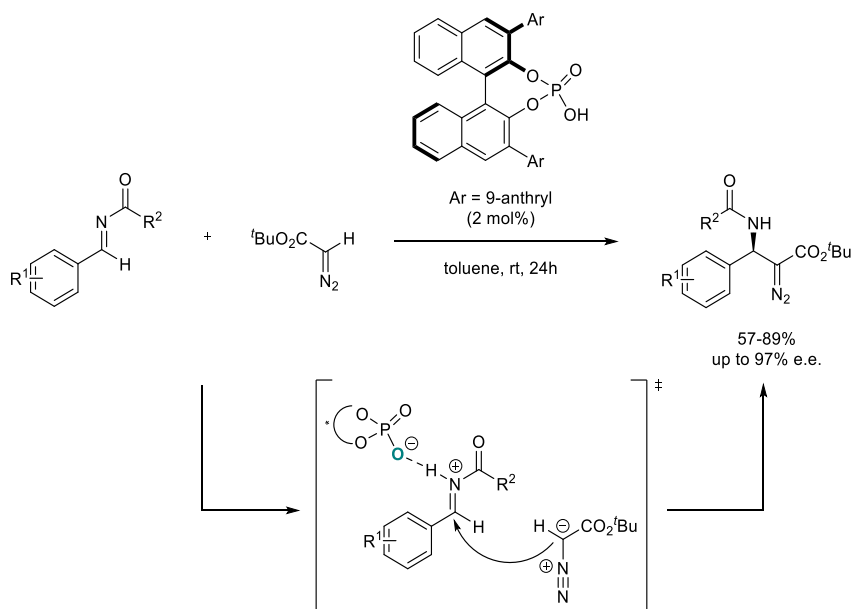
Figure 3.2. Structure and activation of BINOL-based phosphoric acids.

As previously disclosed by Akiyama, the catalytic activity of phosphoric acids has been shown to greatly depend on the nature of the catalyst and in particular, to its Brønsted acidity. In this sense, three different activation modes have been described for the activation of the substrates. The first mode, which is the most frequently found in most literature examples, covers those reactions in which both the nucleophile and the electrophile are activated by the catalyst in a bifunctional mode of activation (Scheme 3.2). Initially the Brønsted acidic part of the catalyst interacts with the available Lewis basic site of the electrophilic substrate while the Lewis basic P=O site of the catalyst can establish hydrogen bonding interactions with the acidic proton of the pronucleophile and therefore, bring together both reacting species whereby the desired transformation occurs in a stereocontrolled environment.



Scheme 3.2. Bifunctional activation mode.

A second possibility for the activation involves the formation of a single contact between the corresponding catalyst and the substrate (monoactivation). As it is exemplified in the following Scheme 3.3, Terada and co-workers demonstrated the direct alkylation of α -diazoesters with *N*-acylimines in the presence of a chiral BINOL-based phosphoric acid, enabling the preparation of the corresponding alkylated secondary amines in good yields and enantioselectivity.¹⁶ The authors proposed a transition state that would involve a single contact activation of the imine, forming an ion-pairing complex with the catalyst, which could be further intercepted by the nucleophilic diazo-species.

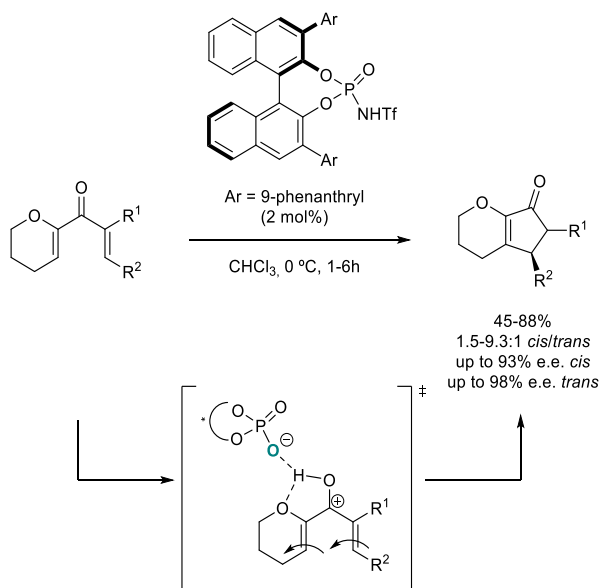


Scheme 3.3. Enantioselective alkylation of diazoesters with imines by Terada.

The third scenario refers to the possibility for the electrophile to display two specific contacts with the catalyst as shown in the example illustrated below in Scheme 3.4. Rueping and co-workers reported a catalytic enantioselective Nazarov cyclization reaction between α -alkoxy ketones in the presence of a chiral *N*-tryflyphosphoramidate to yield optically active cyclopentenones in good yields and

¹⁶ Uraguchi, D.; Sorimachi, K.; Terada, M. *J. Am. Chem. Soc.* **2005**, *127*, 9360.

enantioselectivities.¹⁷ The authors proposed that the key featuring for the observed stereocontrol is the ability of the chiral catalyst to establish a bidentate interaction with the α -alkoxy group and the oxygen of the carbonyl moiety. The next step would be the cyclization and further protonation of the enolate species would afford the products and the regeneration of the catalyst.



Scheme 3.4. Enantioselective Nazarov cyclization by Rueping.

Up to date, a large variety of structures have been already evaluated as catalysts in many different transformations and a summary of the most commonly used chiral phosphoric acid catalysts encountered in the literature have been depicted in Figure 3.3. The archetypical structure relies on the use of the BINOL scaffold incorporating substituents of different nature at the 3- and 3'-positions. A common variation involves the partial hydrogenation of the BINOL core, generating a molecular architecture with a different conformational feature. In addition,

¹⁷ Rueping, M.; leawsuan, W.; Antonchick, A. P.; Nachtseim, B. J. *Angew. Chem. Int. Ed.* **2007**, *46*, 2097.

SPINOL-based scaffold containing central chirality has also shown to catalyze a wide number of transformations in a highly selective manner.

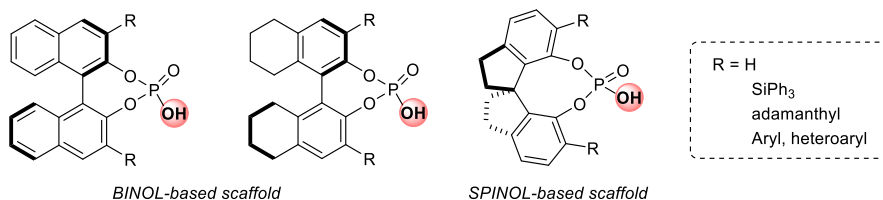


Figure 3.3. Most used chiral Brønsted phosphoric acid catalysts.

On the other hand, although it has been shown that the catalytic activity is highly dependent on the nature of the chiral backbone of the acid catalyst, a relatively scarce number of reports exists regarding detailed studies about the influence of the pK_a on the reactivity of these catalysts. The first general studies were carried out by O'Donogue and Berkessel¹⁸ in 2011 and a complementary theoretical work was reported by Chen and Li afterwards.¹⁹ However, the full study on establishing an acidity scale for the commonly used Brønsted acid catalysts was compiled in 2013 by Rueping and Leito.²⁰ In this work, the authors could distinct three different groups depending on the variation at the acidic site of the catalyst: phosphoric acids, *N*-sulfonyl phosphoramides and sulfonyl imides. As it is illustrated in Figure 3.4, the less acidic phosphoric acids were found to have pK_a values between 12 and 14, in acetonitrile, whereas *N*-sulfonyl phosphoramides have pK_a values between 6 and 7. Finally, sulfonyl imides showed to be the most acidic catalysts with pK_a values around 5. The more acidic the catalyst, the better capacity to efficiently activate weak electrophiles.

¹⁸ Christ, P.; Lindsay, A. G.; Vormittag, S. S.; Neudoerfl, J.-M.; Berkessel, A.; O'Donoghue, A. C. *Chem. Eur. J.* **2011**, *17*, 8524.

¹⁹ Yang, C.; Xue, X.-S.; Jin, J.-L.; Li, X.; Cheng, J.-P. *J. Org. Chem.* **2013**, *78*, 7076.

²⁰ Kaupmees, K.; Tolstoluzhsky, N.; Raja, S.; Rueping, M.; Leito, I. *Angew. Chem., Int. Ed.* **2013**, *52*, 11569.

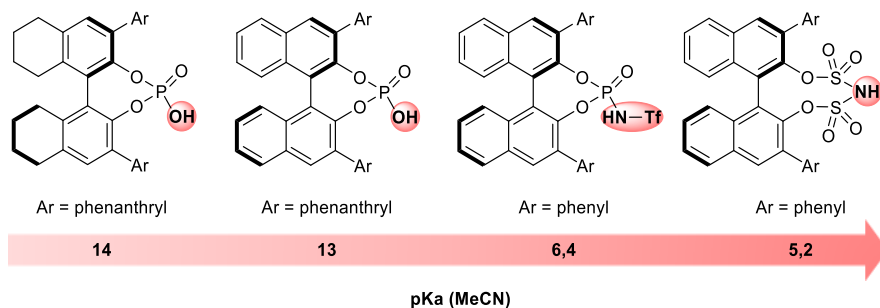


Figure 3.4. Acidity scale for the selected catalysts.

In summary, this portfolio of catalysts have shown to be very versatile systems for the development of highly efficient enantioselective transformations such as S_N1 ,²¹ Friedel-Craft,²² Mannich,²³ multicomponent reactions,²⁴ transfer hydrogenation,²⁵ dearomatization²⁶ or cycloaddition reactions among many others.^{11,27} Due to the relation with the research work developed in this chapter, the application of this type of catalysis to cycloaddition reactions would be described in more detail in the following sections.

²¹ Gualandi, A.; Rodeghiero, G.; Cozzi, P. G. *Asian J. Org. Chem.* **2018**, *7*, 1957.

²² (a) Kang, Q.; Zhao, Z.-A.; You, S.-L. *J. Am. Chem. Soc.* **2007**, *129*, 1484. (b) Itoh, J.; Fuchibe, K.; Akiyama, T. *Angew. Chem. Int. Ed.* **2008**, *47*, 4016. (c) Husmann, R.; Sugiono, E.; Mersmann, S.; Raabe, G.; Rueping, M.; Bolm, C. *Org. Lett.* **2011**, *13*, 1044. (d) Mori, K.; Wakazawa, M.; Akiyama, T. *Chem. Sci.* **2014**, *5*, 1799.

²³ (a) Rueping, M.; Sugiono, E.; Schoepke, F. R. *Synlett* **2007**, 1441. (b) Sickert, M.; Schneider, C. *Angew. Chem. Int. Ed.* **2008**, *47*, 3631. (c) Pansare, S. V.; Paul, E. K. *Chem. Eur. J.* **2011**, *17*, 8770.

²⁴ (a) Gong, L.-Z.; Chen, X.-H.; Xu, X.-Y. *Chem. Eur. J.* **2007**, *13*, 8920. (b) Yue, T.; Wang, M.-X.; Wang, D.-X.; Masson, G.; Zhu, J. *Angew. Chem. Int. Ed.* **2009**, *48*, 6717. (c) Yu, J.; Shi, F.; Gong, L.-Z. *Acc. Chem. Res.* **2011**, *44*, 1156.

²⁵ (a) De Vries, J. G.; Mršić, N. *Catal. Sci. Technol.* **2011**, *1*, 727. (b) Zheng, C.; You, S. L. *Chem. Soc. Rev.* **2012**, *41*, 2498. (c) Foubelo, F.; Yus, M. *Chem. Rec.* **2015**, *15*, 907. (d) Pálvölgyi, Á. M.; Scharinger, F.; Schnürch, M.; Bicaschröder, K. *Eur. J. Org. Chem.* **2021**, 5367.

²⁶ Xia, Z.-L.; Xu-Xu, Q.-F.; Zheng, C.; You, S.-L. *Chem. Soc. Rev.* **2020**, *49*, 286.

²⁷ (a) Monaco, M. R.; Pupo, G.; List, B. *Synlett* **2016**, *27*, 1027. (b) Li, X.; Song, Q. *Chin. Chem. Lett.* **2018**, *29*, 1181. (c) Merad, J.; Lalli, C.; Bernadat, G.; Maury, J.; Masson, G. *Chem. Eur. J.* **2018**, *24*, 3925. (d) Shao, Y.-D.; Cheng, D.-J. *ChemCatChem* **2021**, *13*, 1271. (e) Da, B.-C.; Xiang, S.-H.; Li, S.; Tan, B. *Chin. J. Chem.* **2021**, *39*, 1787.

1.2. Hydrazones in (3+2) cycloaddition reactions: synthesis of pyrazolidines

Pyrazolidines are saturated five-membered azacycloalkanes with two adjacent nitrogen atoms that share a single bond. This type of structural motif can be found at the core of several potential therapeutic agents such as anti-inflammatory, antidepressant, anticancer, antibacterial and antiviral compounds, as well as in unnatural aminoacids, and two examples are provided in Figure 3.5.²⁸

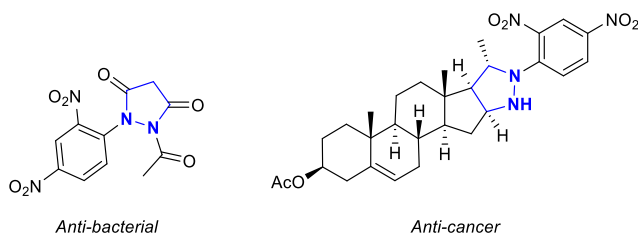


Figure 3.5. Bioactive pyrazolidine-based molecules.

Traditional methods for the stereoselective synthesis of pyrazolidines²⁹ include several cycloaddition reactions, in particular, the 1,3-dipolar or (3+2) cycloaddition between hydrazones and alkenes, in which the former participates as the 1,3-dipole partner (Scheme 3.5). However, the reported examples of this class of cycloadditions often involve Lewis acids,³⁰ under strong heating conditions³¹ or

²⁸ (a) Liu, B.; Brandt, J. D.; Moeller, K. D. *Tetrahedron* **2003**, *59*, 8515. (b) Baucke, D.; Lange, U. E. W.; Hornberger, W.; Mack, H.; Seitz, W.; Hoffken, H. W. *Bioorg. Med. Chem. Lett.* **2006**, *16*, 2648. (c) Davis, L. O. *Org. Pep. Proc. Int.* **2013**, *45*, 437.

²⁹ For reviews on pyrazolidine synthesis, see: (a) Lévai, A. *Chem. Heterocycl. Comp.* **1997**, *33*, 647. (b) Kumar, S.; Bawa, S.; Drabu, S.; Kumar, R.; Gupta, H. *Recent Pat. Anti-Infect. Drug Discovery* **2009**, *4*, 154. (c) Kissane, M.; Maguire, A. R. *Chem. Soc. Rev.* **2010**, *39*, 845. (d) Küchental, C. H.; Maison, W. *Synthesis* **2010**, 719. (e) Deiana, L.; Zhao, G.-L.; Leijonmarck, H.; Sun, J.; Lehmann, C. W.; Córdova, A. *ChemistryOpen* **2012**, *1*, 134.

³⁰ For Lewis acid catalyzed (3+2) cycloadditions of hydrazones, see: (a) Kobayashi, S.; Hirabayashi, R.; Shimizu, H.; Ishitani, H.; Yamashita, Y. *Tetrahedron Lett.* **2003**, *44*, 3351. (b) Frank, E.; Mucsi, Z.; Zupko, I.; Rethy, B.; Falkay, G.; Schneider, G.; Wollfling, J. *J. Am. Chem. Soc.* **2009**, *131*, 3894. (c) Zamfir, A.; Schenker, S.; Bauer, W.; Clark, T.; Tsogoeva, S. B. *Eur. J. Org. Chem.* **2011**, 3706. (d) Xie, H.; Zhu, J.; Chen, Z.; Li, S.; Wu, Y. *Synthesis* **2011**, 2767.

³¹ For (3+2) cycloadditions under thermal conditions, see: (a) Grigg, R.; Kemp, J.; Thompson, N. *Tetrahedron Lett.* **1978**, *19*, 2827. (b) Le Fevre, G.; Hamelin, J. *Tetrahedron Lett.* **1979**, *20*, 1757. (c) Snider, B. B.; Conn, R. S. E.; Sealfon, S. *J. Org. Chem.* **1979**, *44*, 218. (d) Grigg, R.; Dowling,

stoichiometric amounts of the corresponding acid because of the poor reactivity of hydrazones that do not show a particularly high tendency to participate as reactive 1,3-dipoles in cycloaddition chemistry.³² Given the usefulness of this type of molecules, considerable efforts have been devoted to the development of strategies that enable carrying out this particular type of (3+2) cycloadditions under milder conditions and up to date, some examples have been reported for the diastereoselective formation of pyrazolidines from hydrazones and activated alkenes using the chiral auxiliary approach.³⁰ In contrast, the enantioselective version of this reaction is still a challenge and only a few reports are present in the literature. In addition, enantiopure pyrazolidine analogs can also be used in organic synthesis, as direct precursors for the synthesis of chiral 1,3-diamine motifs,³³ through the reductive cleavage of the corresponding N-N bond. These 1,3-diamines have shown to be the key core for many active pharmaceuticals³⁴ and they can potentially serve as ligands in asymmetric catalysis.³⁵

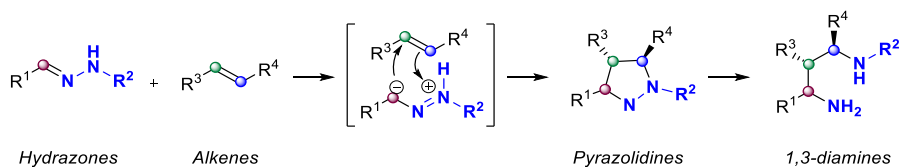
M.; Jordan, M. W.; Sridharan, V. *Tetrahedron* **1987**, *43*, 5873. (e) Khau, V. V.; Martinelli, M. J. *Tetrahedron Lett.* **1996**, *37*, 4323.

³² For stoichiometric achiral Brønsted acid catalysed (3+2) cycloadditions, see: (a) Hesse, K.-D. *Justus Liebigs Ann. Chem.* **1970**, *743*, 50. (b) Le Fevre, G.; Sinbandhit, S.; Hamelin, J. *Tetrahedron* **1979**, *35*, 1821. (c) Fouchet, B.; Joucla, M.; Hamelin, J. *Tetrahedron Lett.* **1981**, *22*, 1333. (d) Shimizu, T.; Hayashi, Y.; Kitora, Y.; Teramura, K. *Bull. Chem. Soc. Jpn.* **1982**, *55*, 2450. (e) Shimizu, T.; Hayashi, Y.; Miki, M.; Teramura, K. *J. Org. Chem.* **1987**, *52*, 2277. (f) Davis, L. O.; Daniel, W. F. M.; Tobey, S. L. *Tetrahedron Lett.* **2012**, *53*, 522.

³³ (a) Kizirian, J.-C. *Chem. Rev.* **2008**, *108*, 140. (b) Ji, X.; Huang, H. *Org. Biomol. Chem.* **2016**, *14*, 10557. (c) Fleurisson, C.; Benedetti, E.; Micouin, L. *Synlett* **2021**, *32*, 858.

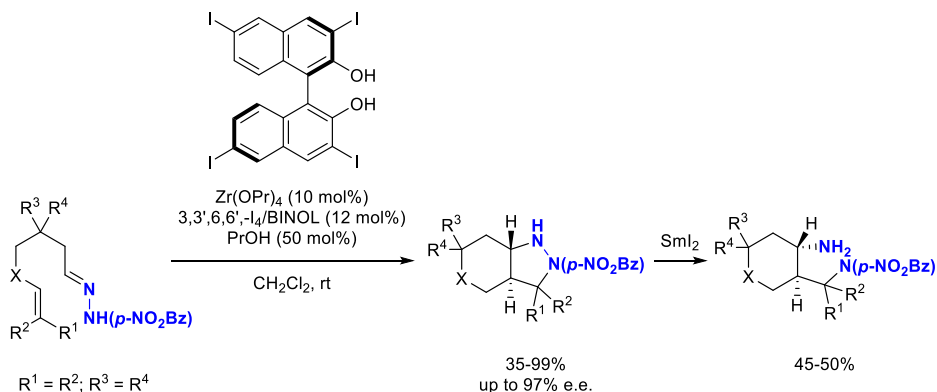
³⁴ (a) Andrews, D. M.; Cherry, P. C.; Humber, D. C.; Jones, P. S.; Kelling, S. P.; Martin, P. F.; Shaw, C. D.; Swanson, S. *Eur. J. Med. Chem.* **1999**, *34*, 563. (b) Chand, P.; Kotian, P. L.; Dehghni, A.; Kattan, Y.-E.; Lin, T.-H.; Hutchison, T. L.; Babu, Y. S.; Bantia, S.; Elliot, A. J.; Montgomery, J. A. *J. Med. Chem.* **2001**, *44*, 4379. (c) Bromba, C. M.; Mason, J. W.; Brant, G. M.; Chan, T.; Lunke, M. D.; Petric, M.; Boulanger, M. J.; Wulff, J. E. *Bioorg. Med. Chem. Lett.* **2011**, *21*, 7137.

³⁵ (a) Pini, D.; Mastantuono, A.; Uccello-Barretta, G. *Tetrahedron* **1993**, *49*, 9613. (b) Vedejs, E.; Kruger, A. W. *J. Org. Chem.* **1998**, *63*, 2792. (c) Yamashita, Y.; Odashima, K.; Koga, K. *Tetrahedron Lett.* **1999**, *40*, 2803. (d) Yamashita, Y.; Emura, Y.; Odashima, K.; Koga, K. *Tetrahedron Lett.* **2000**, *41*, 209. (e) Hems, W. P.; Groarke, M.; Zanotti-Gerosa, A.; Grasa, G. A. *Acc. Chem. Res.* **2007**, *40*, 1340. (f) Kano, T.; Yamaguchi, Y.; Maruoka, K. *Angew. Chem. Int. Ed.* **2009**, *48*, 1838. (g) Kodama, K.; Sugawara, K.; Hirose, T. *Chem. Eur. J.* **2011**, *17*, 13584. (h) Yao, Q. J.; Judeh, Z. M. A. *Tetrahedron* **2011**, *67*, 4086.



Scheme 3.5. Synthesis of pyrazolidine derivatives through 1,3-dipolar cycloaddition reaction.

The first enantioselective 1,3-dipolar cycloaddition was reported in 2002 by Kobayashi and co-workers.³⁶ In this example, the authors were able to develop an efficient chiral Zirconium(IV)/BINOL-based catalytic system for the intramolecular cycloaddition of unsaturated *N*-acylhydrazones giving access to bicyclic pyrazolidine scaffolds with good to excellent yields and total control on both diastereo- and enantioselectivity. Furthermore, the obtained bicyclic adducts could also be transformed into the corresponding chiral 1,3-diamines through a very simple procedure (Scheme 3.6).

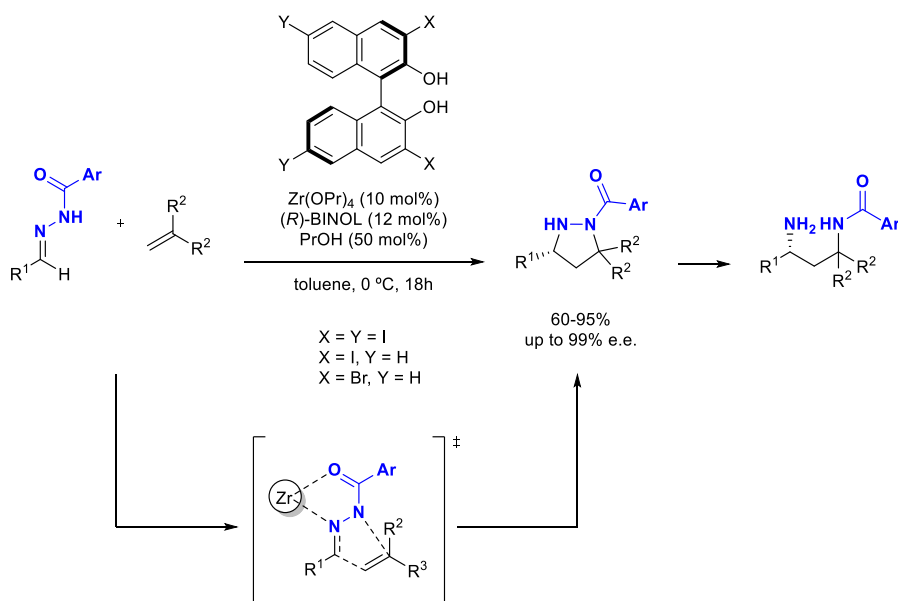


Scheme 3.6. Asymmetric (3+2) cycloaddition of *N*-acylhydrazones/olefins using a chiral Zirconium catalyst.

Two years later, the same research group reported the intermolecular version of this transformation using slightly modified conditions and achieving the first catalytic enantioselective intermolecular (3+2) cycloaddition reaction of *N*-benzoyl

³⁶ Kobayashi, S.; Shimizu, H.; Yamashita, Y.; Ishitani, H.; Kobayashi, J. *J. Am. Chem. Soc.* **2002**, *124*, 13678.

hydrazones to activated alkenes (Scheme 3.7).³⁷ Different substituted pyrazolidine derivatives and 1,3-diamines could be obtained with high yields and enantioselectivities. The group could also demonstrate experimentally that the reaction was proceeding through a concerted mechanism, therefore involving the simultaneous formation of the C-C and C-N bonds of the heterocyclic target.



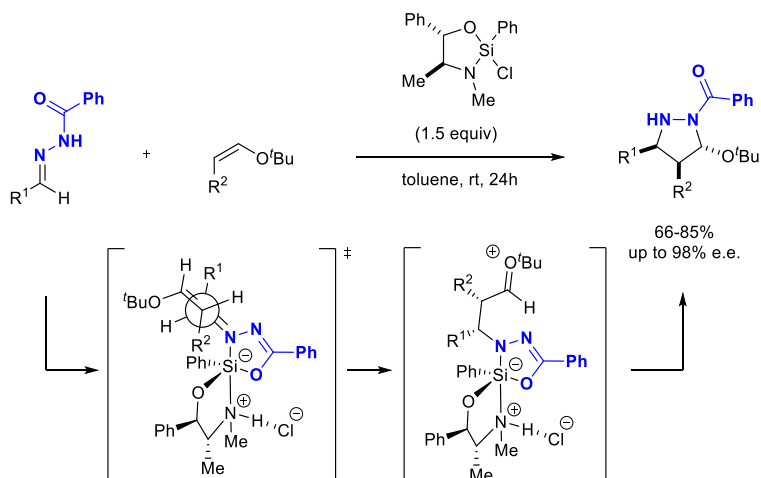
Scheme 3.7. Enantioselective Zr-catalyzed (3+2) cycloaddition of hydrazones with olefins.

In 2005, Leighton and co-workers developed a highly diastereo- and enantioselective (3+2) cycloaddition of benzoylhydrazones to enol ethers catalyzed by a chiral silane Lewis acid (Scheme 3.8).³⁸ Contrarily to the previously concerted mechanism described by Kobayashi, they proposed a stepwise mechanism for the silane-promoted reactions since the *cis*-enol ether led to the final product with a *trans* relationship between the *t*BuO and the R substituents. The authors proposed a model in which the enol ether approaches the more exposed *si* face of the hydrazone, which had previously suffered an isomerization of the C=N bond during

³⁷ Kobayashi, S.; Yamashita, Y. *J. Am. Chem. Soc.* **2004**, *126*, 11279.

³⁸ Shirakawa, S.; Lombardi, P. J.; Leighton, J. L. *J. Am. Chem. Soc.* **2005**, *127*, 9974.

the complexation with the Lewis acid catalyst, acquiring a final orientation in which steric interactions between the *tert*-butoxide bulky group and the complexed hydrazone were minimized during the final stereocontrolled ring closing.

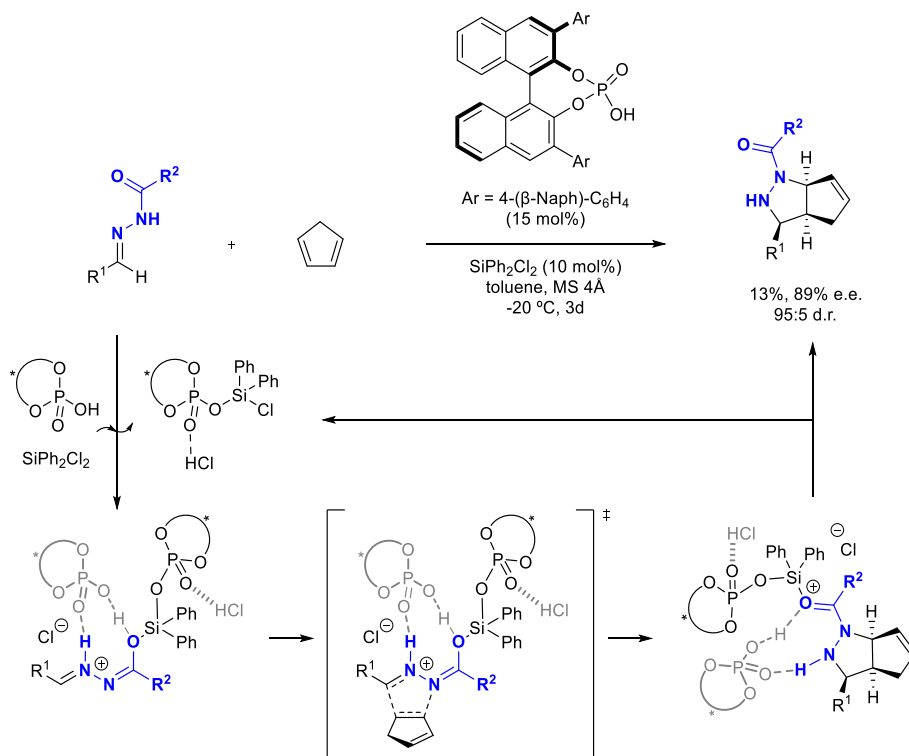


Scheme 3.8. Enantioselective silicon Lewis acid-catalyzed (3+2) cycloaddition reaction between hydrazones and enol ethers.

Inspired by the previous work of Kobayashi and Leighton, the group of Tsogoeva³⁹ reported a novel BINOL phosphate-derived silicon Lewis acid catalytic system for the (3+2) cycloaddition of *N*-benzoylhydrazones to cyclopentadiene. The reaction involved the *in situ* generation of the chiral catalyst, from the corresponding BINOL phosphoric acid and dichlorosilane, being this a suitable catalytic species that would activate the hydrazone and also would be involved in controlling the stereoselectivity of the reaction together with a second molecule of Si-free phosphoric acid. As it is shown in Scheme 3.9, the bifunctional character of the BINOL-based free phosphoric acid played a key role in the reaction outcome. Firstly, the Brønsted acidic part is proposed to coordinate to the hydrazone, stabilizing the proposed transition state and secondly, the P=O moiety is proposed to act as Lewis base that remains coordinated to the generated HCl, therefore

³⁹ (a) Zamfir, A.; Tsogoeva, S. B. *Synthesis* **2011**, 12, 1988. (b) Serdyuk, O. V.; Zamfir, A.; Hampel, F.; Tsogoeva, S. B. *Adv. Synth. Catal.* **2012**, 354, 3115.

preventing the non-enantioselective pathway that would lead to the racemic product. With this strategy they could demonstrate the potential of this new catalytic system by obtaining one example of bicyclic pyrazoline derivative in rather low yield but in high diastereomeric ratio and enantiomeric excess.

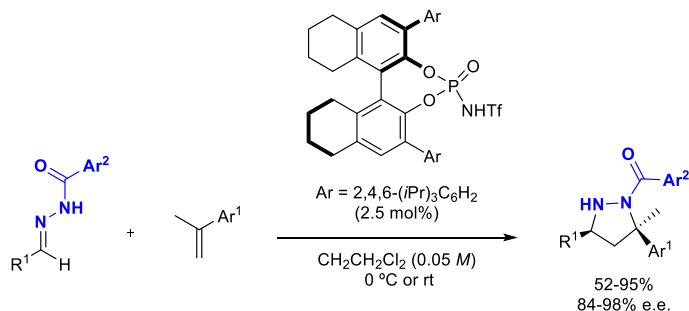


Scheme 3.9. Enantioselective BINOL-phosphate-derived silicon Lewis acid (3+2) cycloaddition between N-acylhydrazones and cyclopentadiene.

Concurrently, Rueping introduced the use of BINOL-based *N*-triflylphosphoramides as the best catalysts for the enantioselective cycloaddition between hydrazones and different alkenes under Brønsted acid catalysis (Scheme 3.10).⁴⁰ The authors found out in this work that the more acidic and active *N*-triflylphosphoramide Brønsted acids promoted the enantioselective (3+2) cycloaddition of a broad range of hydrazones and alkenes, leading to the selective

⁴⁰ Rueping, M.; Maji, M. S.; Küçük, H. B.; Atodiresei, I. *Angew. Chem. Int. Ed.* **2012**, *51*, 12864.

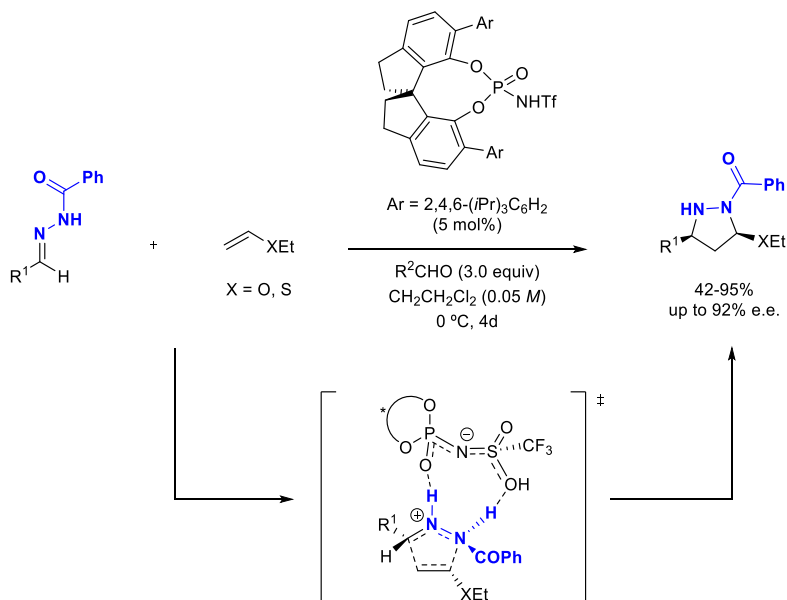
formation of optically active pyrazolidines and their corresponding enantioenriched cyclic 1,3-diamines with good to excellent yields and enantioselectivities.



Scheme 3.10. Enantioselective Brønsted acid catalysed (3+2) cycloaddition reaction.

The origin of the high catalytic efficiency and enantioselectivity of these reactions relies on the specific role of the catalyst during the formation of the transition state. As illustrated below in Scheme 3.11, the phosphoramidate is firstly involved in the formation of the 1,3-dipole through protonation. This leads to the formation of an ion-pair complex having a monopolar hydrazone salt that interacts with the chirality-controlling phosphoramidate anion, leading to the corresponding pyrazolidine products with outstanding results. Furthermore, the authors could observe that SPINOL-derived phosphoramidates provided better results in terms of enantioselectivity than the corresponding BINOL-based catalysts.⁴¹

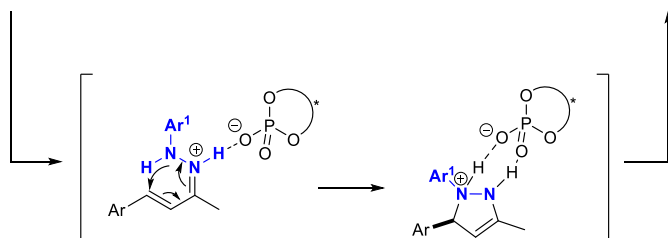
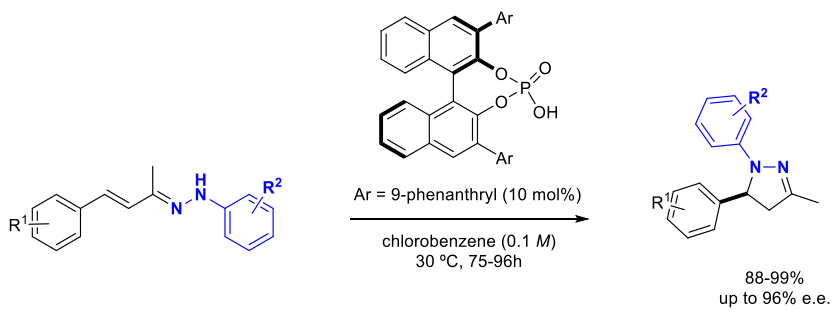
⁴¹ Hong, X.; Küçük, H. B.; Maji, M. S.; Yang, Y.-F.; Rueping, M.; Houk, K. N. *J. Am. Chem. Soc.* **2014**, *136*, 13769.



Scheme 3.11. Enantioselective N-triflylphosphoramidate catalyzed (3+2) cycloaddition between hydrazones and alkenes.

Finally, it has to be highlighted that the use of catalytic chiral Brønsted acids in cycloaddition and pericyclic reactions with hydrazones was already introduced by List and co-workers in 2009. The authors reported a pioneering enantioselective cycloisomerization of α,β -unsaturated hydrazones under BINOL-based chiral Brønsted acid catalysis, in which can be considered as an organocatalytic enantioselective version of the already known Fischer methodology to access pyrazolidines.⁴² As it is depicted in Scheme 3.12, the stereochemical outcome of the reaction was successfully directed by the interaction between the protonated and thus positively charged hydrazone intermediate with the corresponding counteranion of the chiral phosphoric acid. The formation of the specific *s-cis*-intermediate would prompt the further formal 6π -electrocyclization reaction furnishing the corresponding enantioenriched pyrazolines with excellent yields and enantioselectivities.

⁴² Müller, S.; List, B. *Angew. Chem. Int. Ed.* **2009**, *48*, 9975.

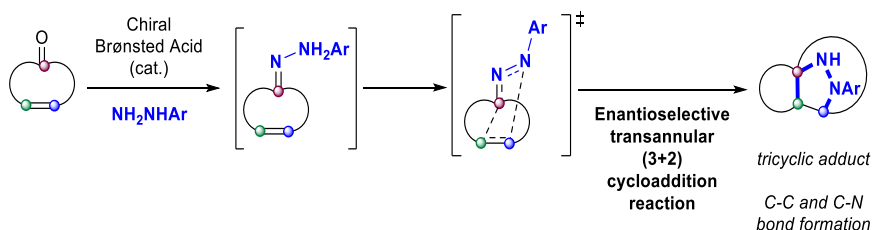


Scheme 3.12. Asymmetric 6 π -electrocyclization reaction.

2. SPECIFIC OBJECTIVES AND WORK PLAN

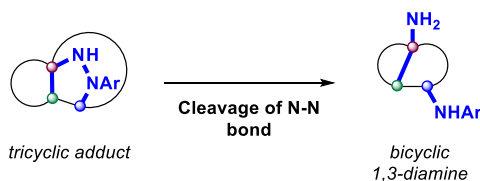
The bibliographic review disclosed in the introduction of this chapter highlights the synthetic utility of (3+2) cycloaddition reactions as an efficient strategy in order to selectively obtain five-membered *N*-heterocyclic rings in the minimum number of steps. In particular, the (3+2) cycloaddition reaction between a hydrazone and an alkene has proven to be an efficient strategy for the synthesis of pyrazolidines, which are frequently present as the basic core of much more complex biologically active structures. Although several inter- and intramolecular versions of this reaction have been already described, to the best of our knowledge there is not any transannular example that involves hydrazones as 1,3-dipoles reported up to date.

With the previously mentioned considerations and taking into account the broad experience of the group in organocatalysis, we decided to evaluate medium-sized cycloalkenones as suitable model systems for the development of a pioneer **catalytic and enantioselective transannular (3+2) cycloaddition reaction between hydrazones and alkenes under chiral Brønsted acid catalysis**. As it is shown in Scheme 3.13, the corresponding hydrazone intermediate would be firstly generated *in situ* after condensation of an hydrazine with the cycloalkenone. The second step would be the formation of the 1,3-dipole after the addition of a Brønsted acid, which will interact with the formed species and control the later transannular (3+2) cycloaddition process with the pending alkene, acting as the dipolarophile. The use of a chiral phosphoric acid catalyst would allow the control of the stereochemistry of the projected reaction.



Scheme 3.13. Specific objective of the project.

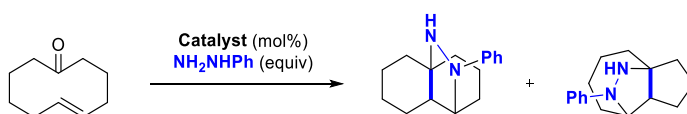
With this transformation, we anticipate the obtention of fused polycyclic pyrazolidine scaffolds through the consecutive formation of a C-C and a C-N bond in a single step. The corresponding obtained products would be good candidates for the direct synthesis of polycyclic 1,3-diamines after carrying out a reductive N-N bond cleavage (Scheme 3.14).



Scheme 3.14. Specific objective of the project.

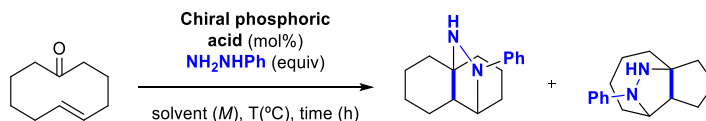
In order to achieve the stated objective, the following work plan was designed:

1. *Proof of concept:* Evaluation of the viability of the proposed reaction on a model cyclic enekoetone substrate and using phenylhydrazine in order to promote the *in situ* formation of the hydrazone intermediate, which can later undergo the transannular cycloaddition. As illustrated in Scheme 3.15, a 10-membered cycloalkenone would be selected as the model system in the presence of an achiral phosphoric acid as catalyst, such as diphenyl phosphate (DPP). Two possible regioisomers can be obtained from the second transannular (3+2) cycloaddition step.



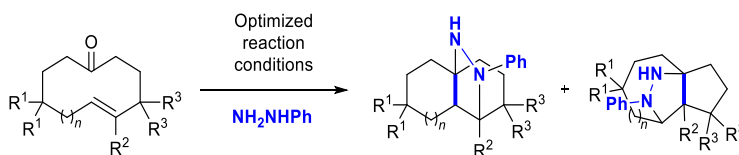
Scheme 3.15. Proof of concept of the envisioned reaction.

2. *Optimization of the reaction:* Chiral BINOL-based phosphoric acids will be evaluated in order to develop the enantioselective version of this transformation. In this sense, a screening of different catalysts, solvents, temperatures and reaction times will also be carried out in order to efficiently afford the desired tricyclic adducts in the highest yields and enantioselectivities (Scheme 3.16).



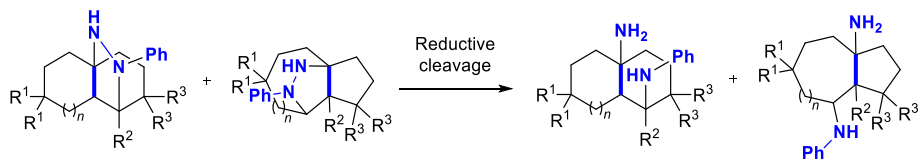
Scheme 3.16. Envisioned model reaction.

3. *Scope of the reaction:* Once the optimal reaction conditions have been established, a study of the influence of the different components of the reaction will be performed. For that, different aryl and alkyl hydrazines will be tested in order to study the electronic and steric influence on the reaction outcome. On the other hand, different cyclic ketones with a variety of substitution patterns and ring sizes will be prepared as well in order to determine the substrate scope of the transannular approach (Scheme 3.17).



Scheme 3.17. Scope of the reaction.

4. *Transformation of the adducts:* We will focus on demonstrating the synthetic applicability of the developed methodology by transforming the obtained enantioenriched polycyclic pyrazolidine scaffolds through reductive cleavage of the N-N bond in order to afford stereodefined bicyclic 1,3-diamines, which should be considered as highly valued molecular frameworks (Scheme 3.18).



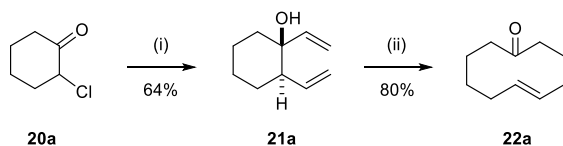
Scheme 3.18. Product transformation.

3. RESULTS AND DISCUSSION

In view of the described precedents on this topic and after establishing the specific objectives of the chapter, we describe here the discussion of the most representative results obtained on this part of the research work.

3.1. Proof of concept

Before testing the viability of the projected transannular (3+2) cycloaddition strategy stated in the work plan of this chapter, we first had to face the synthesis of the starting cyclic eneketone. The corresponding (*E*)-cyclodec-5-en-1-one (**22a**) can be accessed by an already reported two steps sequence, starting from 2-chlorocyclohexan-1-one (**20a**), involving double Grignard addition (i) and a subsequent oxy-Cope rearrangement (ii) as illustrated in Scheme 3.19.⁴³ Both reactions proceeded with good yields in our hands, obtaining the cyclic eneketone **22a** in a 51% overall yield from **20a** and also being able to perform the synthesis in a multigram scale obtaining 2-3 g of **22a**.



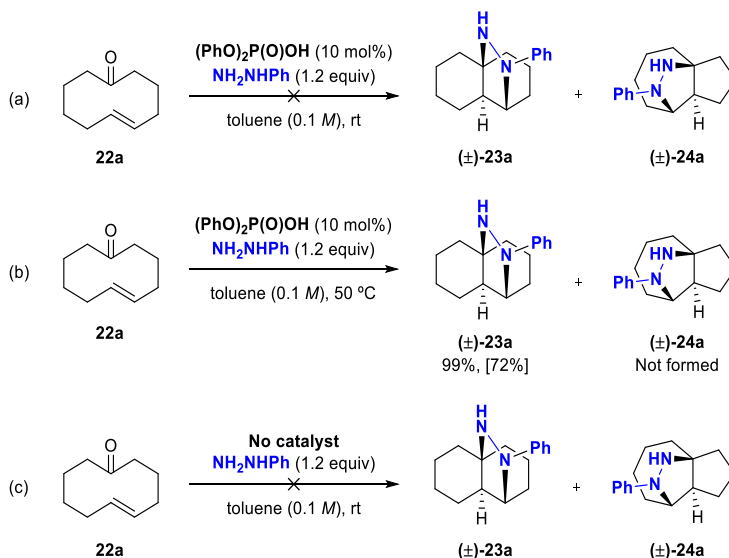
(i) $\text{CH}_2=\text{CHMgBr}$ (2.5 equiv), THF (0.7 M), 0 °C to 55 °C, 16h
(ii) KH (1.3 equiv), 18-crown-6 (2.0 equiv), THF (0.05 M), 0 °C to 80 °C, 3h

Scheme 3.19. Synthetic approach for the synthesis of model substrate **22a**.

With the desired model system in hand, the next step was to test the feasibility of the organocatalytic transannular transformation using phenylhydrazine as the precursor for the *in situ* formation of the hydrazone intermediate (Scheme 3.20). The initial attempt using diphenylphosphoric acid as the catalyst in toluene at room temperature was not successful (Scheme 3.20a) and the starting cycloalkenone

⁴³ (a) T. Kato, H. Kondo, M. Nishino, M. Tanaka, G. Hata, A. Miyake. *Bull. Chem. Soc. Jpn.* **1980**, 53, 2958. (b) G. A. Molander, B. Czakó, M. Rheam. *J. Org. Chem.* **2007**, 72, 1755.

(**22a**) was recovered as the corresponding phenylhydrazone, which was not stable enough and decomposed after purification by flash column chromatography. Nevertheless, this experiment evidenced that the selected hydrazine was able to form *in situ* the hydrazone in the tested reaction conditions. At this point, we thought that the reaction might need to be heated in order to facilitate the reactivity of the generated intermediate with the alkene moiety pending in the cyclic substrate, giving the complete transannular sequence. In fact, when the reaction was performed at 50°C, we could observe full conversion of the starting material towards the formation of the desired cycloaddition product ((±)-**23a**). The reaction took place with good isolated yield and total control on the regio- and the diastereoselectivity (Scheme 3.20b). Compound (±)-**23a** was obtained as a single diastereoisomer of the corresponding cycloaddition adduct containing two fused 6-membered rings and a bridged pyrazolidine scaffold, without observing the formation of the corresponding regioisomer (±)-**24a**. When the reaction was tested without the presence of the acidic catalyst, the unreacted cycloalkenone **22a** was recovered (Scheme 3.20c).

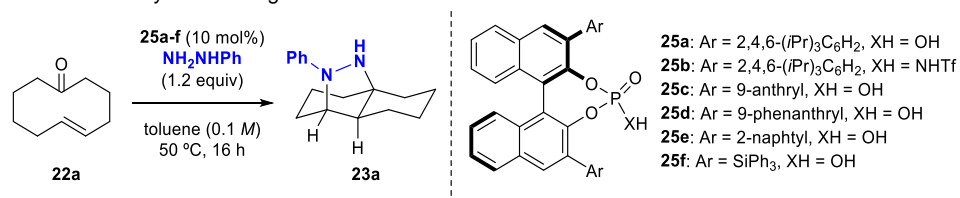


Scheme 3.20. Proof of concept experiments carried out with the model substrate.

3.2. Optimization of the reaction conditions

Once it was demonstrated the ability of (*E*)-cyclodec-5-en-1-one (**22a**) to undergo efficient transannular (3+2) cycloaddition reaction under acid catalysis with total control on the regio- and diastereoselectivity, we next evaluated the possibility of introducing a chiral Brønsted acid catalyst in order to develop the enantioselective version of this transformation to obtain the corresponding chiral tricyclic adduct in an enantioenriched form. For this reason, different chiral BINOL-based phosphoric acids were tested under the previously tested reaction conditions in order to evaluate whether this particular catalyst scaffold would be good to trigger the transformation and to induce enantioselectivity (Table 3.1). To our delight, the first experiment using the archetypical chiral TRIP phosphoric acid catalyst resulted in the complete conversion of the starting material into the tricyclic product (**23a**) with 85% of enantiomeric excess (Entry 1). We also tested the corresponding *N*-trifluoromethylmethanesulfonylamide (**25b**), as a more acidic and therefore potentially more active catalyst, but the reaction performed less efficiently, providing the product with poorer results (Entry 2).

Table 3.1. Optimization of the acid-catalyzed transannular (3+2) cycloaddition using **22a** as model substrate: catalyst screening.^[a]



Entry	Catalyst	Conv.(%), [IY (%)] ^[b]	e.e. (%) ^[c]
1	25a	99	85
2	25b	55, [39]	25
3	25c	99	33
4	25d	99	23
5	25e	99	17
6	25f	99, [92]	88

[a] Reactions were performed with 0.15 mmol of **22a**, **NH₂NHPH** (1.2 equiv), **25a-f** (10 mol%) for 16h.

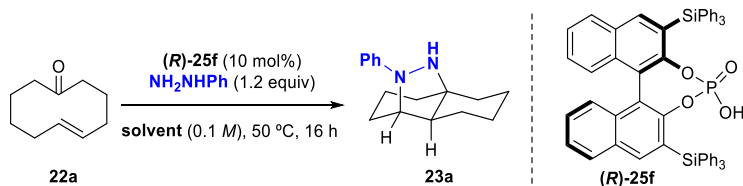
[b] Conversion was calculated by ¹H-NMR as consumption of starting material using 1,3,5-trimethoxybenzene as internal standard; [IY (%)] = isolated yield after flash column chromatography purification.

[c] e.e. was calculated by HPLC on chiral stationary phase after derivatization into the corresponding benzoyl hydrazide.

At this point and since chiral phosphoric acid showed better performance in the reaction outcome, we decided to test different substituents at the 3- and 3'-positions of the BINOL core (Entries 3-6). When the extended π -aryl substituents were placed, high conversions were obtained, however, with a significant decrease in the enantioselectivity (Entries 3-5), whereas the SiPh₃-containing catalyst ((**R**)-**25f**) afforded the product in high isolated yield and slightly better enantioselectivity (88% e.e) (Entry 6).

In view of the obtained results, we next performed a solvent screening in order to see the influence of this parameter in the transannular cycloaddition reaction, using catalyst (**R**)-**25f** as the one that provided the highest enantiocontrol (Table 3.2). When the reaction was performed using different aromatic solvents, the corresponding cycloaddition product was obtained in excellent yields (Entries 1 and 2). However, for the case of chlorobenzene a decrease of the enantioselectivity could be observed (Entry 2). The same trend was observed for protic solvents such as EtOH (Entry 5) whereas for THF or CHCl₃ enantioselectivity was moderate within low conversions (Entries 3 and 4). On the other hand, when the reaction was carried out in CH₂Cl₂, we observed quantitative conversion and the enantioselectivity was as high as in toluene (Entry 6 and 1).

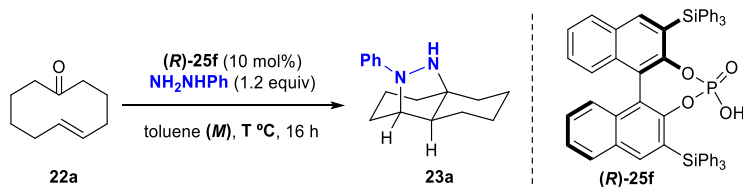
Table 3.2. Optimization of the acid-catalyzed transannular (3+2) cycloaddition using **22a** as model substrate: solvent screening.^[a]



Entry	Solvent	Conv.(%), [IY (%)] ^[b]	e.e. (%) ^[c]
1	toluene	99, [92]	88
2	C ₆ H ₅ Cl	99	21
3	THF	42	53
4	CHCl ₃	33	75
5	EtOH	68	16
6	CH ₂ Cl ₂	99, [91]	89

[a] Reactions were performed with 0.15 mmol of **22a**, NH_2NHPPh (1.2 equiv), **(R)-25f** (10 mol%) for 16 h. [b] Conversion was calculated by ¹H-NMR as consumption of starting material using 1,3,5-trimethoxybenzene as internal standard ; [IY (%)] = isolated yield after flash column chromatography purification. [c] e.e. was calculated by HPLC on chiral stationary phase after derivatization into the corresponding benzoyl hydrazone.

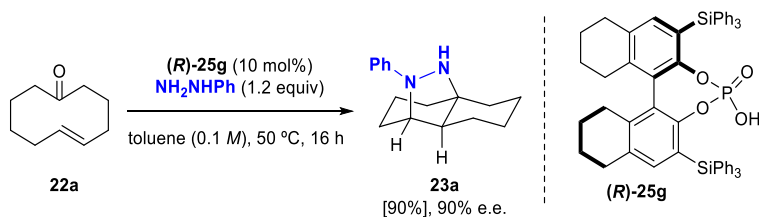
At this stage, the influence of the temperature on the reaction outcome was evaluated in detail, since the preliminary experiments showed that the reaction needed to be heated in order to proceed to completion. As it is illustrated in Table 3.3, when the reaction was performed at room temperature or 30 °C, the corresponding product **23a** could be detected in a rather low yields, together with a considerable amount of the unreacted hydrazone intermediate (Entry 1 and 2). Increasing the temperature to 40 °C favoured the reaction but again, with a moderate performance in terms of both yield and enantioinduction (Entry 3). Therefore, we decided to consider 50 °C (Entry 4) as the optimal temperature and we next evaluated whether carrying out the reaction under more concentrated or diluted conditions could improve these results. Nevertheless, neither more diluted conditions, nor more concentrated ones provided better results (Entries 5 and 6).

Table 3.3. Optimization of the acid-catalyzed transannular (3+2) cycloaddition using **22a** as model substrate: temperature and concentration.^[a]

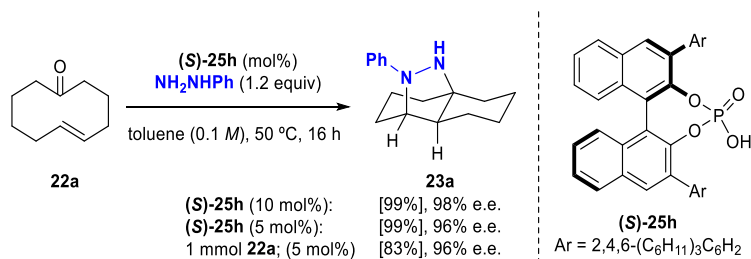
Entry	Solvent	Conc. (M)	T (°C)	Conv.(%) [IY (%)] ^[b]	e.e. (%) ^[c]
1	toluene	0.1	rt	<5 ^[d]	--
2	toluene	0.1	30	25	n.d. ^[e]
3	toluene	0.1	40	46	79
4	toluene	0.1	50	99, [92]	88
5	toluene	0.05	50	99	71
6	toluene	1	50	95	49

[a] Reactions were performed with 0.15 mmol of **22a**, NH_2NHPH (1.2 equiv), **(R)-25f** (10 mol%) for 16 h. [b] Conversion was calculated by $^1\text{H-NMR}$ as consumption of starting material using 1,3,5-trimethoxybenzene as internal standard; [IY (%)] = isolated yield after flash column chromatography purification. [c] e.e. was calculated by HPLC on chiral stationary phase after derivatization into the corresponding benzoyl hydrazide. [d] Starting material was recovered as the corresponding hydrazone. [e] n.d. = not determined.

The study of all the mentioned parameters led us to go backwards in the optimization and to reconsider the structure of the chiral catalysts. We started by evaluating the hydrogenated version of the optimal catalyst **(R)-25f**. To our delight, as illustrated in Scheme 3.21, catalyst **(R)-25g** showed slightly improved results in terms of enantiocontrol.

**Scheme 3.21.** Optimization of the chiral phosphoric acid catalyst.

Complementarily, since TRIP phosphoric acid ((*R*)-**25a**) also showed good values of enantioselectivity, we next decided to synthesize and test the corresponding bulkier analogue ((*S*)-**25h**) shown in Scheme 3.22. In this particular case, the projected transformation performed outstandingly giving higher yields and enantioselectivity values, even decreasing the catalyst loading to a 5 mol%. We also tested the viability of the methodology for preparative purposes by carrying out the reaction on a higher 1.0 mmol scale of the model substrate **22a**.



Scheme 3.22. Optimization of the chiral phosphoric acid catalyst and scale-up.

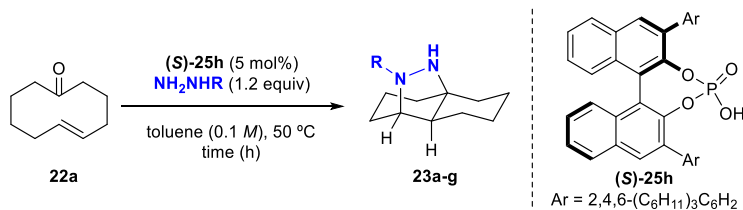
3.3. Scope of the enantioselective transannular (3+2) cycloaddition reaction

Once the optimal conditions were found and with a robust experimental protocol in hand, we proceed to study the scope and limitations of the reaction. First of all, we explored the influence of the hydrazine component and specifically, the nature of the hydrazine substituent using eneketone substrate **22a** as a model system (Table 3.4).

When a series of arylhydrazines containing electron-withdrawing substituents at the *para*-position were tested, the corresponding tricyclic adducts were isolated in excellent yields and enantioselectivities (Entries 1-4). The particular case of *meta*-bis-CF₃-substituted hydrazine provided the desired product but with a decrease of the enantiocontrol (Entry 5). When we moved to electron-donating substituents (CH₃) in the *para*-position of the aryl moiety, the reaction took place very efficiently but longer reaction time was needed in order to proceed to completion (Entry 6). However, when a more electron-rich *para*-methoxy hydrazine was used, the

corresponding hydrazone was identified instead, not observing the formation of the desired tricyclic transannular adduct (Entry 7). All products **23a-g** were formed as single regioisomers and diastereoisomers.

Table 3.4. Scope of the enantioselective transannular (3+2) cycloaddition reaction: Hydrazone component.^[a]

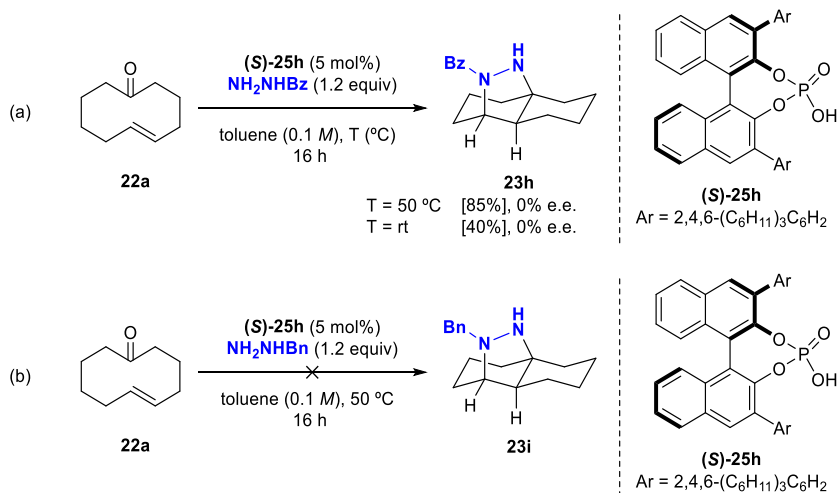


Entry	R	time (h)	[IY%] ^[b]	e.e. (%) ^[c]
1	C ₆ H ₅ (23a)	16	99	96
2	C ₆ F ₅ (23b)	16	96	90
3	4-CF ₃ C ₆ H ₄ (23c)	16	95	83
4	4-BrC ₆ H ₄ (23d)	16	84	96
5	3,5-(CF ₃) ₂ C ₆ H ₃ (23e)	16	90	72
6	4-CH ₃ C ₆ H ₄ (23f)	24	99	94
7	4-CH ₃ OC ₆ H ₄ (23g)	96	<5 ^[d]	n.d. ^[e]

[a] Reactions were performed with 0.15 mmol of **22a**, NH₂NHR (1.2 equiv), (**S**)-**25h** (5 mol%) and toluene (0.1 M) at 50°C. [b] [IY (%)] = isolated yield after flash column chromatography purification.

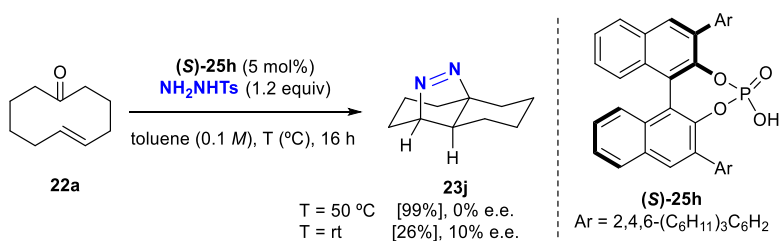
[c] e.e. was calculated by HPLC on chiral stationary phase after derivatization into the corresponding benzoyl or acetyl hydrazone. [d] Starting material was recovered as the corresponding hydrazone. [e] n.d. = not determined.

N-benzoylhydrazine was also reacted under the optimized conditions, and although the reaction took place remarkably fast, the corresponding product was isolated as a completely racemic mixture, even testing it at different temperatures (Scheme 3.23a). On the other hand, benzyl hydrazone was unreactive towards the transannular cycloaddition transformation (Scheme 3.23b).



Scheme 3.23. Transannular (3+2) cycloaddition using *N*-benzoyl and benzylhydrazine.

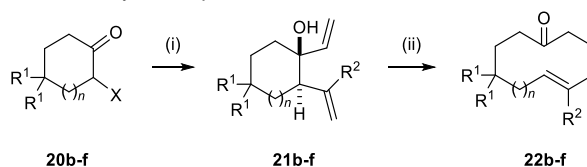
Interestingly, when the reaction was carried out using *p*-toluenesulfonyl hydrazide we could isolate a new product, (**23j**), which resulted from the cycloaddition process followed by elimination of *p*-TsOH in quantitative yield. This compound was isolated as a single regioisomer and as a single diastereoisomer. However, HPLC analysis indicated that it had been formed as a complete racemic mixture, even lowering the temperature from 50 °C to room temperature (Scheme 3.24).



Scheme 3.24. Transannular (3+2) cycloaddition involving *p*-toluenesulfonyl hydrazine.

The next step was to evaluate the influence of the size of the cyclic eneketone substrate on the reaction outcome and the possibility of introducing different substitution patterns. For that purpose, a family of several cycloalkenones were prepared containing different substitution patterns and different ring sizes, following the described methodologies found in the literature and summarized in Table 3.5. The corresponding cyclic eneketones were prepared as described for the model system, through the already reported two steps sequence, containing a first double Grignard addition (i) and a subsequent oxy-Cope rearrangement (ii).⁴³

Table 3.5. Synthetic protocol for substrates **22b-f**.



- (i) 1. $\text{CH}_2=\text{CR}^2\text{MgBr}$ (1.2 equiv), THF (0.7 M), 0 °C to rt, 2h
 2. $\text{CH}_2=\text{CHMgBr}$ (1.2 equiv), THF (0.7 M), 0 °C to 55 °C, 16h
 (ii) KH (1.3 equiv), 18-crown-6 (2.0 equiv), THF (0.05 M), 0 °C to 80 °C, 3h

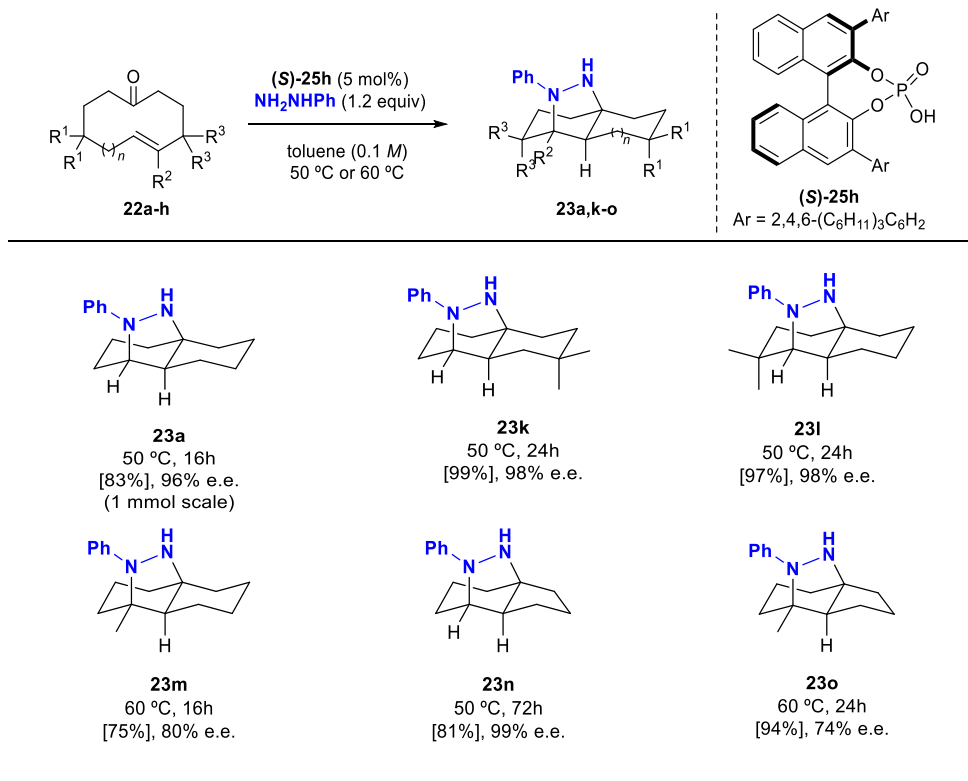
20	<i>n</i>	R¹	R²	X	(i)		(ii)	
					21	[Y%]	22	[Y%]
20b	1	Me	H	Br	21b	36	22b	63
20c	1	H	Me	Cl	21c	55	22c	65
20d	0	H	H	Cl	21d	73	22d	57
20e	2	H	H	Br	21e	59	22e	55
20f	3	H	H	Br	21f	30	22f	13

However, not all the projected starting materials could be prepared following the same synthetic route and an alternative strategy was found in the literature for the preparation of compounds **22g** and **22h** as seen in Scheme 3.25.⁴⁴ In this case, a four steps synthesis was required starting from the ring opening of the corresponding commercially available epoxides (**26a** and **26b**)/Swern oxidation sequence (i), followed by a Grignard addition (ii) and a subsequent oxy-Cope rearrangement (iii).

⁴⁴ (a) K. Tomooka, T. Ezawa, H. Inoue, K. Uehara, K. Igawa. *J. Am. Chem. Soc.* **2011**, 133, 1754. (b) N. S. Rajapaksa, E. N. Jacobsen. *Org. Lett.* **2013**, 15, 4238.

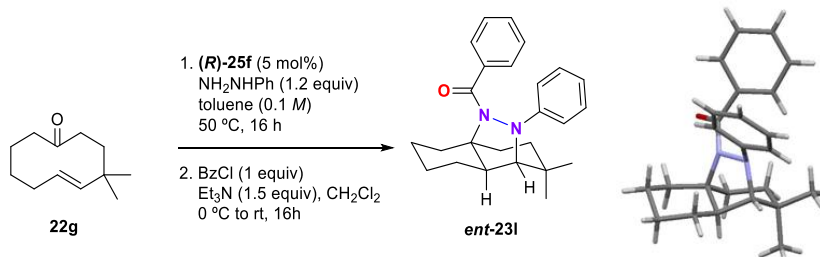
23m and **23o**, in which two α -tertiary hydrazine stereogenic centers are simultaneously generated.

Table 3.6. Scope of the enantioselective transannular (3+2) cycloaddition reaction: Cyclic ketone reagent.^[a]



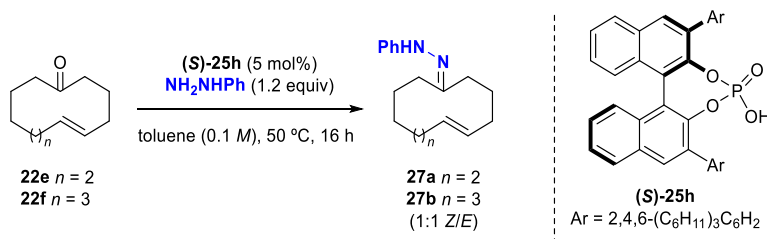
[a] Reactions were performed with 0.15 mmol of **22a-h**, NH_2NHPH (1.2 equiv), **(S)-25h** (5 mol%) and toluene (0.1 M) at the indicated temperature and isolated yields after flash chromatography purification are given. e.e. was calculated by HPLC on chiral stationary phase after derivatization into the corresponding benzoyl hydrazide.

The absolute configuration of the products obtained in the catalytic enantioselective transannular (3+2) cycloaddition reaction could be determined by X-ray analysis of a crystalline sample of the corresponding *N*-benzoyl derivate of compound **ent-23l** (Scheme 3.26). The enantiopure product was obtained following using catalyst **(R)-25f** (See Table 3.1). The configuration of all other adducts were established based on mechanistic analogy.



Scheme 3.26. Absolute stereostructure of compound **ent-231**.

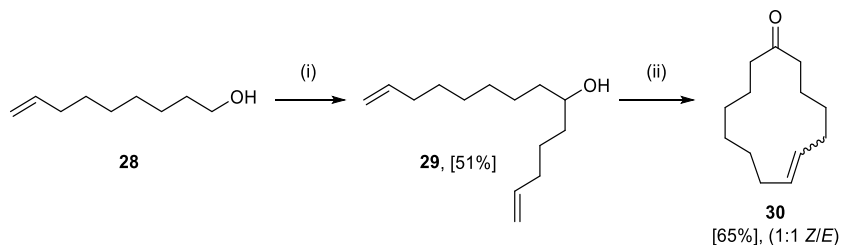
When eleven and twelve-membered cyclic eneketones were tested the projected transannular (3+2) cycloaddition did not occur (Scheme 3.27). Instead, when compounds **22e** and **22f** were subjected to the optimized reaction conditions, we were able to see the *in situ* formation of the corresponding hydrazone intermediate, as a 1:1 mixture of *Z/E* isomers that were unable to further react with the alkene moiety even heating the reaction at different temperatures.



Scheme 3.27. Unsuccessful cycloalkenones.

In order to overcome this situation, we next considered the preparation of a larger macrocyclic system, which could show less rigidity and therefore, to facilitate the spatial approximation of both functional groups. Initial attempts to prepare the previously mentioned substrate following the synthesis used before was not successful and we had to find out a new synthetic route that provided the desired macrocycle in synthetically useful amounts. For that, we decided to establish a new synthetic route based on the ring-closing metathesis (RCM) strategy as it had been

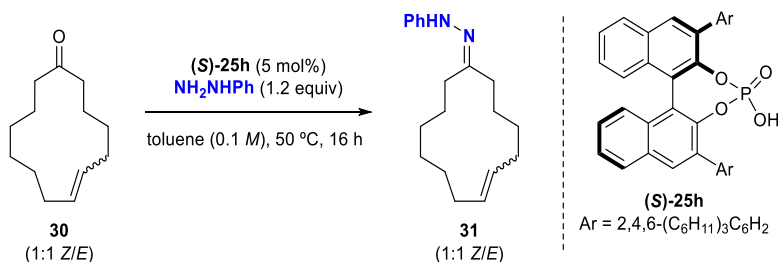
done in some reported examples for the preparation of complex macrolide rings.⁴⁵ As it is shown in Scheme 3.28, the desired macrocyclic precursor was obtained, following the indicated procedure and the resulting cycloalkenone was isolated as a 1:1 mixture of the *Z/E* isomers.



- (i) 1. DMP (2.2 equiv), CH_2Cl_2 (0.1 M), rt, 2h
 2. $\text{CH}_2=\text{CHCH}_2(\text{CH}_2)_n\text{CH}_2\text{MgBr}$ (1.5 equiv), THF (0.1 M), 0 °C to rt, 16h
 (ii) 1. DMP (2.2 equiv), CH_2Cl_2 (0.1 M), rt, 2h
 2. Grubbs 2nd gen. (5 mol%), toluene (0.001 M) (under Ar), reflux, 4h

Scheme 3.28. Synthetic protocol for substrates **30**.

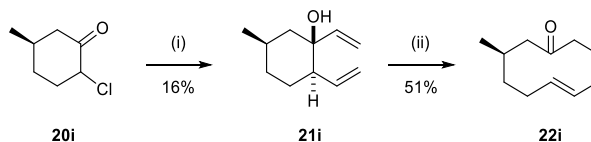
When eneketone **30** (used as *Z/E* mixture of diastereoisomers) was reacted under the optimized conditions, again the hydrazone intermediate was formed but the subsequent transannular cycloaddition step did not occur (Scheme 3.29).



Scheme 3.29. Unsuccessful cycloalkenones.

⁴⁵ Halle, M. B.; Fernandes, R. A. *RSC Adv.* **2014**, *4*, 63342.

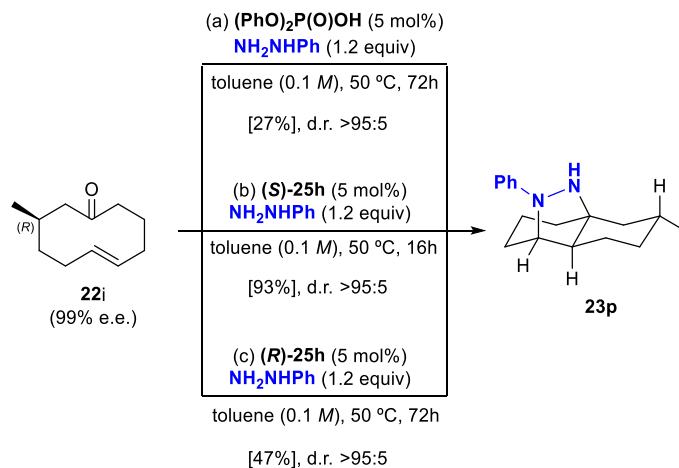
After exploring the scope of the reaction, we next decided to survey a cycloalkenone (**22i**) that contains a stereogenic centre to get further insights into the natural reactivity of this type of starting materials towards the transannular cycloaddition reaction. For this purpose, the cyclic eneketone **22i** was prepared, following the synthetic route used for the preparation of the model system, as illustrated in Scheme 3.30.⁴⁴



(i) $\text{CH}_2=\text{CHMgBr}$ (2.5 equiv), THF (0.7 M), 0 °C to 55 °C, 16h
(ii) KH (1.3 equiv), 18-crown-6 (2.0 equiv), THF (0.05 M), 0 °C to 80 °C, 3h

Scheme 3.30. Synthetic approach for the synthesis of substrate **22i**.

When an achiral catalyst, such as diphenylphosphoric acid, was used we could observe the clean formation of the cycloaddition product **23p** as a single diastereoisomer, although with a low isolated yield, even after long reaction times (Scheme 3.31a). Contrarily, the reaction took place smoothly with the previously described optimized reaction conditions using catalyst **25h**, affording the same product diastereoselectively within higher isolated yield (Scheme 3.31b). However, when the other enantiomer of the catalyst was tested, the obtained diastereoisomer was again the same but providing the desired product in a rather low yield (Scheme 3.31c).



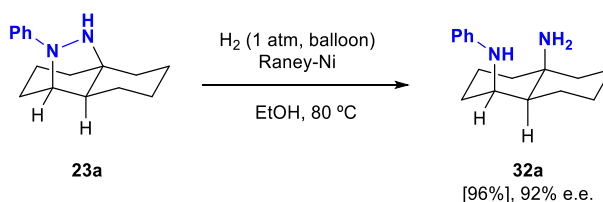
Scheme 3.31. Transannular (3+2) cycloaddition of chiral ketone **22i** as substrate.

The corresponding experiments showed us a strong stereochemical bias due to the presence of chiral information in the starting material. Besides, we can observe an important matched/mismatched scenario when a chiral Brønsted acid is incorporated to the reaction in order to promote the transannular transformation. Therefore, the (R) -ketone/ $(S)\text{-}25\text{h}$ combination of reagents would be the matched scenario whereas the (R) -ketone/ $(R)\text{-}25\text{h}$ the mismatched one.

3.4. Transformation of the adducts: Synthesis of enantioenriched 1,3-diamines

The next challenge we envisaged was to unmask the present 1,3-diamine functionality of the adducts obtained through the established enantioselective transannular (3+2) cycloaddition methodology. Analysing the structure of products **32a,k-p** (Table 3.7), we can see that the nitrogen atoms are located in a particular arrangement that would directly lead to the formation of complex molecular architectures, with decaline or octahydro-1*H*-indene basic core, containing two α -tertiary amine substituents in pseudoaxial positions. This particular *cis*-1,3-diamine scaffolds are challenging structures since they have shown to be difficult to be obtained selectively using conventional approaches.

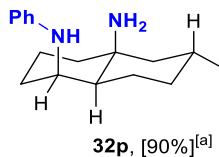
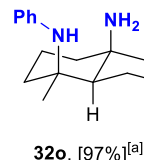
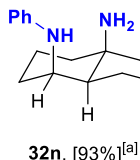
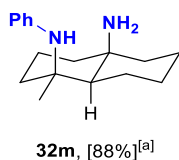
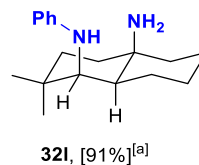
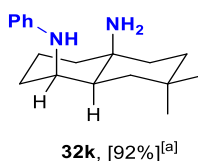
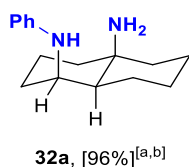
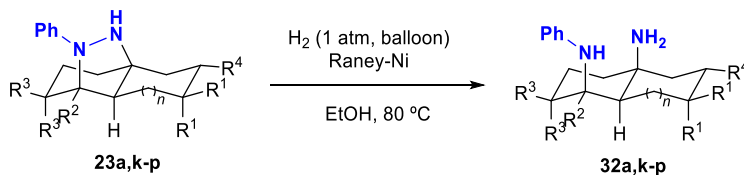
Therefore, the corresponding diamines were obtained by carrying out the hydrogenolytic cleavage of the N-N bond of the corresponding adducts. We optimized the reaction conditions by reacting compound **23a** with hydrogen (1 atm), under Raney-nickel catalysis in ethanol at 80 °C,⁴⁶ and we could obtain the corresponding diamine **32a** in excellent yield. Then, we verified that there was no loss of optical purity during the transformation by high-performance liquid chromatography (HPLC) on a chiral stationary phase under conditions optimized for a racemic standard.



Scheme 3.32. Reductive N-N cleavage of the model system.

With the optimized protocol established, we extended the reaction to all the previously obtained tricyclic adducts (**23k-p**), obtaining in all cases the desired bicyclic *cis*-1,3-diamines (**32k-p**) in excellent isolated yields. As it is summarized in Table 3.7, this strategy gives a direct access to the preparation of octahydronaphthalene-1,4a(2*H*)-diamines (compounds **32a,k-m,p**) or octahydro-3a*H*-indene-3a,7-diamines (**32n-o**) in almost quantitative overall yields and as high enantioenriched materials.

⁴⁶ Wu, X.; Liu, B.; Zhang, Y.; Jeret, M.; Wang, H.; Zheng, P.; Yang, S.; Song, B.-A.; Chi, Y. R. *Angew. Chem. Int. Ed.* **2016**, *55*, 12280.

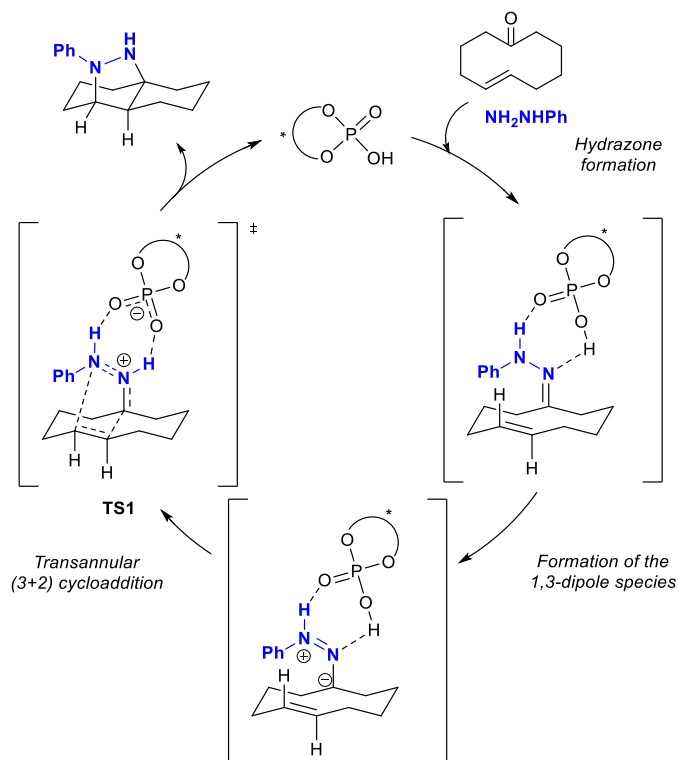
Table 3.7. Reductive cleavage of the hydrazone moiety: Synthesis of enantioenriched 1,3-diamines.

[a] [IY (%)] = isolated yield after flash column chromatography purification. [b] e.e. was determined by HPLC analysis on chiral stationary phase.

3.5. Mechanistic insights and stereochemistry of the reaction

Considering the background knowledge on chiral Brønsted acid catalysis from the previously summarized research works and experimental observations acquired during the development of the current project, the following mechanistic proposal and a rationalized model for the obtained diastereoselectivity are proposed in this section.

In this case we propose an analogous scenario for the transannular (3+2) cycloaddition reaction to that proposed by Rueping⁴¹ on the corresponding Brønsted acid-catalyzed intramolecular (3+2) cycloaddition between hydrazones and alkenes, which is summarized in Scheme 3.33. First of all, condensation of the phenylhydrazine with the ketone moiety should occur leading to the *in situ* formation of the desired hydrazone intermediate, as a mixture of the *Z/E* isomers of the corresponding C=N bond. Then, the chiral phosphoric acid would interact with the intermediate generating a hydrogen bonded complex followed by the formation of the 1,3-dipole reacting species. In contrast to the previous literature reports on intermolecular (3+2) cycloadditions with activated hydrazones described by Rueping,⁴¹ *N*-triflylphosphoramidate catalysts are normally used instead of the weak phosphoric acid, since protonation of the hydrazone is not favoured and larger distortion energy is required for the formed complex to achieve the “ion-pair” type geometry in the cycloaddition transition state and therefore, affords the transformation with high efficiency. However, in our case the isomerization of the hydrazone to the corresponding azomethine imine should occur and at this point, the dienophile would be placed directly in front of the formed 1,3-dipole, favouring the final transannular cycloaddition step. The strain release during the transannular C-C bond formation through a most likely concerted pathway leads to the formation of the final product with two fused 6-membered rings, with a bridged pyrazolidine scaffold that is delivered after releasing the catalyst.



Scheme 3.33. Proposed catalytic cycle.

Remarkably, despite the possibility of having two possible regioisomers from the transannular (3+2) cycloaddition step, in our case we could always observe the final formation of a single isomer containing a decaline scaffold. As it has been already disclosed in the general introduction of this work, the strain release involved for the formation of a decaline scaffold is considerably higher than the one for the formation of the decahydroazulene bicyclic product, meaning that the first system would be less strained and therefore its formation would be favoured (Figure 3.6).

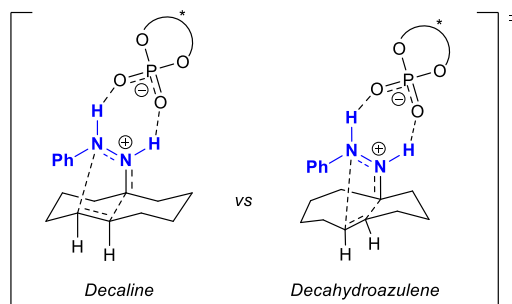


Figure 3.6. Decaline and decahydroazulene scaffolds.

This fact justifies the observed limitations regarding the different ring sizes tested, since in those particular cases not only the dipolarophile would be placed further away from the 1,3-dipole but also the formation of the final bicyclic system would not be prompted for a considerable strain release as for the cyclodecenone substrate. Furthermore, for the particular case of cyclodecenone **22i**, the introduction of a methyl group would fix the more stable conformation of the bicyclic system and thus, in all cases the stereochemistry of this reaction is no longer controlled by the chiral catalyst but through the substrate instead.

Finally, concerning the high enantioselectivity observed in the reaction, we propose the following stereochemical model illustrated in Figure 3.7. The presented bulky chiral phosphoric acid would bind the corresponding azomethine imine species generating a chirality-controlling anion that would stabilize the corresponding transition state (**TS1**). Therefore, the transannular (3+2) cycloaddition step would proceed inside the chiral cavity generated by the catalyst favouring the addition of the 1,3-dipole to the alkene to occur from the illustrated face of the molecule. This configuration is also in agreement with the reported stereochemical model for the intermolecular addition of activated alkenes to hydrazones under phosphoric acid catalysis.⁴¹

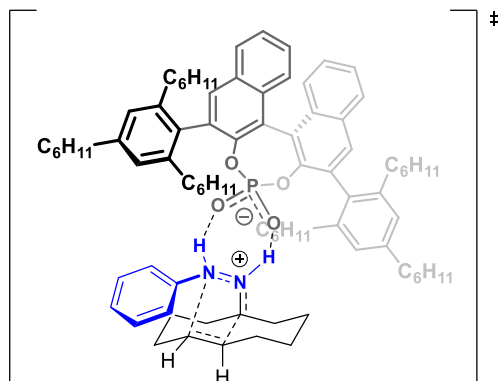


Figure 3.7. Proposed transition-state (TS1) for the transannular (3+2) cycloaddition step.

4. CONCLUSIONS

The following conclusions can be highlighted for this chapter:

1. Cycloalkenone hydrazones generated *in situ* from the corresponding cyclodecenones or cyclononenones can be used as efficient substrates to undergo catalytic and enantioselective transannular formal (3+2) cycloaddition reaction under chiral Brønsted acid catalysis.
2. This methodology enables the straightforward preparation of polycyclic scaffolds with a bridged pyrazolidine ring with high yields and enantioselectivities for a wide substrate scope, including different substitution patterns and ring sizes of the cyclic precursor. Moreover, various hydrazines with different electronic properties can be used to trigger the *in situ* formation of the 1,3-dipole giving in all cases the desired adducts with total control on the diastereoselectivity.
3. The described method has some limitations, showing to be very dependant on the ring size of the used eneketone substrates. In particular, cyclodecenone and cyclononanones have resulted to be the optimal starting materials for the transannular (3+2) cycloaddition reaction.
4. Taking advantage of the obtained molecular arrangement of the synthesized cyclic products, a successful transformation has been performed giving access to enantioenriched decaline- or octahydro-1*H*-indene derived 1,3-diamines containing one or two α -tertiary stereocentres. These compounds have great potential for being used as synthetic intermediates or chiral ligands, which are otherwise difficult to synthesize using other conventional methodologies.

4

4

Switchable Brønsted Acid-Catalyzed Ring Contraction/Enantioselective Allylation of Cyclooctatetraene Oxide

1. INTRODUCTION	129
1.1. Electrocyclic reactions	129
1.2. Cyclooctatetraene systems: structure and reactivity	137
2. SPECIFIC OBJECTIVES AND WORK PLAN	141
3. RESULTS AND DISCUSSION	144
3.1. Proof of concept.....	144
3.2. Mechanistic and computational studies	148
3.3. Enantioselective ring contraction/allylation process	166
4. CONCLUSIONS	174

1. INTRODUCTION

1.1. Electrocyclic reactions

The field of total synthesis of natural products represents a fundamental discipline within the history of organic synthesis, since nearly two centuries ago. Over the past decades, this highly versatile discipline not only includes organic synthesis but also establishes worthwhile synergies with other fields such as physical organic chemistry, spectroscopy, and catalysis, among others. Besides, the evolution of this field has allowed the development of highly selective synthesis of complex natural products, including those synthetic targets considered challenging from the established methodologies (see some representative examples in Figure 4.1).¹

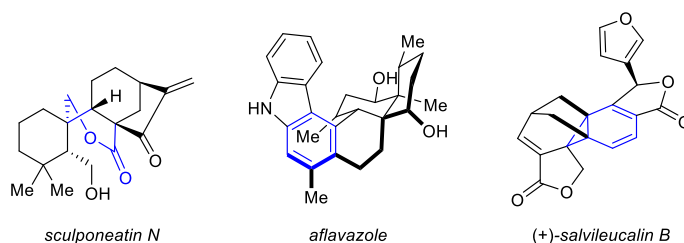


Figure 4.1. Representative natural products synthesized through electrocyclic reactions.

In particular, electrocyclic reactions² have been postulated to be an important class of pericyclic reactions towards the synthesis of structurally complex and biologically active natural products. This type of reactivity allows the construction of carbo- and heteropolycyclic scaffolds with excellent regio- and stereocontrol that can be explained due to the Woodward-Hoffmann rules.³ As it is illustrated in Figure

¹ Reisman, S. E.; Maimone, T. J. *Acc. Chem. Res.* **2021**, *54*, 1815.

² Evans, P. (2011). *Science of Synthesis 2010: Volume 2010/9: Stereoselective Synthesis 3: Stereoselective Pericyclic Reactions, Cross Coupling, CH and CX Activation*; Macmillan Publishers: Stuttgart, p. 383.

³ (a) Woodward, R. B.; Hoffmann, R. *J. Am. Chem. Soc.* **1965**, *87*, 395. (b) Woodward, R. B.; Hoffmann, R. *Angew. Chem. Int. Ed. Engl.* **1969**, *8*, 781. (c) Woodward, R. B.; Hoffmann, R. (1970). *The Conservation of Orbital Symmetry*; Verlag Chemie: Weinheim. (d) Hoffmann, R. *Angew. Chem. Int. Ed.* **1982**, *21*, 711. (e) Fleming, I. (2011). *Molecular Orbitals and Organic Chemical Reactions*; John Wiley: Chichester.

4.2, this set of rules are able to predict the stereochemistry of an electrocyclic reaction, based on recognizing the symmetry of the frontier orbitals (HOMO/LUMO) of the reactant and the corresponding product. The crucial theoretical principle that dictates the viability of a pericyclic transformation is the conservation of orbital symmetry, therefore, meaning that reactant and product orbitals are correlated to each other by geometric distortions, which are function of the reaction coordinate. In this sense, a pericyclic reaction can be classified as either symmetry-allowed or symmetry-forbidden platform, depending on whether a symmetry-imposed barrier exists or not. It has to be highlighted that symmetry-forbidden reactions can still occur if other factors, such as strain release, favours the reaction and the stereochemistry can be modulated according to the conditions, thermal or photochemical.

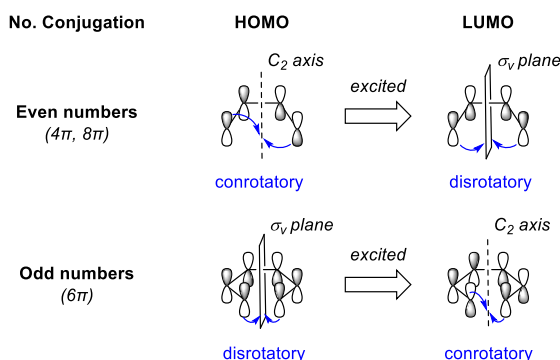


Figure 4.2. The Woodward-Hoffmann rules.

On that context, an electrocyclic process is, in essence, energetically driven by the structural properties of the substrate and it depends far less on the interactions that can be established.^{4,5} The final result of the transformation is the intramolecular conversion of a π bond to a σ bond or viceversa with excellent atom economy,

⁴ Desimoni, G.; Tacconi, G.; Barco, A.; Pollini, G. P. (1983). *Natural Products Synthesis Through Pericyclic Reactions*; ACS Monograph 180, American Chemical Society: Washington D. C.

⁵ Representative examples on the solvent effects of the electrocyclization, see: (a) Huisgen, R.; Dahmen, A.; Huber, H. *Tetrahedron Lett.* **1969**, *10*, 1461. (b) Mayr, H.; Huisgen, R. *J. Chem. Soc., Chem. Commun.* **1976**, 57. (c) Desimoni, G.; Faita, G.; Guidetti, S.; Righetti, P. P. *Eur. J. Org. Chem.* **1999**, 1921.

following a concerted process in a single step. Due to the recent advances in asymmetric catalysis, several enantioselective examples have been developed up to date, however, the total control of the absolute stereochemistry in electrocyclic processes still remains a challenge in comparison with other varieties of pericyclic reactions, such as cycloadditions.⁶

Complementarily, as it has been disclosed throughout the research work described in this thesis, transannular reactions have proven to be a subset of extremely efficient synthetic strategies for preparing complex polycyclic molecules. Although a large number of impressive examples of transannular Diels-Alder and hetero-Diels-Alder^{7,8,9} reactions have been reported in the literature, only a scarce number of transannular electrocyclizations have been described, mostly in a non-asymmetric fashion.

The first example of a transannular electrocyclization was suggested in 1977 by Clardy and co-workers.¹⁰ In this preliminary work, the authors were able to extract Dictyoxepin and Dictyolene from the marine alga *Dictyota acutiloba* and further characterize these two unusual diterpenoids for the first time. As it is summarized in Scheme 4.1, the 1,3-diene *cis*-decalin system could be obtained after cyclization and further oxidation of geranylgeraniol in order to obtain the *trans,cis,trans*-cyclodecatriene scaffold and its corresponding epoxide. These two cyclic polyenes were proposed as direct precursors for the synthesis of the two previously studied diterpenoids through transannular thermally allowed disrotatory ring closure, for the

⁶ For a review on asymmetric electrocyclic reactions, see: Thompson, S.; Coyne, A. G.; Knipe, P. C.; Smith, M. D. *Chem. Soc. Rev.* **2011**, *40*, 4217.

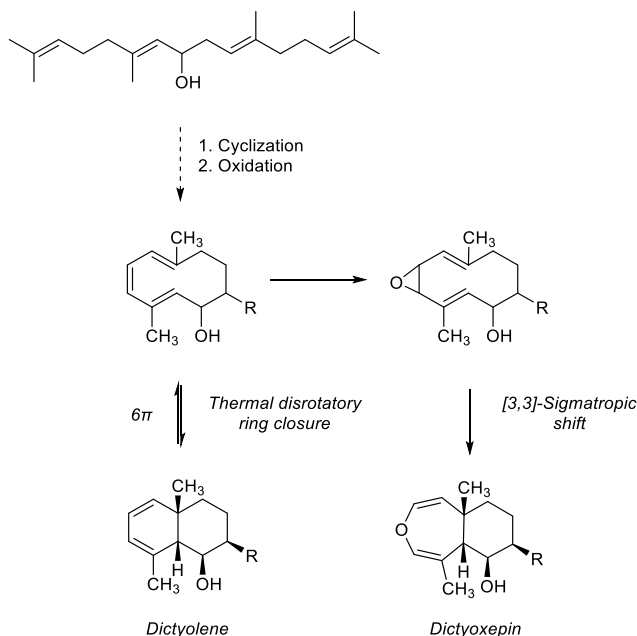
⁷ (a) Marsault, E.; Toró, A.; Nowak, P.; Deslongchamps, P. *Tetrahedron* **2001**, *57*, 4243. (b) Layton, M. E.; Morales, C. A.; Shair, M. D. *J. Am. Chem. Soc.* **2002**, *124*, 773. (c) Balskus, E. P.; Jacobsen, E. N. *Science* **2007**, *317*, 1736.

⁸ For a selected list of natural product syntheses featuring transannular Diels-Alder reactions, see: (a) Vosburg, D. A.; Vanderwal, C. D.; Sorensen, E. J. *J. Am. Chem. Soc.* **2002**, *124*, 4552. (b) Evans, D. A.; Starr, J. T. *Angew. Chem. Int. Ed.* **2002**, *41*, 1787. (c) Vanderwal, C. D.; Weiler, S.; Sorensen, E. J.; Vosburg, D. A. *J. Am. Chem. Soc.* **2003**, *125*, 5393.

⁹ Reyes, E.; Prieto, L.; Carrillo, L.; Uria, U.; Vicario, J. L. *Synthesis* **2022**, *54*, 4167.

¹⁰ Sun, H. H.; Waraszkievicz, S. M.; Erickson, K. L.; Finer, J.; Clardy, J. *J. Am. Chem. Soc.* **1977**, *99*, 3516.

case of Dictyolene, and a [3,3]-sigmatropic rearrangement in the epoxide to afford Dictyoxepin.

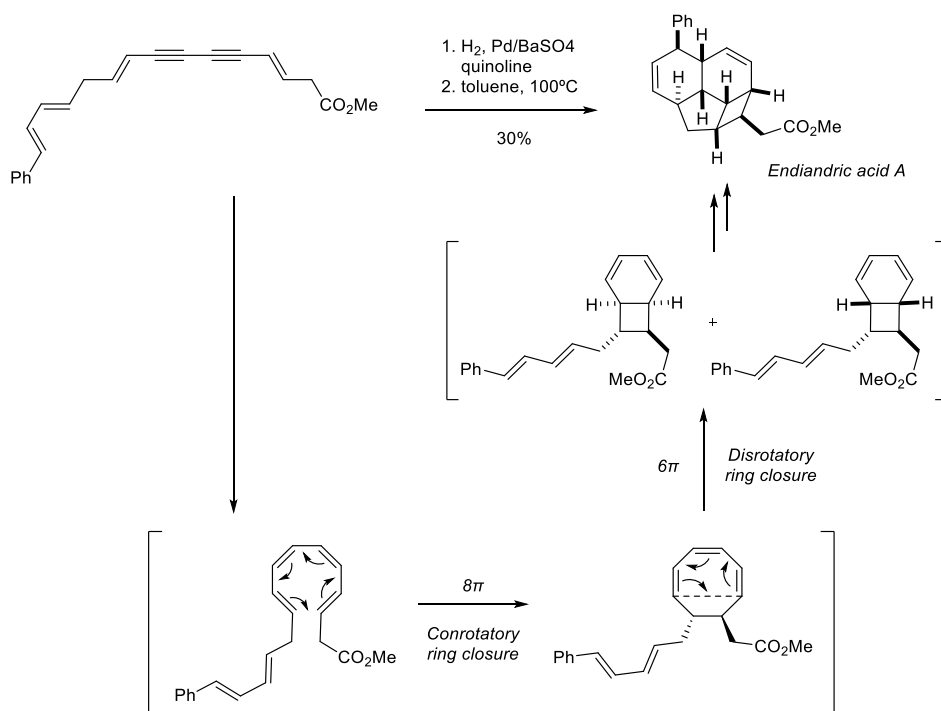


Scheme 4.1. Synthetic approaches for Dictyolene and Dictyoxepin.

The second example of this particular reactivity appeared some years later, by Nicolaou and co-workers,¹¹ who were able to demonstrate that the Lindlar hydrogenation of a diene-diyene system can directly provide bicyclo[4.2.0]octadiene scaffolds in a stereoselective manner (Scheme 4.2). In that sense, the proposed outcome of the reaction starts by the partial reduction of the diyene moiety, generating *in situ* an octatetraene skeleton with a *Z,Z* geometry of the two internal double bonds, which is susceptible to undergo a first 8π conrotatory ring closure. The resulting octatriene system is not stable enough to be isolated and the subsequent transannular 6π -electrocyclization takes place leading to the formation of the indicated bicyclo[4.2.0]octadiene system (endiandric acid D methyl ester and endiandric acid E methyl ester). Interestingly, upon heating the reaction

¹¹ Nicolaou, K. C.; Petasis, N. A.; Zipkin, R. E.; Uenishi, J. *J. Am. Chem. Soc.* **1982**, *104*, 5555.

at 100°C in toluene, these bicyclic intermediates directly provided the tetracyclic endiandric acid A methyl ester in a rather low yield but with total stereocontrol. Within this strategy, the authors exemplified¹² the synthetic utility of this methodology by developing the first stereocontrolled total synthesis of endiandric acids A-D starting from a simple polyene in a single step.¹³



Scheme 4.2. Total synthesis of Endiandric acid A through transannular electrocyclicization.

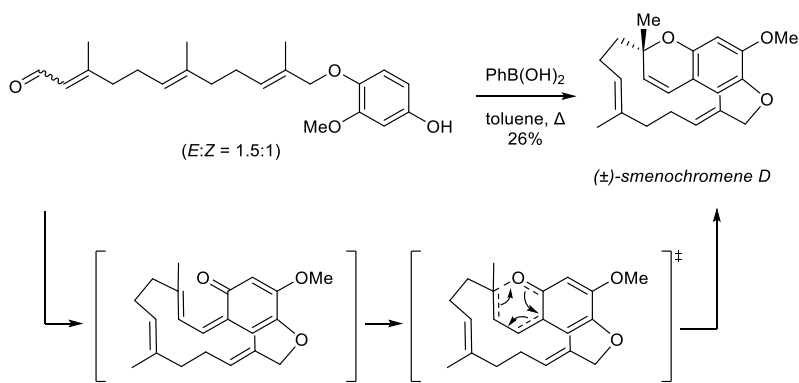
In 2005, the group of Trauner¹⁴ reported the total synthesis of smenocromene D featuring an unprecedented macrocyclization that proceeds through a biomimetic transannular electrocyclicization reaction. As it is highlighted in Scheme 4.3, the

¹² For a previous example suggesting a similar synthetic strategy: Bandaranayake, W. M.; Banfield, J. E.; Black, C. *J. Chem. Soc., Chem. Commun.* **1980**, 902.

¹³ For later examples of related total synthesis, see: (a) Drew, S. L.; Lawrence, A. L.; Sherburn, M. S. *Angew. Chem., Int. Ed.* **2013**, *52*, 4221. (b) Drew, S. L.; Lawrence, A. L.; Sherburn, M. S. *Chem. Sci.* **2015**, *6*, 3886.

¹⁴ Olson, B. S.; Trauner, D. *Synlett* **2005**, *4*, 700.

authors proposed a five-step synthesis of racemic smenochromene D, starting from commercially available farnesyl acetate. The key step to achieve the chromene core of the natural product results from the macrocyclization step, via boronic acid-mediated hydroxyalkylation/elimination sequence, which affords the corresponding *ansa-ortho*-quinone methide intermediate that subsequently goes through a transannular 6π -electrocyclization step affording the final natural product in a rather low yield.

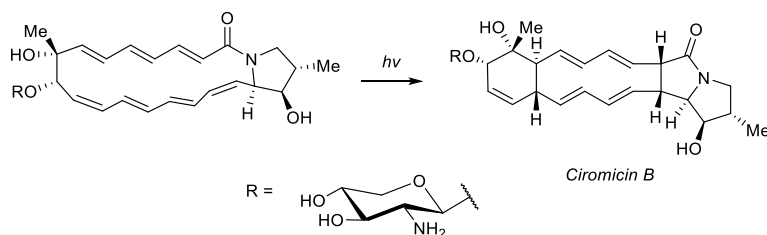


Scheme 4.3. Total synthesis of smenochromene D through transannular 6π -electrocyclization.

On the other hand, Bachmann and co-workers reported a decade later the unique example of a transannular 12π -electrocyclization of a particular family of metabolites containing polyene macrolactam type structures (Scheme 4.4).¹⁵ In this particular case, the authors suggested that a wavelength-dependent chemical process was occurring during the study of the response of actinomycete *Streptomyces coelicolor* to environmental stimuli. After isolation and characterization of the two microbial secondary metabolites Ciromicin A and B, the group of Bachmann were able to rationalize that a diastereoselective visible light-triggered 12π -electrocyclic rearrangement of Ciromicin A was taking place, yielding

¹⁵ Derewacz, D. K.; Covington, B. C.; McLean, J. A.; Bachmann, B. O. *ACS Chem. Biol.* **2015**, *10*, 1998.

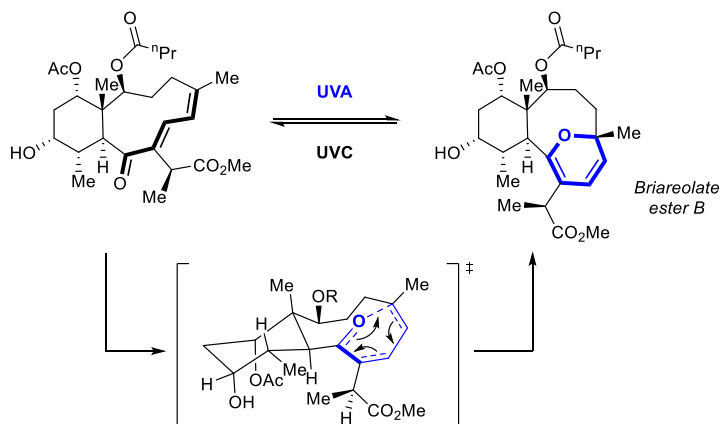
Ciromicin B, and opening an unprecedented pathway for inducing natural product discovery through the mapping of microbial response metabolomes.



Scheme 4.4. Transannular 12π -electrocyclization towards the synthesis of ciromicin B.

Finally, West's research group¹⁶ reported, in 2017, the biomimetic synthesis of briareolate ester B through the unique set of isomerization/transannular oxa- 6π electrocyclization sequence induced by UVA light. As illustrated in detail in the corresponding Scheme 4.5, the proposed reaction involves isomerization of the (*E,Z*)-dienone to the corresponding *Z,Z* configuration and further rotation of the carbonyl moiety (*S-trans* to *S-cis*) occurs, reaching the sterically hindered inside space of the macrocycle and acquiring the desired orientation in order to favour the transannular transformation. Moreover, the authors established a pioneer molecular photochromic switch when UVC irradiation of the product was employed, denoting an alternative synthetic strategy for the synthesis of medium-sized macrocycles.

¹⁶ Hall, A. J.; Roche, S. P.; West, L. M. *Org. Lett.* **2017**, *19*, 576.

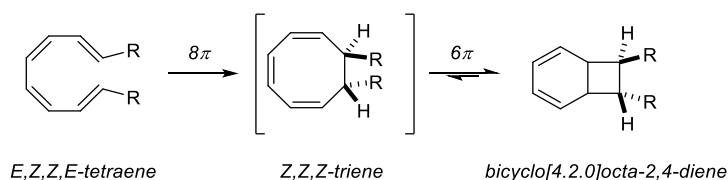


Scheme 4.5. Biomimetic transannular electrocyclicization for the synthesis of briareolate ester B.

In summary, high molecular complexity can be obtained in the minimum number of steps using transannular electrocyclicization reactions of cyclic and acyclic conjugated polyenes. All the aforementioned examples are diastereoselective transannular transformations, in which the stereochemistry of the process is controlled by the present stereogenic centers of the macrocyclic precursor, relying on the use of a chiral starting material. The following section will be focused on the structure and reactivity of cyclooctatetraene systems, as model substrate, for the research work developed in this chapter.

1.2. Cyclooctatetraene systems: structure and reactivity

As it has been introduced in the previous section, conjugated tetraenes with an 8π system usually undergo 8π -electrocyclizations affording diverse cyclic scaffolds under thermal or photochemical conditions. Nevertheless, the resulting octatrienes are in most cases isolated as the corresponding bicyclic dienes (Scheme 4.6), as a result of a subsequent transannular 6π -electrocyclization reaction, whose stereoselectivity can be modulated depending on the terminal substituents present in the precursor.¹⁷

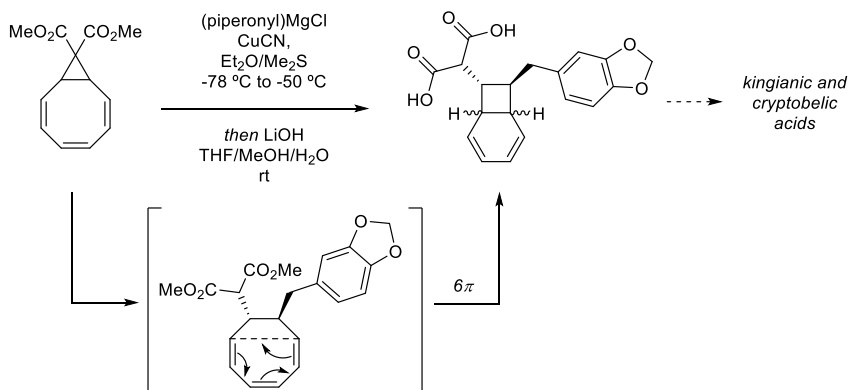


Scheme 4.6. Common rearrangement of cyclooctatetraene systems.

On the other hand, some cyclooctatetraene (COT) analogues have shown to exhibit transannular reactivity. A recent example reported by Fallon and co-workers¹⁸ demonstrates the ability of cyclooctatetraene cyclopropanes to undergo selective ring opening and subsequent transannular 6π -electrocyclicization through the 1,5-addition of an organocopper reagent (Scheme 4.7). With this methodology, the authors showcased a rapid access to functionalized bicyclo[4.2.0]octadiene cores, which could be applied to the total synthesis of the natural products kingianic and cryptobeilic acids, starting from linear diene-diyene systems in a similar approach as the one reported by Nicoulaou.¹¹

¹⁷ Patel, A.; Houk, K. N. *J. Org. Chem.* **2014**, *79*, 11370.

¹⁸ Patel, H. D.; Fallon, T. *Org. Lett.* **2022**, *24*, 2276.

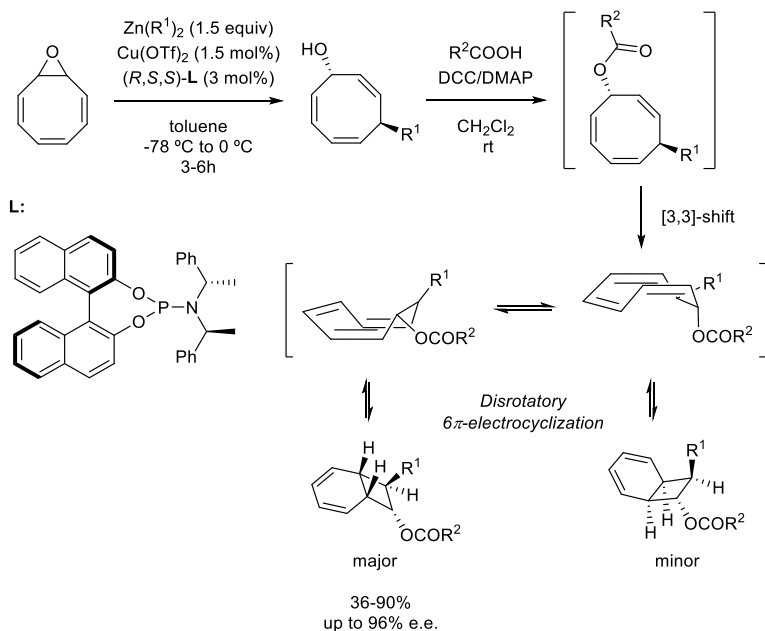


Scheme 4.7. Organocuprate ring opening/ 6π -electrocyclicization sequence of bicyclo[6.1.0]nonatrienes.

The direct oxidation of cyclooctatetraene affords the corresponding cyclooctatetraene oxide derivative,¹⁹ which has showed to be another interesting precursor for the development of transannular reactions. For instance, the group of Pineschi reported a methodology for the preparation of enantiomerically enriched functionalized bicyclo[4.2.0]octa-2,4-dienes through a novel domino sequence of a [3,3]-sigmatropic shift and transannular 6π -electrocyclization, prompted by the subsequent derivatization of the obtained chiral cyclooctatrienols.²⁰ As it is summarized in Scheme 4.8, the stereochemical outcome of the transformation is achieved in the first catalytic copper-phosphoramidite-catalyzed enantioselective alkylation of cyclooctatetraene oxide. The corresponding stereodefined alkylcyclooctatrienols could be selectively transformed by simple esterification of the hydroxyl moiety and the formed intermediate would chain further rearrangements in order to obtain a diastereomeric mixture of different substituted bicyclic compounds by simple thermal treatment.

¹⁹ Wheeler, O. H. *J. Am. Chem. Soc.* **1953**, *74*, 4858.

²⁰ (a) Del Moro, F.; Crotti, P.; Di Bussolo, V.; Macchia, F.; Pineschi, M. *Org. Lett.* **2003**, *5*, 1971. (b) Pineschi, M.; Del Moro, F.; Crotti, P.; Macchia, F. *Eur. J. Org. Chem.* **2004**, 4614.

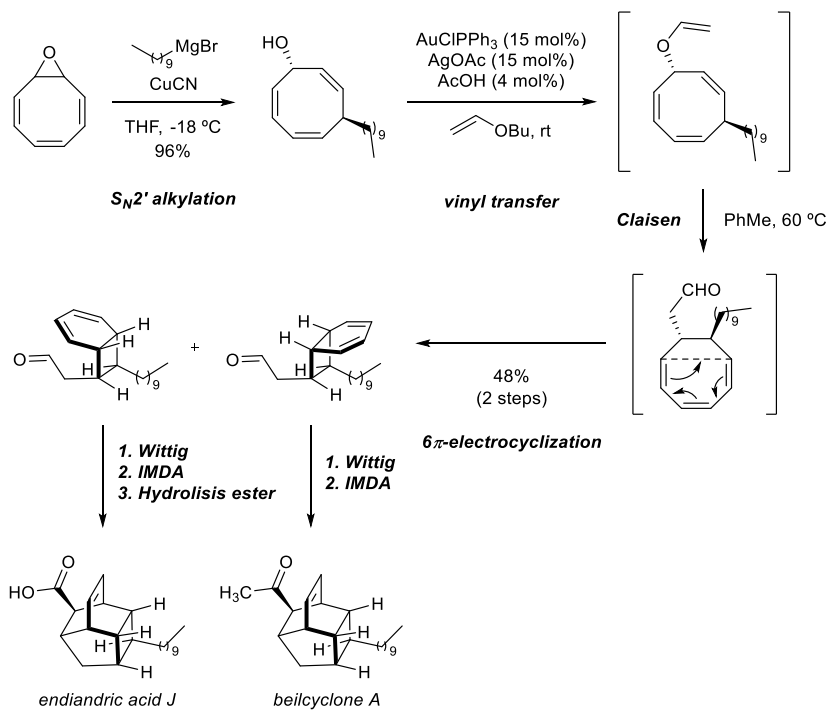


Scheme 4.8. Electrocyclic rearrangement of enantioenriched cyclooctatrienols.

Inspired by the breakthroughs achieved by Pineschi, the group of Fallon has recently developed a complementary strategy for the total synthesis of endiandric acid J and beilcyclone A, from cyclooctatetraene derivatives, in only six and five steps, respectively (Scheme 4.9).²¹ The authors proposed a tactical anti-vicinal difunctionalization of COT oxide through the established stereoselective and enantioselective *anti*- $\text{S}_{\text{N}}2'$ addition/ring opening reaction of cyclooctatetraene oxide followed by pericyclic rearrangements. Nevertheless, previous synthetic approaches relied on the tandem [3,3]-transposition of the derivatized cyclooctatrienols to promote the subsequent electrocyclic reaction. In that work, the corresponding 6π -electrocyclization/IMDA cascade (IMDA = intramolecular Diels-Alder) would be prompted by a vinyl transfer/Claisen rearrangement sequence leading to the construction of bicyclo[4.2.0]octadiene aldehyde intermediates. Final

²¹ Yahiaoui, O.; Almass, A.; Fallon, T. *Chem. Sci.* **2020**, *11*, 9421.

olefination and intramolecular Diels–Alder cycloaddition would allow to complete the total synthesis of both natural products with total stereocontrol.



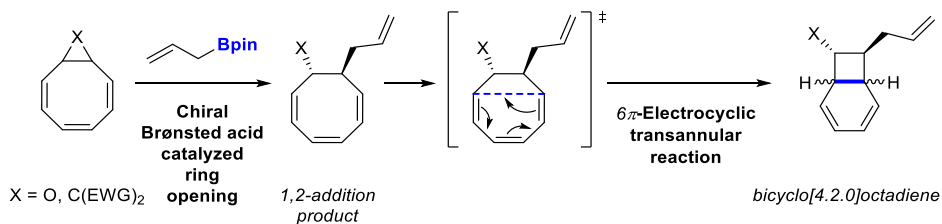
Scheme 4.9. Total synthesis of andiandric acid J and beilcyclone A.

2. SPECIFIC OBJECTIVES AND WORK PLAN

The preceding section summarized the advances regarding the study of the reactivity of different conjugated systems for the synthesis of natural products through pericyclic reactions. Specifically, eight-membered conjugated cyclic systems have proven to be excellent precursors for the direct construction of highly complex polycyclic biologically active compounds, in the minimum number of steps, by means of transannular electrocyclic reactions. Depending on the nature of the precursor and the reagents employed in each methodology, different types of reactivity could be observed leading to the divergent preparation of cyclic polyenic molecular architectures in a non-asymmetric fashion. However, regarding the synthesis of enantiopure molecules using this procedure, a scarce number of examples have been developed relying on the use of chiral organometallic species.

Considering the previously mentioned reactivity of cyclooctatetraene systems and taking into account the scarcely explored 1,2-addition reaction of vinylic epoxides with organoboranes,²² we envisioned to study the reactivity of different cyclooctatetraene derivatives as suitable model systems for the development of a novel **catalytic and enantioselective cascade ring opening allylation/transannular 6 π -electrocyclization under chiral Brønsted acid catalysis**. In that sense, disubstituted and oxabicyclo[6.1.0]nona-2,4,6-trienes, illustrated in Scheme 4.10, would be reacted with a chiral Brønsted phosphoric acid and an allylborane in order to promote the stereoselective direct ring opening through the 1,2-addition of the corresponding allylating agent. According to the selected reported precedents, the resulting substituted *Z,Z,Z*-cyclooctatriene intermediates would undergo subsequent transannular 6 π -electrocyclization reaction affording stereodefined bicyclo[4.2.0]octadiene scaffolds, which have showed to be really useful synthetic intermediates for the synthesis of natural products.

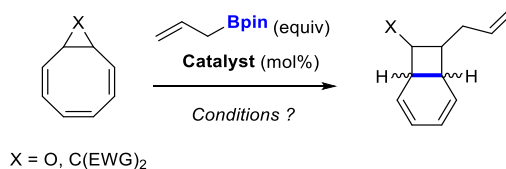
²² (a) Zaidlewicz, M.; Krzemiński, M. P. *Org. Lett.* **2000**, 2, 3897. (b) Lautens, M.; Maddess, M. L.; Sauer, E. L. O.; Ouellet, S. G. *Org. Lett.* **2002**, 4, 83.



Scheme 4.10. Specific objective of the project.

In order to achieve the stated objective, the following work plan was designed:

1. *Proof of concept:* Evaluation of the reaction viability using allylboronic acid pinacol ester and chiral Brønsted acid catalysis in order to promote the direct ring opening allylation/transannular 6 π -electrocyclization sequence taking as model substrates the corresponding cyclooctatetraene derivatives and the allylboronate showed below in Scheme 4.11.



Scheme 4.11. Proof of concept of the envisioned model reaction.

2. *Optimization of the reaction:* Incorporation of a chiral BINOL-based phosphoric acid in order to achieve the enantioselective version of the projected transformation. In that sense, a screening of different catalysts, solvents, temperatures and reaction times will be carried out in order to efficiently provide the desired bicyclic products in high yields and enantioselectivities.

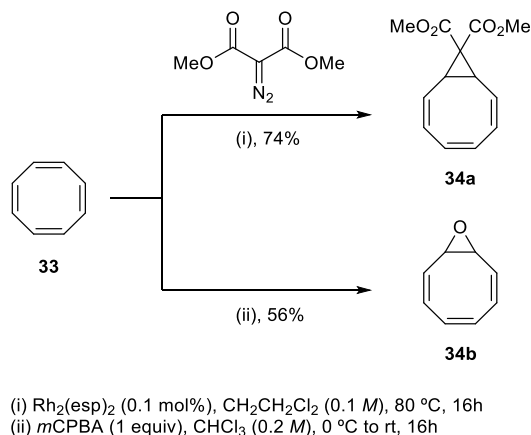
3. *Scope of the reaction:* Once the optimal reaction conditions have been established, a study of the influence of the different components of the reaction will be performed. For that purpose, different allylboranes will be prepared containing diverse substitution patterns along the allylic moiety as well as different boron moieties. On the other hand, in the case of the cyclooctatetraene cyclopropane derivative, different electron-withdrawing and electron-donating groups will be incorporated in order to study their influence on the reaction outcome and determine the general application of the transannular approach.

3. RESULTS AND DISCUSSION

In view of the described precedents on this topic and after establishing the specific objectives of the chapter, we proceed to describe and discuss the most representative results obtained in this part of the research work.

3.1. Proof of concept

Before testing the viability of the projected cascade strategy stated in the work plan of this chapter, our initial efforts were focused on the synthesis of the desired substrates. The corresponding dimethyl (2*Z*,4*Z*,6*Z*)-bicyclo[6.1.0]nona-2,4,6-triene-9,9-dicarboxylate^{18,23} (**34a**) and (2*Z*,4*Z*,6*Z*)-9-oxabicyclo[6.1.0]nona-2,4,6-triene^{20a} (**34b**) were prepared as illustrated in Scheme 4.12, following the reported methodology indicated for each case.

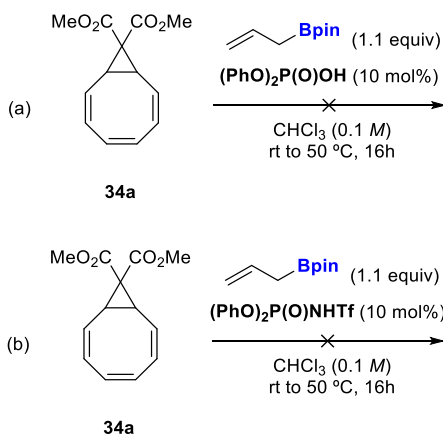


Scheme 4.12. Synthesis of the starting materials **34a-b**.

Once the desired precursors were prepared, the next step was to test the feasibility of the projected organocatalytic ring opening allylation/transannular 6*π*-electrocyclization sequence. As it is showed in Scheme 4.13, the initial attempts

²³ (a) Nanteuil, F.; Waser, J. *Angew. Chem. Int. Ed.* **2011**, *50*, 12075. (b) Racine, S.; Hegedüs, B.; Scopelliti, R.; Waser, J. *Chem. Eur. J.* **2016**, *22*, 11997.

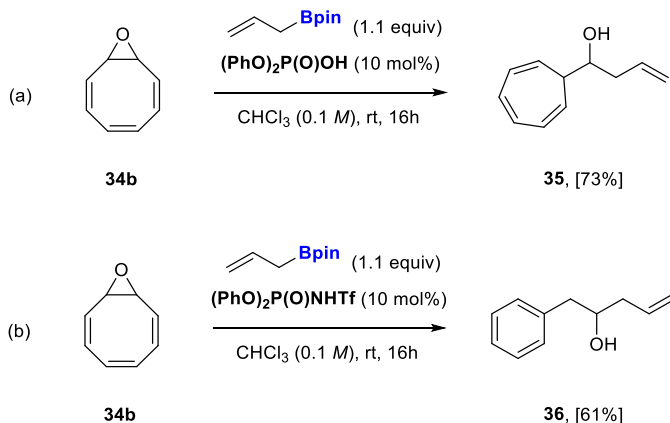
were focused to the corresponding cyclooctatetraene cyclopropane derivative (**34a**). When this substrate was firstly reacted with 2-allyl-4,4,5,5-tetramethyl-1,3,2-dioxaborolane, in the presence of 10 mol% of diphenylphosphoric acid, as catalyst, in chloroform at room temperature, the reaction was not successful and substrate **34a** was recovered by column chromatography (Scheme 4.13a). On the other hand, when the same substrate was tested using the more acidic *N*-triflylphosphoramidate catalyst, the same results were observed, even increasing the reaction temperature progressively, and we only recovered the unreacted starting material (Scheme 4.13b).



Scheme 4.13. Proof of concept of the envisioned reaction with substrate **34a**.

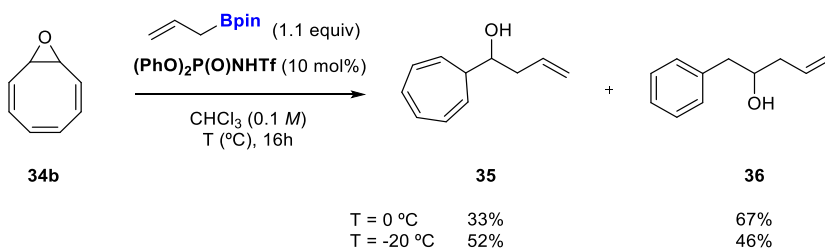
Although the first two attempts did not provide any reactivity, we decided to explore the chemical behaviour of the corresponding cyclooctatetraene oxide (**34b**) under the same reaction conditions tested previously (Scheme 4.14). To our delight, when compound **34b** was reacted with 2-allyl-4,4,5,5-tetramethyl-1,3,2-dioxaborolane, in the presence of catalysts diphenylphosphoric acid (Scheme 4.14a) and *N*-triflylphosphoramidate (Scheme 4.14b), the starting material was completely consumed after 16h. In the first case, the reaction product was confirmed to be cycloheptatrienyl homoallylic alcohol **35**, which was isolated in good yield whereas for the second case, the isolated product was the homoallylic

alcohol **36**, which was exclusively formed and isolated in 61% yield. When the reaction was carried out without any catalyst, the starting material was recovered unchanged.



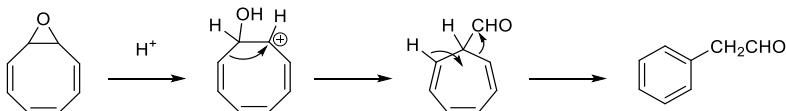
Scheme 4.14. Proof of concept of the envisioned reaction with substrate **34b**.

Interestingly, when the reaction was carried out at lower temperature using *N*-triflylphosphoramidate catalyst, mixtures of compounds **35** and **36** were obtained (Scheme 4.15). This result might suggest a kind of kinetic/thermodynamic control, however, when either pure compound **35** or mixtures of both compounds **35** and **36** were stirred in the presence of 10 mol% of the acidic catalyst, at room temperature, the reaction remained unaltered and therefore, it can be preliminary concluded that the reaction was not reversible and the observed regioselectivity can not be rationalized in terms of thermodynamic control.



Scheme 4.15. Influence of the temperature in the reaction outcome.

The unexpected reactivity observed would be in agreement with pioneer early reports that describe the ring contraction of cyclooctatetraene oxide with different reagents.²⁴ The first example developed by Pettit and co-workers proved that acid catalysis can promote the rearrangement of (2*Z*,4*Z*,6*Z*)-9-oxabicyclo[6.1.0]nona-2,4,6-triene illustrated in Scheme 4.16 to phenylacetaldehyde.²⁵ The authors suggested that the addition of acid potassium permanganate would lead to the initial formation of the corresponding hydroxyl substituted carbo-cation, which after a pinacol-pinacone rearrangement afforded the protonated cyclohepta-2,4,6-trienealdehyde. The presence of oxidizing agents in the reaction medium would favour the evolution of the latter reactive species to the tropylium cation, which would subsequently rearrange to the final phenylacetaldehyde.



Scheme 4.16. Acid-catalyzed ring contraction of cyclooctatetraene oxide.

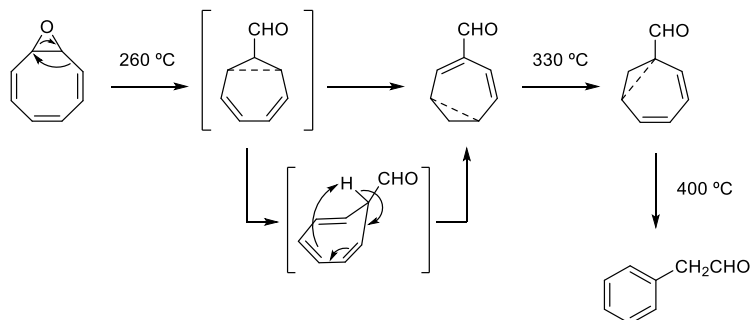
Pyrolysis of the same cyclooctatetraene oxide derivative²⁶ led to the formation of various aldehydes under drastic conditions. Büchi and co-workers suggested an initial rearrangement of the COT oxide to norcaradienecarboxaldehyde, which would go through a rapid transformation to the α -isomer. At this point, although the intramolecular nature of this change is not well-established, the proposed mechanism accommodates a first rearrangement to the β -aldehyde and further isomerization to obtain the most thermodynamically stable linearly conjugated γ -aldehyde. Regarding the final step, the authors mentioned that the transformation

²⁴ For selected examples using organometallic reagents or transition-metal complexes, see: (a) Matsuda, T.; Sugishita, M. *Bull. Chem. Soc. Jpn.* **1967**, *40*, 174. (b) Grigg, R.; Hayes, R.; Sweeney, A. *Chem. Commun.* **1971**, *20*, 1248. (c) Strukul, G.; Viglino, P.; Ros, R.; Graziani, M. *J. Organomet. Chem.* **1974**, *74*, 307. (d) Ogawa, M.; Sugishita, M.; Takagi, M.; Matsuda, T. *Tetrahedron* **1975**, *31*, 299.

²⁵ Ganellin, C. R.; Pettit, R. *J. Chem. Soc.* **1958**, 576.

²⁶ Büchi, G.; Burgess, E. M. *J. Am. Chem. Soc.* **1962**, *84*, 3104.

to phenylacetaldehyde “remains mechanistically obscure and it is conceivable that an acid-catalyzed rather than a thermal process is involved.”



Scheme 4.17. Thermal rearrangement of cyclooctatetraene oxide to phenylacetaldehyde.

Considering the previous interesting observations, we next changed the specific objective of the research work and we envisioned to study the reactivity of cyclooctatetraene oxide as suitable model system for the development of a **novel catalytic Brønsted acid-catalyzed ring contraction/allylation sequence for the synthesis of different substituted homoallylic alcohols**. Besides, in order to gather further insights about the mechanism and the role played by the catalyst of the observed switchable process, a collaboration was established with the research group of Prof. Pedro Merino, from the University of Zaragoza. The obtained mechanistic experiments and computational studies are disclosed in the following section.

3.2. Mechanistic and computational studies

In order to obtain a better understanding of the observed transformation, our initial efforts were focused on the location of the involved intermediates in the reaction. According to the literature data, the possible scenario in this transformation would be the formation of the two possible aldehyde intermediates: cycloheptatriene carboaldehyde (formed after the first ring contraction) and phenylacetaldehyde (generated after the second ring contraction). In that sense, in order to obtain experimental evidences for the formation of both plausible intermediates, preliminary ¹H-NMR experiments were carried out, monitoring the

reaction in absence of the allylboronate reagent. The first experiment was performed treating COT oxide **34b** with 10 mol% of diphenylphosphate catalyst, in CDCl_3 . The $^1\text{H-NMR}$ spectra was recorded every hour during 8h and as showed in Figure 4.3, the formation of cycloheptatrienecarbaldehyde intermediate (**37**) could be observed, increasing its concentration as the reaction times evolved. The structure of **37** could be unambiguously assigned by HSQC-NMR as it can be seen in Figure 4.4.

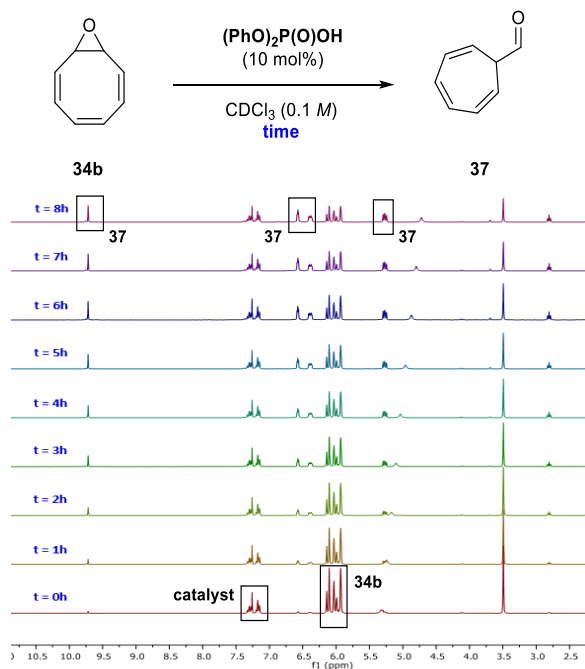


Figure 4.3. $^1\text{H-NMR}$ spectra of the crude reaction using diphenylphosphate catalyst.

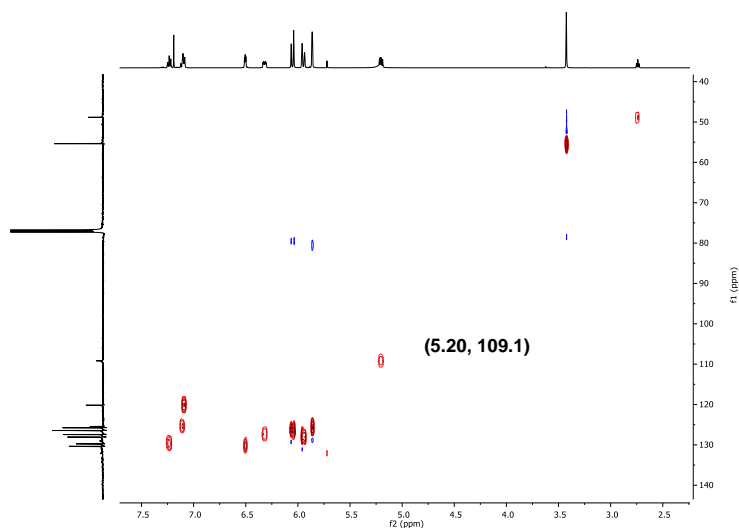


Figure 4.4. HSQC-NMR spectra of reaction at $t = 5\text{h}$.

The same experiment but using the *N*-triflylphosphoramidate catalyst was carried out, observing the instantaneous disappearance of cyclooctatetraene oxide **34b** and the clean quantitative formation of phenylacetaldehyde **38** within less than 2 hours, as shown in Figure 4.5. The presence of both aldehyde intermediates (**37:38**) was detected after 1 hour in an almost 1:2 ratio, which would also point towards the possibility for aldehyde **37** to be converted into aldehyde **38** by the action of the more acidic Brønsted acid *N*-triflylphosphoramidate catalyst.

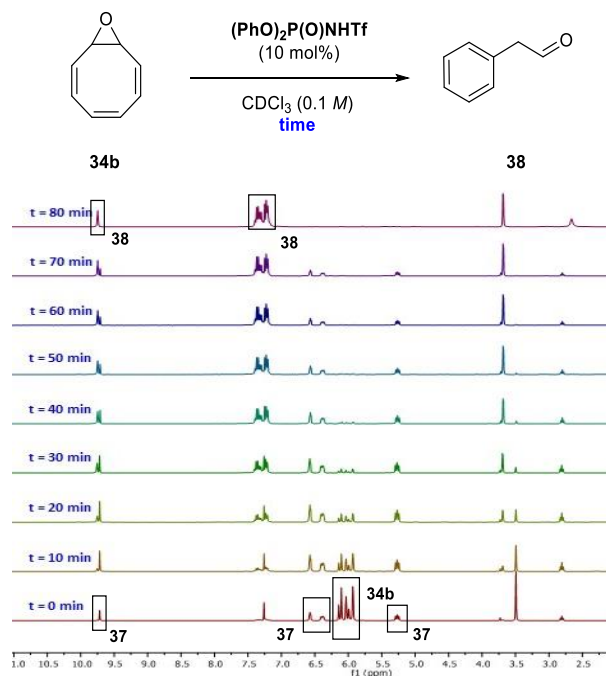
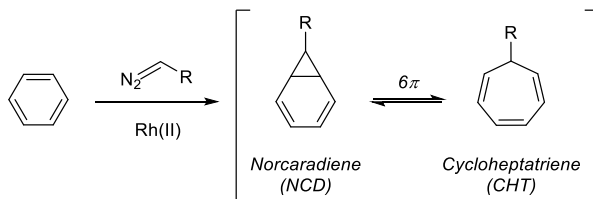


Figure 4.5. $^1\text{H-NMR}$ spectra of the crude reaction using *N*-triflylphosphoramidate catalyst.

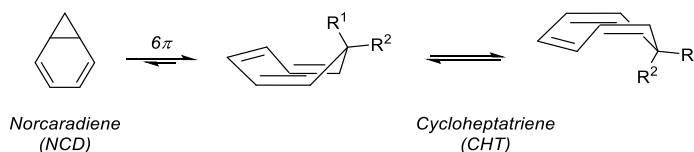
The cycloheptatriene scaffold (CHT) observed for the aldehyde intermediate **37** is an intriguing molecular architecture whose synthesis is a particular challenge by itself due to the limited number of available reactions that enable the preparation of this particular core. The classical approach involves the Buchner reaction through a metal-catalyzed cyclopropanation of arene derivatives to initially provide the norcaradiene (NCD), which is in equilibrium with its cycloheptatriene valence tautomer, after a reversible disrotatory 6π electrocyclic ring opening, to afford the cycloheptatriene system (Scheme 4.18).²⁷

²⁷ (a) Buchner, E.; Curtius, T. *Ber. Dtsch. Chem. Ges.* **1885**, *18*, 2377. (b) Buchner, E. *Ber. Dtsch. Chem. Ges.* **1896**, *29*, 106. For some reviews, see: (a) Reisman, S. E.; Nani, R. R.; Levin, S. *Synlett* **2011**, *17*, 2437. (b) McNamara, O. A.; Maguire, A. R. *Tetrahedron* **2011**, *67*, 9. (c) Jansen, H.; Slootweg, J. C.; Lammertsma, K. *Belstein J. Org. Chem.* **2011**, *7*, 1713. (d) Krüger, S.; Gaich, T. *Belstein J. Org. Chem.* **2014**, *10*, 163.



Scheme 4.18. Conventional approach to cycloheptatrienes through Buchner reaction.

There are several reports directed to the study of the norcaradiene-cycloheptatriene equilibrium by NMR spectroscopy.²⁸ As it is depicted in Scheme 4.19, preliminar studies showed that in most cases the equilibrium is displaced towards the non-planar cycloheptatriene system, which can undergo interconversion between two boat conformations. In 1981, Rubin described the first direct observation of the norcaradiene system and demonstrated that the position of the equilibrium was dramatically altered with structural modification of the substrates and therefore, the number and nature of the substituents.²⁹



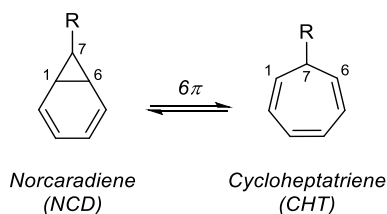
Scheme 4.19. Norcaradiene-Cycloheptatriene (NCD-CHT) equilibrium.

²⁸ (a) Corey, E. J.; Burke, H. J.; Remers, W. A. *J. Am. Chem. Soc.* **1955**, *77*, 4941. (b) Anet, F. A. L. *J. Am. Chem. Soc.* **1964**, *86*, 458. (c) Jensen, F. R.; Smith, L. A. *J. Am. Chem. Soc.* **1964**, *86*, 956. (d) Lambert, J. B.; Durham, L. J.; Lepoutere, P.; Roberts, J. D. *J. Am. Chem. Soc.* **1965**, *87*, 3896. (e) Wehner, R.; Günther, H. *J. Am. Chem. Soc.* **1975**, *97*, 923.

²⁹ (a) Rubin, M. B. *J. Am. Chem. Soc.* **1981**, *103*, 7791. (b) Rubin, M. B. *Tetrahedron Lett.* **1984**, *25*, 4697.

Since the mentioned interconversion of both species is essentially a pericyclic process, various studies were later centered on the study of the possible HOMO-LUMO interactions between the cyclopropane ring and the implied substituents,³⁰ in order to rationalize the previous observations carried out by Rubin and Ciganek.³¹ In this context, the authors disclosed that the cyclopropane ring is a strong π -electron donor and the position of the equilibrium is not only due to the π -interactions but also σ -effects have a significant impact between the two species. In general, as it is summarized in Table 4.1, σ -electron donor substituents have a stabilizing effect towards the norcaradiene, along with π -electron-withdrawing groups, whereas σ -electron-withdrawing substituents favours the displacement of the equilibrium to the cycloheptatriene system.

Table 4.1. Substituent effects on the norcaradiene-cycloheptatriene equilibrium.



Substituen type	C ₁ C ₇ (vicinal)	C ₁ C ₆ (distal)	Major tautomer
π -Acceptor	Longer	Shorter	NCD
π -Donor	Longer	Shorter	NCD
σ -Acceptor	Shorter	Longer	CHT
σ -Donor	Longer	Shorter	NCD

³⁰ (a) Hoffmann, R. *Tetrahedron Lett.* **1970**, 2907. (b) Günther, H. *Tetrahedron Lett.* **1970**, 5173. (c) Hoffmann, R.; Stohrer, W. D. *J. Am. Chem. Soc.* **1971**, *93*, 6941. (d) Staley, S. W.; Fox, M. A.; Cairncross, A. *J. Am. Chem. Soc.* **1977**, *99*, 4524. (e) Allen, F. H. *Acta Crystallogr., Sect. B* **1980**, *36*, 81. (f) Durmaz, S.; Kollmar, H. *J. Am. Chem. Soc.* **1980**, *102*, 6942. (g) Allen, F. H. *Acta Crystallogr., Sect. B* **1981**, *B37*, 890. (h) Allen, F. H. *Acta Crystallogr., Sect. B* **1981**, *B37*, 900. (i) Clark, T.; Spitznagel, G. W.; Klose, R.; Schleyer, R. V. R. *J. Am. Chem. Soc.* **1984**, *106*, 4412.

³¹ (a) Ciganek, E. *J. Am. Chem. Soc.* **1965**, *87*, 652. (b) Ciganek, E. *J. Am. Chem. Soc.* **1967**, *89*, 1454.

In this context, we planned the next experiment aiming to study the reaction of compound **34b** with diphenylphosphoric acid to promote the first ring contraction under the standard conditions (Figure 4.6). After 5h, NMR analysis of the crude reaction showed a 60% conversion of the starting material into aldehyde **37**. Then, the more acidic *N*-triflylphosphoramidate catalyst was added to the reaction crude and we could observe the complete disappearance of **37** and the clean formation of phenylacetaldehyde **38**. With this experiment we could demonstrate that aldehyde **37** (or the corresponding valence isomer) undergoes conversion into **38** in the presence of a strong Brønsted acid catalyst.

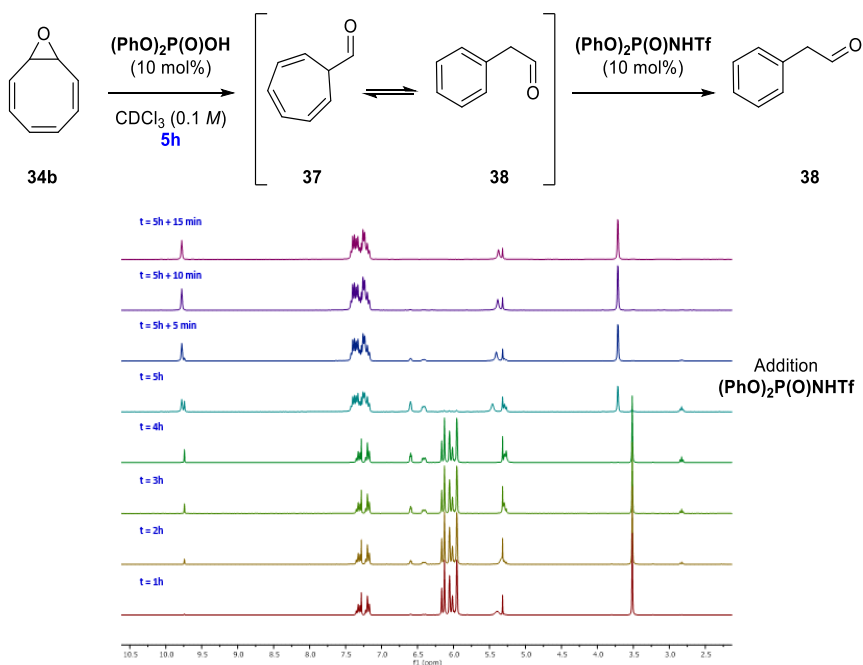
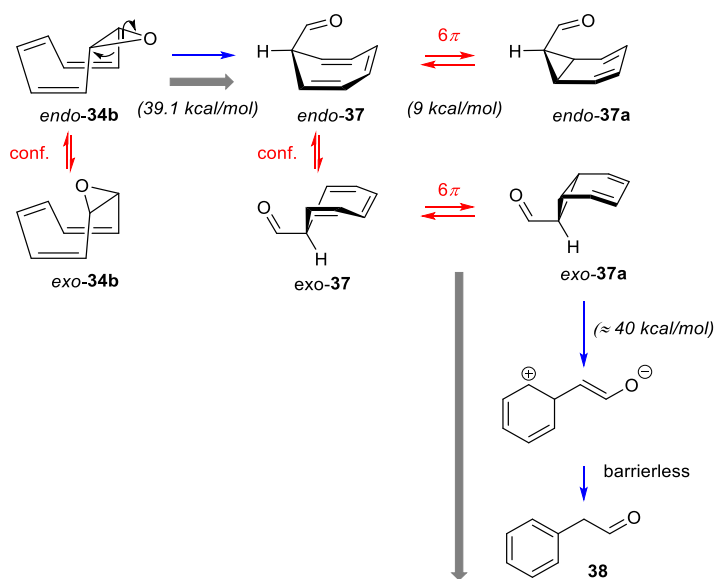


Figure 4.6. $^1\text{H-NMR}$ spectra of the crude reaction with consecutive addition of both catalysts.

After these experimental evidences, a complete computational study of this transformation at DFT level was carried out by the group of Prof. Merino. Firstly, the study of the neutral approach was done, following the previously examples

proposed by Buchi and Burgess,^{26,32} who suggested the formation of phenylacetaldehyde **38** through the grey arrow route depicted in Scheme 4.20, which involves neutral (non-protonated) intermediates, undergoing a thermally induced process (300-400 °C) through several consecutive isomerization processes. The performed calculations showed a barrier of 39.1 kcal/mol when the transition structure was located for the first step and therefore, verifying the connection between **34b** and *endo*-**37**. Considering the aforementioned CHT-NCD equilibrium, the other compounds were subjected to this isomerism process and the energy barrier for the formation of the valence tautomer *endo*-**37a** was found to be of only 9 kcal/mol. In that context, the value of the energy barrier obtained for the first step of the transformation indicated that the neutral route would not be possible under the temperature of our reaction, therefore, the study of the route catalyzed by an acid was considered next.



Scheme 4.20. Proposed pathway for the conversion of cyclooctatetraene oxide.

³² (a) Cope, A. C.; Tiffany, B. *J. Am. Chem. Soc.* **1951**, *73*, 4158. (b) Cope, A. C.; Nelson, N. A.; Smith, D. S. *J. Am. Chem. Soc.* **1954**, *76*, 1100.

When the transformation of **34b** was computed in the presence of diphenylphosphoric acid as the catalyst (**TS1a**), the energetic barrier of the first step decreased and was found to be 22.6 kcal/mol. Regarding the isomerization between *endo*-**37** and *endo*-**37a** through an electrocyclic reaction, it was found to be 8.7 kcal/mol. The intrinsic reaction coordinate (IRC) of **TS1a** identified **34b** as the starting point and aldehyde **37** as the final one, showing the presence of a plateau longer than the one found for the neutral mode, indicating the presence of a possible hidden intermediate.³³ For this reason, an evaluation of the evolution of the electron density of the starting material along the reaction coordinate was carried out at the university of Zaragoza and it was performed through the analysis of the electron localization function (ELF)³⁴ along the entire IRC. This evolution of the electron density is summarized in the following Figure 4.7 and allowed to assign the predominating species in each moment of the reaction. The performed ELF analysis also indicated that a complete proton transfer should occur before the oxirane ring-opening takes place and therefore, this fact would confirm that the pK_a of the acid catalyst is crucial for the reaction to start.

³³ (a) Kraka, E.; Cremer, D. *Acc. Chem. Res.* **2010**, *43*, 591. (b) Ortega, A.; Manzano, R.; Uria, U.; Carrillo, L.; Reyes, E.; Tejero, T.; Merino, P.; Vicario, J. L. *Angew. Chem. Int. Ed.* **2018**, *57*, 8225. (c) Capel, E.; Rodriguez-Rodriguez, M.; Uria, U.; Pedron, M.; Tejero, T.; Vicario, J. L.; Merino, P. *J. Org. Chem.* **2022**, *87*, 693.

³⁴ (a) Savin, A.; Nesper, R.; Wengert, S.; Fässler, T. F. *Angew. Chem. Int. Ed.* **1997**, *36*, 1808. (b) Savin, A. *J. Chem. Sci.* **2005**, *117*, 473. (c) Silvi, B.; Fourre, I. *Monats. Chem.* **2005**, *136*, 855.

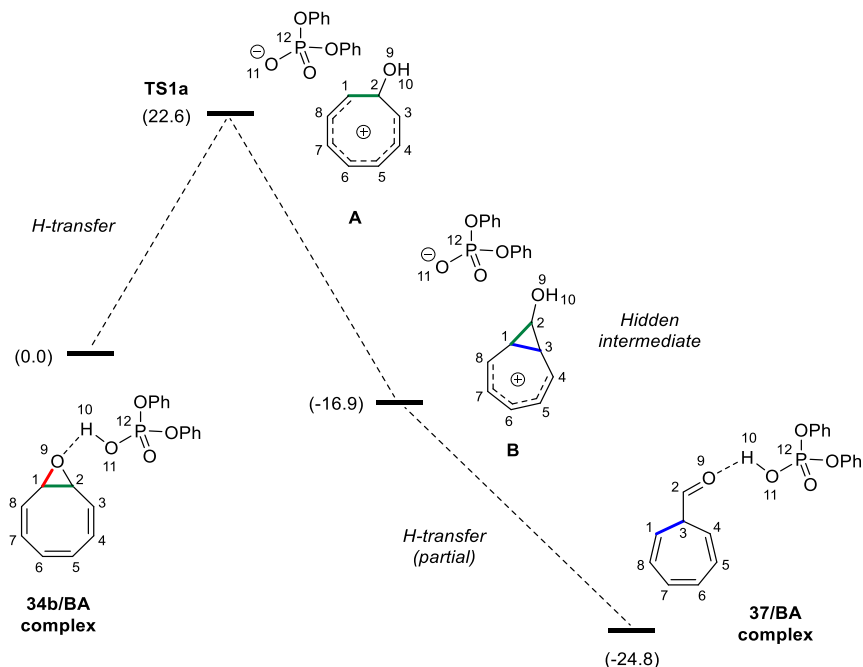


Figure 4.7. Representation of the transient species during the transformation of **34b** to **37** (Energies in kcal/mol).

When the transformation of **34b** into **37** catalyzed by the presence of the *N*-triflylphosphoramidate as the catalyst (**TS1b**) was calculated, the energetic barrier of the first step was found to be 21.9 kcal/mol, similar to **TS1a**. The optimized geometries of both transition structures confirmed the higher acidic character of *N*-triflylphosphoramidate catalyst since the observed distance from the nitrogen to the proton is larger (1.58 Å) and therefore, the proton-transfer is more advanced in that case (Figure 4.8 right) whereas for the case of the phosphoric acid, a partial H-transfer is observed with shorter distance from the oxygen to the proton (1.42 Å) (Figure 4.8 left).

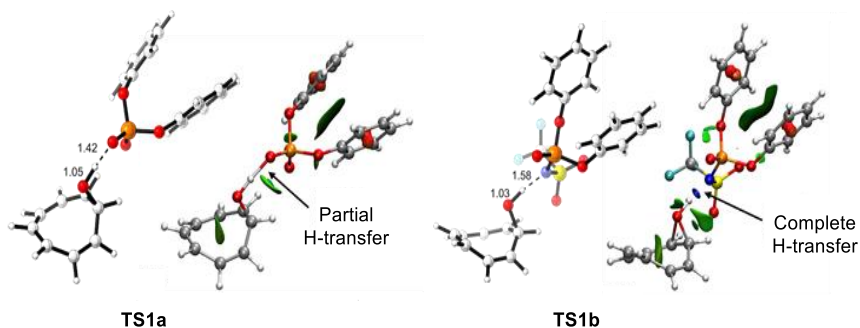


Figure 4.8. Optimized geometries for the transition structures **TS1a** and **TS1b**, corresponding to the formation of **37**.

The next step was to study the second part of the reaction, which consists on the evolution of aldehyde **37** to aldehyde **38**. In the presence of an acid catalyst, the CHT/NCD isomerization proceeds through **TS2a** or **TS2b** with barriers of 7.9 and 8.4 kcal/mol in the presence of diphenylphosphoric acid and *N*-triflylphosphoramidate catalyst, respectively (Figure 4.9). The obtained data indicate that this isomerization is not catalyzed by acids, as the transition state involving the non-protonated form has a slightly lower barrier than the protonated one. On the other hand, the further ring-opening of the cyclopropane would require the protonation of the aldehyde intermediate since the observed barriers are 23.6 kcal/mol for the case of diphenylphosphoric acid and 18.4 kcal/mol for the case of the more acidic catalyst. These results are in accordance with the experimental observations, since it would indicate that the process would be favoured for the case of the *N*-triflylphosphoramidate catalyst with a difference of 5.2 kcal/mol in the energy barrier. The resulting Wheeland intermediate (**WI**) would evolve to the enol in a barrierless process and then, aldehyde **38** would be obtained.

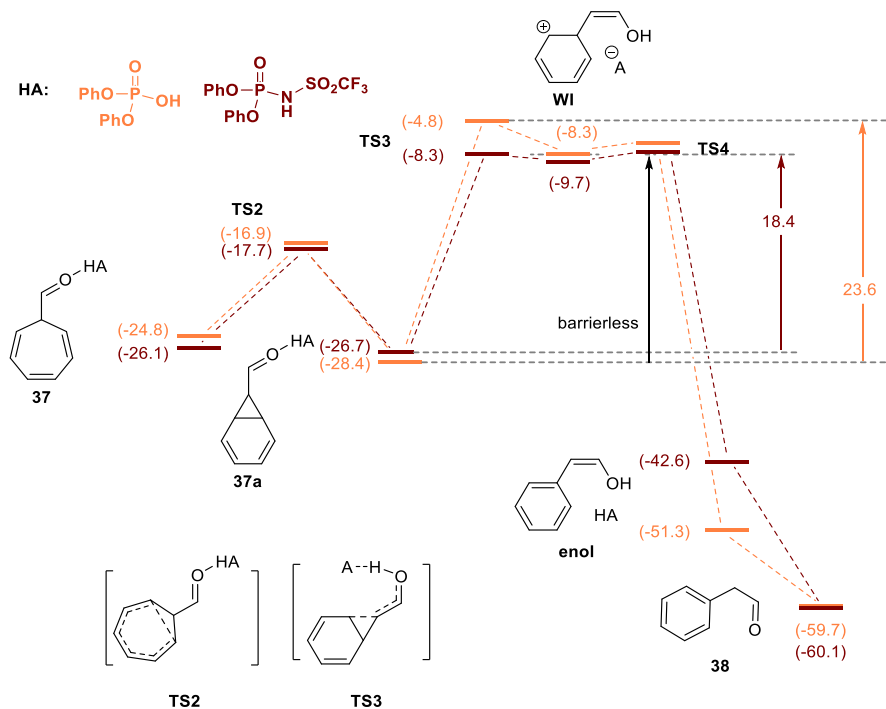


Figure 4.9. Mechanistic proposal for the transformation of **37** to **38**.

The optimized geometries for the previously mentioned transition structures (**TS2a,b** and **TS3a,b**) are given in the following Figure 4.10. The obtained optimized structures for the first case (**TS2a,b**) would clearly indicate that the isomerization of cycloheptatrienecarbaldehyde **37** to formyl norcaradiene **37a** would take place through the non-protonated form since the proton is located closer to the catalyst whereas for the second case (**TS3a,b**), as required for the cyclopropane ring-opening, would correspond to the protonated form of the substrate.

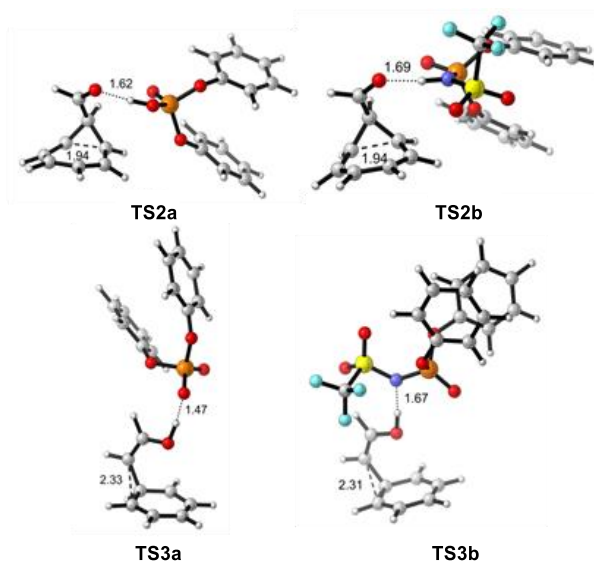


Figure 4.10. Optimized geometries for the transition structures **TS2a,b** and **TS3a,b**, corresponding to the formation of **38**.

With a deeper understanding of the different events during the full concerted reaction outcome, the next step was to perform an analysis of the energy profiles of the transformation (Figure 4.11). This study revealed that for the reaction catalyzed by diphenylphosphate, the rate determining step would be the formation of aldehyde **38** from **37a** (23.6 kcal/mol, through **TS3a**) whereas for the case of the more acidic catalyst, the rate-limiting step would be the first step, corresponding to **TS2b**, with a barrier of 21.9 kcal/mol. The difference observed is of 1.7 kcal/mol, in favour to the more acidic catalyst, and this fact would be enough to justify the different behaviour observed for the two catalysts employed but also the obtained mixture of products when the temperature of the reaction was decreased (Scheme 4.15). Moreover, the different rate-limiting stage for each reaction would also be in agreement with the experimental observations performed by $^1\text{H-NMR}$ in the absence of the allylboronate, for which, at room temperature using diphenylphosphate the only accumulated species is aldehyde **37**.

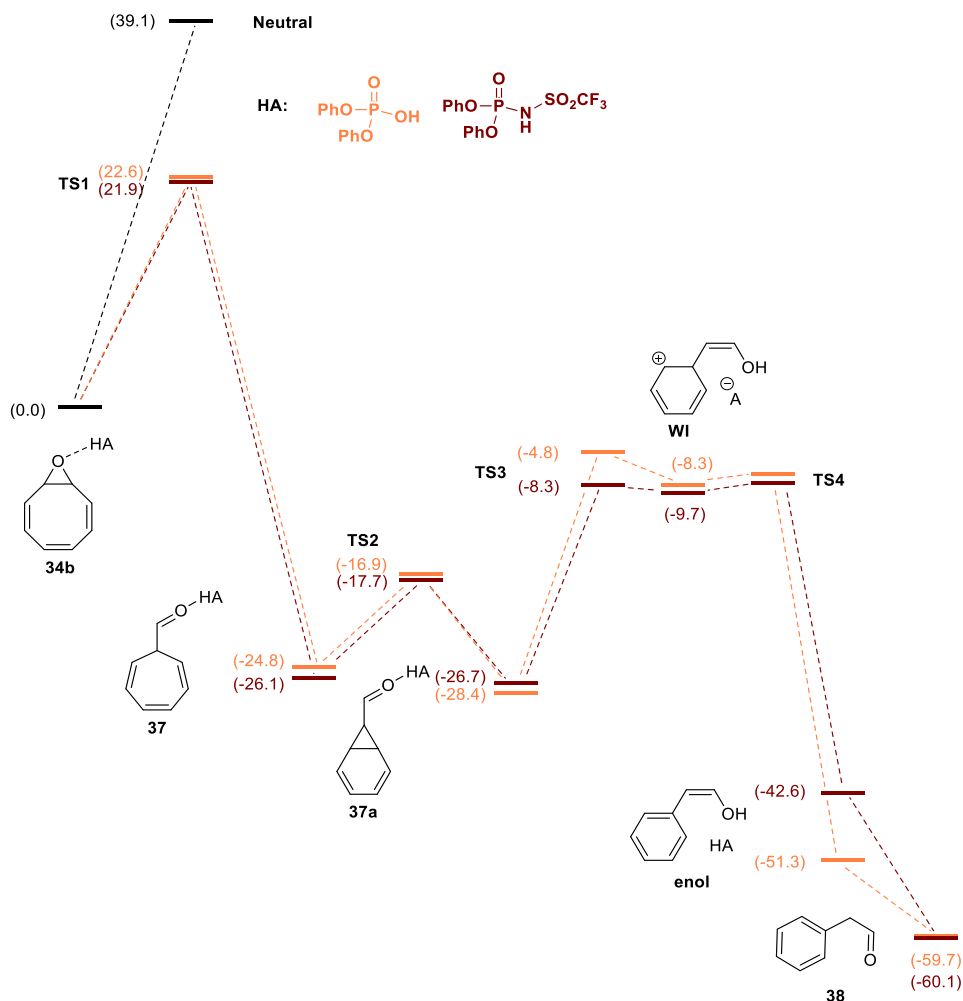
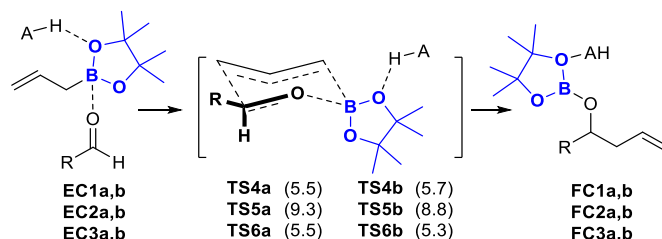


Figure 4.11. Energy profile for the transformation of **34b** into **37** and then **38**.

The next efforts were focused on the study of the energetic profile of the allylboration of the mentioned aldehyde intermediates. The general model for the corresponding interactions between reactants and the Brønsted acid catalyst, during the addition process, was studied computationally in excellent detail for Goodman and co-workers in 2012.³⁵ Thus, according to that model, the allylboronate is proposed to coordinate the carbonyl oxygen of the aldehyde to

³⁵ Grayson, M. N.; Pellegrinet, S. C.; Goodman, J. M. *J. Am. Chem. Soc.* **2012**, *134*, 2716.

reach a classical six-membered ring transition state in which the phosphoric acid would be able to establish a H-bond interaction with the oxygen of the boronate system (Scheme 4.21). For this reason, this reaction would require the presence of the non-protonated form of the aldehyde to participate in the allylation step.



1 series and **TS4a,b** from aldehyde **37**
 2 series and **TS5a,b** from aldehyde **37a**
 3 series and **TS6a,b** from aldehyde **38**

a series using **diphenylphosphate** as a catalyst
 b series using **N-triflylphosphoramidate**
 as a catalyst

Scheme 4.21. Calculation of the allylation process from the corresponding encounter complexes (**EC**) to the final complexes (**FC**). (Barriers are given in kcal/mol relative to the corresponding **EC**).

The obtained barriers for the allylboration were found to be 7.3 kcal/mol for the allylation of **37**, for both catalysts, 10.8 and 9.8 kcal/mol for the allylation of **37a**, 7.5 and 7.2 kcal/mol for the allylation of **38**. Therefore, the calculated values suggest that dependence of the acidity of the catalyst for the allylation step is negligible (representative **TS4a**, **TS5a** and **TS6b** transition structures for the mentioned step are represented in Figure 4.12). Besides, these results are in good agreement with the experimental observations since the lower barrier observed for the allylation with respect to the ring contraction processes indicates a preferred reaction pathway, in which a minimum concentration of non-protonated aldehyde needs to be available. The less acidic catalyst (diphenylphosphate) would allow that enough non-protonated aldehyde is present and thus, the subsequent allylation process could proceed without any problem. On the other hand, for the case of the more acidic catalyst, the aldehyde remains mostly protonated and, consequently, the allylation would not occur instantaneously favouring the isomerization of **37** to **38**. Eventually, with the presence of the allylboronate and without any competitive reactions, aldehyde **38** would be finally allylated.

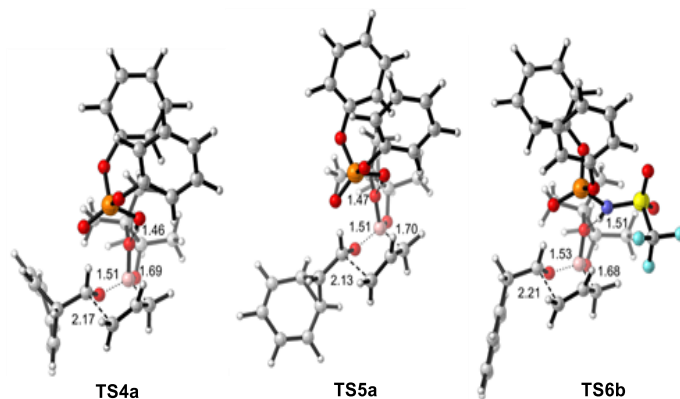


Figure 4.12. Optimized geometries for the transition structures corresponding to the allylboration.

The previously obtained results for the calculated barriers of the allylboration process were supported by comparison of the energies associated to the possible complexes coming from **37**, the two acidic catalysts and the allylboronate. As illustrated in Figure 4.13, the lowest gap between a complex with the acid and the allylating agent, which is required to initiate the allylboration, corresponds to diphenylphosphate with aldehyde **37a** with a value of 3.7 kcal/mol. On the other hand, if we compare the stability of the possible aldehydes with the more acidic *N*-triflylphosphoramidate, the gap is higher with a value of 5 kcal/mol and therefore, indicating that the process would be favoured for the case of the less acidic catalyst.

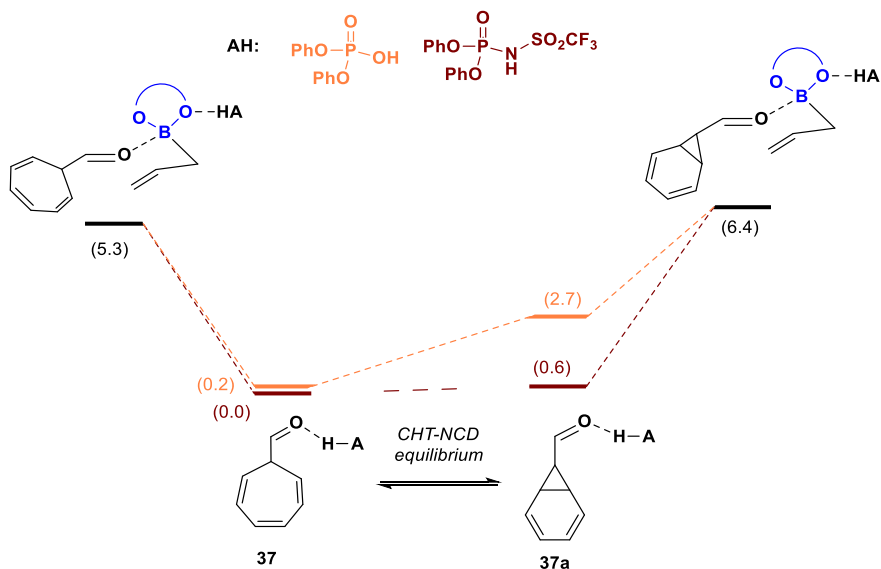


Figure 4.13. Calculated relative energies for the possible different complexes.

Finally, given the crucial role of the acidity of the catalyst, we decided to evaluate the outcome of the reaction using catalysts of different acidity with the aim to establish a correlation between the product selectivity and the pK_a of the Brønsted acid catalyst. As it is illustrated in the following Figure 4.14, we could see that a clear trend was observed between the selectivity of the transformation and the acidity of the catalyst employed in each experiment. In fact, a certain acidity minimum is needed for the reaction to occur, since benzoic acid ($pK_a = 21.5$) and perfluorophenol ($pK_a = 20.1$)³⁶ were unable to transform the starting material into any of the ring contraction products. When 4- $CF_3C_6F_4OH$ ($pK_a = 16.6$) was employed, only small conversion towards the formation of cycloheptatrienyl-substituted homoallylic alcohol **35** was observed after a prolonged reaction time. With the corresponding phosphoric acid ($pK_a = 13.6$), employed in our previous proof of concept experiments, complete disappearance of **34b** was obtained and

³⁶ Kütt, A.; Tshpelevitsh, S.; Saame, J.; Lõkov, M.; Kaljurand, I.; Selberg, S.; Leito, I. *Eur. J. Org. Chem.* **2021**, 1407.

as catalyst acidity increased, the formation of compound **36** gained prevalence on the crude reaction mixtures.

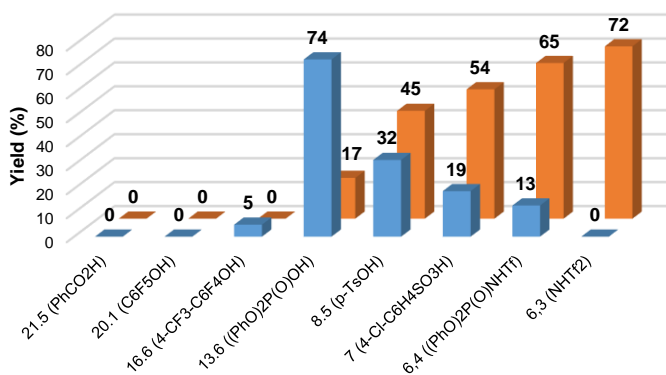
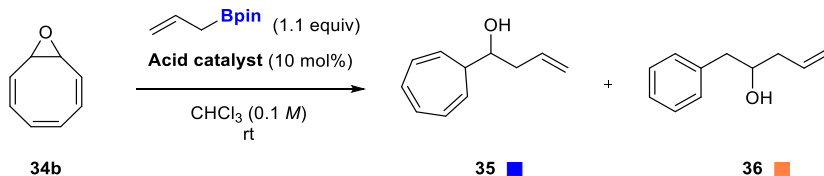


Figure 4.14. Correlation between selectivity and catalyst acidity.

3.3. Enantioselective ring contraction/allylation process

With an extensive understanding of the mechanism operating in this transformation and knowing that Brønsted acids are able to catalyze the addition of allylboronates to aldehydes,³⁷ we next became interested in the optimization of the enantioselective version of the coupled ring contraction and further allylation process. The incorporation of a chiral phosphoric acid would enable the direct and easy preparation of cycloheptatrienyl-substituted homoallylic alcohols from a readily available starting material such as cyclooctatetraene oxide and being an alternative of the conventional approach through the described Buchner reaction. At this point, we have not considered the possibility of developing the enantioselective double ring contraction/allylation reaction sequence towards enantioenriched 1-phenylpent-4-en-2-ols since their preparation is more straightforward using directly commercially available phenylacetaldehyde through the same type of chiral Brønsted acid-catalyzed allylboration reaction.^{35,38}

We focused on the reaction between (2Z,4Z,6Z)-9-oxabicyclo[6.1.0]nona-2,4,6-triene (**34b**) and 2-allyl-4,4,5,5-tetramethyl-1,3,2-dioxaborolane, as model system, and we first proceed to evaluate different BINOL-based chiral phosphoric acids in order to obtain high levels of asymmetric induction. For the initial experiments, we decided to carry out the reactions using a solvent of low polarity, such as toluene, in order to potentially maximize the possible H-bonding interactions between the substrate and the catalyst contributing therefore to obtain higher enantioselectivities. As it can be seen in the following Table 4.2, from the different phosphoric acids tested (Entries 1-12), the archetypical TRIP-phosphoric acid (**39a**) provided the highest value of enantioselectivity in 67% yield (Entry 1). Other catalysts with different substituents at the 3- and 3'-positions of the BINOL core

³⁷ For selected reviews about chiral Brønsted acid-catalyzed allylation of carbonyl compounds, see: (a) Yus, M.; González-Gómez, J. C.; Foubelo, F. *Chem. Rev.* **2011**, *111*, 7774. (b) Sedgwick, D. M.; Grayson, M. N.; Fustero, S.; Barrio, P. *Synthesis* **2018**, *50*, 1935.

³⁸ For seminal contributions on chiral Brønsted acid-catalyzed allylboration of aldehydes, see: (a) Jain, P.; Antilla, J. C. *J. Am. Chem. Soc.* **2010**, *132*, 11884. (b) Wang, H.; Jain, P.; Antilla, J. C.; Houk, K. N. *J. Org. Chem.* **2013**, *78*, 1208.

were tested, although, without significant improvements in terms of both yields and enantioselectivities (Entries 2-7). Similar reactivity trend was observed when extended π -aryl substituents were placed at the 3- and 3'-positions of the BINOL core, although observing slightly better yields but with lower enantioselectivity (Entries 8-12).

Table 4.2. Optimization of the acid-catalyzed ring contraction/allylation reaction using **34b** as model substrate: catalyst screening.^[a]

34b $\xrightarrow[\text{toluene (0.1 M), rt, 20-24h}]{\text{Bpin (1.1 equiv), Catalyst (10 mol\%)}}$ **35**

39a: Ar = 2,4,6-(*i*Pr)₃C₆H₂
39b: Ar = H
39c: Ar = 2,4,6-(C₆H₁₁)₃C₆H₂
39d: Ar = 2,4,6-(C₅H₁₀)₃C₆H₂
39g: Ar = SiPh₃
39h: Ar = 9-phenanthryl
39i: Ar = Ph
39j: Ar = 9-anthracenyl
39k: Ar = Bisphenyl
39l: Ar = 3,5-(CF₃)₂C₆H₃

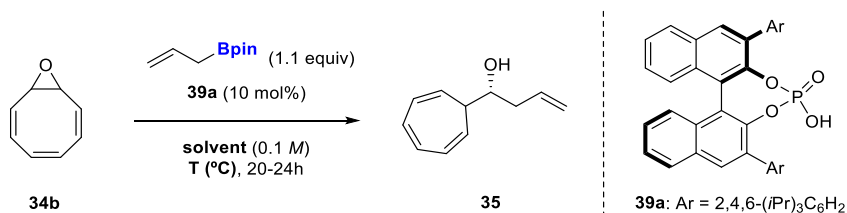
39e

39f

Entry	Catalyst	[IY%] ^[b]	e.e. (%) ^[c]
1	39a	67	82
2	39b	63	0
3	39c	62	64
4	39d	19	n.d. ^[d]
5	39e	57	0
6	39f	43	0
7	39g	46	12
8 ^[e]	39h	78	34
9 ^[e]	39i	96	0
10 ^[f]	39j	79	54
11 ^[g]	39k	80	4
12 ^[g]	39l	89	24

[a] Reactions were performed with 0.1 mmol of **34b**, allylboronate (1.1 equiv), **catalyst** (10 mol%) in toluene (0.1 M) at rt for 20-24h. [b] [IY] (%) = isolated yield after flash column chromatography purification. [c] e.e. was calculated by HPLC on chiral stationary phase. [d] n.d. = not determined. [e] Reaction time = 4h. [f] Reaction time = 6h. [g] Reaction time = 2h.

We next evaluated the influence of the solvent on the outcome of the projected ring contraction/allylation sequence using TRIP (**39a**) as the best performing catalyst (Entry 1). As summarized in the following Table 4.3, when other arenes such as mesitylene or xylene were used as solvents, similar yields were obtained but with lower values of enantiocontrol (Entries 2 and 3). Contrarily, when different halogenated reagents were tested, an outstanding outcome of the reaction was observed, increasing both yields and enantioselectivity (Entries 4-8). In particular, the best results were obtained when 1,2-dichloroethane was used as the solvent, obtaining a quantitative yield of the corresponding homoallylic alcohol **35** with 84% e.e. (Entry 5). Other more polar solvents were also tested but the reaction was much less efficient, not only with respect to enantiocontrol but also in terms of chemical yield (Entries 9-12). Since 1,2-dichloroethane showed to be the optimal solvent, we next performed the reaction at lower temperatures in order to improve the enantioselectivities (Entries 13 and 14). Working at slightly lower temperature (15 °C) enables increasing the e.e. to 86% (Entry 13) whereas when the reaction was carried out at 0 °C, became extremely slow, not observing significant conversion after 24h (Entry 14).

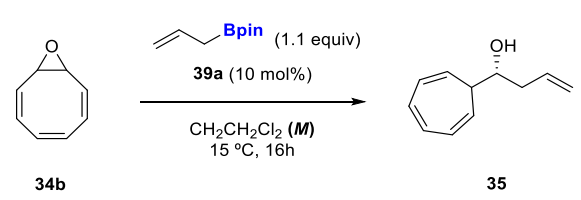
Table 4.3. Optimization of the acid-catalyzed ring contraction/allylation reaction using **34b** as model substrate: solvent and temperature screening.^[a]

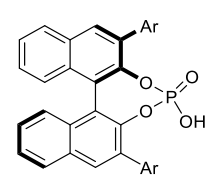
Entry	Solvent	T (°C)	[Y%] ^[b]	e.e. (%) ^[c]
1	toluene	rt	67	82
2	mesitylene	rt	65	64
3	<i>o</i> -xylene	rt	68	72
4 ^[e]	CH ₂ Cl ₂	rt	99	82
5 ^[e]	CH ₂ CH ₂ Cl ₂	rt	99	84
6	CHCl ₃	rt	86	80
7 ^[e]	C ₆ H ₅ Cl	rt	99	82
8 ^[e]	trifluorotoluene	rt	99	80
9	THF	rt	-	n.d. ^[d]
10	Et ₂ O	rt	15	10
11	1,4-dioxane	rt	-	n.d. ^[d]
12	EtOAc	rt	<5	n.d. ^[d]
13	CH ₂ CH ₂ Cl ₂	15	99	86
14	CH ₂ CH ₂ Cl ₂	0	<5	n.d. ^[d]

[a] Reactions were performed with 0.1 mmol of **34b**, allylboronate (1.1 equiv), **39a** (10 mol%) in solvent (0.1 M) at rt for 20-24h. [b] [Y] (%) = isolated yield after flash column chromatography purification. [c] e.e. was calculated by HPLC on chiral stationary phase. [d] n.d. = not determined. [e] Reaction time = 16h.

With these promising results, we next decided to test the transformation at different concentrations in order to further increase the enantioselectivity (Table 4.4, Entries 1-5). We could observe that the more concentrated the reaction, the higher e.e. values were obtained, being 1.5 M of **34b** the optimal one (Entry 4), maintaining the excellent yield and increasing the enantioselectivity to a 89%. Besides, addition of molecular sieves or lowering the catalyst loading did not show any significant improvement and a slightly decrease of the enantiocontrol was obtained (Entries 6 and 7).

Table 4.4. Optimization of the acid-catalyzed ring contraction/allylation reaction using **34b** as model substrate: concentration screening.^[a]



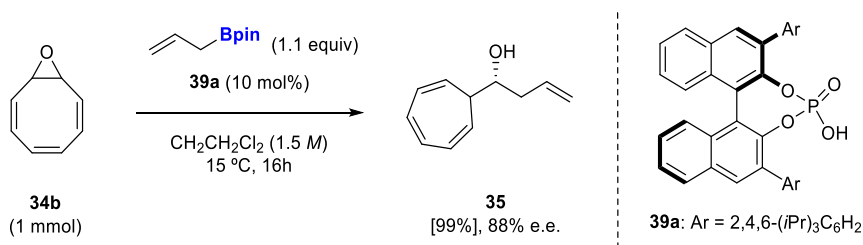


39a: Ar = 2,4,6-(*i*Pr)₃C₆H₂

Entry	Concentration (M)	[IY%] ^[b]	e.e. (%) ^[c]
1	0.01	76	64
2	0.1	99	84
3	1	99	86
4 ^[d]	1.5	99	89
5 ^[d]	2	99	86
6 ^[d,e]	2	67	84
7 ^[d,f]	1.5	99	86

[a] Reactions were performed with 0.1 mmol of **34b**, allylboronate (1.1 equiv), **39a** (10 mol%) in CH₂CH₂Cl₂ (M) at 15°C for 16h. [b] [IY] (%) = isolated yield after flash column chromatography purification. [c] e.e. was calculated by HPLC on chiral stationary phase. [d] 0.2 mmol of **34b**. [e] 5 mol% of **39a**. [f] 4Å MS as additive.

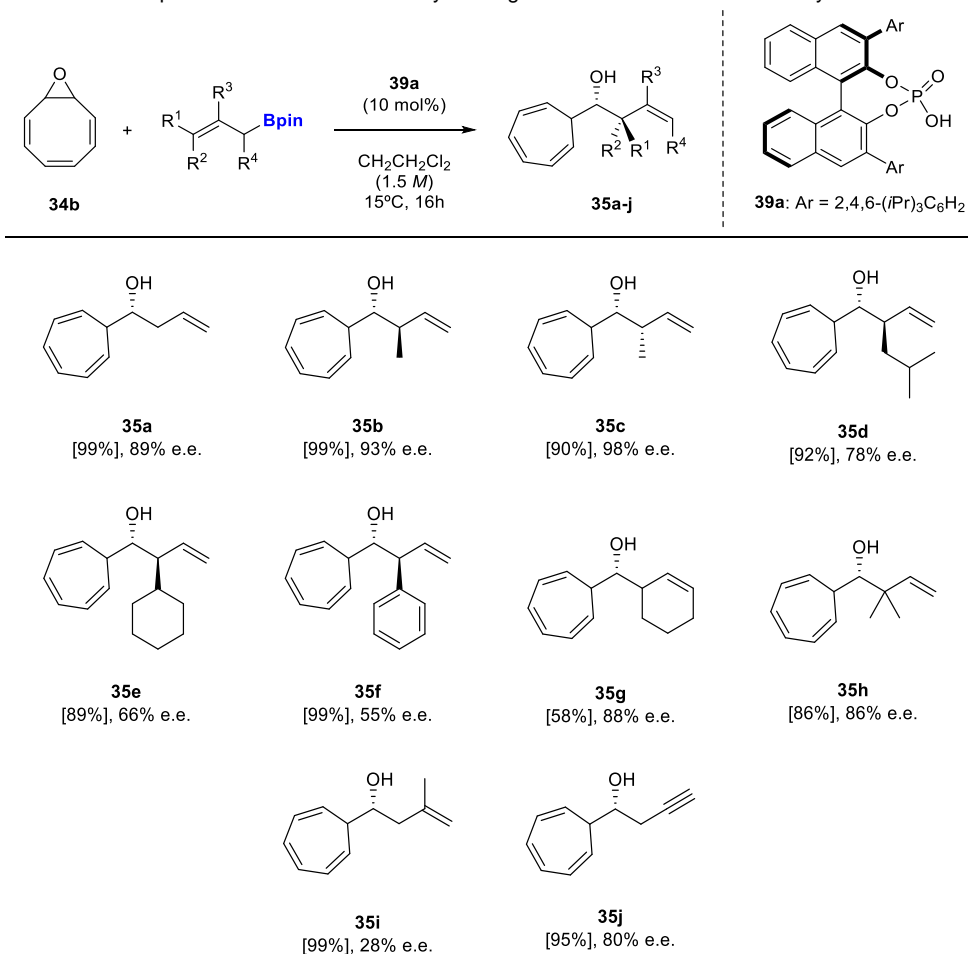
In order to demonstrate the synthetic utility of the described transformation we also performed the reaction with the model system on a larger scale. As it can be seen in the following Scheme 4.22, the reaction outcome was not affected and the corresponding homoallylic alcohol **35** could be obtained in excellent yield and enantioselectivity starting from 1 mmol of **34b**.



Scheme 4.22. Scale-up experiment with the model system.

With a robust protocol in hand, we next proceeded to evaluate the scope of the catalytic enantioselective Brønsted acid-catalyzed ring contraction/allylation process, using a variety of allylboronates, some of them provided by researchers from the group of Prof. Elena Fernández, from the Rovira i Virgili University.

As it is summarized in the following Table 4.5, we started by evaluating the influence of incorporating a substituent at the γ -position of the allylboronate. Therefore, when (*E*)-crotylboronate was used under the optimized reaction conditions, the corresponding homoallylic alcohol **35b** was isolated in a quantitative yield and as a single *anti*-diastereoisomer of very high enantiomeric excess. Remarkably, (*Z*)-crotylboronate also provided the ring contraction/allylation product leading to the formation of the syn-configured adduct **35c** as a single diastereoisomer and with excellent yield and enantioselectivity. When bulkier γ -substituents were incorporated, the reaction proceeded with excellent to good yields and complete control on the diastereoselectivity affording compounds **35d**, **35e** and **35f**. Nevertheless, the enantiocontrol of the process became significantly affected as the size of the substituent increased. A cyclic α,γ -disubstituted allylboronate was also tested and the addition product **35g** was obtained in a moderate yield presumably due to the inherent instability of the boronate reagent, but the adduct was obtained again as a single diastereoisomer and high enantiomeric purity. When a more challenging γ,γ -disubstituted allylboronate was tested, the corresponding homoallylic alcohol **35h** was isolated with good yield and enantioselectivity and again, with total diastereocontrol. On the other hand, the incorporation of a β -substituent at the allylborane reagent affected the reaction outcome providing the desired product **35i** with excellent yield but with a rather low value of enantioinduction. Finally, when an allenylboronate was used as the nucleophile in the reaction, the corresponding homopropargyl alcohol **35j** was obtained in high yield and moderate enantioselectivity.

Table 4.5. Scope of the Brønsted acid-catalyzed ring contraction/enantioselective allylation.^[a]

[a] Reactions were performed with 0.2 mmol of **34b**, allylboronates (1.1 equiv), **39a** (10 mol%) and $\text{CH}_2\text{CH}_2\text{Cl}_2$ (1.5 M) at 15 °C for 16h. Isolated yields after flash chromatography purification and e.e. calculated by HPLC on chiral stationary phase are given.

Computational calculations using the Goodman's model were also performed at the University of Zaragoza employing the optimal chiral catalyst (**39a**) in order to gain mechanistic understanding of the source of the enantiocontrol. The selected model system was the addition of 2-allyl-4,4,5,5-tetramethyl-1,3,2-dioxaborolane to aldehyde **37** in the presence of **39a** exploring both *Re* and *Si* faces as well as the conformational variability of the transition structures. In this case, calculations

predicted the formation of the enantiomer coming from the *Re* attack (**TS7a-Re**) to be predominant with the possibility of obtaining a minor amount of the other enantiomer, coming from the *Si* attack (**TS7a-Si**) with a difference of 3 kcal/mol (Figure 4.15). This fact could be rationalized due to the steric hindrance present in the case of **TS7a-Si** between the Bpin moiety and the substituents at the 3- and 3'-positions of the catalyst (**39a**).

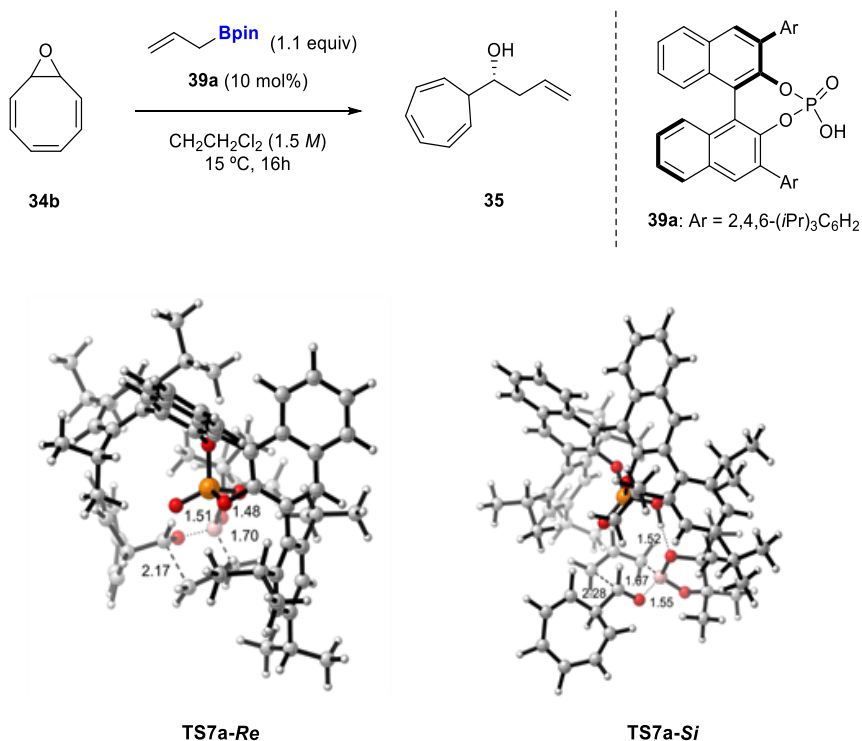


Figure 4.15. Optimized geometries of the transition structures for the allylation process.

4. CONCLUSIONS

Considering the obtained results in this chapter, the following conclusions can be highlighted:

1. Cyclooctatetraene derivatives did not undergo direct ring opening allylation/transannular 6π -electrocyclization reaction sequence under Brønsted acid catalysis. Instead, cyclooctatetraene oxide reacted with allylboronates under Brønsted acid catalysis through ring contraction/allylboration reaction sequence.
2. The described ring contraction/allylboration reactivity exhibited an influence of the pK_a along the ring contraction process. A clear trend was identified regarding the selectivity of the process when the reaction was performed using catalysts of different acidity. Therefore, a certain pK_a value is needed in order to promote the desired transformation towards the single ring contraction product whereas the second ring contraction is favoured as the catalyst acidity increases.
3. Computational and mechanistic studies, performed in collaboration with the group of Prof. Pedro Merino, allowed to understand the overall reaction mechanism. Theoretical results, supported by experimental proofs, demonstrated the switchable behaviour of cyclooctatetraene oxide under Brønsted acid catalysis towards the formation of different homoallylic alcohols due to the existence of different aldehyde intermediates, having different rate-determining steps, depending on the acidic catalyst. In that sense, the rate determining step for the less acidic diphenylphosphate catalyst showed to be the formation of phenylacetaldehyde (**38**) from **37a** whereas for the case of the more acidic *N*-triflylphosphoramidate, the rate determining step would be the isomerization of **37** to **37a**. Moreover, it has also been demonstrated that the second allylation step does not fully depend

on the nature of the catalyst but on the most stable aldehyde intermediate that can be accumulated and further reacted with the allylboronate.

4. This methodology enables the straightforward preparation of enantioenriched cycloheptatrienyl-substituted homoallylic alcohols when a chiral phosphoric acid is used as the selected catalyst. The transformation exhibited a wide substrate scope, including different substitution patterns along the allylboronate skeleton, and the corresponding products were obtained in high yields and enantioselectivities.

5

5

Final Conclusions

1. CONCLUSIONS

The present work covers the study and development of novel enantioselective transannular reactions relying on the use of catalytic organoboron chemistry and organocatalysis as efficient systems to generate new C-B and C-C bonds. Experimental results collected during the accomplishment of this work lead to the following general conclusions:

Copper(I)-catalyzed stereoselective conjugate borylation/transannular aldol reaction sequence. It has been demonstrated that medium-sized keto-enones are ideal model systems to conduct copper-catalyzed conjugate borylation and subsequent transannular aldol reaction triggering a highly diastereoselective transformation that enables the construction of complex polycyclic scaffolds. The *in situ* generation of the nucleophilic Cu-Bpin species, by activation of B₂pin₂ with an efficient CuCl/ligand/base catalytic system, is essential for this purpose. The reaction rendered the desired polycyclic organoboranes as a single diastereoisomer with good results, including different ring sizes of the substrates as well as showing good tolerance to the incorporation of fused aromatic rings with different bulkiness and electronic properties. The utility of the transformation was extended with the incorporation of a chiral ligand obtaining the desired borylated adducts in a highly enantioselective fashion.

Cycloalkenone hydrazones acting as 1,3-dipoles in the enantioselective transannular (3+2) cycloaddition reaction under chiral Brønsted acid catalysis. The work verified that cycloalkenone hydrazones generated *in situ* from the corresponding cyclodecenones or cyclononenones could efficiently undergo transannular (3+2) cycloaddition reactions under chiral Brønsted acid catalysis. The reaction enabled the straightforward preparation of stereodefined polycyclic scaffolds with a bridged pyrazolidine ring, showing a wide substrate scope including different substitution patterns and ring sizes of the cyclic precursor and various hydrazines with different electronic properties for the formation of the 1,3-dipole. Synthetically challenging decaline- and octahydro-1*H*-indene *cis*-1,3-diamines

could be obtained after reductive cleavage of the obtained pyrazolidine ring with excellent yields and without loss of optical purity during the transformation.

Switchable Brønsted acid-catalyzed ring contraction/allylboration reaction of cyclooctatetraene oxide. The ability of cyclooctatetraene oxide to undergo single or double ring contraction processes, under Brønsted acid catalysis, has been confirmed and has been shown that it could be modulated through the pK_a of the chosen Brønsted acid catalyst, leading selectively to cycloheptatrienecarbaldehyde or phenylacetaldehyde in a switchable manner. This ring contraction process could be coupled to an allylboration reaction that enabled the synthesis of enantioenriched cycloheptatrienyl-substituted homoallylic alcohols in good yields and enantioselectivities when a chiral BINOL-based chiral phosphoric acid is used as the catalyst. The mechanism of the isomerization processes, together with the high dependence of the reaction with the pK_a , has been disclosed in detail with the support of mechanistic and computational studies performed in collaboration with the group of Prof. Pedro Merino from the University of Zaragoza.

6

6

Experimental

1. GENERAL METHODS AND MATERIALS	187
2. CATALYTIC STEREOSELECTIVE BORYLATIVE TRANSANNULAR REACTIONS	191
2.1. Synthesis of the starting materials	191
2.2. Cu/dppf catalyzed transannular conjugated borylation/aldol cyclization ...	194
2.3. Cu/Josiphos catalyzed transannular conjugated borylation/aldol cyclization	204
2.4. Oxidation procedures	210
3. TRANSANNULAR ENANTIOSELECTIVE (3+2) CYCLOADDITION OF CYCLOALKENONE HYDRAZONES	212
3.1. Synthesis of the starting materials	212
3.2. Enantioselective transannular (3+2) cycloaddition	221
3.3. Derivatization procedures for the cycloaddition adducts	231
3.4. Reductive cleavage for the synthesis of enantioenriched 1,3-diamines....	240
4. SWITCHABLE BRØNSTED ACID-CATALYZED RING CONTRACTION/ENANTIOSELECTIVE ALLYLATION	245
4.1. Synthesis of the starting materials	245
4.2. Enantioselective ring contraction/allylation reaction	246

1. GENERAL METHODS AND MATERIALS

Analytical grade *solvents* and commercially available *reagents* were used without further purification. Anhydrous solvents were purified and dried with activated molecular sieves prior to use.¹ For reactions carried out under inert conditions, the argon was previously dried through a column of P₂O₅ and a column of KOH and CaCl₂. All the glassware was dried for 12 hours prior to use in an oven at 140 °C, and allowed to cool under a dehumidified atmosphere.² Reactions at reduced temperatures were carried out using Isotemp refrigerator. Reactions were monitored using analytical thin layer chromatography (TLC), in pre-coated silica-backed plates (Merck Kieselgel 60 F₂₅₄ 400-630 mesh) and visualized by ultraviolet irradiation, *p*-anisaldehyde, phosphomolybdic acid, potassium permanganate, Hanessian stain or iodine dips.³ For flash chromatography Silicycle 40-63, 230-400 mesh silica gel was used.⁴ For removal of solvents under reduced pressure Büchi R-210 rotatory evaporators were used. For precision weighing Sartorius Analytical Balance Practum 224-1S was used (± 0.1 mg).

Monodimensional and/or bidimensional nuclear magnetic resonance proton and carbon spectra (¹H NMR, ¹³C NMR, ¹¹B NMR and ¹⁹F NMR) were acquired at 25 °C on a Bruker AC-300 spectrometer (300 MHz for ¹H, 75.5 MHz for ¹³C and 283 MHz for ¹⁹F), Bruker AC-500 spectrometer (500 MHz for ¹H and 125.7 MHz for ¹³C) or Varian Goku 400 or a Varian Mercury 400 spectrometer (400 MHz for ¹H, 100 MHz for ¹³C and 128.3 MHz for ¹¹B) at the indicated temperature. Chemical shifts (δ) are reported in ppm relative to residual solvent signals⁵ (CHCl₃, 7.26 ppm for ¹H NMR, CDCl₃, 77.16 ppm for ¹³C NMR) and coupling constants (*J*) in hertz (Hz). The following abbreviations are used to indicate the multiplicity in NMR spectra: s, singlet; d, doublet; t, triplet; q, quartet; app, apparent; m, multiplet; bs, broad signal.

¹ (a) Perrin, D. D.; Armarego, W. L. F. (1988). *Purification of Laboratory Chemicals*; Pergamon Press; 3r Edition. (b) Williams, D. B. G.; Lawton, M. J. *Org. Chem.* **2010**, *75*, 8351.

² Kramer, G. W.; Levy, A. B.; Midland, M. M. (1975). *Organic Synthesis via Boranes*; John Wiley & Sons: New York.

³ Stahl, E. (1969). *Thin Layer Chromatography*; Springer-Verlag: Berlin.

⁴ Still, W. C.; Kahn, H.; Mitra, A. J. *J. Org. Chem.* **1978**, *43*, 2923.

⁵ Gottlieb, H. E.; Kotlyar, V.; Nudelman, A. *J. Org. Chem.* **1997**, *62*, 7512.

^{13}C NMR spectra were acquired on a broad band decoupled mode using DEPT experiments (Distorsionless Enhancement by Polarization Transfer) for assigning different types of carbon environment. Selective n.O.e., NOESY, COSY, HSQC and HMBC experiments were acquired to confirm precise molecular configurations and to assist in convoluting complex multiplet signals.⁶

Infrared spectra (IR) were measured in a Jasco FT/IR 4100 (ATR) in the interval between 4000 and 400 cm^{-1} with a 4 cm^{-1} resolution. Only characteristic bands are given in each case. *Melting points (M.p.)* were measured in a Stuart SMP30 apparatus in open capillary tubes and are uncorrected.

Mass spectra (MS) were recorded on an Agilent 7890A gas chromatograph coupled to an Agilent 5975 quadrupole mass spectrometer under electronic impact ionization (EI) 70 eV or on a HP6890 gas chromatograph and an Agilent Technologies 5973 Mass selective detector (Waldbronn, Germany) equipped with an achiral capillary column HP-5 (30 m, 0.25 mm, i.d., 0.25 μm thickness) using He as the carrier gas. The obtained data is presented in mass units (m/z) and the values found in brackets belong to the relative intensities comparing to the base peak (100%).

High-resolution mass spectra (HRMS) were recorded on an Acquity UPLC coupled to a QTOF mass spectrometer (SYNAPT G2 HDMS) using electrospray ionization (ESI^+ or ESI^-) or on a 6210 Time of Flight (TOF) mass spectrometer from Agilent Technologies (Waldbronn, Germany) with and ESI interface.

The enantiomeric excess (e.e.) of the products was determined by *High Performance Liquid Chromatography (HPLC)* on a chiral stationary phase in a Waters chromatograph coupled to a Waters photodiode array detector or in an Agilent Technologies 1200 Series HPLC-DAD instrument equipped. Daicel Chiralpak IA, IC, ID, IF, AD-H, AD-3, AS-H, AZ-3, AY-3 and Chiralcel OD and OD-

⁶ Kinss, M.; Sanders, J. K. M. *J. Mag. Res.* **1984**, 56, 518.

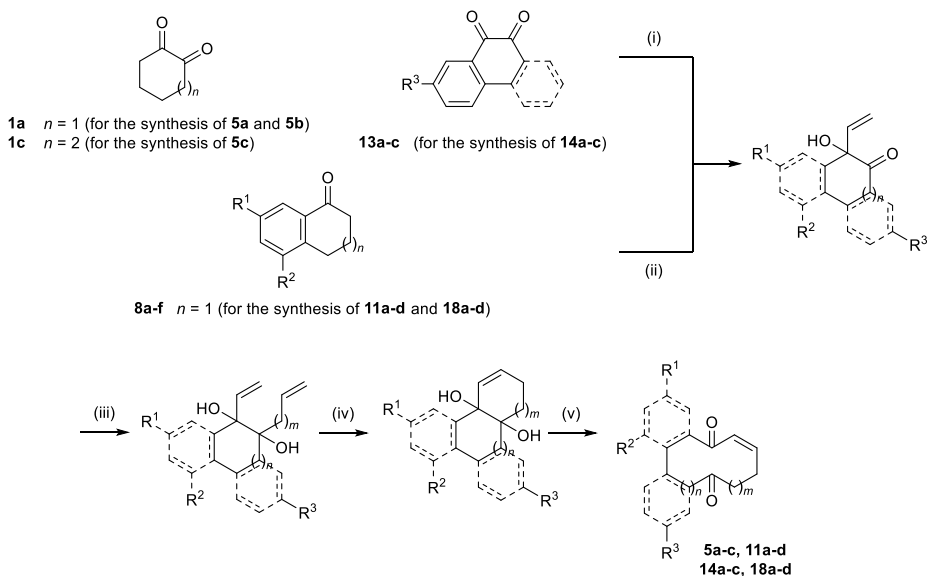
3 columns (0.46 × 25 cm) were used; specific conditions are indicated for each case.

Specific optical rotations ($[\alpha]_D^{20}$) were measured at 20 °C on a Jasco P-2000 polarimeter with sodium lamp at 589 nm and a path of length of 1 dm or at 25 °C on a Perkin-Elmer MC240 polarimeter. Solvent and concentration are specified in each case.

X-ray data collections were performed in an Agilent Supernova diffractometer equipped with an Atlas CCD area detector, and a CuK α micro-focus source with multilayer optics ($\lambda = 1.54184 \text{ \AA}$, 250 μm FWHM beam size). The sample was kept at 150 K with an Oxford Cryosystems Cryostream 700 cooler. The quality of the crystals was checked under a polarizing microscope, and a suitable crystal or fragment was mounted on a Mitegen Micromount™ using Paratone N inert oil and transferred to the diffractometer.

2. CATALYTIC STEREOSELECTIVE BORYLATIVE TRANSANNULAR REACTIONS

2.1. Synthesis of the starting materials



- (i) $\text{CH}_2=\text{CHMgBr}$ (2 equiv), THF (0.1 M), 0 °C to rt, 16h
 (ii) 1. PIDA (1.1 equiv), KOH (3 equiv), MeOH, 12 h, then HCl, EtOH
 2. $\text{CH}_2=\text{CHMgBr}$ (2 equiv), THF (0.1 M), 0 °C to rt, 16h
 3. IBX (3 equiv), EtOAc (0.5 M), reflux, 16h
 (iii) $\text{CH}_2=\text{CHCH}_2(\text{CH}_2)_m\text{MgBr}$ (3.8 equiv), THF (0.5 M), 0 °C to 40 °C, 2h
 (iv) Grubbs 2nd gen. (2.5 mol%), CH_2Cl_2 (33 mM), reflux
 (v) $\text{Pb}(\text{OAc})_4$ (1 equiv), CH_2Cl_2 (0.4 M), rt, 30 min

Non-aromatic substrates

5a $n = 1; m = 1$

5b $n = 1; m = 2$

5c $n = 2; m = 1$

Fused aromatic substrates

11a $n = m = 1; \text{R}^1 = \text{R}^2 = \text{Me}$

11b $n = m = 1; \text{R}^1 = \text{OMe}; \text{R}^2 = \text{H}$

11c $n = m = 1; \text{R}^1 = \text{H}; \text{R}^2 = \text{OMe}$

11d $n = m = 1; \text{R}^1 = \text{F}; \text{R}^2 = \text{H}$

14a $n = m = 1; \text{R}^1 = \text{R}^2 = \text{R}^3 = \text{H}$

14a $n = m = 1; \text{R}^1 = \text{R}^2 = \text{H}; \text{R}^3 = \text{Br}$

14c $n = m = 1; \text{R}^1 = \text{R}^2 = \text{R}^3 = \text{H}$ (2 Ar)

18a $n = 1; m = 2; \text{R}^1 = \text{R}^2 = \text{Me}$

18b $n = 1; m = 2; \text{R}^1 = \text{OMe}; \text{R}^2 = \text{H}$

18c $n = 1; m = 2; \text{R}^1 = \text{R}^2 = \text{H}$

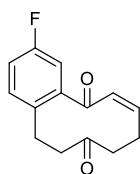
18d $n = 1; m = 2; \text{R}^1 = \text{Br}; \text{R}^2 = \text{H}$

Scheme 6.1. General overview of the synthesis of starting materials.

Compounds **5a-c**, **11a-d**, **11a-c** and **18a-d** were synthesized using our previous literature procedure.⁷ The synthesis of compounds **11d** and **14a-c** were performed using the same protocol with some modifications at the last step.

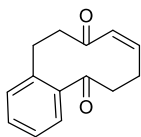
General Procedure V for the synthesis of substrates **11d** and **14a-c**: To a solution of $\text{Pb}(\text{OAc})_4$ (4.00 mmol) in CH_2Cl_2 (10 mL) was added a solution of the corresponding 1,2-diol (4.00 mmol) in CH_2Cl_2 (10 mL) and it was stirred at room temperature for 60-120 min (monitored by TLC). The reaction mixture was concentrated, taken up in ether and the solids were removed by filtration through a short pad of silica gel. The filtrate was concentrated and purified by column chromatography on silica gel (*vide infra*) to yield the desired product.

(Z)-3-fluoro-8,9,11,12-tetrahydrobenzo[10]annulene-5,10-dione (11d).

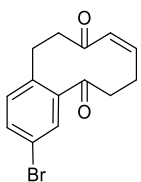


Following the *General Procedure V*, compound **11d** (226 mg, 0.98 mmol) was isolated by flash chromatography (petroleum ether/EtOAc 7:3) in 70% yield as a colorless oil starting from 6-fluoro-1,2,9,10-tetrahydrophenanthrene-4a,10a-diol (327 mg, 1.4 mmol) and $\text{Pb}(\text{OAc})_4$ (681 mg, 1.5 mmol). $^1\text{H-NMR}$ (δ , ppm) (400 MHz, CDCl_3): 7.27-7.19 (m, 1H, CH_{arom}), 7.10 (td, $J = 8.3, 2.8$ Hz, 1H, CH_{arom}), 6.96 (dd, $J = 8.5, 2.8$ Hz, 1H, CH_{arom}), 6.42 (dt, $J = 12.1, 1.0$ Hz, 1H, **H-6**), 6.31 (dt, $J = 12.1, 8.5$ Hz, 1H, **H-7**), 3.08-3.00 (m, 2H, **H-12**), 2.70-2.62 (m, 2H, **H-11**), 2.49-2.42 (m, 2H, **H-9**), 2.28-2.18 (m, 2H, **H-8**). $^{13}\text{C-NMR}$ (δ , ppm) (100 MHz, CDCl_3): 210.3 (**C-10**), 197.3 (**C-5**), 162.4 (C_{arom}), 159.9 (C_{arom}), 143.4 (**C-7**), 134.3 (C_{arom}), 133.1 (**C-6**), 132.4 (CH_{arom}), 117.5 (CH_{arom}), 113.4 (CH_{arom}), 43.9 (**C-11**), 43.3 (**C-9**), 28.4 (**C-8**), 22.3 (**C-12**). HRMS (ESI-TOF) for $\text{C}_{14}\text{H}_{13}\text{FNaO}_2$ $[\text{M}+\text{Na}]^+$: calculated: 255.0797, found: 255.0796.

⁷ R. Mato, R. Manzano, E. Reyes, L. Carrillo, U. Uria, J. L. Vicario. *J. Am. Chem. Soc.* **2019**, *141*, 9495.

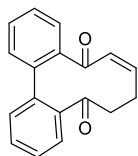
(Z)-6,7,11,12-tetrahydrobenzo[10]annulene-5,10-dione (14a).

Following the *General Procedure V*, compound **14a** (348 mg, 1.62 mmol) was isolated by flash chromatography (petroleum ether/ethyl acetate 7:3) in 65% yield as a white solid starting from 3,4,9,10-tetrahydrophenanthrene-4a,10a-diol (543 mg, 2.5 mmol) and $\text{Pb}(\text{OAc})_4$ (1.225 g, 2.8 mmol). $^1\text{H-NMR}$ (δ , ppm) (400 MHz, CDCl_3): 7.41 (td, $J = 7.5, 1.5$ Hz, 1H, CH_{arom}), 7.30 (dt, $J = 7.7, 1.4$ Hz, 2H, 2 x CH_{arom}), 7.27-7.19 (m, 1H, CH_{arom}), 6.16 (dt, $J = 11.9, 1.2$ Hz, 1H, **H-9**), 5.88 (dt, $J = 11.8, 8.4$ Hz, 1H, **H-8**), 3.28-3.20 (m, 2H, **H-11**), 2.94-2.86 (m, 2H, **H-12**), 2.68-2.55 (m, 4H, **H-6** and **H-7**). $^{13}\text{C-NMR}$ (δ , ppm) (100 MHz, CDCl_3): 207.6 (**C-5**), 204.9 (**C-10**), 139.3 (**C-8**), 138.9 (C_{arom}), 138.6 (C_{arom}), 131.6 (**C-9**), 131.3 (CH_{arom}), 131.0 (CH_{arom}), 126.2 (CH_{arom}), 126.0 (CH_{arom}), 46.4 (**C-11**), 42.7 (**C-6**), 27.5 (**C-12**), 24.6 (**C-7**). HRMS (ESI-TOF) for $\text{C}_{14}\text{H}_{14}\text{KO}_2$ [$\text{M}+\text{K}$] $^+$: calculated: 253.0631, found: 253.0635.

(Z)-3-bromo-6,7,11,12-tetrahydrobenzo[10]annulene-5,10-dione (14b).

Following the *General Procedure V*, compound **14b** (445 mg, 1.51 mmol) was isolated by flash chromatography (dichloromethane/MeOH gradient from 100:0 to 96:4) in 70% yield as a brown solid starting from 6-bromo-3,4,9,10-tetrahydrophenanthrene-4a,10a-diol (640 mg, 2.17 mmol) and $\text{Pb}(\text{OAc})_4$ (1.057 g, 2.4 mmol). $^1\text{H-NMR}$ (δ , ppm) (400 MHz, CDCl_3): 7.52 (dd, $J = 8.3, 2.1$ Hz, 1H, CH_{arom}), 7.42 (d, $J = 2.1$ Hz, 1H, CH_{arom}), 7.18 (d, $J = 8.3$ Hz, 1H, CH_{arom}), 6.16 (dt, $J = 11.7, 1.2$ Hz, 1H, **H-9**), 5.88 (dt, $J = 11.8, 8.3$ Hz, 1H, **H-8**), 3.22-3.14 (m, 2H, **H-11**), 2.94-2.84 (m, 2H, **H-12**), 2.67-2.56 (m, 4H, **H-6** and **H-7**). $^{13}\text{C-NMR}$ (δ , ppm) (100 MHz, CDCl_3): 205.8 (**C-5**), 204.5 (**C-10**), 141.0 (C_{arom}), 138.9 (**C-8**), 137.6 (C_{arom}), 134.0 (**C-9**), 133.0 (CH_{arom}), 131.5 (CH_{arom}), 128.8 (CH_{arom}), 120.0 (C_{arom}), 46.0 (**C-11**), 42.5 (**C-6**), 27.2 (**C-12**), 24.4 (**C-7**). HRMS (ESI-TOF) for $\text{C}_{14}\text{H}_{13}\text{BrNaO}_2$ [$\text{M}+\text{Na}$] $^+$: calculated: 314.9996, found: 314.9991.

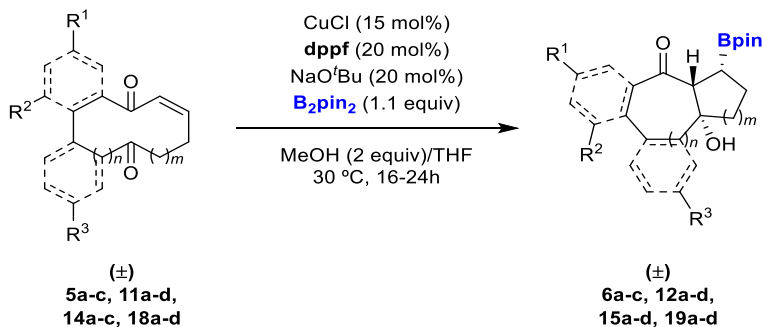
(Z)-6,7-dihydrodibenzo[a,c][10]annulene-5,10-dione (14c). Following the



General Procedure V, compound **14c** (118 mg, 0.45 mmol) was isolated by flash chromatography (petroleum ether/ethyl acetate gradient from 7:3 to 6:4) in 29% yield as a brown solid starting from 1,2-dihydrotriphenylene-4a,12b-diol (407 mg, 1.54 mmol) and

$\text{Pb}(\text{OAc})_4$ (751 g, 1.7 mmol). $^1\text{H-NMR}$ (δ , ppm) (400 MHz, CDCl_3): 7.67-7.60 (m, 1H, CH_{arom}), 7.52-7.47 (m, 2H, 2 x CH_{arom}), 7.40-7.36 (m, 2H, 2 x CH_{arom}), 7.35-7.31 (m, 1H, CH_{arom}), 7.28-7.20 (m, 1H, CH_{arom}), 7.13-7.06 (m, 1H, CH_{arom}), 5.77 (dd, $J = 12.2, 1.1$ Hz, 1H, **H-9**), 5.74-5.63 (m, 1H, **H-8**), 2.77-2.63 (m, 1H, **H_a-6**), 2.57-2.47 (m, 1H, **H_b-6**), 2.16-2.04 (m, 2H, **H-7**). $^{13}\text{C-NMR}$ (δ , ppm) (100 MHz, CDCl_3): 207.0 (**C-5**), 197.1 (**C-10**), 142.0 (C_{arom}), 140.7 (C_{arom}), 139.2 (**C-9**), 138.8 (C_{arom}), 137.1 (C_{arom}), 131.7 (**C-9**), 130.8 (CH_{arom}), 130.7 (CH_{arom}), 130.5 (CH_{arom}), 129.5 (CH_{arom}), 128.7 (CH_{arom}), 127.8 (CH_{arom}), 124.3 (CH_{arom}), 42.8 (**C-6**), 24.2 (**C-7**). HRMS (ESI-TOF) for $\text{C}_{18}\text{H}_{14}\text{KO}_2$ [$\text{M}+\text{K}$] $^+$: calculated: 301.0631, found: 301.0633.

2.2. Cu/dppf catalyzed transannular conjugated borylation/aldol cyclization

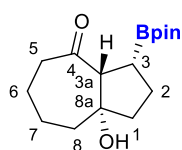


Scheme 6.2. General procedure for the Cu/dppf transannular borylation/aldol reaction sequence.

General Procedure A: To an oven-dried Schlenk tube, equipped with a magnetic stirring bar, CuCl (15 mol%, 0.03 mmol), dppf (20 mol%, 0.04 mmol), NaO^tBu (20 mol%, 0.04 mmol) and B_2pin_2 (1.1 equiv, 0.22 mmol) were added followed by dry THF (3 mL), under Argon. The reaction mixture was stirred at 30 °C for 30 min. A solution of the corresponding enone (1 equiv, 0.2 mmol) in THF (1 mL) was then

added, followed by THF (2 mL) and MeOH (0.4 mmol) and the resulting mixture was stirred at 30 °C for 16h. The reaction crude was filtered through Celite® and eluted with CH₂Cl₂. Afterwards, the solvent was concentrated in vacuo and the resulting mixture was purified by column chromatography.

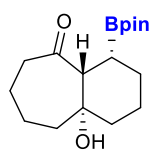
***rac*-(3*R*,3*aR*,8*aS*)-8*a*-hydroxy-3-(4,4,5,5-tetramethyl-1,3,2-dioxaborolan-2-yl)octahydroazulen-4(1*H*)-one (6*a*).** Following the *General Procedure A*, *rac*-6*a*



(25.3 mg, 0.08 mmol) was isolated after 16h at 30 °C by flash chromatography (pentane/ethyl acetate 20:1) in 86% yield as a colorless oil starting from **5a** (16.6 mg, 0.1 mmol) and B₂pin₂ (27.9 mg, 0.11 mmol) using 1,1'-bis(diphenylphosphino)ferrocene

(11.1 mg, 0.02 mmol), CuCl (1.5 mg, 0.015 mmol) and NaO^tBu (1.9 mg, 0.02 mmol). ¹H-NMR (δ, ppm) (400 MHz, CDCl₃): 4.46 (s, 1H, OH), 3.37 (d, *J* = 8.5 Hz, 1H, H-3a), 2.53-2.48 (m, 1H, H_a-5), 2.42-2.35 (m, 1H, H_b-5), 2.20 (dt, *J* = 14.1, 3.0 Hz, 1H, H_a-2), 1.96 (ddd, *J* = 9.4, 6.5, 1.5 Hz, 2H, H-6), 1.88-1.72 (m, 6H, H-1, H-7 and H-8), 1.60 (m, 2H, H_b-2 and H-3), 1.32 (s, 6H, 2 x CH₃-Bpin), 1.27 (s, 6H, 2 x CH₃-Bpin). ¹¹B-NMR (δ, ppm) (128.3 MHz, CDCl₃): 33.2 (br s). ¹³C-NMR (δ, ppm) (100 MHz, CDCl₃): 213.1 (C-4), 83.6 (C-Bpin), 81.2 (C-8a), 65.8 (C-3a), 44.5 (C-5), 42.3 (C-1), 42.2 (C-8), 24.8 (C-3), 24.6 (CH₃-Bpin), 24.6 (C-6), 23.9 (C-7), 23.5 (C-2). HRMS (ESI-TOF) for C₁₆H₂₈BO₄ [M+H]⁺: calculated: 295.2081, found: 295.2085.

***rac*-(4*R*,4*aR*,9*aS*)-9*a*-hydroxy-4-(4,4,5,5-tetramethyl-1,3,2-dioxaborolan-2-yl)decahydro-5*H*-benzo[7]annulen-5-one (6*b*).** Following the *General Procedure*

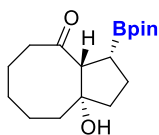


A, *rac*-6*b* (40.0 mg, 0.13 mmol) was isolated after 16h at 30 °C by flash chromatography (pentane/ethyl acetate 10:1) in 65% yield as a colorless oil starting from **5b** (36.0 mg, 0.2 mmol) and B₂pin₂ (55.9 mg, 0.22 mmol) using 1,1'-bis(diphenylphosphino)ferrocene (22.2

mg, 0.04 mmol), CuCl (2.9 mg, 0.03 mmol) and NaO^tBu (3.8 mg, 0.04 mmol). ¹H-NMR (δ, ppm) (400 MHz, CDCl₃): 5.07 (s, 1H, OH), 3.05 (d, *J* = 6.4 Hz, 1H, H-3a), 2.51-2.47 (m, 2H, H-5), 1.89-1.98 (m, 2H, H-9), 1.75-1.52 (m, 8H, H-1, H-6, H-7 and H-8), 1.43-1.40 (m, 3H, H-2 and H-3), 1.33 (s, 6H, 2 x CH₃-Bpin), 1.29 (s, 6H, 2 x CH₃-Bpin). ¹¹B-NMR (δ, ppm) (128.3 MHz, CDCl₃): 31.8 (br s). ¹³C-NMR (δ,

ppm) (100 MHz, CDCl₃): 216.2 (**C-4**), 83.4 (**C-Bpin**), 70.2 (**C-9a**), 59.0 (**C-3a**), 46.5 (**C-5**), 43.0 (**C-8**), 42.5 (**C-9**), 24.8 (**C-6**), 24.7 (**CH₃-Bpin**), 24.6 (**CH₃-Bpin**), 23.5 (**C-3**), 23.4 (**C-1**), 18.7 (**C-2**). HRMS (ESI-TOF) for C₁₇H₃₀BO₄ [M+H]⁺: calculated: 309.2237, found: 309.2237.

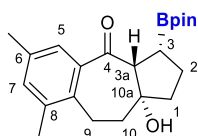
rac-(3R,3aR,9aS)-9a-hydroxy-3-(4,4,5,5-tetramethyl-1,3,2-dioxaborolan-2-yl)decahydro-4H-cyclopenta[8]annulen-4-one (6c). Following the *General*



Procedure A, *rac-6c* (51.6 mg, 0.16 mmol) was isolated after 16h at 30 °C by flash chromatography (pentane/ethyl acetate 6:1) in 84% yield as a colorless oil starting from **5c** (36.0 mg, 0.2 mmol) and B₂pin₂ (55.9 mg, 0.22 mmol) using 1,1'-

bis(diphenylphosphino)ferrocene (22.2 mg, 0.04 mmol), CuCl (2.9 mg, 0.03 mmol) and NaO^tBu (3.8 mg, 0.04 mmol). ¹H-NMR (δ, ppm) (400 MHz, CDCl₃): 3.17 (d, *J* = 8.6 Hz, 1H, **H-3a**), 2.54-2.47 (m, 1H, **H_a-5**), 2.35-2.27 (m, 1H, **H_b-5**), 2.10-1.98 (m, 3H, **H_a-1**, **H_a-2** and **H_a-6**), 1.89-1.79 (m, 2H, **H_b-1** and **H_b-6**), 1.68-1.53 (m, 5H, **H_b-2**, **H-3** and **H-9**), 1.39-1.31 (m, 1H, **H-3**), 1.26-1.22 (m, 2H, **H-7**), 1.19 (s, 6H, 2 x **CH₃-Bpin**), 1.18 (s, 6H, 2 x **CH₃-Bpin**). ¹¹B-NMR (δ, ppm) (128.3 MHz, CDCl₃): 34.1 (br s). ¹³C-NMR (δ, ppm) (100 MHz, CDCl₃): 218.9 (**C-4**), 84.4 (**C-9a**), 83.2 (**C-Bpin**), 57.0 (**C-3a**), 44.8 (**C-5**), 41.7 (**C-1**), 35.9 (**C-9**), 28.4 (**C-6**), 24.8 (**CH₃-Bpin**), 24.6 (**C-3**), 23.3 (**C-7**), 22.4 (**C-8**), 19.3 (**C-2**). HRMS (ESI-TOF) for C₁₇H₂₉NaBO₄ [M+Na]⁺: calculated: 331.2056, found: 331.2058.

rac-(3R,3aR,10aR)-10a-hydroxy-6,8-dimethyl-3-(4,4,5,5-tetramethyl-1,3,2-dioxaborolan-2-yl)-2,3,3a,9,10,10a-hexahydrobenzo[*f*]azulen-4(1H)-one (12a).

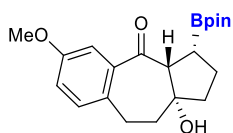


Following the *General Procedure A*, *rac-12a* (63.7 mg, 0.17 mmol) was isolated after 16h at 30 °C by flash chromatography (pentane/ethyl acetate 3:1) in 86% yield as a yellow oil starting from **11a** (48.5 mg, 0.2 mmol) and B₂pin₂ (55.9 mg, 0.22 mmol)

using 1,1'-bis(diphenylphosphino)ferrocene (22.2 mg, 0.04 mmol), CuCl (2.9 mg, 0.03 mmol) and NaO^tBu (3.8 mg, 0.04 mmol). ¹H-NMR (δ, ppm) (400 MHz, CDCl₃): 7.21 (s, 1H, **CH_{arom}**), 7.07 (s, 1H, **CH_{arom}**), 3.51 (d, *J* = 1.5 Hz, 1H, **H-3a**), 3.09 (dd, *J* = 17.9, 11.3 Hz, 1H, **H_a-9**), 2.97 (dd, *J* = 17.9, 6.6 Hz, 1H, **H_b-9**), 2.29 (s, 6H, 2 x

CH₃), 2.21 (ddt, $J = 12.3, 8.1, 3.1$ Hz, 1H, H-3), 2.07-2.03 (m, 1H, H_a-10), 1.82-1.65 (m, 5H, H-1, H-2 and H_b-10), 1.29 (s, 6H, 2 x CH₃-Bpin), 1.25 (s, 6H, 2 x CH₃-Bpin). ¹¹B-NMR (δ , ppm) (128.3 MHz, CDCl₃): 33.5 (br s). ¹³C-NMR (δ , ppm) (100 MHz, CDCl₃): 204.1 (C-4), 139.2 (C_{arom}), 138.9 (C_{arom}), 136.7 (C_{arom}), 135.2 (C_{arom}), 133.6 (CH_{arom}), 127.0 (CH_{arom}), 85.2 (C-10a), 83.0 (C-Bpin), 66.2 (C-3a), 40.0 (C-1), 39.1 (C-10), 26.3 (C-9), 25.0 (CH₃-Bpin), 24.9 (CH₃-Bpin), 24.7 (C-3), 20.7 (CH₃), 20.4 (C-2). HRMS (ESI-TOF) for C₂₂H₃₂BO₄ [M+H]⁺: calculated: 371.2394, found: 371.2398.

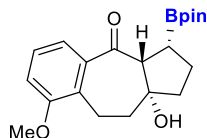
***rac*-(3*R*,3*aR*,10*aR*)-10*a*-hydroxy-6-methoxy-3-(4,4,5,5-tetramethyl-1,3,2-dioxaborolan-2-yl)-2,3,3*a*,9,10,10*a*-hexahydrobenzo[*f*]azulen-4(1*H*)-one (12*b*).**



Following the *General Procedure A*, *rac*-**12b** (22.7 mg, 0.06 mmol) was isolated after 16h at 30 °C by flash chromatography (pentane/ethyl acetate 3:1) in 31% yield as a yellow oil starting from **11b** (48.9 mg, 0.2 mmol) and B₂pin₂

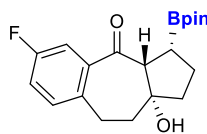
(55.9 mg, 0.22 mmol) using 1,1'-bis(diphenylphosphino)ferrocene (22.2 mg, 0.04 mmol), CuCl (2.9 mg, 0.03 mmol) and NaO^tBu (3.8 mg, 0.04 mmol). ¹H-NMR (δ , ppm) (400 MHz, CDCl₃): 7.20 (d, $J = 2.9$ Hz, 1H, CH_{arom}), 7.11 (d, $J = 8.3$ Hz, 1H, CH_{arom}), 6.92 (dd, $J = 2.9, 1.5$ Hz, 1H, CH_{arom}), 3.79 (s, 3H, OCH₃), 3.49-3.47 (m, 1H, H-3a), 3.27 (ddd, $J = 15.2, 9.7, 3.2$ Hz, 1H, H_a-9), 2.82 (ddd, $J = 15.3, 8.1, 3.4$ Hz, 1H, H_b-9), 2.26 (ddd, $J = 14.0, 8.1, 3.2$ Hz, 1H, H-3), 2.12-2.08 (m, 1H, H_a-10), 2.03-1.99 (m, 2H, H-1), 1.84-1.82 (m, 2H, H-2), 1.39 (s, 6H, 2 x CH₃-Bpin), 1.32 (s, 6H, 2 x CH₃-Bpin), 1.27-1.24 (m, 1H, H_b-4). ¹¹B-NMR (δ , ppm) (128.3 MHz, CDCl₃): 34.7 (br s). ¹³C-NMR (δ , ppm) (100 MHz, CDCl₃): 203.6 (C-4), 157.1 (C_{arom}), 139.6 (C_{arom}), 133.2 (C_{arom}), 132.1 (CH_{arom}), 118.4 (CH_{arom}), 113.4 (CH_{arom}), 83.9 (C-Bpin), 81.4 (C-10a), 66.1 (OCH₃), 55.4 (C-3a), 44.6 (C-1), 38.5 (C-10), 30.0 (C-9), 24.8 (CH₃-Bpin), 24.7 (C-3), 22.3 (C-2). HRMS (ESI-TOF) for C₂₁H₂₉NaBO₅ [M+Na]⁺: calculated: 395.2005, found: 395.2005.

***rac*-(3*R*,3*aR*,10*aR*)-10*a*-hydroxy-8-methoxy-3-(4,4,5,5-tetramethyl-1,3,2-dioxaborolan-2-yl)-2,3,3*a*,9,10,10*a*-hexahydrobenzo[*f*]azulen-4(1*H*)-one (12*c*).**



Following the *General Procedure A*, *rac*-**12c** (34.7 mg, 0.09 mmol) was isolated after 16h at 30 °C by flash chromatography (pentane/ethyl acetate 2:1) in 47% yield as a yellow oil starting from **11c** (48.8 mg, 0.2 mmol) and B₂pin₂ (55.9 mg, 0.22 mmol) using 1,1'-bis(diphenylphosphino)ferrocene (22.2 mg, 0.04 mmol), CuCl (2.9 mg, 0.03 mmol) and NaO^tBu (3.8 mg, 0.04 mmol). ¹H-NMR (δ, ppm) (400 MHz, CDCl₃): 7.23-7.16 (m, 2H, 2 x CH_{arom}), 6.95 (dd, *J* = 7.5, 1.9 Hz, 1H, CH_{arom}), 3.86 (s, 3H, OCH₃), 3.53 (d, *J* = 7.2 Hz, 1H, H-3*a*), 3.35 (ddd, *J* = 18.5, 7.1, 1.2 Hz, 1H, H_a-9), 3.01-2.87 (m, 1H, H_b-9), 2.28 (ddt, *J* = 15.1, 7.2, 1.3 Hz, 1H, H-3), 2.23-2.16 (m, 1H, H_a-10), 2.07 (ddt, *J* = 13.0, 11.0, 8.7 Hz, 1H, H_b-10), 1.90-1.72 (m, 2H, H-1), 1.72-1.60 (m, 2H, H-2), 1.29 (s, 6H, 2 x CH₃-Bpin), 1.25 (s, 6H, 2 x CH₃-Bpin). ¹¹B-NMR (δ, ppm) (128.3 MHz, CDCl₃): 32.8 (br s). ¹³C-NMR (δ, ppm) (100 MHz, CDCl₃): 203.4 (C-4), 157.1 (C_{arom}), 140.1 (C_{arom}), 132.6 (C_{arom}), 126.6 (CH_{arom}), 120.6 (CH_{arom}), 112.7 (CH_{arom}), 85.3 (C-10*a*), 83.0 (C-Bpin), 66.4 (OCH₃), 55.9 (C-3*a*), 39.8 (C-1), 39.0 (C-10), 25.1 (C-9), 24.7 (CH₃-Bpin), 22.5 (C-2). HRMS (ESI-TOF) for C₂₁H₃₀BO₅ [M+H]⁺: calculated: 373.2186, found: 373.2187.

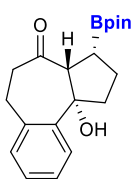
***rac*-(3*R*,3*aR*,10*aR*)-6-fluoro-10*a*-hydroxy-3-(4,4,5,5-tetramethyl-1,3,2-dioxaborolan-2-yl)-2,3,3*a*,9,10,10*a*-hexahydrobenzo[*f*]azulen-4(1*H*)-one (12*d*).**



Following the *General Procedure A*, *rac*-**12d** (33.0 mg, 0.09 mmol) was isolated after 16h at 30 °C by flash chromatography (pentane/ethyl acetate 10:1) in 46% yield as a colorless oil starting from **11d** (46.4 mg, 0.2 mmol) and B₂pin₂ (55.9 mg, 0.22 mmol) using 1,1'-bis(diphenylphosphino)ferrocene (22.2 mg, 0.04 mmol), CuCl (2.9 mg, 0.03 mmol) and NaO^tBu (3.8 mg, 0.04 mmol). ¹H-NMR (δ, ppm) (400 MHz, CDCl₃): 7.38 (dd, *J* = 9.4, 2.9 Hz, 1H, CH_{arom}), 7.19 (dd, *J* = 8.4, 5.3 Hz, 1H, CH_{arom}), 7.05 (td, *J* = 8.1, 2.9 Hz, 1H, CH_{arom}), 3.47 (d, *J* = 8.6 Hz, 1H, H-3*a*), 3.28 (ddd, *J* = 15.3, 9.1, 3.4 Hz, 1H, H_a-9), 2.88 (ddd, *J* = 15.3, 8.5, 3.5 Hz, 1H, H_b-9), 2.28 (ddd, *J* = 14.1, 8.5, 3.4 Hz, 1H, H-3), 2.22-2.05 (m, 1H, H_a-10), 2.05-1.98 (m, 2H, H-1), 1.83 (dtt, *J* = 13.0, 10.2, 3.2 Hz, 3H, H-2 and H_b-10), 1.37 (s, 6H, 2 x CH₃-

Bpin), 1.31 (s, 6H, 2 x CH₃-Bpin). ¹¹B-NMR (δ, ppm) (128.3 MHz, CDCl₃): 33.7 (br s). ¹³C-NMR (δ, ppm) (100 MHz, CDCl₃): 202.2 (C-4), 158.3 (C_{arom}), 139.7 (C_{arom}), 136.8 (C_{arom}), 131.9 (CH_{arom}), 119.0 (CH_{arom}), 115.3 (CH_{arom}), 84.0 (C-Bpin), 81.6 (C-10a), 66.3 (C-3a), 49.7 (C-1), 38.8 (C-10), 31.4 (C-9), 24.7 (CH₃-Bpin), 24.7 (C-3), 23.0 (C-2). HRMS (ESI-TOF) for C₂₀H₂₆NaBFO₄ [M+Na]⁺: calculated: 383.1805, found: 383.1801.

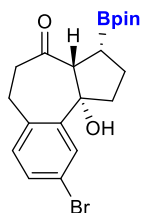
***rac*-(3*R*,3*aR*,10*bS*)-10*b*-hydroxy-3-(4,4,5,5-tetramethyl-1,3,2-dioxaborolan-2-yl) 2,3,3*a*,5,6,10*b*-hexahydrobenzo[*e*]azulen-4(1*H*)-one (15*a*)**. Following the



General Procedure A, *rac*-15*a* (40.0 mg, 0.12 mmol) was isolated after 16h at 30 °C by flash chromatography (pentane/ethyl acetate 10:1) in 60% yield as a colorless oil starting from 14*a* (42.9 mg, 0.2 mmol) and B₂pin₂ (55.9 mg, 0.22 mmol) using 1,1'-bis(diphenylphosphino)ferrocene (22.2 mg, 0.04 mmol), CuCl (2.9

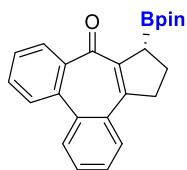
mg, 0.03 mmol) and NaO^tBu (3.8 mg, 0.04 mmol). ¹H-NMR (δ, ppm) (400 MHz, CDCl₃): 7.55-7.53 (m, 1H, CH_{arom}), 7.30-7.22 (m, 3H, 3 x CH_{arom}), 4.37 (s, 1H, OH), 3.54 (d, *J* = 10.2 Hz, 1H, H-3*a*), 3.37 (ddd, *J* = 14.9, 10.9, 2.0 Hz, 1H, H_a-6), 3.03 (ddd, *J* = 14.9, 8.8, 2.5 Hz, 1H, H_b-6), 2.80 (ddd, *J* = 14.7, 8.8, 2.0 Hz, 1H, H_a-5), 2.64-2.55 (m, 2H, H_a-1 and H_b-5), 2.45-2.39 (m, 1H, H_b-1), 1.96-1.91 (m, 2H, H-2), 1.76 (ddd, *J* = 16.9, 11.5, 6.5 Hz, 1H, H-3), 1.39 (s, 6H, 2 x CH₃-Bpin), 1.33 (s, 6H, 2 x CH₃-Bpin). ¹¹B-NMR (δ, ppm) (128.3 MHz, CDCl₃): 33.5 (br s). ¹³C-NMR (δ, ppm) (100 MHz, CDCl₃): 211.6 (C-4), 141.9 (C_{arom}), 139.2 (C_{arom}), 130.9 (CH_{arom}), 127.9 (CH_{arom}), 127.3 (CH_{arom}), 126.7 (CH_{arom}), 84.0 (C-10*b*), 83.6 (C-Bpin), 65.6 (C-3*a*), 44.0 (C-5), 42.2 (C-1), 31.5 (C-6), 24.9 (CH₃-Bpin), 24.7 (C-3), 22.2 (C-2). HRMS (ESI-TOF) for C₂₀H₂₇NaBO₄ [M+Na]⁺: calculated: 365.1900, found: 365.1906.

***rac*-(3*R*,3*aR*,10*bS*)-9-bromo-10*b*-hydroxy-3-(4,4,5,5-tetramethyl-1,3,2-dioxaborolan-2-yl)-2,3,3*a*,5,6,10*b*-hexahydrobenzo[*e*]azulen-4(1*H*)-one (15*b*).**



Following the *General Procedure A*, *rac*-**15b** (59.8 mg, 0.14 mmol) was isolated after 16h at 30 °C by flash chromatography (pentane/ethyl acetate 10:1) in 71% yield as a white solid starting from **14b** (58.6 mg, 0.2 mmol) and B₂pin₂ (55.9 mg, 0.22 mmol) using 1,1'-bis(diphenylphosphino)ferrocene (22.2 mg, 0.04 mmol), CuCl (2.9 mg, 0.03 mmol) and NaO^tBu (3.8 mg, 0.04 mmol). ¹H-NMR (δ, ppm) (400 MHz, CDCl₃): 7.64 (d, *J* = 2.1 Hz, 1H, CH_{arom}), 7.35 (dd, *J* = 8.1, 2.1 Hz, 1H, CH_{arom}), 7.07 (d, *J* = 8.1 Hz, 1H, CH_{arom}), 3.47 (d, *J* = 10.1 Hz, 1H, H-3*a*), 3.30 (ddd, *J* = 15.0, 11.0, 2.0 Hz, 1H, H_a-6), 2.95 (ddd, *J* = 15.0, 8.7, 2.5 Hz, 1H, H_b-6), 2.77 (ddd, *J* = 14.8, 8.8, 2.0 Hz, 1H, H_a-5), 2.59-2.50 (m, 2H, H_a-1 and H_b-5), 2.36 (ddd, *J* = 13.2, 7.5, 3.3 Hz, 1H, H_b-1), 1.96-1.85 (m, 2H, H-2), 1.76 (td, *J* = 10.0, 5.5 Hz, 1H, H-3), 1.36 (s, 6H, 2 x CH₃-Bpin), 1.30 (s, 6H, 2 x CH₃-Bpin). ¹¹B-NMR (δ, ppm) (128.3 MHz, CDCl₃): 33.6 (br s). ¹³C-NMR (δ, ppm) (100 MHz, CDCl₃): 210.3 (C-4), 144.1 (C_{arom}), 139.1 (C_{arom}), 132.5 (CH_{arom}), 130.8 (CH_{arom}), 130.6 (CH_{arom}), 120.4 (C_{arom}), 83.8 (C-Bpin), 83.6 (C-10*b*), 65.5 (C-3*a*), 42.3 (C-5), 42.0 (C-1), 30.5 (C-6), 24.9 (CH₃-Bpin), 24.7 (C-3), 22.5 (C-2). HRMS (ESI-TOF) for C₂₀H₂₆NaBBrO₄ [M+Na]⁺: calculated: 443.1005, found: 443.1006.

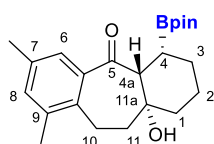
***rac*-(*R*)-7-(4,4,5,5-tetramethyl-1,3,2-dioxaborolan-2-yl)-6,7-dihydrodibenzo[*e,g*]azulen-8(5*H*)-one (15*d*).**



Following the *General Procedure A*, *rac*-**15d** (43.2 mg, 0.11 mmol) was isolated after 16h at 30 °C by flash chromatography (pentane/ethyl acetate 10:1) in 58% yield as a colorless oil starting from **14c** (52.5 mg, 0.2 mmol) and B₂pin₂ (55.9 mg, 0.22 mmol) using 1,1'-bis(diphenylphosphino)ferrocene (22.2 mg, 0.04 mmol), CuCl (2.9 mg, 0.03 mmol) and NaO^tBu (3.8 mg, 0.04 mmol). ¹H-NMR (δ, ppm) (400 MHz, CDCl₃): 7.95 (dd, *J* = 7.8, 1.6 Hz, 1H, CH_{arom}), 7.88-7.84 (m, 2H, 2 x CH_{arom}), 7.64-7.60 (m, 2H, 2 x CH_{arom}), 7.54 (td, *J* = 7.5, 1.3 Hz, 1H, CH_{arom}), 7.48-7.46 (m, 2H, 2 x CH_{arom}), 3.29-3.20 (m, 2H, H-6), 2.96-2.91 (m, 1H, H-7*a*), 2.22-2.13 (m, 1H, H_a-7), 1.91 (dq, *J* = 12.3, 8.0 Hz, 1H, H_b-7), 1.29 (s, 6H, 2 x CH₃-Bpin), 1.26 (s, 6H, 2 x CH₃-Bpin). ¹¹B-

NMR (δ , ppm) (128.3 MHz, CDCl_3): 33.2 (br s). ^{13}C -NMR (δ , ppm) (100 MHz, CDCl_3): 191.9 (**C**-8), 147.6 (**C**-5), 147.1 (**C**_{arom}), 140.3 (**C**_{arom}), 137.9 (**C**_{arom}), 137.5 (**C**_{arom}), 133.9 (**CH**_{arom}), 131.4 (**CH**_{arom}), 130.8 (**CH**_{arom}), 130.5 (**CH**_{arom}), 128.5 (**C**-7b), 128.1 (**CH**_{arom}), 128.0 (**CH**_{arom}), 127.9 (**CH**_{arom}), 127.5 (**CH**_{arom}), 84.3 (**C**-Bpin), 39.2 (**C**-7a), 24.7 (**CH**₃-Bpin), 24.6 (**C**-6), 23.0 (**C**-7). HRMS (ESI-TOF) for $\text{C}_{24}\text{H}_{26}\text{BO}_3$ [$\text{M}+\text{H}$]⁺: calculated: 373.1975, found: 373.1974.

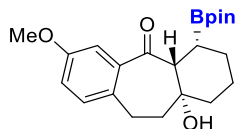
***rac*-(4*R*,4*aR*,11*aR*)-11*a*-hydroxy-7,9-dimethyl-4-(4,4,5,5-tetramethyl-1,3,2-dioxaborolan-2-yl)-1,2,3,4,4*a*,10,11,11*a*-octahydro-5*H*-**



dibenzo[*a,d*][7]annulen-5-one (19a). Following the *General*

Procedure A, *rac*-**19a** (16.9 mg, 0.04 mmol) was isolated after 16h at 30 °C by flash chromatography (pentane/ethyl acetate 10:1) in 22% yield as a colorless oil starting from **18a** (51.3 mg, 0.2 mmol) and B_2pin_2 (55.9 mg, 0.22 mmol) using 1,1'-bis(diphenylphosphino)ferrocene (22.2 mg, 0.04 mmol), CuCl (2.9 mg, 0.03 mmol) and NaO^tBu (3.8 mg, 0.04 mmol). ^1H -NMR (δ , ppm) (400 MHz, CDCl_3): 7.19 (s, 1H, **CH**_{arom}), 6.99 (s, 1H, **CH**_{arom}), 5.54 (s, 1H, **OH**), 3.11 (d, $J = 5.1$ Hz, 1H, **H**-4a), 3.08-3.03 (m, 1H, **H**_a-10), 2.69 (ddd, $J = 16.6, 9.5, 2.0$ Hz, 1H, **H**_b-10), 2.25 (s, 3H, **CH**₃), 2.19 (s, 3H, **CH**₃), 1.99-1.86 (m, 2H, **H**-11), 1.71-1.60 (m, 2H, **H**_a-1 and **H**-4), 1.48 (m, 1H, **H**_b-1), 1.38-1.36 (m, 2H, **H**_a-2 and **H**_a-3), 1.33 (s, 6H, 2 x **CH**₃-Bpin), 1.29 (s, 6H, 2 x **CH**₃-Bpin), 1.20-1.17 (m, 2H, **H**_b-2 and **H**_b-3). ^{11}B -NMR (δ , ppm) (128.3 MHz, CDCl_3): 34.4 (br s). ^{13}C -NMR (δ , ppm) (100 MHz, CDCl_3): 207.1 (**C**-5), 140.5 (**C**_{arom}), 137.9 (**C**_{arom}), 136.0 (**C**_{arom}), 135.2 (**C**_{arom}), 133.8 (**CH**_{arom}), 126.5 (**CH**_{arom}), 83.9 (**C**-Bpin), 71.9 (**C**-11a), 59.8 (**C**-4a), 42.5 (**C**-11), 40.6 (**C**-1), 25.3 (**C**-10), 25.1 (**CH**₃-Bpin), 24.7 (**C**-4), 24.4 (**CH**₃), 20.5 (**C**-2), 19.3 (**C**-3). HRMS (ESI-TOF) for $\text{C}_{23}\text{H}_{34}\text{BO}_4$ [$\text{M}+\text{H}$]⁺: calculated: 385.2550, found: 385.2555.

***rac*-(4*R*,4*aR*,11*aR*)-11*a*-hydroxy-7-methoxy-4-(4,4,5,5-tetramethyl-1,3,2-dioxaborolan-2-yl)-1,2,3,4,4*a*,10,11,11*a*-octahydro-5*H*-dibenzo[*a,d*][7]annulene**

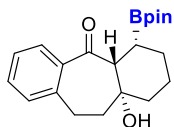


-5-one (19b). Following the *General Procedure A*, *rac*-**19b**

(54.1 mg, 0.14 mmol) was isolated after 16h at 30 °C by flash chromatography (pentane/ethyl acetate 10:1) in 70% yield as a colorless oil starting from **18b** (51.7 mg, 0.2 mmol) and

B₂pin₂ (55.9 mg, 0.22 mmol) using 1,1'-bis(diphenylphosphino)ferrocene (22.2 mg, 0.04 mmol), CuCl (2.9 mg, 0.04 mmol) and NaO^tBu (3.8 mg, 0.04 mmol). ¹H-NMR (δ, ppm) (400 MHz, CDCl₃): 7.18 (d, *J* = 2.9 Hz, 1H, CH_{arom}), 7.10 (d, *J* = 8.3 Hz, 1H, CH_{arom}), 6.90 (dd, *J* = 8.3, 2.9 Hz, 1H, CH_{arom}), 5.57 (s, 1H, OH), 3.79 (s, 3H, OCH₃), 3.19 (d, *J* = 5.8 Hz, 1H, H-4*a*), 3.16-3.10 (m, 1H, H_a-10), 2.80 (ddd, *J* = 16.2, 9.9, 1.7 Hz, 1H, H_b-10), 2.14-2.05 (m, 1H, H_a-11), 1.95 (ddd, *J* = 14.3, 9.8, 1.9 Hz, 1H, H_b-11), 1.77 (ddt, *J* = 23.5, 11.4, 2.8 Hz, 3H, H-1 and H-4), 1.63-1.51 (m, 3H, H-2 and H_a-3), 1.48 (br s, 1H, H_b-3), 1.39 (s, 6H, 2 x CH₃-Bpin), 1.36 (s, 6H, 2 x CH₃-Bpin). ¹¹B-NMR (δ, ppm) (128.3 MHz, CDCl₃): 32.4 (br s). ¹³C-NMR (δ, ppm) (100 MHz, CDCl₃): 206.0 (C-5), 157.8 (C_{arom}), 140.0 (C_{arom}), 135.1 (C_{arom}), 131.3 (CH_{arom}), 118.5 (CH_{arom}), 111.8 (CH_{arom}), 84.0 (C-Bpin), 71.7 (C-11*a*), 59.8 (OCH₃), 55.5 (C-4*a*), 43.4 (C-11), 41.1 (C-1), 30.5 (C-10), 25.2 (CH₃-Bpin), 24.8 (C-4), 24.5 (C-2), 19.3 (C-3). HRMS (ESI-TOF) for C₂₂H₃₂BO₅ [M+H]⁺: calculated: 387.2343, found: 387.2347.

***rac*-(4*R*,4*aR*,11*aR*)-11*a*-hydroxy-4-(4,4,5,5-tetramethyl-1,3,2-dioxaborolan-2-yl)-1,2,3,4,4*a*,10,11,11*a*-octahydro-5*H*-dibenzo[*a,d*][7]annulene-5-one (19c).**



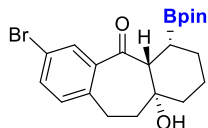
Following the *General Procedure A*, *rac*-**19c** (45.6 mg, 0.13 mmol)

was isolated after 16h at 30 °C by flash chromatography (pentane/ethyl acetate 10:1) in 64% yield as a colorless oil starting from **18c** (45.7 mg, 0.2 mmol) and **B₂pin₂** (55.9 mg, 0.22 mmol)

using 1,1'-bis(diphenylphosphino)ferrocene (22.2 mg, 0.04 mmol), CuCl (2.9 mg, 0.03 mmol) and NaO^tBu (3.8 mg, 0.04 mmol). ¹H-NMR (δ, ppm) (400 MHz, CDCl₃): 7.58 (dd, *J* = 7.6, 1.4 Hz, 1H, CH_{arom}), 7.34 (td, *J* = 7.5, 1.5 Hz, 1H, CH_{arom}), 7.24-7.18 (m, 2H, 2 x CH_{arom}), 5.61 (s, 1H, OH), 3.27 (ddd, *J* = 16.1, 9.8, 2.1 Hz, 1H, H_a-10), 3.20 (d, *J* = 5.7 Hz, 1H, H-4*a*), 2.84 (ddd, *J* = 16.1, 9.3, 2 Hz, 1H, H_b-10), 2.10

(ddt, $J = 14.4, 9.7, 1.7$ Hz, 1H, H_{a-11}), 1.99 (ddd, $J = 14.4, 9.2, 2.1$ Hz, 1H, H_{b-11}), 1.80-1.71 (m, 3H, H_{a-1} , H_{a-3} and $H-4$), 1.59-1.51 (m, 3H, H_{b-1} and $H-2$), 1.47 (t, $J = 2.4$ Hz, 1H, H_{b-3}), 1.40 (s, 6H, 2 x CH_3 -Bpin), 1.36 (s, 6H, 2 x CH_3 -Bpin). ^{11}B -NMR (δ , ppm) (128.3 MHz, $CDCl_3$): 32.2 (br s). ^{13}C -NMR (δ , ppm) (100 MHz, $CDCl_3$): 206.5 ($C-5$), 142.2 (C_{arom}), 139.7 (C_{arom}), 131.2 (CH_{arom}), 129.9 (CH_{arom}), 128.3 (CH_{arom}), 126.2 (CH_{arom}), 83.9 (C -Bpin), 71.6 ($C-11a$), 60.1 ($C-4a$), 43.1 ($C-11$), 41.3 ($C-1$), 31.2 ($C-10$), 25.3 (CH_3 -Bpin), 24.7 ($C-4$), 24.5 ($C-2$), 19.3 ($C-3$). HRMS (ESI-TOF) for $C_{21}H_{30}BO_4$ $[M+H]^+$: calculated: 357.2237, found: 357.2226.

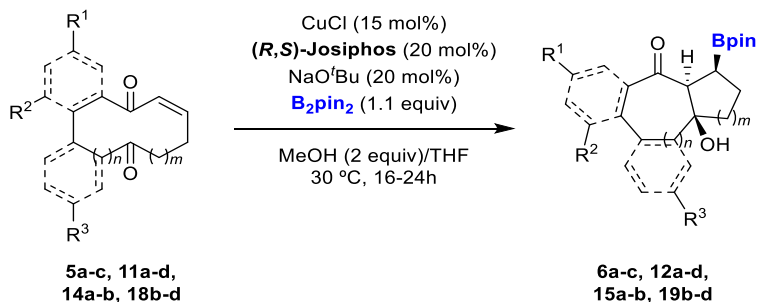
***rac*-(4*R*,4*aR*,11*aR*)-7-bromo-11*a*-hydroxy-4-(4,4,5,5-tetramethyl-1,3,2-dioxaborolan-2-yl)-1,2,3,4,4*a*,10,11,11*a*-octahydro-5*H*-**



dibenzo[*a,d*][7]annulen-5-one (19d). Following the *General Procedure A*, *rac*-**19d** (27.4 mg, 0.06 mmol) was isolated after 16h at 30 °C by flash chromatography (pentane/ethyl acetate 20:1) in 32% yield as a colorless oil starting from **18d** (61.4 mg,

0.2 mmol) and B_2pin_2 (55.9 mg, 0.22 mmol) using 1,1'-bis(diphenylphosphino)ferrocene (22.2 mg, 0.04 mmol), CuCl (2.9 mg, 0.03 mmol) and NaOtBu (3.8 mg, 0.04 mmol). 1H -NMR (δ , ppm) (400 MHz, $CDCl_3$): 7.70 (d, $J = 2.2$ Hz, 1H, CH_{arom}), 7.45 (dd, $J = 8.1, 2.2$ Hz, 1H, CH_{arom}), 7.08 (d, $J = 8.1$ Hz, 1H, CH_{arom}), 5.62 (s, 1H, OH), 3.23 (ddd, $J = 16.1, 9.9, 2.1$ Hz, 1H, H_{a-10}), 3.16 (d, $J = 5.6$ Hz, 1H, $H-4a$), 2.77 (ddd, $J = 16.1, 9.1, 2.0$ Hz, 1H, H_{b-10}), 2.07 (ddt, $J = 14.6, 9.7, 1.7$ Hz, 1H, H_{a-11}), 1.98 (ddd, $J = 14.4, 9.1, 2.1$ Hz, 1H, H_{b-11}), 1.79-1.69 (m, 3H, $H-1$ and $H-4$), 1.54-1.48 (m, 4H, $H-2$ and $H-3$), 1.39 (s, 6H, 2 x CH_3 -Bpin), 1.35 (s, 6H, 2 x CH_3 -Bpin). ^{11}B -NMR (δ , ppm) (128.3 MHz, $CDCl_3$): 33.5 (br s). ^{13}C -NMR (δ , ppm) (100 MHz, $CDCl_3$): 205.3 ($C-5$), 141.4 (C_{arom}), 141.0 (C_{arom}), 133.9 (CH_{arom}), 131.7 (CH_{arom}), 131.0 (CH_{arom}), 120.1 (C_{arom}), 84.1 (C -Bpin), 71.6 ($C-11a$), 60.2 ($C-4a$), 42.9 ($C-11$), 41.3 ($C-1$), 30.6 ($C-10$), 25.2 (CH_3 -Bpin), 24.7 ($C-4$), 24.5 ($C-2$), 19.2 ($C-3$). HRMS (ESI-TOF) for $C_{21}H_{28}NaBBro_4$ $[M+Na]^+$: calculated: 457.1161, found: 457.1160.

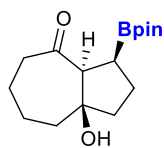
2.3. Cu/Josiphos catalyzed transannular conjugated borylation/aldol cyclization



Scheme 6.3. General procedure for enantioselective reaction.

General Procedure B: To an oven-dried Schlenk tube, equipped with a magnetic stirring bar, CuCl (15 mol%, 0.03 mmol), (*R,S*)-Josiphos (20 mol%, 0.04 mmol), NaO'Bu (20 mol%, 0.04 mmol) and B₂pin₂ (1.1 equiv, 0.22 mmol) were added followed by dry THF (3 mL), under Argon. The reaction mixture was stirred at 30 °C for 30 min. A solution of the corresponding enone (1 equiv, 0.2 mmol) in THF (1 mL) was then added, followed by THF (2 mL) and MeOH (0.4 mmol) and the resulting mixture was stirred at 30 °C for 16-24h. The reaction crude was filtered through Celite® and eluted with CH₂Cl₂. Afterwards, the solvent was concentrated in vacuo and the resulting mixture was purified by column chromatography.

(3*S*,3*aS*,8*aR*)-8*a*-hydroxy-3-(4,4,5,5-tetramethyl-1,3,2-dioxaborolan-2-yl)octahydroazulen-4(1*H*)-one (6a). Following the *General Procedure B*, (+)-**6a**

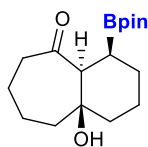


(56.1 mg, 0.19 mmol) was isolated after 16h at 30 °C by flash chromatography (pentane/ethyl acetate 20:1) in 95% yield as a colorless oil starting from **5a** (33.2 mg, 0.2 mmol) and B₂pin₂ (55.9 mg, 0.22 mmol) using (*R*)-1-[(*S*)-2-(Diphenylphosphino)

ferrocenyl]ethylidicyclohexylphosphine (25.6 mg, 0.04 mmol), CuCl (2.9 mg, 0.03 mmol) and NaO'Bu (3.8 mg, 0.04 mmol). All spectroscopic data matched with those described for *rac*-**6a**. The enantiomeric excess (e.e.) was determined by HPLC-DAD using a CHIRALPAK® IC column (hexane/*i*-PrOH 90:10, 1 mL/min, 210 nm,

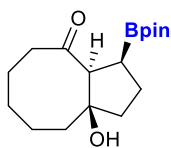
25°C); t_r (major) = 5.48 min, t_r (minor) = 6.27 min (92% ee). $[\alpha]_D^{25}$: +17.6 (c = 1.26, CH_2Cl_2).

(4*S*,4*aS*,9*aR*)-9*a*-hydroxy-4-(4,4,5,5-tetramethyl-1,3,2-dioxaborolan-2-yl)decahydro-5*H*-benzo[7]annulen-5-one (6*b*). Following the *General Procedure*



B, (+)-**6b** (44.2 mg, 0.14 mmol) was isolated after 16h at 30 °C by flash chromatography (pentane/ethyl acetate 10:1) in 72% yield as a colorless oil starting from **5b** (36.0 mg, 0.2 mmol) and B_2pin_2 (55.9 mg, 0.22 mmol) using (*R*)-1-[(*S_P*)-2-(Diphenylphosphino)ferrocenyl]ethylidicyclohexylphosphine (25.6 mg, 0.04 mmol), CuCl (2.9 mg, 0.03 mmol) and NaO^tBu (3.8 mg, 0.04 mmol). All spectroscopic data matched with those described for *rac*-**6b**. The enantiomeric excess (e.e.) was determined by HPLC-DAD using a CHIRALPAK® IC column (hexane/*i*-PrOH 90:10, 1 mL/min, 210 nm, 25°C); t_r (major) = 4.93 min, t_r (minor) = 6.07 min (88% ee). $[\alpha]_D^{25}$: +37.4 (c = 0.38, CH_2Cl_2).

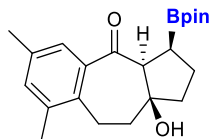
(3*S*,3*aS*,9*aR*)-9*a*-hydroxy-3-(4,4,5,5-tetramethyl-1,3,2-dioxaborolan-2-yl)decahydro-4*H*-cyclopenta[8]annulen-4-one (6*c*). Following the *General*



Procedure B, (-)-**6c** (49.9 mg, 0.16 mmol) was isolated after 16h at 30 °C by flash chromatography (pentane/ethyl acetate 6:1) in 81% yield as a colorless oil starting from **5c** (36.0 mg, 0.2 mmol) and B_2pin_2 (55.9 mg, 0.22 mmol) using (*R*)-1-[(*S_P*)-2-

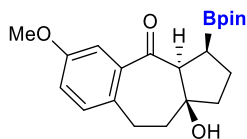
(Diphenylphosphino)ferrocenyl]ethylidicyclohexylphosphine (25.6 mg, 0.04 mmol), CuCl (2.9 mg, 0.03 mmol) and NaO^tBu (3.8 mg, 0.04 mmol). All spectroscopic data matched with those described for *rac*-**6c**. The enantiomeric excess (e.e.) was determined by HPLC-DAD using a CHIRALPAK® ID column (hexane/*i*-PrOH 80:20, 1 mL/min, 205 nm, 25°C); t_r (major) = 11.45 min, t_r (minor) = 14.52 min (88% ee). $[\alpha]_D^{25}$: -0.9 (c = 1.0, CH_2Cl_2).

(3*S*,3*aS*,10*aS*)-10*a*-hydroxy-6,8-dimethyl-3-(4,4,5,5-tetramethyl-1,3,2-dioxaborolan-2-yl)-2,3,3*a*,9,10,10*a*-hexahydrobenzo[*f*]azulen-4(1*H*)-one (12*a*).



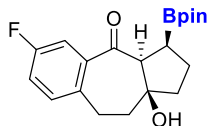
Following the *General Procedure B*, (+)-**12a** (66.2 mg, 0.18 mmol) was isolated after 20h at 30 °C by flash chromatography (pentane/ethyl acetate 3:1) in 89% yield as a yellow oil starting from **11a** (48.5 mg, 0.2 mmol) and B₂pin₂ (55.9 mg, 0.22 mmol) using (*R*)-1-[(*S*_P)-2-(Diphenylphosphino)ferrocenyl]ethylidicyclohexylphosphine (25.6 mg, 0.04 mmol), CuCl (2.9 mg, 0.03 mmol) and NaO^tBu (3.8 mg, 0.04 mmol). All spectroscopic data matched with those described for *rac*-**12a**. The enantiomeric excess (e.e.) was determined by HPLC-DAD using a CHIRALPAK® IA column (hexane/*i*-PrOH 70:30, 1 mL/min, 210 nm, 25°C); t_r (major) = 4.15 min, t_r (minor) = 5.16 min (74% ee). [α]_D²⁵: +31.4 (c= 0.74, CH₂Cl₂).

(3*S*,3*aS*,10*aS*)-10*a*-hydroxy-6-methoxy-3-(4,4,5,5-tetramethyl-1,3,2-dioxaborolan-2-yl)-2,3,3*a*,9,10,10*a*-hexahydrobenzo[*f*]azulen-4(1*H*)-one (12*b*).



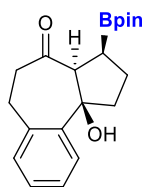
Following the *General Procedure B*, (-)-**12b** (73.6 mg, 0.19 mmol) was isolated after 24h at 30 °C by flash chromatography (pentane/ethyl acetate 3:1) in 98% yield as a yellow oil starting from **11b** (48.9 mg, 0.2 mmol) and B₂pin₂ (55.9 mg, 0.22 mmol) using (*R*)-1-[(*S*_P)-2-(Diphenylphosphino)ferrocenyl]ethylidicyclohexylphosphine (25.6 mg, 0.04 mmol), CuCl (2.9 mg, 0.03 mmol) and NaO^tBu (3.8 mg, 0.04 mmol). All spectroscopic data matched with those described for *rac*-**12b**. The enantiomeric excess (e.e.) was determined by HPLC-DAD using a CHIRALPAK® IC column (hexane/*i*-PrOH 90:10, 1 mL/min, 210 nm, 25°C); t_r (major) = 6.66 min, t_r (minor) = 7.28 min (>99% ee). [α]_D²⁵: -106.6 (c= 0.77, CH₂Cl₂).

(3*S*,3*aS*,10*aS*)-6-fluoro-10*a*-hydroxy-3-(4,4,5,5-tetramethyl-1,3,2-dioxaborolan-2-yl)-2,3,3*a*,9,10,10*a*-hexahydrobenzo[*f*]azulen-4(1*H*)-one (12*d*).



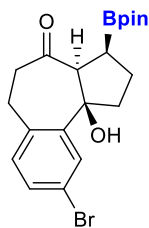
Following the *General Procedure B*, (-)-**12d** (31.1 mg, 0.08 mmol) was isolated after 16h at 30 °C by flash chromatography (pentane/ethyl acetate 10:1) in 43% yield as a colorless oil starting from **11d** (46.4 mg, 0.2 mmol) and B₂pin₂ (55.9 mg, 0.22 mmol) using (*R*)-1-[(*S*_P)-2-(Diphenylphosphino)ferrocenyl]ethylidicyclohexylphosphine (25.6 mg, 0.04 mmol), CuCl (2.9 mg, 0.03 mmol) and NaO^tBu (3.8 mg, 0.04 mmol). All spectroscopic data matched with those described for *rac*-**12d**. The enantiomeric excess (e.e.) was determined by HPLC-DAD using a CHIRALPAK® ID column (hexane/*i*-PrOH 80:20, 1 mL/min, 210 nm, 25°C); t_r (major) = 5.97 min, t_r (minor) = 5.13 min (74% ee). [α]_D²⁵: -1.6 (c= 1.0, CH₂Cl₂).

(3*S*,3*aS*,10*bR*)-10*b*-hydroxy-3-(4,4,5,5-tetramethyl-1,3,2-dioxaborolan-2-yl)-2,3,3*a*,5,6,10*b*-hexahydrobenzo[*e*]azulen-4(1*H*)-one (15*a*).



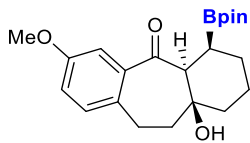
Following the *General Procedure B*, (+)-**15a** (44.5 mg, 0.13 mmol) was isolated after 20h at 30 °C by flash chromatography (pentane/ethyl acetate 10:1) in 65% yield as a colorless oil starting from **14a** (42.9 mg, 0.2 mmol) and B₂pin₂ (55.9 mg, 0.22 mmol) using (*R*)-1-[(*S*_P)-2-(Diphenylphosphino)ferrocenyl]ethylidicyclohexylphosphine (25.6 mg, 0.04 mmol), CuCl (2.9 mg, 0.03 mmol) and NaO^tBu (3.8 mg, 0.04 mmol). All spectroscopic data matched with those described for *rac*-**15a**. The enantiomeric excess (e.e.) was determined by HPLC-DAD using a CHIRALPAK® ID column (hexane/*i*-PrOH 80:20, 1 mL/min, 210 nm, 25°C); t_r (major) = 6.31 min, t_r (minor) = 7.12 min (84% ee). [α]_D²⁵: +3.6 (c= 0.76, CH₂Cl₂).

(3*S*,3*aS*,10*bR*)-9-bromo-10*b*-hydroxy-3-(4,4,5,5-tetramethyl-1,3,2-dioxaborolan-2-yl)-2,3,3*a*,5,6,10*b*-hexahydrobenzo[*e*]azulen-4(1*H*)-one (15*b*).



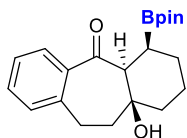
Following the *General Procedure B*, (+)-**15b** (62.3 mg, 0.14 mmol) was isolated after 16h at 30 °C by flash chromatography (pentane/ethyl acetate 10:1) in 74% yield as a white solid starting from **14b** (58.6 mg, 0.2 mmol) and B₂pin₂ (55.9 mg, 0.22 mmol) using (*R*)-1-[(*S_P*)-2-(Diphenylphosphino)ferrocenyl]ethyl dicyclohexylphosphine (25.6 mg, 0.04 mmol), CuCl (2.9 mg, 0.03 mmol) and NaO^tBu (3.8 mg, 0.04 mmol). All spectroscopic data matched with those described for *rac*-**15b**. The enantiomeric excess (e.e.) was determined by HPLC-DAD using a CHIRALPAK® IC column (hexane/*i*-PrOH 90:10, 1 mL/min, 210 nm, 25°C); t_r (major) = 7.41 min, t_r (minor) = 6.65 min (88% ee). [α]_D²⁵: +9.2 (c= 1.5, CH₂Cl₂). M.p.: 110-111 °C (EtOAc/hexane).

(4*S*,4*aS*,11*aS*)-11*a*-hydroxy-7-methoxy-4-(4,4,5,5-tetramethyl-1,3,2-dioxaborolan-2-yl)-1,2,3,4,4*a*,10,11,11*a*-octahydro-5*H*-dibenzo[*a,d*][7]annulen



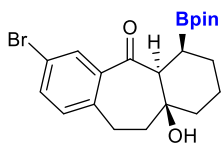
-5-one (19b). Following the *General Procedure B*, (-)-**19b** (43.5 mg, 0.11 mmol) was isolated after 16h at 30 °C by flash chromatography (pentane/ethyl acetate 10:1) in 56% yield as a colorless oil starting from **18b** (51.7 mg, 0.2 mmol) and B₂pin₂ (55.9 mg, 0.22 mmol) using (*R*)-1-[(*S_P*)-2-(Diphenylphosphino)ferrocenyl]ethyldicyclohexylphosphine (22.2 mg, 0.04 mmol), CuCl (2.9 mg, 0.03 mmol) and NaO^tBu (3.8 mg, 0.04 mmol). All spectroscopic data matched with those described for *rac*-**19b**. The enantiomeric excess (e.e.) was determined by HPLC-DAD using a CHIRALPAK® IC column (hexane/*i*-PrOH 90:10, 1 mL/min, 210 nm, 25°C); t_r (major) = 6.81 min, t_r (minor) = 7.88 min (88% ee). [α]_D²⁵: +69.9 (c= 0.34, CH₂Cl₂).

(4*S*,4*aS*,11*aS*)-11*a*-hydroxy-4-(4,4,5,5-tetramethyl-1,3,2-dioxaborolan-2-yl)-1,2,3,4,4*a*,10,11,11*a*-octahydro-5*H*-dibenzo[*a,d*][7]annulen-5-one (19c).



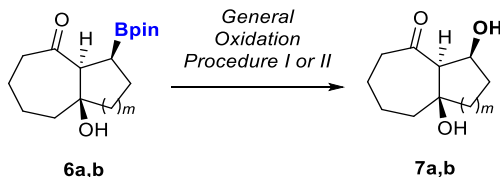
Following the *General Procedure B*, (+)-**19c** (36.1 mg, 0.1 mmol) was isolated after 16h at 30 °C by flash chromatography (pentane/ethyl acetate 10:1) in 67% yield as a colorless oil starting from **18c** (35.0 mg, 0.15 mmol) and B₂pin₂ (40.6 mg, 0.16 mmol) using (*R*)-1-[(*S_P*)-2-(Diphenylphosphino)ferrocenyl]ethyldicyclohexylphosphine (19.2 mg, 0.03 mmol), CuCl (2.2 mg, 0.02 mmol) and NaO^tBu (2.9 mg, 0.03 mmol). All spectroscopic data matched with those described for *rac*-**19c**. The enantiomeric excess (e.e.) was determined by HPLC-DAD using a CHIRALPAK® IC column (hexane/*i*-PrOH 90:10, 1 mL/min, 210 nm, 25°C); t_r (major) = 4.97 min, t_r (minor) = 6.50 min (62% ee). [α]_D²⁵: +48.0 (c= 1.0, CH₂Cl₂).

(4*S*,4*aS*,11*aS*)-7-bromo-11*a*-hydroxy-4-(4,4,5,5-tetramethyl-1,3,2-dioxaborolan-2-yl)-1,2,3,4,4*a*,10,11,11*a*-octahydro-5*H*-



dibenzo[*a,d*][7]annulen-5-one (19d). Following the *General Procedure B*, (+)-**19d** (38.5 mg, 0.08 mmol) was isolated after 16h at 30 °C by flash chromatography (pentane/ethyl acetate 20:1) in 44% yield as a colorless oil starting from **18d** (61.4 mg, 0.2 mmol) and B₂pin₂ (55.9 mg, 0.22 mmol) using (*R*)-1-[(*S_P*)-2-(Diphenylphosphino)ferrocenyl]ethyldicyclohexylphosphine (25.6 mg, 0.04 mmol), CuCl (2.9 mg, 0.03 mmol) and NaO^tBu (3.8 mg, 0.04 mmol). All spectroscopic data matched with those described for *rac*-**19d**. The enantiomeric excess (e.e.) was determined by HPLC-DAD using a CHIRALPAK® IC column (hexane/*i*-PrOH 95:05, 1 mL/min, 210 nm, 25°C); t_r (major) = 5.25 min, t_r (minor) = 5.96 min (64% ee). [α]_D²⁵: +14.7 (c= 1.0, CH₂Cl₂).

2.4. Oxidation procedures

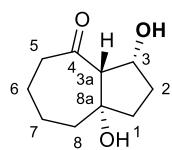


Scheme 6.4. Oxidation procedures of the borylated products.

General Oxidation Procedure I: To a solution of *rac*-**6a** (0.8 equiv, 0.03 mmol) in THF (0.1 mL, 0.3 M) was added Oxone® (2.2 equiv, 0.08 mmol) as a slurry in THF (0.4 mL) and H₂O (0.5 mL). The reaction mixture was stirred at room temperature until full conversion (TLC). Then, Na₂S₂O₅ (4.0 equiv) was added and the mixture was diluted with H₂O and EtOAc. The phases were separated and the aqueous phase was extracted with EtOAc. The combined organic layers were dried over Na₂SO₄, filtered and evaporated. The oxidized product was purified by flash column chromatography.

General Oxidation Procedure II: In a vial equipped with a stirring bar, *rac*-**6b** (1 equiv, 0.1 mmol) was diluted in THF (1 mL). NaBO₃·H₂O (10 equiv, 1 mmol) was added, and followed by the addition of H₂O (0.5 mL). Then, the reaction mixture was stirred at room temperature until completion of the reaction (TLC). The crude was quenched with a saturated solution of NaCl (1 mL) and extracted with EtOAc. The aqueous layer was cleaned with ethyl acetate (3 x 5 mL) and the resulting organic phases were dried over MgSO₄ and concentrated in vacuo. The oxidized product was purified by flash column chromatography.

***rac*-(3*R*,3*aR*,8*aS*)-3,8*a*-dihydroxyoctahydroazulen-4(1*H*)-one (7*a*).** Following

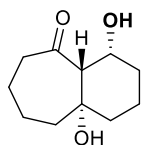


the *General Oxidation Procedure I*, *rac*-**7a** (4.0 mg, 0.02 mmol) was isolated after 4h at room temperature by flash chromatography (petroleum ether/ethyl acetate 70:30) in 64% yield as a white solid starting from *rac*-**6a** (10.0 mg, 0.03 mmol)

and oxone (47 mg, 0.08 mmol). ¹H-NMR (δ, ppm) (400 MHz, CDCl₃): 4.65-4.62 (m, 1H, OH), 4.22 (s, 1H, OH), 3.33 (d, *J* = 2.4 Hz, 1H, H-3), 2.88 (d, *J* = 2.8 Hz, 1H,

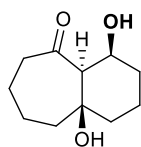
H-3a), 2.66-2.57 (m, 1H, **H_a-5**), 2.53-2.41 (m, 1H, **H_b-5**), 2.30-2.26 (m, 1H, **H_a-2**), 2.24-2.16 (m, 1H, **H_a-1**), 2.07-2.01 (m, 1H, **H_a-6**), 1.98-1.88 (m, 2H, **H_b-2** and **H_b-6**), 1.85-1.78 (m, 1H, **H_a-7**), 1.77-1.64 (m, 3H, **H_b-1**, **H_b-7** and **H_a-8**), 1.63-1.51 (m, 1H, **H_b-8**). ¹³C-NMR (δ, ppm) (100 MHz, CDCl₃): 216.0 (**C-4**), 81.3 (**C-8a**), 76.1 (**C-3**), 64.0 (**C-3a**), 44.3 (**C-5**), 43.0 (**C-8**), 42.4 (**C-1**), 30.5 (**C-2**), 24.7 (**C-6**), 23.5 (**C-7**). HRMS (ESI-TOF) for C₁₀H₁₆NaO₃ [M+Na]⁺: calculated: 207.0997, found: 207.1007. M.p.: 68-69 °C (EtOAc/hexane).

rac-(4R,4aR,9aS)-4,9a-dihydroxydecahydro-5H-benzo[7]annulen-5-one (7b).



Following the *General Oxidation Procedure II*, *rac-7b* (15.1 mg, 0.07 mmol) was isolated after 3h at room temperature by flash chromatography (pentane/ethyl acetate 5:1) in 76% yield as a colorless oil starting from *rac-6b* (30.8 mg, 0.1 mmol) and NaBO₃·H₂O (100 mg, 1 mmol). ¹H-NMR (δ, ppm) (400 MHz, CDCl₃): 4.70 (s, 1H, OH), 4.37 (d, *J* = 1.5 Hz, 1H, **H-3**), 4.25 (s, 1H, OH), 2.64-2.59 (m, 2H, **H-5**), 2.57 (d, *J* = 1.4 Hz, 1H, **H-3a**), 2.01-1.93 (m, 4H, **H_a-2**, **H_a-6**, **H_a-7** and **H_a-9**), 1.81-1.76 (m, 1H, **H_b-6**), 1.63-1.52 (m, 4H, **H_a-1**, **H_b-2**, **H_b-7** and **H_b-9**), 1.51-1.39 (m, 2H, **H_a-8** and **H_b-1**), 1.37-1.29 (m, 1H, **H_b-8**). ¹³C-NMR (δ, ppm) (100 MHz, CDCl₃): 217.3 (**C-4**), 72.6 (**C-9a**), 68.8 (**C-3a**), 57.0 (**C-3**), 44.9 (**C-5**), 44.6 (**C-8**), 41.4 (**C-9**), 31.0 (**C-2**), 23.0 (**C-6**), 22.3 (**C-7**), 15.2 (**C-1**). HRMS (ESI-TOF) for C₁₁H₁₈NaO₃ [M+Na]⁺: calculated: 221.1153, found: 221.1153.

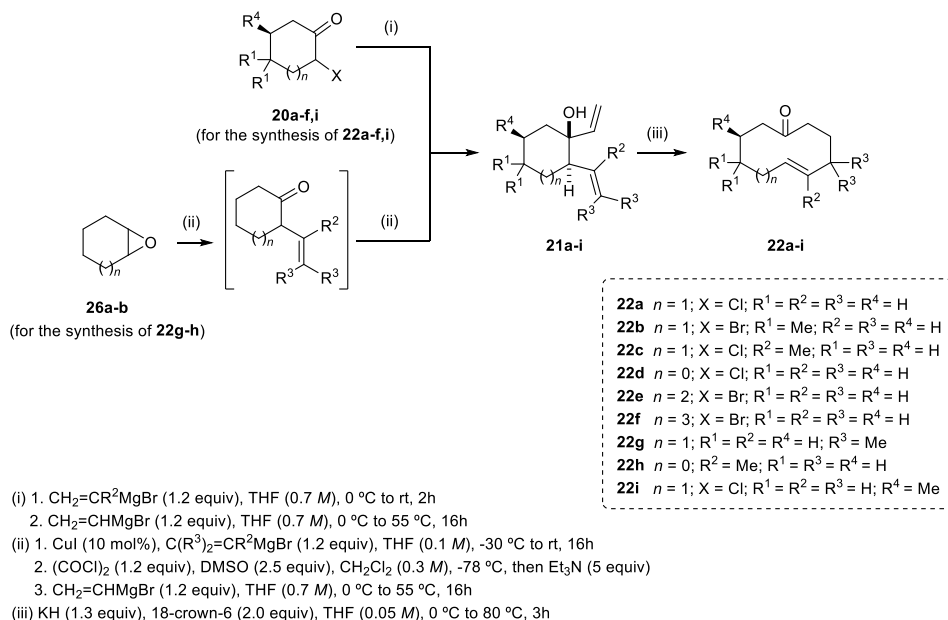
(4R,4aR,9aS)-4,9a-dihydroxydecahydro-5H-benzo[7]annulen-5-one (7b).



Following the *General Oxidation Procedure II*, **(+)-7b** (16.7 mg, 0.08 mmol) was isolated after 3h at room temperature by flash chromatography (pentane/ethyl acetate 5:1) in 99% yield as a colorless oil starting from **(+)-6b** (26.2 mg, 0.09 mmol) and NaBO₃·H₂O (85.0 mg, 0.85 mmol). All spectroscopic data matched with those described for *rac-7b*. The enantiomeric excess (e.e.) was determined by HPLC-DAD using a CHIRALPAK® ID column (hexane/*i*-PrOH 70:30, 1 mL/min, 210 nm, 25°C); *t_r* (major) = 7.84 min, *t_r* (minor) = 8.68 min (82% ee). [α]_D²⁵: +54.4 (*c* = 0.84, CH₂Cl₂).

3. TRANSANNULAR ENANTIOSELECTIVE (3+2) CYCLOADDITION OF CYCLOALKENONE HYDRAZONES

3.1. Synthesis of the starting materials



Scheme 6.5. General overview of the synthesis of starting materials.

Compounds **20a**, **20d** and **26a-b** were commercially available and used without further purification. Compounds **20b** and **20i** were synthesized according to procedures previously described in the literature and used without further purification.⁸

General Procedure I for the synthesis of substrates **21a-f,i**: These compounds were prepared following the procedure described in the literature. Spectroscopic data of substrates **21a**, **21c**, **21d**, **21e** and **21f** were consistent with those reported

⁸ (a) Faeh, C.; Kuehne, H.; Luebberts, T.; Mattei, P.; Maugeais, C.; Pflieger, P. (2007). *Preparation of heteroaryl and benzyl amide compounds as CETP inhibitors for treating dyslipidemia and other diseases*. (U.S. Pat. Appl. Publ. No. 20070185113). (b) Riss, B.; Garreau, M.; Fricero, P.; Podsiadly, P.; Berton, N.; Buchter, S. *Tetrahedron* **2017**, 73, 3202.

in the literature.⁹

A solution of 2-chlorocycloalkanone (1 equiv) in THF and vinylmagnesium bromide solution (0.5-1 M in THF, 1.25 equiv) were added dropwise to THF at 0 °C, over 1 hour under argon atmosphere. After that time, the reaction was left stirring for 1 hour additional before the addition of the Grignard reagent in THF (0.5-1 M in THF, 1.25 equiv) over a period of 10 minutes. The reaction was allowed to warm up to 55 °C and kept stirring overnight. Upon completion, saturated aqueous NH₄Cl was added, the phases separated and the aqueous phase was extracted with Et₂O (3 x 10 mL). The combined organic layers were washed with brine, dried over Na₂SO₄, filtered and the solvent evaporated under reduced pressure. The obtained crude was purified by column chromatography.

General Procedure III for the synthesis of substrates **21g-h**: These compounds were prepared following the procedure described in the literature. Spectroscopic data of **21h** were consistent with those reported in the literature.^{9d-e,10}

An oven-dried round-bottom flask was charged with CuI (0.15 equiv), dissolved in THF and cooled to -30 °C under argon atmosphere. To the formed suspension, the corresponding Grignard reagent in THF was added (1.5 equiv) over a period of 30 minutes and left stirring for additional 10 minutes at -30 °C. After the mentioned time, *meso*-epoxide (1 equiv) was added dropwise over 10 minutes and the reaction mixture was allowed to gradually warm up to room temperature and left stirring overnight. Upon reaction completion, the crude solution was cooled to 0 °C and quenched with saturated aqueous NH₄Cl and diluted with H₂O, the phases separated and the aqueous phase was extracted with Et₂O (3 x 10 mL). The combined organic layers were washed with brine, dried over Na₂SO₄, filtered and

⁹ (a) Thies, R. W.; Billigmeier, J. E. *J. Am. Chem. Soc.* **1974**, *96*, 200. (b) Thies, R. W.; Seitz, E. P. *J. Chem. Soc., Chem. Commun.* **1976**, 846. (c) Kato, T.; Kondo, H.; Nishino, M.; Tanaka, M.; Hata, G.; Miyake, A. *Bull. Chem. Soc. Jpn.* **1980**, *53*, 2958. (d) Molander, G. A.; Czako, B.; Rheam, M. *J. Org. Chem.* **2007**, *72*, 1755. (e) Tomooka, K.; Ezawa, T.; Inoue, H.; Uehara, K.; Igawa, K. *J. Am. Chem. Soc.* **2011**, *133*, 1754.

¹⁰ Rajapaksa, N. S.; Jacobsen, E. N. *Org. Lett.* **2013**, *15*, 4238.

the solvent evaporated under reduced pressure. The crude was used without further purification as follows.

To a solution of oxalyl chloride (1.2 equiv) in CH_2Cl_2 at $-78\text{ }^\circ\text{C}$ was added dropwise a solution of DMSO (2.5 equiv) in CH_2Cl_2 and stirred at the mentioned temperature for 10 minutes. Then, a solution of the crude alcohol (1 equiv) in CH_2Cl_2 was added dropwise and the crude solution was stirred for 1 hour at $-78\text{ }^\circ\text{C}$. The reaction was quenched by the addition of Et_3N (5 equiv) and immediately warmed up to room temperature. The contents were diluted with H_2O , the phases separated and the aqueous phase was extracted with Et_2O (3 x 10 mL). The combined organic layers were washed with brine, dried over Na_2SO_4 , filtered and the solvent evaporated under reduced pressure. The crude was used without further purification as follows.

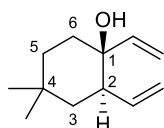
A solution of the unsaturated ketone (1 equiv) in THF was cooled down to $0\text{ }^\circ\text{C}$ before the dropwise addition of the Grignard reagent in THF (0.5-1 M in THF, 1.25 equiv) under argon atmosphere. The reaction was allowed to warm up to room temperature and kept stirring overnight. Upon completion, saturated aqueous NH_4Cl was added, the phases separated and the aqueous phase was extracted with Et_2O (3 x 10 mL). The combined organic layers were washed with brine, dried over Na_2SO_4 , filtered and the solvent evaporated under reduced pressure. The obtained crude was purified by column chromatography.

General Procedure III for the synthesis of substrates **22a-i**: These compounds were prepared following the procedure described in the literature. Spectroscopic data of substrates **22a**, **22c**, **22d**, **22e**, **22f** and **22h** were consistent with those reported in the literature.^{8,9a}

An oven-dried round-bottom flask was charged with KH (1.3 equiv), dissolved in THF and cooled to $0\text{ }^\circ\text{C}$ under argon atmosphere. Then, a solution of 18-crown-6 (2 equiv) and a solution of divinyl alcohol (1 equiv) were added dropwise *via* cannula. The reaction was allowed to warm up to $80\text{ }^\circ\text{C}$ and it was left under reflux for 2-3h. Upon completion, saturated aqueous NH_4Cl was added, the phases

separated and the aqueous phase was extracted with Et₂O (3 x 10 mL). The combined organic layers were washed with brine, dried over Na₂SO₄, filtered and the solvent evaporated under reduced pressure. The obtained crude was purified by column chromatography.

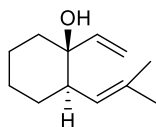
rac-(1S,2R)-4,4-dimethyl-1,2-divinylcyclohexan-1-ol (21b). Following the



General Procedure I, compound **21b** (0.38 g, 2.08 mmol) was isolated after 16h at 55 °C by flash chromatography (petroleum ether/EtOAc 9:1) in 36% yield as a colourless oil starting from **20b** (1.19 g, 5.80 mmol), vinylmagnesium bromide solution (0.6 M in

THF, 14.50 mmol) and THF (10 mL). ¹H-NMR (δ, ppm) (300 MHz, CDCl₃): 5.97-5.77 (m, 2H, 2 x CH=CH₂), 5.22 (dd, *J* = 17.3, 1.4 Hz, 1H, CH=CH₂), 5.13-4.98 (m, 3H, 3 x CH=CH₂), 2.34-2.23 (m, 1H, **H-2**), 1.73-1.43 (m, 4H, **H-3_a**, **H-5_a** and **H-6**), 1.21 (dt, *J* = 12.4, 2.5 Hz, 2H, **H-3_b** and **H-5_b**), 0.98 (s, 3H, CH₃), 0.94 (s, 3H, CH₃). ¹³C-NMR (δ, ppm) (75.5 MHz, CDCl₃): 145.9 (CH=CH₂), 138.7 (CH=CH₂), 116.1 (CH=CH₂), 111.9 (CH=CH₂), 72.8 (**C-1**), 43.9 (**C-2**), 38.5 (**C-3**), 34.1 (**C-6**), 33.7 (**C-5**), 33.0 (**C-4**), 30.0 (CH₃), 24.0 (CH₃). IR (ATR) cm⁻¹: 3486, 2950, 2927, 1364, 1219, 913, 772. MS (EI, 70 eV) *m/z* (%): 195 (4), 181 (15), 180 (M⁺, 11), 179 (22), 178 (10), 177 (11), 176 (5), 174 (4), 164 (12), 163 (87), 162 (100), 161 (23), 160 (15), 159 (6), 158 (11), 156 (5). HRMS (ESI⁺) for C₁₂H₁₉ [M-H₂O+H]⁺: calculated: 163.1487, found: 163.1490.

rac-(1S,2R)-2-(2-methylprop-1-en-1-yl)-1-vinylcyclohexan-1-ol (21g).

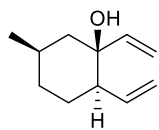


Following the *General Procedure II*, compound **21g** (0.56 g, 3.11 mmol) was isolated after 16h at room temperature by flash chromatography (petroleum ether/EtOAc 19:1) in 38% yield as a pale green oil starting from vinylmagnesium bromide solution (0.7

M in THF, 9.70 mmol) and THF (15 mL). ¹H-NMR (δ, ppm) (300 MHz, CDCl₃): 5.80 (dd, *J* = 17.4, 10.8 Hz, 1H, CH=CH₂), 5.15-4.86 (m, 3H, CH=CH₂ and CH=C(CH₃)₂), 2.26-2.09 (m, 1H, **H-2**), 1.63 (s, 3H, CH₃), 1.53 (s, 3H, CH₃), 1.50-1.46 (m, 3H, **H-4_a**, **H-5_a** and **H-6_a**), 1.40 (ddd, *J* = 10.5, 6.1, 2.4 Hz, 4H, **H-3_a**, **H-5_b**, **H-4_b** and **H-6_b**), 1.24 (ddt, *J* = 12.3, 8.3, 3.7 Hz, 1H, **H-3_b**). ¹³C-NMR (δ, ppm) (75.5 MHz, CDCl₃):

146.0 (CH=CH₂), 132.0 (CH=C(CH₃)₂), 124.9 (CH=C(CH₃)₂), 111.1 (CH=CH₂), 73.7 (C-1), 44.2 (C-2), 37.7 (C-6), 28.3 (C-4), 25.8 (C-3), 25.3 (CH₃), 21.3 (C-5), 18.2 (CH₃). IR (ATR) cm⁻¹: 3480, 2927, 2853, 1444, 1375, 966, 916. MS (EI, 70 eV) *m/z* (%): 179 (10), 178 (6), 177 (14), 176 (4), 175 (4), 164 (16), 163 (100), 162 (63), 161 (26), 160 (15), 159 (5), 158 (6), 156 (4), 119 (6). HRMS (ESI⁺) for C₁₃H₂₁O₃ [M+HCOOH-H]⁺: calculated: 225.1491, found: 225.1488.

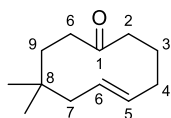
(1S,2R,5R)-5-methyl-1,2-divinylcyclohexan-1-ol (21i). Following the *General*



Procedure I, compound **21i** (315.70 mg, 1.90 mmol) was isolated after 3h at 80 °C by flash chromatography (petroleum ether/EtOAc 8:2) in 34% yield as a pale brown oil starting from **20i** (0.94 g, 5.65 mmol), vinylmagnesium bromide solution (0.8 *M* in THF, 13.00

mmol) and THF (7.8 mL). ¹H-NMR (δ, ppm) (300 MHz, CDCl₃): 5.88 (ddd, *J* = 17.3, 10.7, 5.4 Hz, 2H, 2 x CH=CH₂), 5.26-4.94 (m, 4H, 4 x CH=CH₂), 2.11-2.01 (m, 1H, H-2), 1.89-1.59 (m, 5H, H-3_a, H-4_a, H-5 and H-6), 1.45 (s, 1H, OH), 1.13 (dd, *J* = 13.7, 12.1 Hz, 1H, H-4_b), 1.04-0.92 (m, 1H, H-3_b), 0.89 (d, *J* = 6.4 Hz, 3H, CH₃). ¹³C-NMR (δ, ppm) (75.5 MHz, CDCl₃): 145.9 (CH=CH₂), 138.7 (CH=CH₂), 116.2 (CH=CH₂), 111.7 (CH=CH₂), 73.8 (C-1), 47.7 (C-2), 46.5 (C-6), 34.2 (C-4), 27.3 (C-5), 25.7 (C-3), 22.1 (CH₃). [α]_D²⁰: +173.6 (*c* = 0.9, CH₂Cl₂). IR (ATR) cm⁻¹: 3502, 2989, 1275, 1260, 763, 750. MS (EI, 70 eV) *m/z* (%): 164 (5), 150 (12), 149 (97), 148 (100), 147 (15), 146 (9), 144 (3), 66 (6), 55 (9), 54 (6), 53 (7), 51 (6). HRMS (ESI⁺) for C₁₁H₁₉O [M+H]⁺: calculated: 167.1436, found: 167.1432.

(E)-8,8-dimethylcyclodec-5-en-1-one (22b). Following the *General Procedure III*,

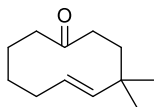


compound **22b** (226.50 mg, 1.26 mmol) was isolated after 3 h at 80°C by flash chromatography (petroleum ether/EtOAc 19:1) in 63% yield as a white crystalline solid starting from **21b** (360.0 g, 2.00 mmol), KH (347 mg, 2.60 mmol), 18-crown-6 (1.06 g, 4.00

mmol) and THF (31 mL). ¹H-NMR (δ, ppm) (300 MHz, CDCl₃): 5.51-5.40 (m, 1H, CH), 5.09 (dd, *J* = 15.0, 7.4 Hz, 1H, CH), 2.79-2.68 (m, 1H, H-2_a), 2.29-2.02 (m, 6H, H-2_b, H-4, H-6 and H-7_a), 1.87-1.67 (m, 4H, H-3, H-7_b and H-9_a), 1.32-1.20 (m, 1H, H-9_b), 0.99-0.90 (m, 6H, 2 x CH₃). ¹³C-NMR (δ, ppm) (75.5 MHz, CDCl₃): 212.6

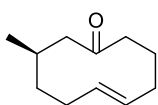
(C-1), 135.6 (CH), 128.1 (CH), 46.2 (C-7), 43.0 (C-2), 40.5 (C-6), 34.2 (CH₃), 34.1 (CH₃), 34.0 (C-9), 33.6 (C-4), 28.3 (C-8), 24.3 (C-3). IR (ATR) cm⁻¹: 2942, 2925, 1705, 1364, 1106, 986, 772. MS (EI, 70 eV) *m/z* (%): 181 (5), 180 (M⁺, 11), 179 (10), 178 (5), 177 (4), 164 (14), 163 (100), 162 (65), 161 (18), 160 (16), 158 (5). HRMS (ESI⁺) for C₁₂H₁₉ [M-H₂O+H]⁺: calculated: 163.1487, found: 163.1485. M.p.: 41-42 °C (EtOAc/hexane).

(E)-4,4-dimethylcyclodec-5-en-1-one (22g). Following the *General Procedure III*,



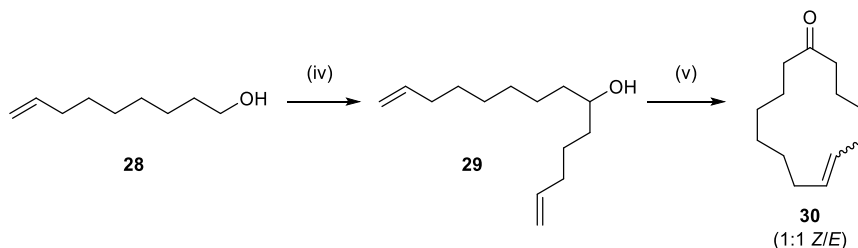
compound **22g** (368.00 mg, 2.04 mmol) was isolated after 3 h at 80°C by flash chromatography (petroleum ether/EtOAc 9:1) in 66% yield as a colourless oil starting from **21g** (560.00 mg, 3.11 mmol), KH (540 mg, 4.04 mmol), 18-crown-6 (1.64 g, 6.22 mmol) and THF (48 mL). ¹H-NMR (δ, ppm) (300 MHz, CDCl₃): 5.31-5.04 (m, 2H, 2 x CH), 2.53-1.25 (m, 12H, H-2, H-3, H-7, H-8, H-9 and H-10), 1.01 (s, 6H, 2 x CH₃). ¹³C-NMR (δ, ppm) (75.5 MHz, CDCl₃): 213.0 (C-1), 143.0 (CH), 126.5 (CH), 45.7 (C-6), 41.8 (C-2), 39.2 (C-3), 36.8 (C-7), 33.3 (C-8), 28.6 (CH₃), 22.1 (C-9). IR (ATR) cm⁻¹: 2954, 2924, 1707, 1445, 1364, 1195, 989. MS (EI, 70 eV) *m/z* (%): 181 (4), 180 (M⁺, 7), 179 (7), 178 (5), 177 (6), 164 (9), 163 (70), 162 (100), 161 (32), 160 (17), 158 (7), 156 (4). HRMS (ESI⁺) for C₁₂H₁₉ [M-H₂O+H]⁺: calculated: 163.1487, found: 163.1491.

(R,E)-9-methylcyclodec-5-en-1-one (22i). Following the *General Procedure III*,



compound **22i** (158.90 mg, 0.96 mmol) was isolated after 2 h at 80°C by flash chromatography (petroleum ether/EtOAc 9:1) in 51% yield as a colourless oil starting from **21i** (315.7 mg, 1.90 mmol), KH (330 mg, 2.50 mmol), 18-crown-6 (1.0 g, 3.80 mmol) and THF (33 mL). ¹H-NMR (δ, ppm) (300 MHz, CDCl₃): 5.29 (ddd, *J* = 14.0, 10.2, 3.3 Hz, 1H, CH), 5.10 (ddd, *J* = 15.1, 10.5, 3.5 Hz, 1H, CH), 2.53 (dd, *J* = 16.7, 8.6 Hz, 1H, H-6_a), 2.17 (tt, *J* = 14.8, 6.0 Hz, 7H, H-2, H-4, H-6_b and H-7), 1.93 (dtd, *J* = 13.5, 11.2, 10.1, 2.8 Hz, 1H, H-9), 1.81-1.70 (m, 2H, H-3), 1.63 (ddt, *J* = 14.2, 5.6, 2.6 Hz, 1H, H-8_a), 1.17 (q, *J* = 12.0, 11.4 Hz, 1H, H-8_b), 0.92 (d, *J* = 7.1 Hz, 3H, CH₃). ¹³C-NMR (δ, ppm) (75.5 MHz, CDCl₃): 212.0 (C-1), 134.8 (CH), 130.8 (CH), 53.8 (C-6), 42.8 (C-2), 37.3 (C-8), 34.1 (C-7), 32.2 (C-4), 28.4 (C-9), 27.8 (C-3), 24.9 (CH₃). [α]_D²⁰: +522.7 (*c* = 0.3,

CH₂Cl₂). IR (ATR) cm⁻¹: 2989, 1275, 1260, 763, 750. MS (EI, 70 eV) *m/z* (%): 167 (17), 166 (M⁺, 14), 165 (23), 150 (15), 149 (100), 148 (86), 147 (14), 146 (8), 145 (10), 143 (6). HRMS (ESI⁺) for C₁₁H₁₉O [M+H]⁺: calculated: 167.1436, found: 167.1436.



- (iv) 1. DMP (2.2 equiv), CH₂Cl₂ (0.1 M), rt, 2h
 2. CH₂=CHCH₂(CH₂)_nCH₂MgBr (1.5 equiv), THF (0.1 M), 0 °C to rt, 16h
 (v) 1. DMP (2.2 equiv), CH₂Cl₂ (0.1 M), rt, 2h
 2. Grubbs 2nd gen. (5 mol%), toluene (0.001 M) (under Ar), reflux, 4h

Scheme 6.6. Synthesis of substrate **30**.

Compound **28** was commercially available and used without further purification.

General Procedure IV for the synthesis of compound **29**: This compound was prepared following the procedure described in the literature.¹¹

To a solution of alcohol **28** (1 equiv) in CH₂Cl₂ (0.1 M) was added DMP (2.2 equiv). The resulting mixture was stirred at room temperature for 2h. It was then quenched with a solution of 10% aq. Na₂S₂O₃ and sat. aq. NaHCO₃ (1:1) and extracted with CH₂Cl₂. The combined organic layers were washed with brine, dried over Na₂SO₄, filtered and the solvent evaporated under reduced pressure. The crude was used without further purification as follows.

To a solution of the obtained crude (1 equiv) in THF at 0 °C was added vinylmagnesium bromide solution (0.5-1 M in THF, 1.5 equiv) dropwise. The reaction was allowed to warm up to room temperature and kept stirring overnight. Upon completion, saturated aqueous NH₄Cl was added, the phases separated and

¹¹ (a) Halle, M. B.; Fernandes, R. A. *RSC Adv.* **2014**, *4*, 63342. (b) Curton, N.; Ornelas, J.; Uhrinak, A.; Rhem, B.; Coulter, J.; Zhang, J.; Joyner, P. M.; White, J. B. *Tetrahedron Lett.* **2016**, *57*, 4061.

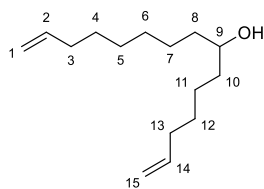
the aqueous phase was extracted with Et₂O (3 x 10 mL). The combined organic layers were washed with brine, dried over Na₂SO₄, filtered and the solvent evaporated under reduced pressure. The obtained crude was purified by column chromatography.

General Procedure V for the synthesis of compound **30**: This compound was prepared following the procedure described in the literature.¹¹

To a solution of alcohol **29** (1 equiv) in CH₂Cl₂ (0.1 M) was added DMP (2.2 equiv). The resulting mixture was stirred at room temperature for 2h. It was then quenched with a solution of 10% aq. Na₂S₂O₃ and sat. aq. NaHCO₃ (1:1) and extracted with CH₂Cl₂. The combined organic layers were washed with brine, dried over Na₂SO₄, filtered and the solvent evaporated under reduced pressure. The crude was used without further purification as follows.

To a solution of the obtained crude (1 equiv) in dry and degassed toluene (0.001 M) was added Grubbs 2nd gen. (5 mol%) under Ar. The mixture was allowed to warm up until reflux and left stirring until completion. Then, the reaction was cooled down to room temperature, filtered through a small pad of Celite® and the obtained crude was purified by column chromatography.

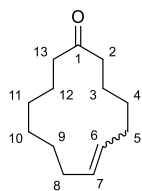
Pentadeca-1,14-dien-7-ol (29). Following *General Procedure IV*, compound **29**



(0.26 g, 1.16 mmol) was isolated after 16h at room temperature by flash chromatography (petroleum ether/EtOAc 9:1) in 51% yield as a colourless oil. ¹H-NMR (δ, ppm) (300 MHz, CDCl₃): 5.81 (ddt, *J* = 16.9, 10.2, 6.7 Hz, 2H, 2xCH=CH₂), 5.06-4.88 (m, 4H, 2xCH=CH₂), 3.58 (dd, *J* = 7.0, 3.8 Hz, 1H, H-9), 2.05 (p, *J* = 6.9 Hz, 4H, H-3 and H-13), 1.49-1.26 (m, 17H, H-4, H-5, H-6, H-7, H-8, H-10, H-11, H-12 and OH). ¹³C-NMR (δ, ppm) (75.5 MHz, CDCl₃): 139.3 (CH=CH₂), 139.1 (CH=CH₂), 114.5 (CH=CH₂), 114.3 (CH=CH₂), 72.1 (C-9), 37.6 (C-8), 37.5 (C-10), 33.9 (C-3), 33.9 (C-13), 29.7 (C-4), 29.2 (C-5), 29.1 (C-6), 29.0 (C-12), 25.7 (C-7), 25.3 (C-11). IR (ATR) cm⁻¹: 3339, 2925, 2854. MS (EI, 70 eV) *m/z* (%): 224 (M⁺, 5), 223 ([M-H]⁺, 100), 221 (30), 219

(14), 207 (53), 206 (52), 205 (44), 203 (14), 125 (13), 111 (55). HRMS (ESI⁺) for C₁₅H₂₉O [M+H]⁺: calculated: 225.2136, found: 225.2130.

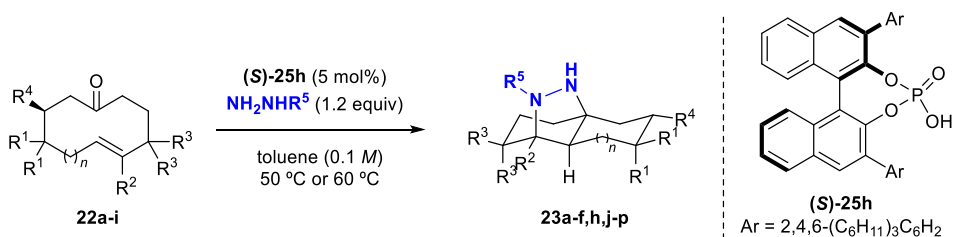
(E)-cyclotridec-6-enone (30). Following *General Procedure V*, compound **30** (25.1



mg, 0.13 mmol) was isolated after 4h under reflux by flash chromatography (petroleum ether/EtOAc 19:1) in 65% yield as a colourless oil. ¹H-NMR (δ, ppm) (300 MHz, CDCl₃): 5.45-5.17 (m, 2H, **H-6** and **H-7**), 2.38 (dq, *J* = 13.5, 6.6 Hz, 4H, **H-2** and **H-13**), 2.11-1.91 (m, 4H, **H-5** and **H-8**), 1.71-1.54 (m, 4H, **H-3** and **H-12**), 1.51-

1.36 (m, 4H, **H-4** and **H-9**), 1.30-1.20 (m, 4H, **H-10** and **H-11**). ¹³C-NMR (δ, ppm) (75.5 MHz, CDCl₃)(*denotes the signals of the other diastereoisomer): 213.8* (**C-1**), 212.6 (**C-1**), 131.9 (**CH=CH**), 131.3 (**CH=CH**), 131.0* (**CH=CH**), 130.3* (**CH=CH**), 43.2* (**C-13**), 42.7 (**C-13**), 40.7* (**C-2**), 39.9 (**C-2**), 31.5 (**C-8**), 31.4 (**C-5**), 28.2* (**C-8**), 27.8* (**C-5**), 27.0 (**C-4**), 26.9 (**C-9**), 26.5* (**C-4**), 26.3 (**C-9**), 26.1* (**C-12**), 25.7 (**C-12**), 25.7* (**C-10**), 25.1* (**C-10**), 24.6* (**C-11**), 23.6 (**C-11**), 23.3* (**C-3**), 22.3 (**C-3**). IR (ATR) cm⁻¹: 2925, 2850, 1709. MS (EI, 70 eV) *m/z* (%): 195 (25), 194 (M⁺, 12), 193 (31), 192 (10), 177 (18), 98 (12), 81 (16), 79 (30), 77 (17), 68 (12), 67 (68), 65 (18), 56 (16), 55 (100), 54 (64), 53 (54), 52 (12), 51 (12). HRMS (ESI⁺) for C₁₃H₂₃O [M+H]⁺: calculated: 195.1721, found: 195.1728.

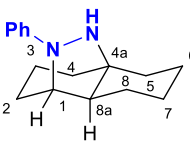
3.2. Enantioselective transannular (3+2) cycloaddition



Scheme 6.7. General procedure for the enantioselective transannular (3+2) cycloaddition.

General Procedure A for the synthesis of **23a-f,h,j-p**: To an oven-dried screw-top vial, equipped with a magnetic stirring bar, the enone **22a-i** (1 equiv, 0.15 mmol), catalyst **(S)-25h** (5 mol%, 0.008 mmol) and the corresponding hydrazine (1.2 equiv, 0.18 mmol) were added followed by dry toluene (1.5 mL). The vial was sealed with a plastic cap and the resulting mixture was left stirring at the indicated temperature in each case, until consumption of the starting material was observed by TLC. The solvent was evaporated under reduced pressure and the NMR yield was calculated through comparison to an internal standard (1,3,5-trimethoxybenzene). Purification by column chromatography afforded the desired products. Racemic standards for HPLC separation were prepared under the same reaction conditions, using diphenylphosphoric acid (DPP) (0.015 mmol) as catalyst.

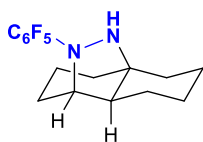
(1*S*,4*aR*,8*aS*)-10-phenyloctahydro-2*H*-1,4*a*-epidiazanonaphthalene (**23a**)



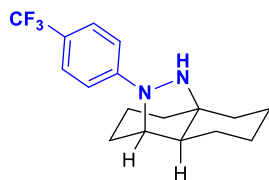
Following the *General Procedure A*, **23a** (36.10 mg, 0.15 mmol) was isolated after 16h at 50 °C by flash chromatography (petroleum ether/EtOAc 19:1) in 99% yield as a colourless oil starting from **22a** (22.80 mg, 0.15 mmol), phenylhydrazine (18 μL , 0.18 mmol), **(S)-25h** (7.50 mg, 0.008 mmol) and toluene (1.5 mL, 0.1 M). ¹H-NMR (δ , ppm) (300 MHz, CDCl₃): 7.19 (dd, J = 8.7, 7.3 Hz, 2H, 2 x CH_{arom}), 6.90 (d, J = 8 Hz, 2H, 2 x CH_{arom}), 6.65 (tt, J = 7.2, 11.2 Hz, 1H, CH_{arom}), 4.06 (br s, 1H, NH), 3.88 (d, J = 4.4 Hz, 1H, H-1), 2.21-2.10 (m, 1H, H-7_a), 1.89-1.73 (m, 2H, H-6_a and H-8_a), 1.71-1.50 (m, 5H, H-2_a, H-3_a, H-4_a, H-5_a and H-7_b), 1.44-1.33 (m, 5H, H-2_b, H-3_b, H-6_b, H-8_a and H-8_b), 1.89-1.73 (m, 2H, H-4_b and H-5_b). ¹³C-NMR (δ , ppm)

(75.5 MHz, CDCl₃): 149.2 (**C**_{arom}), 128.7 (**CH**_{arom}), 116.2 (**CH**_{arom}), 113.0 (**CH**_{arom}), 62.1 (**C**-1), 59.5 (**C**-4a), 49.8 (**C**-8a), 40.4 (**C**-5), 31.0 (**C**-4), 28.0 (**C**-2), 25.8 (**C**-7), 24.5 (**C**-6), 21.7 (**C**-8), 18.8 (**C**-3). The enantiomeric excess (e.e.) was determined by HPLC after derivatization of the corresponding product following the *General Procedure B*. [α]_D²⁰: -12.0 (*c* = 1.0, CH₂Cl₂). IR (ATR) cm⁻¹: 2928, 1590, 1219, 770. MS (EI, 70 eV) *m/z* (%): 243 (11), 242 (M⁺, 60), 21 (5), 213 (4), 200 (15), 199 (100), 198 (4), 171 (4), 157 (6), 135 (6), 134 (8), 130 (6), 117 (5), 108 (4), 107 (6), 104 (7), 94 (4), 93 (8), 92 (4), 91 (11), 81 (4), 79 (10), 78 (6), 77 (37), 67 (7), 65 (6), 55 (4), 53 (4), 51 (8). HRMS (ESI⁺) for C₁₆H₂₃N₂ [M+H]⁺: calculated: 243.1861, found: 243.1866.

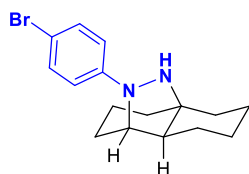
(1*S*,4*aR*,8*aS*)-10-(perfluorophenyl)octahydro-2*H*-1,4*a*-epidiazanonaphthalene (23b). Following the *General Procedure A*, **23b** (48.00 mg, 0.14 mmol) was isolated



after 16h at 50 °C by flash chromatography (petroleum ether/EtOAc 19:1) in 96% yield as a pale orange oil starting from **22a** (22.80 mg, 0.15 mmol), pentafluorophenylhydrazine (35.60 mg, 0.18 mmol), **(S)-25h** (7.50 mg, 0.008 mmol) and toluene (1.5 mL, 0.1 M). ¹H-NMR (δ , ppm) (300 MHz, CDCl₃): 4.37 (br s, 1H, NH), 3.90 (s, 1H, **H**-1), 1.85-1.68 (m, 5H, **H**-5_a, **H**-6_a, **H**-7 and **H**-8_a), 1.59-1.53 (m, 5H, **H**-2_a, **H**-3, **H**-4_a and **H**-8_b), 1.49-1.37 (m, 3H, **H**-2_b, **H**-6_b and **H**-8_a), 1.28-1.18 (m, 2H, **H**-5_b and **H**-4_b). ¹³C-NMR (δ , ppm) (75.5 MHz, CDCl₃): 66.4 (**C**-1), 59.8 (**C**-4a), 49.0 (**C**-8a), 40.0 (**C**-5), 30.9 (**C**-4), 30.1 (**C**-2), 25.7 (**C**-7), 24.4 (**C**-6), 21.3 (**C**-8), 18.8 (**C**-3), (Fluor containing C_{arom} do not relax). ¹⁹F-NMR (δ , ppm) (282 MHz, CDCl₃): -150.81, -150.83, -150.88, -150.89, -164.62, -164.70, -164.77, -171.33, -171.35, -171.39, -171.41, -171.43, -171.47, -171.49, -171.51. The enantiomeric excess (e.e.) was determined by HPLC after derivatization of the corresponding product following the *General Procedure B*. [α]_D²⁰: +29.8 (*c* = 0.7, CH₂Cl₂). IR (ATR) cm⁻¹: 2934, 1515, 1491, 1051, 749. MS (EI, 70 eV) *m/z* (%): 345 (2), 334 (2), 333 (18), 332 (M⁺, 100), 331 (77), 330 (26), 329 (4), 328 (2), 165 (3), 136 (7), 135 (42), 134 (21), 133 (3), 133 (3). HRMS (ESI⁺) for C₁₆H₁₈N₂F₅ [M+H]⁺: calculated: 333.1390, found: 333.1393.

(1S,4aR,8aS)-10-(4-(trifluoromethyl)phenyl)octahydro-2H-1,4a-**epidiazanonaphthalene (23c).** Following the *General Procedure A*, **23c** (44.20mg, 0.14 mmol) was isolated after 16h at 50 °C by flash chromatography (petroleum ether/EtOAc 19:1) in 95% yield as a yellow oil starting from **22a** (22.80 mg, 0.15 mmol), 4-(trifluoromethyl)phenylhydrazine (31.70 mg, 0.18 mmol), (**S**)-**25h** (7.50 mg, 0.008 mmol) and toluene

(1.5 mL, 0.1 M). $^1\text{H-NMR}$ (δ , ppm) (300 MHz, CDCl_3): 7.40 (d, $J = 8.6$ Hz, 2H, 2 x CH_{arom}), 6.88 (br s, 2H, 2 x CH_{arom}), 4.12 (s, 1H, NH), 3.91 (d, $J = 4.3$ Hz, 1H, H-1), 2.13 (dd, $J = 7.7, 4.3$ Hz, 1H, H-7_a), 1.81 (dd, $J = 11.2, 4.8$ Hz, 2H, H-6_a and H-8_a), 1.76-1.54 (m, 5H, H-2_a, H-3_a, H-4_a, H-5_a and H-7_b), 1.47-1.34 (m, 5H, H-2_b, H-3_b, H-6_b, H-8_a and H-8_b), 1.26-1.16 (m, 2H, H-4_b and H-5_b). $^{13}\text{C-NMR}$ (δ , ppm) (75.5 MHz, CDCl_3): 151.0 (C_{arom}), 126.0 (CH_{arom}), 117.6 (C_{arom}), 117.2 (CF_3), 112.0 (CH_{arom}), 62.2 (C-1), 59.7 (C-4_a), 49.7 (C-8_a), 40.1 (C-5), 30.8 (C-4), 27.7 (C-2), 25.7 (C-7), 24.4 (C-6), 21.6 (C-8), 18.7 (C-3). $^{19}\text{F-NMR}$ (δ , ppm) (282 MHz, CDCl_3): -60.66. The enantiomeric excess (e.e.) was determined by HPLC after derivatization of the corresponding product following the *General Procedure C*. $[\alpha]_{\text{D}}^{20}$: +14.9 ($c = 0.9$, CH_2Cl_2). IR (ATR) cm^{-1} : 2857, 1611, 1321, 1105, 750, 763. MS (EI, 70 eV) m/z (%): 311 (19), 310 (M^+ , 100), 309 (85), 308 (10), 292 (5), 291 (21). HRMS (ESI⁺) for $\text{C}_{17}\text{H}_{22}\text{N}_2\text{F}_3$ [$\text{M}+\text{H}$]⁺: calculated: 311.1735, found: 311.1734.

(1S,4aR,8aS)-10-(4-bromophenyl)octahydro-2H-1,4a-epidiazanonaphthalene**(23d).** Following the *General Procedure A*, **23d** (40.60 mg, 0.13 mmol) was isolatedafter 20h at 50 °C by flash chromatography (petroleum ether/EtOAc 19:1) in 84% yield as a brown oil starting from **22a** (22.80 mg, 0.15 mmol), 4-bromophenylhydrazine¹² (33.7 mg, 0.18 mmol), (**S**)-**25h** (7.50 mg, 0.008 mmol) and

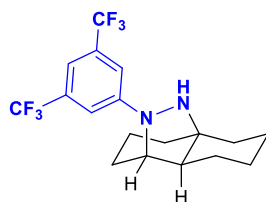
toluene (1.5 mL, 0.1 M). $^1\text{H-NMR}$ (δ , ppm) (300 MHz, CDCl_3): 7.28 (d, $J = 8.8$ Hz, 2H, 2 x CH_{arom}), 6.81 (d, $J = 8.3$ Hz, 2H, 2 x CH_{arom}), 4.06 (s, 1H, NH), 3.85 (d, $J =$

¹² The hydrazine was extracted from the corresponding hydrochloride following the procedure described: Dey, R.; Kumar, P.; Banerjee, P. *J. Org. Chem.* **2018**, *83*, 5438.

4.3 Hz, 1H, **H-1**), 2.12 (dt, $J = 8.7, 4.2$ Hz, 1H, **H-7_a**), 1.83-1.52 (m, 6H, **H-2_a**, **H-3_a**, **H-5_a**, **H-6_a**, **H-7_b** and **H-8_a**), 1.48-1.33 (m, 6H, **H-2_b**, **H-3_b**, **H-4_a**, **H-6_b**, **H-8_a** and **H-8_b**), 1.29-1.21 (m, 2H, **H-4_b** and **H-5_b**). $^{13}\text{C-NMR}$ (δ , ppm) (75.5 MHz, CDCl_3): 148.3 (**C_{arom}**), 131.3 (**CH_{arom}**), 114.9 (**CH_{arom}**), 108.0 (**C_{arom}**), 62.4 (**C-1**), 59.7 (**C-4_a**), 49.9 (**C-8_a**), 40.3 (**C-5**), 30.9 (**C-4**), 27.8 (**C-2**), 25.8 (**C-7**), 24.4 (**C-6**), 21.6 (**C-8**), 18.7 (**C-3**). The enantiomeric excess (e.e.) was determined by HPLC after derivatization of the corresponding product following the *General Procedure B*. $[\alpha]_{\text{D}}^{20}$: +19.7 ($c = 0.8, \text{CH}_2\text{Cl}_2$). IR (ATR) cm^{-1} : 2929, 1587, 1484, 1259, 763, 750. MS (EI, 70 eV) m/z (%): 337 (5), 336 (11), 335 (13), 334 (13), 331 (10), 322 (31), 321 (80), 320 (M^+ , 100), 319 (70), 318 (87), 317 (7), 311 (4), 304 (4), 184 (5), 183 (4), 170 (4), 164 (4), 151 (4), 147 (4), 144 (4), 136 (4), 135 (7), 134 (13). HRMS (ESI $^+$) for $\text{C}_{16}\text{H}_{20}\text{N}_2\text{Br}$ $[\text{M}+\text{H}]^+$: calculated: 319.0810, found: 319.0811.

(1*S*,4*aR*,8*aS*)-10-(3,5-bis(trifluoromethyl)phenyl)octahydro-2*H*-1,4*a*-

epidiazanonaphthalene (23e). Following the *General Procedure A*, **23e** (50.90

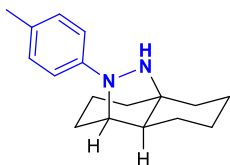


mg, 0.14 mmol) was isolated after 16h at 50 °C by flash chromatography (petroleum ether/EtOAc 19:1) in 90% yield as a yellow oil starting from **22a** (22.80 mg, 0.15 mmol), 3,5-bis(trifluoromethyl)phenylhydrazine (43.9 mg, 0.18 mmol), (**S**)-**25h** (7.50 mg, 0.008 mmol) and toluene

(1.5 mL, 0.1 M). $^1\text{H-NMR}$ (δ , ppm) (300 MHz, CDCl_3): 7.09 (s, 1H, **CH_{arom}**), 4.15 (s, 1H, **NH**), 3.94 (d, $J = 4.3$ Hz, 1H, **H-1**), 2.12-2.03 (m, 1H, **H-7_a**), 1.88-1.78 (m, 2H, **H-6_a** and **H-8_a**), 1.75-1.56 (m, 5H, **H-2_a**, **H-3_a**, **H-4_a**, **H-5_a** and **H-7_b**), 1.52-1.30 (m, 5H, **H-2_b**, **H-3_b**, **H-6_b**, **H-8_b** and **H-8_a**), 1.28-1.15 (m, 2H, **H-4_b** and **H-5_b**). $^{13}\text{C-NMR}$ (δ , ppm) (75.5 MHz, CDCl_3): 149.6 (**C_{arom}**), 125.6 (**C_{arom}**), 122.0 (**CF₃**), 112.3 (**CH_{arom}**), 109.0 (**CH_{arom}**), 62.6 (**C-1**), 59.9 (**C-4_a**), 49.7 (**C-8_a**), 39.9 (**C-5**), 30.7 (**C-4**), 27.4 (**C-2**), 25.7 (**C-7**), 24.3 (**C-6**), 21.5 (**C-8**), 18.5 (**C-3**). $^{19}\text{F-NMR}$ (δ , ppm) (282 MHz, CDCl_3): -62.97. The enantiomeric excess (e.e.) was determined by HPLC after derivatization of the corresponding product following the *General Procedure C*. $[\alpha]_{\text{D}}^{20}$: +9.9 ($c = 1.4, \text{CH}_2\text{Cl}_2$). IR (ATR) cm^{-1} : 2937, 1615, 1275, 763, 750. MS (EI, 70 eV) m/z (%): 393 (1), 392 (1), 390 (1), 380 (2), 379 (22), 378 (M^+ , 100), 377

(70), 376 (12), 375 (1), 373 (1), 135 (2), 134 (1). HRMS (ESI⁺) for C₁₈H₂₁N₂F₆ [M+H]⁺: calculated: 379.1609, found: 379.1608.

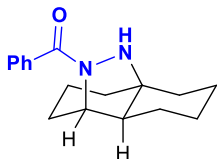
(1*S*,4*aR*,8*aS*)-10-(*p*-tolyl)octahydro-2*H*-1,4*a*-epidiazanonaphthalene (23f).



Following the *General Procedure A*, **23f** (38.50 mg, 0.15 mmol) was isolated after 20h at 50 °C by flash chromatography (petroleum ether/EtOAc 19:1) in 99% yield as a brown oil starting from **22a** (22.80 mg, 0.15 mmol), *p*-tolylhydrazine¹² (21.9 mg, 0.18 mmol), (**S**)-**25h** (7.50 mg, 0.008 mmol) and toluene (1.5 mL, 0.1 *M*). ¹H-NMR (δ, ppm) (300 MHz, CDCl₃): 7.01 (d, *J* = 8.2 Hz, 2H, 2 x CH_{arom}), 6.83 (d, *J* = 8.2 Hz, 2H, 2 x CH_{arom}), 4.03 (s, 1H, NH), 3.85 (d, *J* = 4.3 Hz, 1H, H-1), 2.25 (s, 3H, CH₃), 2.20-2.06 (m, 1H, H-7_a), 1.84-1.19 (m, 14H, H-2, H-3, H-4, H-5, H-6, H-7_b, H-8 and H-8a). ¹³C-NMR (δ, ppm) (75.5 MHz, CDCl₃): 147.2 (C_{arom}), 129.2 (CH_{arom}), 125.3 (C_{arom}), 113.2 (CH_{arom}), 62.2 (C-1), 59.5 (C-4a), 49.9 (C-8a), 40.5 (C-5), 31.1 (C-4), 28.1 (C-2), 24.5 (C-7), 21.7 (C-6), 20.4 (C-8), 18.9 (C-3). The enantiomeric excess (e.e.) was determined by HPLC after derivatization of the corresponding product following the *General Procedure C*. [α]_D²⁰: -14.4 (*c* = 0.7, CH₂Cl₂). IR (ATR) cm⁻¹: 2927, 1592, 1275, 1260, 763, 750. MS (EI, 70 eV) *m/z* (%): 257 (20), 256 (M⁺, 100), 255 (95), 254 (23), 213 (5), 212 (14). HRMS (ESI⁺) for C₁₇H₂₅N₂ [M+H]⁺: calculated: 257.2018, found: 257.2022.

((1*S*,4*aR*,8*aS*)-octahydro-2*H*-1,4*a*-epidiazanonaphthalen-10-

yl)(phenyl)methanone (23h). Following the *General Procedure A*, **23h** (34.40 mg,

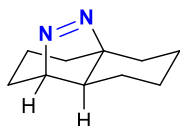


0.13 mmol) was isolated after 16h at 50 °C by flash chromatography (petroleum ether/EtOAc 2:8) in 85% yield as a colourless oil starting from **22a** (22.80 mg, 0.15 mmol), benzoylhydrazine (24.5 mg, 0.18 mmol), (**S**)-**25h** (7.50 mg, 0.008 mmol) and toluene (1.5 mL, 0.1 *M*). ¹H-NMR (δ, ppm) (300 MHz, CDCl₃): 7.46-7.40 (m, 2H, 2 x CH_{arom}), 7.34-7.30 (m, 3H, 3 x CH_{arom}), 5.30 (br s, 1H, NH), 3.70 (d, *J* = 4.5 Hz, 1H, H-1), 1.97-1.84 (m, 1H, H-7_a), 1.82-1.73 (m, 1H, H-6_a), 1.72-1.55 (m, 5H, H-2_a, H-3_a, H-5_a, H-7_b and H-8_a), 1.46-1.25 (m, 6H, H-2_b, H-3_b,

H-4a, **H-6b**, **H-8b** and **H-8a**), 1.20-1.02 (m, 1H, **H-5b**), 0.88-0.70 (m, 1H, **H-4b**). ^{13}C -NMR (δ , ppm) (75.5 MHz, CDCl_3): 166.9 (**C=O**), 135.9 (**C_{arom}**), 130.0 (**CH_{arom}**), 128.3 (**CH_{arom}**), 128.1 (**CH_{arom}**), 127.9 (**CH_{arom}**), 127.2 (**CH_{arom}**), 64.8 (**C-1**), 59.8 (**C-4a**), 49.3 (**C-8a**), 39.6 (**C-5**), 31.5 (**C-4**), 30.5 (**C-2**), 25.4 (**C-7**), 24.0 (**C-6**), 21.1 (**C-8**), 19.2 (**C-3**). The enantiomeric excess (e.e.) was determined by HPLC using a CHIRALPAK® AD-H column (hexane/*i*-PrOH 90:10, 1 mL/min, 250 nm, 25°C); t_r (major) = 18.75 min, t_r (minor) = 16.79 min (0% ee). IR (ATR) cm^{-1} : 3235, 2929, 1613, 1275, 1261, 764, 750. MS (EI, 70 eV) m/z (%): 271 (17), 270 (M^+ , 29), 269 (25), 166 (16), 165 (100), 163 (8), 137 (12), 136 (69), 135 (39), 134 (21), 133 (8), 104 (20). HRMS (ESI⁺) for $\text{C}_{17}\text{H}_{23}\text{N}_2\text{O}$ [$\text{M}+\text{H}$]⁺: calculated: 271.1810, found: 271.1818.

(1S,4aR,8aS)-1,3,4,5,6,7,8,8a-octahydro-2H-1,4a-epidiazenonaphthalene

(23j). Following the *General Procedure A*, **23j** (32.80 mg, 0.2 mmol) was isolated

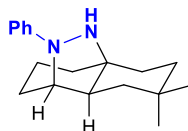


after 16 h at 50°C by flash chromatography (petroleum ether/EtOAc 1:1) in 99% yield as a colourless oil starting from **22a** (22.80 mg, 0.15 mmol), benzoylhydrazine (24.5 mg, 0.18 mmol),

(S)-25h (7.50 mg, 0.008 mmol) and toluene (1.5 mL, 0.1 M). ^1H -NMR (δ , ppm) (300 MHz, CDCl_3): 4.75 (d, $J = 4.3$ Hz, 1H, **H-1**), 2.74 (dt, $J = 14.4, 3.0$ Hz, 1H, **H-7_a**), 1.78 (dt, $J = 12.2, 5.3$ Hz, 1H, **H-6_a**), 1.73-1.66 (m, 1H, **H-8_a**), 1.63-1.46 (m, 4H, **H-2_a**, **H-3_a**, **H-4_a** and **H-5_a**), 1.41 (dt, $J = 13.6, 6.4$ Hz, 1H, **H-7_b**), 1.35-1.23 (m, 3H, **H-2_b**, **H-3_b** and **H-6_b**), 1.14 (ddt, $J = 17.9, 11.3, 5.3$ Hz, 1H, **H-8_a**), 1.10-1.01 (m, 1H, **H-8_b**), 0.91 (dtd, $J = 23.6, 12.7, 6.6$ Hz, 1H, **H-4_b**), 0.64-0.48 (m, 1H, **H-5_b**). ^{13}C -NMR (δ , ppm) (75.5 MHz, CDCl_3): 86.6 (**C-1**), 85.9 (**C-4a**), 47.6 (**C-8a**), 31.6 (**C-5**), 29.9 (**C-4**), 25.9 (**C-2**), 23.5 (**C-7**), 22.4 (**C-6**), 21.9 (**C-8**), 17.9 (**C-3**). The enantiomeric excess (e.e.) was determined by HPLC using a CHIRALPAK® OD-3 column (hexane/*i*-PrOH 98:02, 1 mL/min, 324 nm, 25°C); t_r (major) = 5.04 min, t_r (minor) = 6.16 min (0% ee). HRMS (ESI⁺) for $\text{C}_{10}\text{H}_{17}\text{N}_2$ [$\text{M}+\text{H}$]⁺: calculated: 165.1392, found: 165.1405.

(1S,4aS,8aS)-7,7-dimethyl-10-phenyloctahydro-2H-1,4a-

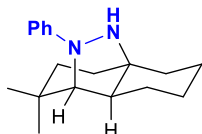
epidiazanonaphthalene (23k). Following the *General Procedure A*, **23k** (40.40



mg, 0.15 mmol) was isolated after 20h at 50 °C by flash chromatography (petroleum ether/EtOAc 19:1) in 99% yield as a yellow oil starting from **22b** (27.00 mg, 0.15 mmol), phenylhydrazine (18 μ L, 0.18 mmol), **(S)-25h** (7.50 mg, 0.008 mmol) and toluene (1.5 mL, 0.1 M). $^1\text{H-NMR}$ (δ , ppm) (300 MHz, CDCl_3): 7.20 (dd, $J = 8.7, 7.3$ Hz, 2H, 2 x CH_{arom}), 6.90 (d, $J = 8.0$ Hz, 2H, 2 x CH_{arom}), 6.66 (tt, $J = 7.2, 1.1$ Hz, 1H, CH_{arom}), 4.04 (s, 1H, NH), 3.86 (d, $J = 4.3$ Hz, 1H, H-1), 2.18 (ddd, $J = 9.3, 4.0, 2.1$ Hz, 1H, H-6a), 1.94 (dd, $J = 11.0, 6.6$ Hz, 1H, H-8a), 1.70-1.58 (m, 3H, H-2a, H-3a and H-5a), 1.39-1.23 (m, 8H, H-2b, H-3b, H-4, H-5b, H-6b, H-8b and H-8a), 0.95 (s, 3H, CH_3), 0.92 (s, 3H, CH_3). $^{13}\text{C-NMR}$ (δ , ppm) (75.5 MHz, CDCl_3): 149.0 (C_{arom}), 128.7 (CH_{arom}), 116.3 (CH_{arom}), 113.1 (CH_{arom}), 62.1 (C-1), 58.8 (C-4a), 46.6 (C-8a), 40.1 (C-5), 38.3 (C-4), 34.1 (C-2), 32.8 (CH_3), 30.1 (CH_3), 28.0 (C-7), 27.5 (C-6), 23.4 (C-8), 18.8 (C-3). The enantiomeric excess (e.e.) was determined by HPLC after derivatization of the corresponding product following the *General Procedure B*. $[\alpha]_{\text{D}}^{20}$: -20.9 ($c = 0.3, \text{CH}_2\text{Cl}_2$). IR (ATR) cm^{-1} : 2935, 1596, 1219, 770. MS (EI, 70 eV) m/z (%): 283 (4), 271 (16), 270 (M^+ , 53), 269 (100), 268 (65), 266 (6), 265 (6), 248 (5), 225 (5), 224 (4), 205 (4), 203 (4), 177 (7), 163 (4), 162 (10), 161 (5), 159 (5), 145 (5), 142 (4), 127 (6), 126 (4), 93 (5). HRMS (ESI $^+$) for $\text{C}_{18}\text{H}_{27}\text{N}_2$ [$\text{M}+\text{H}$] $^+$: calculated: 271.2174, found: 271.2179.

(1R,4aR,8aS)-2,2-dimethyl-10-phenyloctahydro-2H-1,4a-

epidiazanonaphthalene (23l). Following the *General Procedure A*, **23l** (38.10 mg,

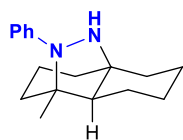


0.14 mmol) was isolated after 20h at 50 °C by flash chromatography (petroleum ether/EtOAc 19:1) in 94% yield as a colourless oil starting from **22g** (27.00 mg, 0.15 mmol), phenylhydrazine (18 μ L, 0.18 mmol), **(S)-25h** (7.50 mg, 0.008 mmol) and toluene (1.5 mL, 0.1 M). $^1\text{H-NMR}$ (δ , ppm) (300 MHz, CDCl_3): 7.19 (dd, $J = 8.8, 7.2$ Hz, 2H, 2 x CH_{arom}), 7.03 (d, $J = 8.1$ Hz, 2H, 2 x CH_{arom}), 6.69 (tt, $J = 7.2, 1.2$ Hz, 1H, CH_{arom}), 3.39 (br s, 1H, NH), 3.18 (s, 1H, H-1), 1.89 (dd, $J = 11.8, 5.2$ Hz, 1H, H-7a), 1.79-1.60 (m, 4H, H-5a, H-6a, H-7b and H-8a), 1.55-1.26 (m, 6H,

H-3, H-4_a, H-6_b, H-8_b, H-8_a, 1.21-1.09 (m, 1H, **H-5_b**), 1.07 (s, 3H, **CH₃**), 1.01 (s, 3H, **CH₃**), 0.94-0.80 (m, 1H, **H-4_b**). ¹³C-NMR (δ , ppm) (75.5 MHz, CDCl₃): 154.0 (**C_{arom}**), 128.6 (**CH_{arom}**), 116.8 (**CH_{arom}**), 112.5 (**CH_{arom}**), 76.3 (**C-1**), 59.9 (**C-4_a**), 44.4 (**C-8_a**), 38.0 (**C-5**), 36.3 (**C-4**), 33.4 (**C-2**), 32.4 (**C-7**), 29.7 (**CH₃**), 25.9 (**C-6**), 24.9 (**C-8**), 24.4 (**CH₃**), 21.7 (**C-3**). The enantiomeric excess (e.e.) was determined by HPLC after derivatization of the corresponding product following the *General Procedure B*. $[\alpha]_D^{20}$: -202.6 ($c = 0.4$, CH₂Cl₂). IR (ATR) cm⁻¹: 2923, 1593, 1219, 775. MS (EI, 70 eV) m/z (%): 297 (4), 285 (7), 284 (7), 283 (5), 282 (10), 281 (4), 280 (6), 271 (12), 270 (M⁺, 60), 269 (94), 268 (100), 267 (6), 266 (21), 263 (4), 261 (4), 199 (4), 198 (4), 197 (4), 177 (6), 171 (4), 164 (4), 163 (10), 162 (18), 161 (6), 159 (4), 158 (4), 157 (4), 149 (4), 108 (4), 104 (6). HRMS (ESI⁺) for C₁₈H₂₇N₂ [M+H]⁺: calculated: 271.2174, found: 271.2166.

(1S,4aR,8aR)-1-methyl-10-phenyloctahydro-2H-1,4a-epidiazanonaphthalene

(23m). Following the *General Procedure A*, **23m** (26.70 mg, 0.10 mmol) was

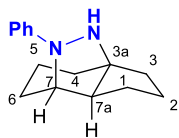


isolated after 20h at 60 °C by flash chromatography (petroleum ether/EtOAc 19:1) in 69% yield as a yellow oil starting from **22c** (25.00 mg, 0.15 mmol), phenylhydrazine (18 μ L, 0.18 mmol), **(S)-25h** (7.50 mg, 0.008 mmol) and toluene (1.5 mL, 0.1 M). ¹H-NMR

(δ , ppm) (300 MHz, CDCl₃): 7.18 (d, $J = 5.1$ Hz, 4H, 4 x **CH_{arom}**), 6.70 (dq, $J = 5.6$, 3.0 Hz, 1H, **CH_{arom}**), 2.21 (t, $J = 9.6$ Hz, 1H, **H-7_a**), 1.82-1.69 (m, 3H, **H-6_a**, **H-7_b** and **H-8_a**), 1.66 (dd, $J = 11.4$, 5.1 Hz, 2H, **H-2_a** and **H-3_a**), 1.56 (s, 3H, **CH₃**), 1.52-1.45 (m, 2H, **H-4_a** and **H-6_b**), 1.44-1.32 (m, 5H, **H-2_b**, **H-3_b**, **H-5_b**, **H-8_a** and **H-8_b**), 1.29-1.12 (m, 1H, **H-4_b**). ¹³C-NMR (δ , ppm) (75.5 MHz, CDCl₃): 149.8 (**C_{arom}**), 128.4 (**CH_{arom}**), 121.7 (**C_{arom}**), 117.0 (**CH_{arom}**), 114.8 (**CH_{arom}**), 67.0 (**C-1**), 57.8 (**C-4_a**), 56.4 (**C-8_a**), 40.4 (**C-5**), 35.1 (**C-4**), 31.1 (**C-2**), 24.7 (**C-7**), 23.6 (**CH₃**), 23.0 (**C-6**), 21.7 (**C-8**), 19.4 (**C-3**). The enantiomeric excess (e.e.) was determined by HPLC after derivatization of the corresponding product following the *General Procedure B*. $[\alpha]_D^{20}$: -8.1 ($c = 0.1$, CH₂Cl₂). IR (ATR) cm⁻¹: 2928, 1595, 1219, 767. MS (EI, 70 eV) m/z (%): 257 (7), 256 (M⁺, 33), 241 (11), 227 (5), 214 (17), 213 (100), 212 (5), 186 (6), 150 (5), 149 (38), 148 (4), 133 (5), 130 (4), 121 (4), 119 (5), 118 (6), 117 (5), 114 (4), 108 (8), 107 (18), 106 (6), 105 (14), 95 (5), 93 (20), 92 (8), 91 (27), 81 (23),

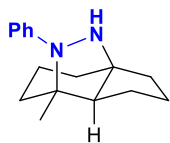
80 (4), 79 (22), 78 (9), 77 (66), 69 (4), 67 (12), 65 (10), 55 (9), 53 (8), 51 (17). HRMS (ESI⁺) for C₁₇H₂₅N₂ [M+H]⁺: calculated: 257.2018, found: 257.2025.

(3aR,7S,7aS)-8-phenyloctahydro-3a,7-epidiazanoindene (23n).



Following the *General Procedure A*, **23n** (26.10 mg, 0.11 mmol) was isolated after 72h at 50 °C by flash chromatography (petroleum ether/EtOAc 19:1) in 88% yield as a colourless oil starting from **22d** (18.00 mg, 0.13 mmol), phenylhydrazine (18 μL, 0.18 mmol), **(S)-25h** (7.500 mg, 0.008 mmol) and toluene (1.5 mL, 0.1 M). ¹H-NMR (δ, ppm) (300 MHz, CDCl₃): 7.20 (dd, *J* = 8.5, 7.2 Hz, 2H, 2 x CH_{arom}), 6.91 (d, *J* = 8.0 Hz, 2H, 2 x CH_{arom}), 6.74-6.63 (m, 1H, CH_{arom}), 4.22 (d, *J* = 4.3 Hz, 1H, CH_{arom}), 3.65 (br s, 1H, NH), 2.22-2.12 (m, 1H, H-1_a), 2.04-1.79 (m, 6H, H-1_b, H-2_a, H-3_a, H-4_a, H-6_a and H-7_a), 1.73-1.56 (m, 2H, H-2_b and H-3_b), 1.49-1.20 (m, 5H, H-4_b, H-5, H-6_b and H-7). ¹³C-NMR (δ, ppm) (75.5 MHz, CDCl₃): 149.2 (C_{arom}), 129.1 (CH_{arom}), 128.7 (CH_{arom}), 116.5 (CH_{arom}), 113.4 (CH_{arom}), 70.1 (C-3a), 60.3 (C-7), 55.6 (C-7a), 36.4 (C-3), 33.4 (C-4), 27.9 (C-6), 26.6 (C-2), 22.6 (C-1), 18.4 (C-5). The enantiomeric excess (e.e.) was determined by HPLC after derivatization of the corresponding product following the *General Procedure B*. [α]_D²⁰: +62.0 (*c* = 0.3, CH₂Cl₂). IR (ATR) cm⁻¹: 2936, 1595, 1219, 774. MS (EI, 70 eV) *m/z* (%): 243 (9), 242 (13), 240 (5), 229 (12), 228 (M⁺, 73), 227 (100), 226 (52), 225 (8), 223 (15), 222 (4), 213 (5), 211 (4), 150 (4), 143 (4), 142 (4), 133 (4), 121 (5), 120 (20), 119 (4), 118 (5), 93 (4). HRMS (ESI⁺) for C₁₅H₂₁N₂ [M+H]⁺: calculated: 229.1705, found: 229.1711.

(3aR,7S,7aR)-7-methyl-8-phenyloctahydro-3a,7-epidiazanoindene (23o).

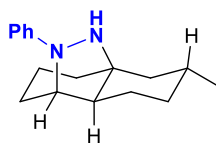


Following the *General Procedure A*, **23o** (33.60 mg, 0.14 mmol) was isolated after 24h at 60 °C by flash chromatography (petroleum ether/EtOAc 19:1) in 92% yield as a yellow oil starting from **22h** (23.00 mg, 0.15 mmol), phenylhydrazine (18 μL, 0.18 mmol), **(S)-25h** (7.50 mg, 0.008 mmol) and toluene (1.5 mL, 0.1 M). ¹H-NMR (δ, ppm) (300 MHz, CDCl₃): 7.22-7.11 (m, 4H, 4 x CH_{arom}), 6.71 (tt, *J* = 6.8, 1.6 Hz, 1H, CH_{arom}), 4.04 (br s, 1H, NH), 2.24 (ddd, *J* = 8.3, 3.9, 1.5 Hz, 1H, H-1_a), 1.94-1.74

(m, 8H, **H-1_b**, **H-2**, **H-3**, **H-4_a**, **H-6_a** and **H-7_a**), 1.64 (s, 3H, **CH₃**), 1.45-1.35 (m, 4H, **H-4_b**, **H-5** and **H-6_b**). ¹³C-NMR (δ , ppm) (75.5 MHz, CDCl₃): 129.1 (**C_{arom}**), 128.4 (**CH_{arom}**), 117.4 (**C_{arom}**), 114.9 (**CH_{arom}**), 77.2 (**C-7**), 66.9 (**C-3_a**), 63.3 (**C-7_a**), 35.8 (**C-3**), 34.3 (**C-4**), 33.4 (**C-6**), 25.2 (**C-2**), 23.8 (**CH₃**), 22.3 (**C-1**), 19.6 (**C-5**). The enantiomeric excess (e.e.) was determined by HPLC after derivatization of the corresponding product following the *General Procedure B*. $[\alpha]_D^{20}$: -14.4 ($c = 0.5$, CH₂Cl₂). IR (ATR) cm⁻¹: 2934, 1595, 1219, 767. MS (EI, 70 eV) m/z (%): 242 (M⁺, 8), 241 (61), 240 (6), 239 (36), 220 (8), 210 (8), 181 (7), 176 (5), 172 (8), 167 (5), 146 (7), 145 (7), 139 (5), 136 (5), 135 (100), 134 (40), 132 (10), 132 (8), 131 (6), 107 (5), 104 (6), 94 (6). HRMS (ESI⁺) for C₁₆H₂₃N₂ [M+H]⁺: calculated: 243.1861, found: 243.1865.

(1S,4aS,6R,8aS)-6-methyl-10-phenyloctahydro-2H-1,4a-

epidiazanonaphthalene (23p). Following the *General Procedure A*, **23p** (35.80



mg, 0.14 mmol) was isolated after 16h at 50 °C by flash chromatography (petroleum ether/EtOAc 19:1) in 93% yield as a crystalline white solid starting from **22i** (24.90 mg, 0.15 mmol), phenylhydrazine (18 μ L, 0.18 mmol), **(S)-25h** (7.50

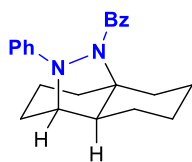
mg, 0.008 mmol) and toluene (1.5 mL, 0.1 M). ¹H-NMR (δ , ppm) (300 MHz, CDCl₃): 7.19 (dd, $J = 8.5, 7.1$ Hz, 2H, 2 x **CH_{arom}**), 6.90 (d, $J = 8.0$ Hz, 2H, 2 x **CH_{arom}**), 6.66 (td, $J = 7.2, 1.2$ Hz, 1H, **CH_{arom}**), 4.04 (br s, 1H, **NH**), 3.91 (d, $J = 4.4$ Hz, 1H, **H-1**), 2.23-2.09 (m, 1H, **H-7_a**), 1.92-1.52 (m, 7H, **H-2_a**, **H-3_a**, **H-4_a**, **H-5_a**, **H-6**, **H-7_b** and **H-8_a**), 1.46-1.25 (m, 5H, **H-2_b**, **H-3_b**, **H-4_b**, **H-8_a** and **H-8_b**), 1.06 (dd, $J = 14.3, 12.3$ Hz, 1H, **H-5_b**), 0.93 (d, $J = 6.3$ Hz, 3H, **CH₃**). ¹³C-NMR (δ , ppm) (75.5 MHz, CDCl₃): 149.2 (**C_{arom}**), 128.7 (**CH_{arom}**), 116.2 (**CH_{arom}**), 113.1 (**CH_{arom}**), 61.9 (**C-1**), 60.4 (**C-4_a**), 49.5 (**C-8_a**), 40.5 (**C-5**), 40.0 (**C-4**), 33.3 (**C-2**), 28.1 (**C-7**), 28.0 (**C-6**), 26.0 (**C-8**), 22.4 (**CH₃**), 18.7 (**C-3**). $[\alpha]_D^{20}$: +32.3 ($c = 0.8$, CH₂Cl₂). IR (ATR) cm⁻¹: 2924, 1596, 1494, 1275, 1260, 763, 749. MS (EI, 70 eV) m/z (%): 256 (M⁺, 6), 255 (5), 253 (8), 252 (7), 242 (4), 241 (38), 240 (100), 239 (52), 238 (4), 237 (5), 236 (8), 235 (5), 231 (6), 223 (4), 214 (6), 213 (10), 212 (9), 211 (9), 209 (4), 181 (4), 148 (4), 106 (4). HRMS (ESI⁺) for C₁₇H₂₅N₂ [M+H]⁺: calculated: 257.2018, found: 257.2014.

3.3. Derivatization procedures for the cycloaddition adducts

General Procedure B for the benzylation of **23a**, **23b**, **23d**, **23k**, **23l**, **23m**, **23n** and **23o**: To a cooled solution of **23a**, **23b**, **23d**, **23k**, **23l**, **23m**, **23n** or **23o** (1.1 equiv) in CH₂Cl₂ (2 mL/mmol) at 0 °C, triethylamine (1.5 equiv) was added dropwise followed by the addition of benzoyl chloride (1 equiv). The reaction mixture was left overnight stirring at room temperature. Upon reaction completion, the crude was diluted with CH₂Cl₂, washed with a solution of HCl 1 N, dried over Na₂SO₄, filtered and the solvent was evaporated under reduced pressure. Purification by column chromatography afforded the desired products.

General Procedure C for the acetylation of **23c**, **23e** and **23f**: To a cooled solution of **23c**, **23e** or **23f** (1 equiv) and DMAP (20 mol%) in DCM (0.1 M) at 0 °C, pyridine (10 equiv) was added dropwise followed by the addition of acetyl chloride (10 equiv). The reaction mixture was left 2h stirring at room temperature. Upon reaction completion, the crude was diluted with CH₂Cl₂, washed with a solution of HCl 1 N, dried over Na₂SO₄, filtered and the solvent was evaporated under reduced pressure. Purification by column chromatography afforded the desired products.

Phenyl((1*S*,4*aR*,8*aS*)-10-phenyloctahydro-2*H*-1,4*a*-epidiazanonaphthalen-9-yl)methanone (23a'**)**. Following the *General Procedure B*, **23a'** (42.00 mg, 0.12

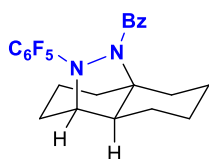


mmol) was isolated after 16h at room temperature by flash chromatography (petroleum ether/EtOAc 6:4) in 81% yield as a colourless oil starting from **23a** (36.10 mg, 0.15 mmol), triethylamine (25 μ L, 0.18 mmol), benzoyl chloride (14 μ L, 0.12 mmol) and CH₂Cl₂ (0.20 mL). ¹H-NMR (δ , ppm) (300 MHz, CDCl₃): 8.17-8.09 (m, 2H, 2 x CH_{arom}), 7.90 (dd, J = 7.9, 1.8 Hz, 1H, CH_{arom}), 7.69-7.57 (m, 1H, CH_{arom}), 7.52-7.44 (m, 2H, 2 x CH_{arom}), 7.18-7.04 (m, 2H, 2 x CH_{arom}), 6.92-6.77 (m, 2H, 2 x CH_{arom}), 6.62 (t, J = 7.1 Hz, 1H, CH_{arom}), 3.82 (d, J = 3.8 Hz, 1H, H-1), 3.37 (d, J = 11.0 Hz, 1H, H-7_a), 2.67 (dd, J = 13.6, 6.1 Hz, 1H, H-6_a), 2.36-2.19 (m, 1H, H-8_a), 2.08 (dt, J = 12.0, 6.2 Hz, 1H, H-2_a), 1.92-1.78 (m, 3H, H-4_a, H-5_a and H-7_b), 1.62 (m, 3H, H-3_a, H-6_b and H-8_b), 1.52-1.41 (m, 2H, H-2_b and H-8_a), 1.26 (m, 2H, H-3_b and H-5_b), 1.12 (m, 1H, H-4_b). ¹³C-NMR (δ , ppm) (75.5 MHz, CDCl₃): 172.0 (C=O),

151.5 (**C**_{arom}), 137.1 (**C**_{arom}), 133.7 (**CH**_{arom}), 130.2 (**CH**_{arom}), 129.7 (**CH**_{arom}), 129.4 (**CH**_{arom}), 128.4 (**CH**_{arom}), 128.3 (**CH**_{arom}), 127.1 (**CH**_{arom}), 119.9 (**CH**_{arom}), 68.9 (**C**-4a), 68.0 (**C**-1), 51.3 (**C**-8a), 34.7 (**C**-5), 32.6 (**C**-4), 25.6 (**C**-2), 24.8 (**C**-7), 22.3 (**C**-6), 21.6 (**C**-8), 19.6 (**C**-3). The enantiomeric excess (e.e.) was determined by HPLC using a CHIRALPAK® AD-3 column (hexane/*i*-PrOH 90:10, 1 mL/min, 210.5 nm, 25°C); *t*_r (major) = 11.11 min, *t*_r (minor) = 12.98 min (96% ee). [α]_D²⁰: -3.9 (*c* = 0.6, CH₂Cl₂). IR (ATR) cm⁻¹: 1687, 1219, 775. MS (EI, 70 eV) *m/z* (%): 348 (4), 347 (31), 346 (*M*⁺, 100), 241 (4). HRMS (ESI⁺) for C₂₃H₂₇N₂O [*M*+H]⁺: calculated: 347.2123, found: 347.2130.

((1*S*,4*aR*,8*aS*)-10-(perfluorophenyl)octahydro-2*H*-1,4*a*-

epidiazanonaphthalen-9-yl)(phenyl)methanone (23b'**)**. Following the *General*

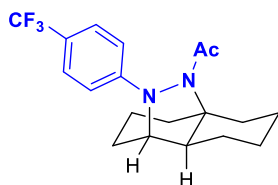


Procedure B, **23b'** (41.90 mg, 0.09 mmol) was isolated after 16h at room temperature by flash chromatography (petroleum ether/EtOAc 6:4) in 64% yield as a white foam starting from **23b** (48.00 mg, 0.14 mmol), triethylamine (23 μL, 0.17 mmol),

benzoyl chloride (13 μL, 0.11 mmol) and CH₂Cl₂ (0.20 mL). ¹H-NMR (δ, ppm) (300 MHz, toluene-*d*₈): 7.66 (d, *J* = 6.9 Hz, 1H, **CH**_{arom}), 7.38 (br s, 1H, **CH**_{arom}), 6.83-6.70 (m, 3H, 3 x **CH**_{arom}), 3.58-3.45 (m, 1H, **H**-1), 2.59 (dd, *J* = 13.6, 5.9 Hz, 1H, **H**-7a), 2.01-1.88 (m, 3H, **H**-6a, **H**-7b and **H**-8a), 1.61-1.39 (m, 3H, **H**-2a, **H**-3a and **H**-5a), 1.30 (dd, *J* = 11.4, 5.8 Hz, 2H, **H**-4a and **H**-6b), 1.17 (dt, *J* = 8.1, 4.2 Hz, 2H, **H**-8a and **H**-8b), 1.09-0.96 (m, 4H, **H**-2b, **H**-3b, **H**-4b and **H**-5b). ¹³C-NMR (δ, ppm) (75.5 MHz, toluene-*d*₈): 168.6 (**C**=O), 137.0 (**C**_{arom}), 129.3 (**C**_{arom}), 129.1 (**C**_{arom}), 127.7 (**CH**_{arom}), 127.6 (**CH**_{arom}), 127.0 (**CH**_{arom}), 126.9 (**CH**_{arom}), 68.7 (**C**-1), 68.0 (**C**-4a), 50.7 (**C**-8a), 39.2 (**C**-5), 34.5 (**C**-4), 32.0 (**C**-2), 30.8 (**C**-7), 30.2 (**C**-6), 25.6 (**C**-8), 24.5 (**C**-3). ¹⁹F-NMR (δ, ppm) (282 MHz, toluene-*d*₈): -149.72, -149.80, -150.31, -150.39, -150.48, -150.56, -153.76, -163.93, -164.00, -164.08, -164.52, -164.60, -164.68, -164.77, -164.84, -166.76, -166.84, -166.92, -167.74, -167.82, -167.90. The enantiomeric excess (e.e.) was determined by HPLC using a CHIRALPAK® IA column (hexane/*i*-PrOH 90:10, 1 mL/min, 250 nm, 25°C); *t*_r (major) = 7.87 min, *t*_r (minor) = 7.21 min (90% ee). [α]_D²⁰: +84.7 (*c* = 2.1, CH₂Cl₂). IR (ATR) cm⁻¹: 1638, 1515, 1497, 1048, 982, 764, 749. MS (EI, 70 eV) *m/z* (%): 438 (4), 437 (26), 436

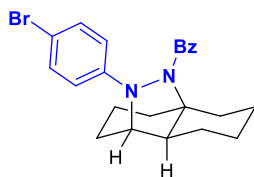
(M⁺, 100), 331 (2). HRMS (ESI⁺) for C₂₃H₂₂N₂O₂F₅ [M+H]⁺: calculated: 437.1652, found: 437.1656. M.p.: >200 °C (EtOAc/hexane).

1-((1S,4aR,8aS)-10-(4-(trifluoromethyl)phenyl)octahydro-2H-1,4a-epidiazanonaphthalen-9-yl)ethan-1-one (23c'). Following the *General Procedure*



C, **23c'** (27.40 mg, 0.08 mmol) was isolated after 2h at room temperature by flash chromatography (petroleum ether/EtOAc 1:1) in 80% yield as a colourless oil starting from **23c** (31.30 mg, 0.10 mmol), DMAP (2.40 mg, 0.02 mmol), pyridine (81 μL, 1 mmol), acetyl chloride (71 μL, 1 mmol) and CH₂Cl₂ (0.83 mL). ¹H-NMR (δ, ppm) (300 MHz, CDCl₃): 7.53-7.45 (m, 2H, 2 x CH_{arom}), 7.17 (dd, *J* = 9.0, 2.5 Hz, 1H, CH_{arom}), 6.83 (dd, *J* = 8.4, 2.5 Hz, 1H, CH_{arom}), 3.79 (d, *J* = 2.3 Hz, 1H, H-1), 3.07 (dd, *J* = 11.5, 4.4 Hz, 1H, H-7_a), 2.50 (dd, *J* = 13.1, 5.1 Hz, 1H, H-6_a), 2.05 (s, 3H, COCH₃), 1.86-1.21 (m, 11H, H-2, H-3, H-4_a, H-5_a, H-6_b, H-7_b, H-8 and H-8_a), 1.14-0.99 (m, 1H, H-5_b), 0.97-0.85 (m, 1H, H-4_b). ¹³C-NMR (δ, ppm) (75.5 MHz, CDCl₃): 176.7 (C=O), 155.3 (C_{arom}), 126.4 (C_{arom}), 122.4 (CF₃), 116.4 (CH_{arom}), 114.0 (CH_{arom}), 68.5 (C-1), 64.3 (C-4_a), 51.8 (C-8_a), 34.4 (C-5), 32.3 (C-4), 31.9 (COCH₃), 25.7 (C-2), 25.3 (C-7), 23.9 (C-6), 22.2 (C-8), 19.9 (C-3). ¹⁹F-NMR (δ, ppm) (282 MHz, CDCl₃): -61,48. The enantiomeric excess (e.e.) was determined by HPLC using a CHIRALPAK® IA column (hexane/*i*-PrOH 99:01, 1 mL/min, 250 nm, 30°C); t_r (major) = 13.58 min, t_r (minor) = 12.75 min (83% ee). [α]_D²⁰: +60.5 (*c* = 1.2, CH₂Cl₂). IR (ATR) cm⁻¹: 1666, 1611, 1321, 763, 750. MS (EI, 70 eV) *m/z* (%): 354 (3), 353 (23), 352 (M⁺, 100), 350 (1), 310 (1), 309 (3). HRMS (ESI⁺) for C₁₉H₂₄N₂O₂F₃ [M+H]⁺: calculated: 353.1841, found: 353.1845.

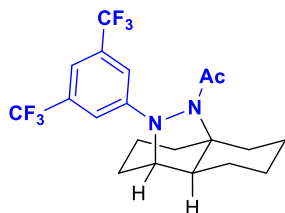
1-((1S,4aR,8aS)-10-(4-bromophenyl)octahydro-2H-1,4a-epidiazanonaphthalen-9-yl)(phenyl)methanone (23d'). Following the *General Procedure B*, **23d'** (27.60



mg, 0.07 mmol) was isolated after 16h at room temperature by flash chromatography (petroleum ether/EtOAc 7:3) in 54% yield as a colourless oil starting from **23d** (40.60 mg, 0.13 mmol), triethylamine (25 μL, 0.18 mmol), benzoyl

chloride (14 μL , 0.12 mmol) and CH_2Cl_2 (0.20 mL). $^1\text{H-NMR}$ (δ , ppm) (300 MHz, CDCl_3): 7.95-7.80 (m, 2H, 2 x CH_{arom}), 7.45 (dd, $J = 13.2, 7.1$ Hz, 2H, 2 x CH_{arom}), 7.31 (d, $J = 8.7$ Hz, 1H, CH_{arom}), 7.22-7.08 (m, 3H, 3 x CH_{arom}), 6.72-6.53 (m, 2H, 2 x CH_{arom}), 3.76 (d, $J = 2.7$ Hz, 1H, **H-1**), 3.33 (d, $J = 11.2$ Hz, 1H, **H-7_a**), 2.65 (dd, $J = 13.6, 6.0$ Hz, 1H, **H-6_a**), 2.24 (d, $J = 9.2$ Hz, 1H, **H-8_a**), 1.91-1.75 (m, 3H, **H-2_a**, **H-5_a** and **H-7_b**), 1.71-1.36 (m, 6H, **H-2_b**, **H-3_a**, **H-4_a**, **H-6_b**, **H-8_a** and **H-8_b**), 1.17-0.98 (m, 3H, **H-3_b**, **H-4_b** and **H-5_b**). $^{13}\text{C-NMR}$ (δ , ppm) (75.5 MHz, CDCl_3): 171.1 (**C=O**), 150.8 (**C_{arom}**), 136.9 (**C_{arom}**), 131.3 (**CH_{arom}**), 129.9 (**CH_{arom}**), 128.3 (**CH_{arom}**), 127.3 (**CH_{arom}**), 112.0 (**C_{arom}**), 68.9 (**C-4_a**), 68.2 (**C-1**), 51.3 (**C-8_a**), 39.6 (**C-5**), 34.5 (**C-4**), 32.5 (**C-2**), 25.7 (**C-7**), 24.7 (**C-6**), 22.3 (**C-8**), 19.5 (**C-3**). The enantiomeric excess (e.e.) was determined by HPLC using a CHIRALPAK® IA column (hexane/*i*-PrOH 90:10, 1 mL/min, 250 nm, 25°C); t_r (major) = 12.99 min, t_r (minor) = 19.15 min (96% ee). $[\alpha]_D^{20}$: -1.4 ($c = 2.0$, CH_2Cl_2). IR (ATR) cm^{-1} : 1637, 1260, 1275, 763, 750. MS (EI, 70 eV) m/z (%): 427 (26), 426 (94), 425 (26), 424 (M^+ , 100). HRMS (ESI⁺) for $\text{C}_{23}\text{H}_{26}\text{N}_2\text{OBr}$ [$\text{M}+\text{H}$]⁺: calculated: 425.1229, found: 425.1222.

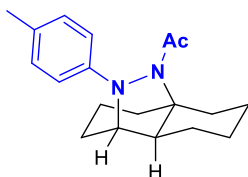
1-((1*S*,4*aR*,8*aS*)-10-(3,5-bis(trifluoromethyl)phenyl)octahydro-2*H*-1,4*a*-epidiazanonaphthalen-9-yl)ethan-1-one (23e'**)**. Following the *General Procedure*



C, **23e'** (27.70 mg, 0.07 mmol) was isolated after 3h at room temperature by flash chromatography (petroleum ether/EtOAc 1:1) in 88% yield as a pale yellow oil starting from **23e** (29.60 mg, 0.08 mmol), DMAP (1.90 mg, 0.02 mmol), pyridine (65 μL , 0.80 mmol), acetyl chloride (57 μL , 0.80 mmol) and CH_2Cl_2 (0.66 mL). $^1\text{H-NMR}$ (δ , ppm) (300 MHz, CDCl_3): 7.51 (s, 1H, CH_{arom}), 7.36 (s, 1H, CH_{arom}), 7.15 (s, 1H, CH_{arom}), 3.79 (d, $J = 3.2$ Hz, 1H, **H-1**), 3.07 (dd, $J = 12.2, 4.9$ Hz, 1H, **H-7_a**), 2.53 (dd, $J = 12.9, 5.0$ Hz, 1H, **H-6_a**), 2.04 (s, 3H, COCH_3), 1.91-1.53 (m, 6H, **H-2_a**, **H-3_a**, **H-4_a**, **H-5_a**, **H-7_b** and **H-8_a**), 1.50-1.24 (m, 5H, **H-2_b**, **H-3_b**, **H-6_b**, **H-8_b** and **H-8_a**), 1.17-1.00 (m, 1H, **H-5_b**), 0.88-0.70 (m, 1H, **H-4_b**). $^{13}\text{C-NMR}$ (δ , ppm) (75.5 MHz, CDCl_3): 176.5 (**C=O**), 154.0 (**C_{arom}**), 132.7 (**C_{arom}**), 132.3 (**C_{arom}**), 125.0 (**CF₃**), 121.4 (**CF₃**), 116.4 (**CH_{arom}**), 114.0 (**CH_{arom}**), 113.8 (**CH_{arom}**), 69.1 (**C-1**), 68.8 (**C-4_a**), 51.8 (**C-8_a**), 34.3 (**C-5**), 32.2 (**C-4**), 31.7 (COCH_3), 25.9 (**C-2**), 24.5 (**C-7**), 23.8 (**C-6**),

22.2 (**C-8**), 19.8 (**C-3**). $^{19}\text{F-NMR}$ (δ , ppm) (282 MHz, CDCl_3): -62.99, -63.18. The enantiomeric excess (e.e.) was determined by HPLC using a CHIRALPAK[®] IC column (hexane/*i*-PrOH 95:05, 1 mL/min, 250 nm, 25°C); t_r (major) = 6.73 min, t_r (minor) = 7.29 min (72% ee). $[\alpha]_{\text{D}}^{20}$: -23.4 ($c = 2.0$, CH_2Cl_2). IR (ATR) cm^{-1} : 1671, 1275, 1260, 763, 750. MS (EI, 70 eV) m/z (%): 422 (3), 421 (23), 420 (M^+ , 100), 418 (1), 378 (2), 377 (6), 376 (2). HRMS (ESI⁺) for $\text{C}_{20}\text{H}_{23}\text{N}_2\text{O}_6$ $[\text{M}+\text{H}]^+$: calculated: 421.1715, found: 421.1715.

1-((1S,4aR,8aS)-10-(*p*-tolyl)octahydro-2H-1,4a-epidiazanonaphthalen-9-yl)ethan-1-one (23f'**)**. Following the *General Procedure C*, **23f'** (36.80 mg, 0.12

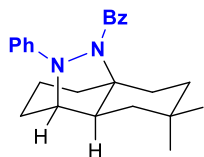


mmol) was isolated after 3h at room temperature by flash chromatography (petroleum ether/EtOAc 1:1) in 87% yield as a colourless oil starting from **23f** (38.50 mg, 0.15 mmol), DMAP (3.60 mg, 0.03 mmol), pyridine (122 μL , 1.5 mmol), acetyl chloride (107 μL , 1.5 mmol) and CH_2Cl_2 (1.25 mL).

$^1\text{H-NMR}$ (δ , ppm) (300 MHz, CDCl_3): 7.07-7.04 (m, 3H, 3 x CH_{arom}), 6.69-6.67 (m, 1H, CH_{arom}), 3.70 (d, $J = 4.0$ Hz, 1H, **H-1**), 3.12 (dd, $J = 13.5, 5.0$ Hz, 1H, **H-7a**), 2.49 (dd, $J = 13.1, 5.4$ Hz, 1H, **H-6a**), 2.27 (s, 3H, CH_3), 2.06 (s, 3H, COCH_3), 1.84-1.38 (m, 9H, **H-2a**, **H-3a**, **H-4a**, **H-5a**, **H-6b**, **H-7b**, **H-8** and **H-8a**), 1.38-1.01 (m, 4H, **H-2b**, **H-3b**, **H-4b** and **H-5b**). $^{13}\text{C-NMR}$ (δ , ppm) (75.5 MHz, CDCl_3): 176.8 (**C=O**), 150.3 (C_{arom}), 129.6 (CH_{arom}), 129.2 (C_{arom}), 116.8 (CH_{arom}), 114.5 (CH_{arom}), 68.3 (**C-1**), 68.2 (**C-4a**), 52.0 (**C-8a**), 34.7 (**C-5**), 32.5 (**C-4**), 32.4 (**C-2**), 25.6 (**C-7**), 24.8 (**C-6**), 24.1 (COCH_3), 22.2 (**C-8**), 20.4 (CH_3), 20.0 (**C-3**). The enantiomeric excess (e.e.) was determined by HPLC using a CHIRALPAK[®] IC column (hexane/*i*-PrOH 90:10, 1 mL/min, 254.8 nm, 25°C); t_r (major) = 14.02 min, t_r (minor) = 12.81 min (94% ee). $[\alpha]_{\text{D}}^{20}$: +47.4 ($c = 2.6$, CH_2Cl_2). IR (ATR) cm^{-1} : 1661, 1275, 1260, 763, 750. MS (EI, 70 eV) m/z (%): 312 (1), 300 (4), 299 (25), 298 (M^+ , 100), 297 (4), 296 (1), 256 (1), 255 (4), 254 (3), 240 (1), 134 (1). HRMS (ESI⁺) for $\text{C}_{19}\text{H}_{27}\text{N}_2\text{O}$ $[\text{M}+\text{H}]^+$: calculated: 299.2123, found: 299.2130.

((1*S*,4*aS*,8*aS*)-7,7-dimethyl-10-phenyloctahydro-2*H*-1,4a-

epidiazanonaphthalen-9-yl)(phenyl)methanone (23k'). Following the *General*

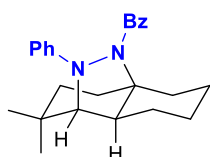


Procedure B, **23k'** (55.40 mg, 0.14 mmol) was isolated after 16h at room temperature by flash chromatography (petroleum ether/EtOAc 7:3) in 99% yield as a colourless oil starting from **23k** (40.40 mg, 0.15 mmol), triethylamine (29 μ L, 0.21 mmol), benzoyl chloride (16 μ L, 0.14 mmol) and CH_2Cl_2 (0.23 mL). ^1H -

NMR (δ , ppm) (300 MHz, CDCl_3): 7.88 (dd, $J = 7.8, 1.9$ Hz, 2H, 2 x CH_{arom}), 7.59-7.48 (m, 1H, CH_{arom}), 7.42 (d, $J = 7.4$ Hz, 1H, CH_{arom}), 7.23-7.17 (m, 1H, CH_{arom}), 7.14-7.05 (m, 3H, 3 x CH_{arom}), 6.82 (t, $J = 7.2$ Hz, 1H, CH_{arom}), 6.69-6.56 (m, 1H, CH_{arom}), 3.83-3.74 (m, 1H, **H-1**), 3.27 (dt, $J = 14.7, 3.4$ Hz, 1H, **H-6a**), 2.70 (dd, $J = 13.5, 6.1$ Hz, 1H, **H-8a**), 2.31-2.20 (m, 1H, **H-5a**), 1.99 (dd, $J = 12.4, 6.1$ Hz, 2H, **H-2a** and **H-3a**), 1.87-1.70 (m, 2H, **H-6b** and **H-8b**), 1.60-1.51 (m, 4H, **H-2b**, **H-3b**, **H-4a** and **H-8a**), 1.30 (ddd, $J = 16.1, 6.1, 2.8$ Hz, 2H, **H-4b** and **H-5b**), 0.86 (s, 3H, CH_3), 0.71 (s, 3H, CH_3). ^{13}C -NMR (δ , ppm) (75.5 MHz, CDCl_3): 162.3 (**C=O**), 137.2 (C_{arom}), 134.5 (C_{arom}), 130.5 (CH_{arom}), 129.6 (CH_{arom}), 128.8 (CH_{arom}), 128.3 (CH_{arom}), 127.1 (CH_{arom}), 120.0 (CH_{arom}), 68.2 (**C-1**), 68.1 (**C-4a**), 48.4 (**C-8a**), 39.4 (**C-5**), 37.7 (**C-4**), 34.9 (**C-2**), 32.8 (CH_3), 32.2 (**C-7**), 29.8 (CH_3), 28.2 (**C-6**), 23.5 (**C-8**), 19.7 (**C-3**). The enantiomeric excess (e.e.) was determined by HPLC using a CHIRALPAK[®] IA column (hexane/*i*-PrOH 95:05, 1 mL/min, 250 nm, 25°C); t_r (major) = 11.29 min, t_r (minor) = 13.65 min (98% ee). $[\alpha]_{\text{D}}^{20}$: -6.6 ($c = 2.1, \text{CH}_2\text{Cl}_2$). IR (ATR) cm^{-1} : 1698, 1219, 769. MS (EI, 70 eV) m/z (%): 376 (5), 375 (32), 374 (M^+ , 100), 269 (2). HRMS (ESI⁺) for $\text{C}_{25}\text{H}_{31}\text{N}_2\text{O}$ $[\text{M}+\text{H}]^+$: calculated: 375.2436, found: 375.2443.

((1*R*,4*aR*,8*aS*)-2,2-dimethyl-10-phenyloctahydro-2*H*-1,4a-

epidiazanonaphthalen-9-yl)(phenyl)methanone (231'**)**. Following the *General*



Procedure B, **231'** (51.30 mg, 0.14 mmol) was isolated after

16h at room temperature by flash chromatography (petroleum ether/EtOAc 7:3) in 98% yield as a colourless oil starting from

231 (38.10 mg, 0.14 mmol), triethylamine (28 μ L, 0.20 mmol),

benzoyl chloride (15 μ L, 0.13 mmol) and CH_2Cl_2 (0.22 mL). $^1\text{H-NMR}$ (δ , ppm) (300

MHz, CDCl_3): 8.19 (dd, $J = 8.4, 1.4$ Hz, 1H, CH_{arom}), 7.87 (dd, $J = 7.9, 1.8$ Hz, 2H,

2 x CH_{arom}), 7.60-7.51 (m, 1H, CH_{arom}), 7.42 (dt, $J = 5.5, 1.6$ Hz, 1H, CH_{arom}), 7.12

(qt, $J = 7.1, 1.2$ Hz, 2H, 2 x CH_{arom}), 6.99-6.82 (m, 2H, 2 x CH_{arom}), 6.70-6.59 (m,

1H, CH_{arom}), 3.45-3.38 (m, 1H, **H-1**), 3.26 (d, $J = 16.0$ Hz, 1H, **H-7_a**), 2.64-2.50 (m,

1H, **H-6_a**), 2.15 (t, $J = 8.7$ Hz, 1H, **H-8_a**), 1.94-1.76 (m, 1H, **H-5_a**), 1.74-1.45 (m, 8H,

H-3, **H-4**, **H-6_b**, **H-7_b**, **H-8_b** and **H-8_a**), 1.38 (s, 3H, CH_3), 1.28-1.17 (m, 1H, **H-5_b**)

1.11 (s, 3H, CH_3). $^{13}\text{C-NMR}$ (δ , ppm) (75.5 MHz, CDCl_3) (presence of rotatory

isomers): 171.1 (**C=O**), 152.1 (**C_{arom}**), 137.3 (**C_{arom}**), 134.5 (**CH_{arom}**), 130.5 (**CH_{arom}**),

129.5 (**CH_{arom}**), 128.0 (**CH_{arom}**), 127.1 (**CH_{arom}**), 120.0 (**CH_{arom}**), 78.7 (**C-1**), 68.6 (**C-**

4a), 46.2 (**C-8_a**), 36.0 (**C-5**), 33.1 (**C-4**), 32.3 (**C-2**), 32.1 (**C-7**), 29.7 (CH_3), 25.8 (**C-**

6), 25.5 (CH_3), 25.0 (**C-8**), 22.4 (**C-3**). The enantiomeric excess (e.e.) was

determined by HPLC using a CHIRALPAK[®] IA column (hexane/*i*-PrOH 90:10, 1

mL/min, 250 nm, 25°C); t_r (major) = 8.90 min, t_r (minor) = 7.52 min (98% ee). $[\alpha]_{\text{D}}^{20}$:

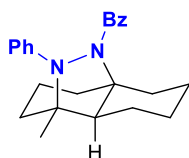
+11.6 ($c = 1.00, \text{CH}_2\text{Cl}_2$). IR (ATR) cm^{-1} : 1683, 1219, 771. MS (EI, 70 eV) m/z (%):

376 (4), 375 (30), 374 (M^+ , 100), 372 (1), 269 (3). HRMS (ESI⁺) for $\text{C}_{25}\text{H}_{31}\text{N}_2\text{O}$

$[\text{M}+\text{H}]^+$: calculated: 375.2436, found: 375.2444.

((1*S*,4*aR*,8*aS*)-1-methyl-10-phenyloctahydro-2*H*-1,4a-epidiazanonaphthalen-

9-yl)(phenyl)methanone (23m'**)**. Following the *General Procedure B*, **23m'** (24.70



mg, 0.07 mmol) was isolated after 16h at room temperature by

flash chromatography (petroleum ether/EtOAc 6:4) in 69% yield

as a colourless oil starting from **23m** (26.70 mg, 0.10 mmol),

triethylamine (19 μ L, 0.14 mmol), benzoyl chloride (11 μ L, 0.09

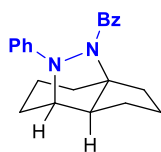
mmol) and CH_2Cl_2 (0.15 mL). $^1\text{H-NMR}$ (δ , ppm) (300 MHz, CDCl_3): 7.66 (dd, $J =$

7.6, 2.1 Hz, 2H, 2 x CH_{arom}), 7.48-7.33 (m, 1H, CH_{arom}), 7.22-7.13 (m, 2H, 2 x

CH_{arom}), 7.03 (d, $J = 6.4$ Hz, 2H, 2 x CH_{arom}), 6.98-6.84 (m, 2H, 2 x CH_{arom}), 6.66 (t, $J = 7.3$ Hz, 1H, CH_{arom}), 3.50 (dd, $J = 13.8, 2.5$ Hz, 1H, **H-7_a**), 2.63 (dd, $J = 13.8, 6.2$ Hz, 1H, **H-6_a**), 2.20-1.90 (m, 3H, **H-5_a**, **H-7_b** and **H-8_a**), 1.85-1.66 (m, 7H, **H-2**, **H-3_a**, **H-4_a**, **H-6_b**, **H-8_a** and **H-8_b**), 1.32-1.17 (m, 3H, **H-3_b**, **H-4_b** and **H-5_b**), 1.15 (s, 3H, CH_3). $^{13}\text{C-NMR}$ (δ , ppm) (75.5 MHz, CDCl_3) (presence of rotatory isomers): 168.9 ($\text{C}=\text{O}$), 148.6 (C_{arom}), 137.6 (C_{arom}), 130.4 (CH_{arom}), 128.9 (CH_{arom}), 128.1 (CH_{arom}), 126.9 (CH_{arom}), 121.6 (CH_{arom}), 119.5 (CH_{arom}), 66.2 (**C-1**), 64.6 (**C-4_a**), 55.0 (**C-8_a**), 40.0 (**C-5**), 35.4 (**C-4**), 32.9 (**C-2**), 24.9 (**C-7**), 23.1 (CH_3), 22.3 (**C-6**), 21.4 (**C-8**), 19.6 (**C-3**). The enantiomeric excess (e.e.) was determined by HPLC using a CHIRALPAK® IA column (hexane/*i*-PrOH 90:10, 1 mL/min, 250 nm, 25°C); t_r (major) = 13.18 min, t_r (minor) = 10.42 min (80% ee). $[\alpha]_{\text{D}}^{20}$: -9.1 ($c = 0.5$, CH_2Cl_2). IR (ATR) cm^{-1} : 1686, 1219, 771. MS (EI, 70 eV) m/z (%): 362 (5), 361 (29), 360 (M^+ , 100), 358 (1), 255 (3), 254 (1), 148 (1). HRMS (ESI⁺) for $\text{C}_{24}\text{H}_{29}\text{N}_2\text{O}$ [$\text{M}+\text{H}$]⁺: calculated: 361.2280, found: 361.2287.

Phenyl((3*a*R,7*S*,7*a*S)-8-phenyloctahydro-3*a*,7-epidiazainden-9-yl)methanone (**23n'**).

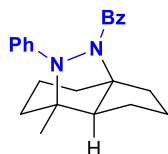
Following the *General Procedure B*, **23n'** (16.60 mg, 0.05 mmol) was isolated after 16h at room temperature by flash chromatography (petroleum ether/EtOAc 7:3) in 70% yield as a colourless oil starting from **23n** (17.80 mg, 0.07 mmol), triethylamine (13 μL , 0.09 mmol), benzoyl chloride (7 μL , 0.06 mmol) and CH_2Cl_2 (0.10 mL). $^1\text{H-NMR}$ (δ , ppm) (300 MHz, CDCl_3): 7.94 (dd, $J = 7.8, 1.9$ Hz, 2H, 2 x CH_{arom}), 7.16-7.06 (m, 3H, 3 x CH_{arom}), 6.99 (td, $J = 7.1, 2.4$ Hz, 2H, 2 x CH_{arom}), 6.76 (d, $J = 8.1$ Hz, 2H, 2 x CH_{arom}), 6.66 (dd, $J = 7.9, 6.7$ Hz, 1H, CH_{arom}), 4.18 (dd, $J = 3.9, 1.9$ Hz, 1H, **H-1_a**), 3.16-3.01 (m, 1H, **H-3_a**), 2.95 (dd, $J = 13.3, 6.1$ Hz, 1H, **H-2_a**), 2.27 (dt, $J = 13.0, 5.1$ Hz, 1H, **H-4_a**), 2.13-2.01 (m, 1H, **H-6_a**), 2.01-1.46 (m, 9H, **H-1_b**, **H-2_b**, **H-3_b**, **H-4_b**, **H-5**, **H-6_b**, **H-7** and **H-7_a**). $^{13}\text{C-NMR}$ (δ , ppm) (75.5 MHz, CDCl_3): 168.8 ($\text{C}=\text{O}$), 150.9 (C_{arom}), 136.5 (C_{arom}), 129.8 (CH_{arom}), 128.3 (CH_{arom}), 127.2 (CH_{arom}), 120.4 (CH_{arom}), 115.0 (CH_{arom}), 66.7 (**C-7**), 56.7 (**C-7_a**), 36.2 (**C-3_a**), 34.8 (**C-3**), 32.3 (**C-4**), 31.7 (**C-6**), 26.3 (**C-2**), 22.8 (**C-1**), 19.7 (**C-5**). The enantiomeric excess (e.e.) was determined by HPLC using a CHIRALPAK® AD-H column (hexane/*i*-PrOH 90:10, 1 mL/min, 250 nm, 25°C); t_r



(major) = 11.16 min (>99% ee). $[\alpha]_D^{20}$: +22.9 ($c = 1.3$, CH_2Cl_2). IR (ATR) cm^{-1} : 1624, 1218, 771. MS (EI, 70 eV) m/z (%): 334 (4), 333 (25), 332 (M^+ , 100), 227 (2), 105 (1). HRMS (ESI⁺) for $\text{C}_{22}\text{H}_{25}\text{N}_2\text{O}$ $[\text{M}+\text{H}]^+$: calculated: 333.1967, found: 333.1977.

((3aR,7S,7aS)-7-methyl-8-phenyloctahydro-3a,7-epidiazanoinden-9-

yl)(phenyl)methanone (23o'). Following the *General Procedure B*, **23o'** (27.80



mg, 0.08 mmol) was isolated after 16h at room temperature by

flash chromatography (petroleum ether/EtOAc 7:3) in 57% yield as a colourless oil starting from **23o** (33.60 mg, 0.14 mmol),

triethylamine (28 μL , 0.20 mmol), benzoyl chloride (15 μL , 0.13

mmol) and CH_2Cl_2 (0.22 mL). $^1\text{H-NMR}$ (δ , ppm) (300 MHz, CDCl_3):

7.73-7.67 (m, 2H, 2 x CH_{arom}), 7.65-7.54 (m, 1H, CH_{arom}), 7.50-7.38 (m, 1H, CH_{arom}),

7.23-7.12 (m, 1H, CH_{arom}), 7.09-7.00 (m, 2H, 2 x CH_{arom}), 6.98-6.89 (m, 2H, 2 x

CH_{arom}), 6.78-6.62 (m, 1H, CH_{arom}), 3.31-3.10 (m, 1H, H-1_a), 2.91 (dd, $J = 13.3$, 6.1

Hz, 1H, H-3_a), 2.13-1.93 (m, 5H, H-2_a , H-4_a , H-6_a , H-1_b and H-7_a), 1.94-1.67 (m,

5H, H-2_b , H-3_b , H-4_b , H-5_a and H-6_b), 1.47-1.38 (m, 1H, H-5_b), 1.20 (s, 3H, CH_3).

$^{13}\text{C-NMR}$ (δ , ppm) (75.5 MHz, CDCl_3): 167.9 ($\text{C}=\text{O}$), 148.4 (C_{arom}), 136.9 (C_{arom}),

130.6 (CH_{arom}), 129.1 (CH_{arom}), 128.1 (CH_{arom}), 126.9 (CH_{arom}), 122.1 (CH_{arom}),

118.9 (CH_{arom}), 76.7 (C-7), 66.7 (C-3_a), 62.0 (C-7_a), 41.0 (C-3), 34.9 (C-4), 32.1

(C-6), 25.0 (C-2), 23.1 (CH_3), 22.1 (C-1), 20.4 (C-5). The enantiomeric excess (e.e.)

was determined by HPLC using a CHIRALPAK[®] AD-H column (hexane/*i*-PrOH

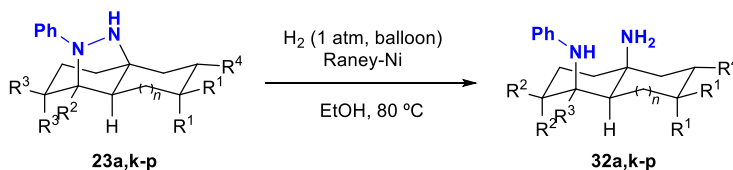
90:10, 1 mL/min, 250 nm, 25°C); t_r (major) = 12.34 min, t_r (minor) = 9.86 min (74%

ee). $[\alpha]_D^{20}$: +4.3 ($c = 1.0$, CH_2Cl_2). IR (ATR) cm^{-1} : 1683, 1219, 766. MS (EI, 70 eV)

m/z (%): 348 (4), 347 (30), 346 (M^+ , 100), 344 (1), 241 (2), 135 (2), 134 (1), 105

(1). HRMS (ESI⁺) for $\text{C}_{23}\text{H}_{27}\text{N}_2\text{O}$ $[\text{M}+\text{H}]^+$: calculated: 347.2123, found: 347.2129.

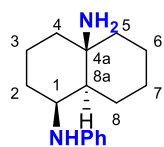
3.4. Reductive cleavage for the synthesis of enantioenriched 1,3-diamines



Scheme 6.8. General procedure for the synthesis of enantioenriched 1,3-diamines.

General Procedure D for the synthesis of enantioenriched 1,3-diamines **32a,k-p**: To a two-neck round-bottom flask equipped with a magnetic stir bar, **23a,k-p** (15.0 mg, 0.062 mmol), Raney Ni (~200 mg, washed three times with EtOH before addition) and EtOH (4 mL). The system was filled with H₂ (balloon, 1 atm), purged (vacuum/H₂ cycles) and it was refluxed at 80 °C for 40 minutes. After reaction completion, the mixture was filtered through a short pad of Celite® and extensively washed with EtOH. Purification by column chromatography afforded the desired products.¹³

(1*S*,4*aR*,8*aS*)-*N*¹-phenyloctahydronaphthalene-1,4*a*(2*H*)-diamine (**32a**).

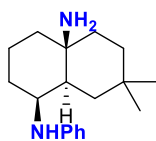


Following the *General Procedure D*, **32a** (14.90 mg, 0.06 mmol) was isolated after 40 min at 80 °C by flash chromatography (petroleum ether/EtOAc 1:1) in 98% yield as a colourless oil starting from **23a** (15.00 mg, 0.06 mmol). ¹H-NMR (δ, ppm) (300 MHz, CDCl₃): 7.11 (dd, *J* = 8.4, 7.2 Hz, 2H, 2 x CH_{arom}), 6.58-6.51 (m, 3H, 3 x CH_{arom}), 3.54 (q, *J* = 3.2 Hz, 1H, **H-1**), 2.03 (dtd, *J* = 13.5, 4.9, 4.4, 1.8 Hz, 1H, **H-5_a**), 1.98-1.83 (m, 1H, **H-4_a**), 1.76 (ddd, *J* = 14.4, 4.3, 2.2 Hz, 1H, **H-2_a**), 1.65-1.46 (m, 2H, **H-7_a** and **H-8_a**), 1.45-1.18 (m, 10H, **H-2_b**, **H-3**, **H-4_b**, **H-5_b**, **H-6**, **H-7_b**, **H-8_b** and **H-8_a**). ¹³C-NMR (δ, ppm) (75.5 MHz, CDCl₃): 148.6 (C_{arom}), 129.1 (CH_{arom}), 115.1 (CH_{arom}), 112.4 (CH_{arom}), 52.3 (C-1), 51.6 (C-8_a), 46.0 (C-4_a), 43.8 (C-5), 41.6 (C-4), 29.8 (C-2), 26.4 (C-7), 26.3 (C-6), 21.5 (C-8), 16.8 (C-3). The enantiomeric excess (e.e.) was determined by HPLC using a CHIRALPAK® OD-3 column

¹³ Wu, x.; Liu, B.; Zhang, Y.; Jeret, M.; Wang, H.; Zheng, P.; Yang, S.; Song, B.-A.; Chi, Y. R. *Angew. Chem. Int. Ed.* **2016**, *55*, 12280.

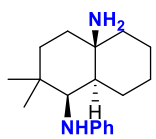
(hexane/*i*-PrOH 90:10, 1 mL/min, 250 nm, 25°C); t_r (major) = 4.35 min, t_r (minor) = 5.17 min (92% ee). $[\alpha]_D^{20}$: -59.5 ($c=2.5$, CH_2Cl_2). IR (ATR) cm^{-1} : 3005, 2989, 2926, 1600, 1508, 1275, 1260, 763, 750. MS (EI, 70 eV) m/z (%): 259 (4), 246 (15), 245 (68), 244 (M^+ , 100), 243 (7), 241 (7), 228 (6), 227 (9), 226 (20), 225 (9), 224 (4), 134 (5). HRMS (ESI⁺) for $\text{C}_{16}\text{H}_{25}\text{N}_2$ [$\text{M}+\text{H}$]⁺: calculated: 245.2018, found: 245.2024.

(1S,4aS,8aS)-7,7-dimethyl-*N*¹-phenyloctahydronaphthalene-1,4a(2H)-diamine (32k). Following the *General Procedure D*, **32k** (22.60 mg, 0.08 mmol) was isolated



after 40 min at 80 °C by flash chromatography (petroleum ether/EtOAc 1:1) in 92% yield as a colourless oil starting from **23k** (24.30 mg, 0.09 mmol). ¹H-NMR (δ , ppm) (300 MHz, CDCl_3): 7.06 (t, $J = 7.7$ Hz, 2H, 2 x CH_{arom}), 6.58-6.41 (m, 3H, 3 x CH_{arom}), 3.05-2.93 (br s, 1H, **H-1**), 1.96 (t, $J = 13.8$ Hz, 1H, **H-5_a**), 1.78-1.16 (m, 12H, **H-2**, **H-3**, **H-4**, **H-5_b**, **H-6**, **H-8** and **H-8_a**), 1.07 (s, 3H, CH_3), 0.93 (s, 3H, CH_3). ¹³C-NMR (δ , ppm) (75.5 MHz, CDCl_3): 150.7 (C_{arom}), 129.0 (CH_{arom}), 114.3 (CH_{arom}), 111.6 (CH_{arom}), 62.2 (**C-1**), 43.6 (**C-4_a**), 42.1 (**C-8_a**), 37.3 (**C-5**), 36.2 (**C-4**), 30.3 (**C-2**), 29.7 (CH_3), 28.9 (CH_3), 26.3 (**C-6**), 26.1 (**C-7**), 25.8 (**C-8**), 21.5 (**C-3**). $[\alpha]_D^{20}$: +228.2 ($c=1.5$, CH_2Cl_2). IR (ATR) cm^{-1} : 3303, 2924, 2848, 1599, 1508, 1275, 1260, 763, 749. MS (EI, 70 eV) m/z (%): 274 (6), 273 (42), 272 (M^+ , 100), 118 (6), 93 (4), 92 (3), 82 (5), 77 (5), 71 (3), 69 (4), 65 (3), 57 (3), 56 (4), 55 (5). HRMS (ESI⁺) for $\text{C}_{18}\text{H}_{29}\text{N}_2$ [$\text{M}+\text{H}$]⁺: calculated: 273.2331, found: 273.2337.

(1R,4aR,8aS)-2,2-dimethyl-*N*¹-phenyloctahydronaphthalene-1,4a(2H)-diamine (32l). Following the *General Procedure D*, **32l** (24.70 mg, 0.09 mmol) was

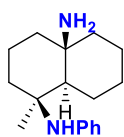


isolated after 40 min at 80 °C by flash chromatography (petroleum ether/EtOAc 1:1) in 91% yield as a colourless oil starting from **23l** (27.00 mg, 0.1 mmol). ¹H-NMR (δ , ppm) (300 MHz, CDCl_3): 7.18-7.08 (m, 2H, 2 x CH_{arom}), 6.65-6.43 (m, 1H, CH_{arom}), 3.49 (d, $J = 2.9$ Hz, 1H, **H-1**), 2.04 (ddd, $J = 14.6, 3.9, 1.7$ Hz, 1H, **H-5_a**), 1.93 (dt, $J = 14.1, 3.6$ Hz, 1H, **H-4_a**), 1.59 (dd, $J = 5.2, 2.3$ Hz, 2H, **H-7_a** and **H-8_a**), 1.54-1.44 (m, 2H, **H-3_a** and **H-6_a**), 1.41-1.31 (m, 3H, **H-4_b**, **H-5_b** and **H-6_b**), 1.30-1.22 (m, 2H, **H-3_b** and **H-7_b**), 1.14-1.06 (m, 1H, **H8_b**), 1.05-1.01 (m, 1H, **H-8_a**), 0.95 (d, $J = 2.3$ Hz, 6H, 2 x CH_3).

^{13}C -NMR (δ , ppm) (75.5 MHz, CDCl_3): 148.6 (C_{arom}), 129.1 (CH_{arom}), 115.2 (CH_{arom}), 112.5 (CH_{arom}), 52.4 (**C-1**), 51.4 (**C-4a**), 41.3 (**C-8a**), 40.9 (**C-5**), 39.9 (**C-2**), 39.3 (**C-4**), 34.3 (**C-7**), 33.3 (**C-3**), 30.9 (CH_3), 29.7 (CH_3), 24.8 (**C-6**), 16.9 (**C-8**). $[\alpha]_{\text{D}}^{20}$: +138.1 ($c=1.1$, CH_2Cl_2). IR (ATR) cm^{-1} : 3325, 2924, 2855, 1600, 1518, 1275, 1260, 763, 749. MS (EI, 70 eV) m/z (%): 273 (29), 272 (M^+ , 100). HRMS (ESI $^+$) for $\text{C}_{18}\text{H}_{29}\text{N}_2$ [$\text{M}+\text{H}$] $^+$: calculated: 273.2331, found: 273.2336.

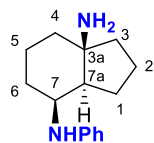
(1*S*,4*aR*,8*aR*)-1-methyl-*N*¹-phenyloctahydronaphthalene-1,4*a*(2*H*)-diamine

(32m). Following the *General Procedure D*, **32m** (22.80 mg, 0.09 mmol) was



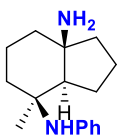
isolated after 40 min at 80 °C by flash chromatography (EtOAc/MeOH 3%) in 88% yield as a colourless oil starting from **23m** (25.60 mg, 0.10 mmol). ^1H -NMR (δ , ppm) (300 MHz, CDCl_3): 7.11 (dd, $J=8.5, 7.2$ Hz, 2H, 2 x CH_{arom}), 6.78 (dd, $J=8.5, 1.2$ Hz, 2H, 2 x CH_{arom}), 6.71 (t, $J=$

7.4 Hz, 1H, CH_{arom}), 2.30-2.20 (m, 1H, **H-5_a**), 1.90-1.75 (m, 3H, **H-2_a**, **H-4_a** and **H-7_a**), 1.61-1.54 (m, 3H, **H-2_b**, **H-3_a** and **H-8_a**), 1.42-1.36 (m, 2H, **H-3_b** and **H-4_b**), 1.33 (s, 3H, CH_3), 1.28-1.22 (m, 2H, **H-5_b** and **H-6_a**), 1.10 (td, $J=13.0, 12.4, 3.1$ Hz, 4H, **H-6_b**, **H-7_b**, **H-8_b** and **H-8_a**). ^{13}C -NMR (δ , ppm) (75.5 MHz, CDCl_3): 147.5 (C_{arom}), 128.7 (CH_{arom}), 118.4 (CH_{arom}), 115.7 (CH_{arom}), 56.2 (**C-8a**), 53.4 (**C-1**), 43.1 (**C-4a**), 41.6 (**C-5**), 35.7 (**C-4**), 29.7 (**C-2**), 28.7 (**C-7**), 26.8 (CH_3), 21.3 (**C-6**), 20.9 (**C-8**), 17.7 (**C-3**). $[\alpha]_{\text{D}}^{20}$: +326.7 ($c=0.5$, CH_2Cl_2). IR (ATR) cm^{-1} : 3270, 2929, 2857, 1597, 1496, 1275, 1260, 763, 750. MS (EI, 70 eV) m/z (%): 260 (14), 259 (75), 258 (M^+ , 100), 256 (4), 255 (5), 149 (5), 148 (4). HRMS (ESI $^+$) for $\text{C}_{17}\text{H}_{27}\text{N}_2$ [$\text{M}+\text{H}$] $^+$: calculated: 259.2174, found: 259.2176.

(3aR,7S,7aS)-N⁷-phenyloctahydro-3aH-indene-3a,7-diamine (32n).

Following the *General Procedure D*, **32n** (21.30 mg, 0.09 mmol) was isolated after 40 min at 80 °C by flash chromatography (EtOAc/MeOH 3%) in 93% yield as a colourless oil starting from **23n** (22.80 mg, 0.10 mmol). ¹H-NMR (δ, ppm) (300 MHz, CDCl₃): 7.11 (dd, *J* = 8.5, 7.1

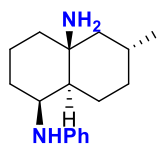
Hz, 2H, 2 x CH_{arom}), 6.61 (d, *J* = 8.1 Hz, 3H, 3 x CH_{arom}), 3.84 (d, *J* = 3.1 Hz, 1H, H-7), 2.10-1.60 (m, 7H, H-1, H-2, H-3a, H-4a and H-6a), 1.52-1.30 (m, 6H, H-3b, H-4b, H-5, H-6b and H-7a). ¹³C-NMR (δ, ppm) (75.5 MHz, CDCl₃): 148.7 (C_{arom}), 129.0 (CH_{arom}), 116.1 (CH_{arom}), 113.2 (CH_{arom}), 60.0 (C-3a), 50.0 (C-7a), 48.2 (C-7), 37.8 (C-3), 30.2 (C-4), 29.7 (C-6), 24.1 (C-2), 19.0 (C-1), 17.2 (C-5). [α]_D²⁰: +463.7 (*c* = 0.4, CH₂Cl₂). IR (ATR) cm⁻¹: 3306, 2929, 2875, 1600, 1508, 1275, 1260, 763, 750. MS (EI, 70 eV) *m/z* (%): 232 (5), 231 (38), 230 (M⁺, 100), 229 (3), 227 (4), 214 (4), 213 (6), 212 (6). HRMS (ESI⁺) for C₁₅H₂₃N₂ [M+H]⁺: calculated: 231.1861, found: 231.1858.

(3aR,7S,7aR)-7-methyl-N⁷-phenyloctahydro-3aH-indene-3a,7-diamine (32o).

Following the *General Procedure D*, **32o** (12.90 mg, 0.05 mmol) was isolated after 40 min at 80 °C by flash chromatography (petroleum ether/EtOAc 1:1) in 97% yield as a colourless oil starting from **23o** (13.10 mg, 0.05 mmol). ¹H-NMR (δ, ppm) (300 MHz, CDCl₃): 7.12 (dd,

J = 8.6, 7.2 Hz, 2H, 2 x CH_{arom}), 6.77 (d, *J* = 7.4 Hz, 2H, 2 x CH_{arom}), 6.68 (tt, *J* = 7.3, 1.1 Hz, 1H, CH_{arom}), 2.79 (br s, 2H, NH₂), 2.35 (d, *J* = 13.1 Hz, 1H, H-1a), 1.90-1.66 (m, 6H, H-1b, H-2, H-3a, H-4a and H-6a), 1.54-1.44 (m, 2H, H-3b and H-5a), 1.42-1.38 (m, 1H, H-4b), 1.36 (s, 3H, CH₃), 1.27 (d, *J* = 7.5 Hz, 2H, H-5b and H-6b), 1.04 (td, *J* = 13.4, 3.7 Hz, 1H, H-7a). ¹³C-NMR (δ, ppm) (75.5 MHz, CDCl₃): 147.7 (C_{arom}), 128.7 (CH_{arom}), 117.6 (CH_{arom}), 117.5 (CH_{arom}), 58.8 (C-7a), 55.7 (C-3a), 55.7 (C-7), 42.4 (C-3), 39.2 (C-4), 35.1 (C-6), 28.4 (C-2), 21.1 (CH₃), 19.0 (C-1), 18.7 (C-5). [α]_D²⁰: +181.0 (*c* = 1.0, CH₂Cl₂). IR (ATR) cm⁻¹: 3270, 2930, 2872, 1598, 1496, 1275, 1260, 763, 750. MS (EI, 70 eV) *m/z* (%): 246 (10), 245 (74), 244 (M⁺, 100), 241 (4). HRMS (ESI⁺) for C₁₆H₂₅N₂ [M+H]⁺: calculated: 245.2018, found: 245.2022.

(1S,4aS,6R,8aS)-6-methyl-N¹-phenyloctahydronaphthalene-1,4a(2H)-diamine (32p). Following the *General Procedure D*, **32p** (22.20 mg, 0.09 mmol) was isolated

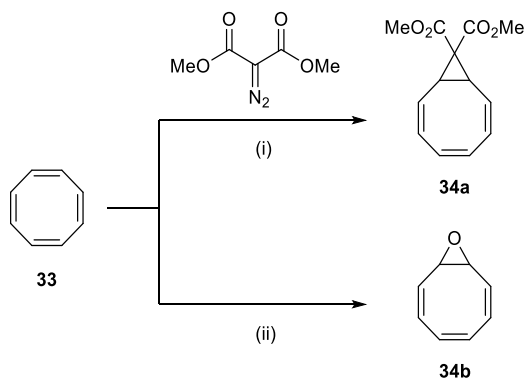


after 40 min at 80 °C by flash chromatography (petroleum ether/EtOAc 1:1) in 90% yield as a colourless oil starting from **23p** (25.00 mg, 0.1 mmol). ¹H-NMR (δ, ppm) (300 MHz, CDCl₃): 7.11 (t, *J* = 7.8 Hz, 2H, 2 x CH_{arom}), 6.64-6.50 (m, 3H, 3 x CH_{arom}), 3.57 (d,

J = 3.3 Hz, 1H, H-1), 2.12-1.85 (m, 2H, H-4_a and H-5_a), 1.84-1.60 (m, 3H, H-2_a, H-7_a and H-8_a), 1.50 (d, *J* = 13.3 Hz, 1H, H-3_a), 1.33 (tdd, *J* = 16.2, 7.9, 3.3 Hz, 6H, H-2_b, H-3_b, H-4_b, H-5_b, H-6 and H-7_b), 1.13-0.96 (m, 2H, H-8_a and H-8_b), 0.89 (d, *J* = 6.2 Hz, 3H, CH₃). ¹³C-NMR (δ, ppm) (75.5 MHz, CDCl₃): 148.7 (C_{arom}), 129.1 (CH_{arom}), 115.3 (CH_{arom}), 112.6 (CH_{arom}), 52.6 (C-1), 52.1 (C-8_a), 45.6 (C-4_a), 41.4 (C-5), 35.2 (C-4), 29.9 (C-2), 29.7 (C-7), 27.8 (C-6), 26.3 (C-8), 22.4 (CH₃), 16.7 (C-3). [α]_D²⁰: +249.9 (*c* = 1.3, CH₂Cl₂). IR (ATR) cm⁻¹: 3305, 2922, 2862, 1599, 1508, 1275, 1260, 763, 749. MS (EI, 70 eV) *m/z* (%): 260 (5), 259 (33), 258 (M⁺, 100), 118 (3), 92 (3), 77 (4), 57 (4), 55 (3). HRMS (ESI⁺) for C₁₇H₂₇N₂ [M+H]⁺: calculated: 259.2174, found: 259.2173.

4. SWITCHABLE BRØNSTED ACID-CATALYZED RING CONTRACTION/ ENANTIOSELECTIVE ALLYLATION

4.1. Synthesis of the starting materials



(i) $\text{Rh}_2(\text{esp})_2$ (0.1 mol%), $\text{CH}_2\text{CH}_2\text{Cl}_2$ (0.1 M), 80 °C, 16h
 (ii) *m*CPBA (1 equiv), CHCl_3 (0.2 M), 0 °C to rt, 16h

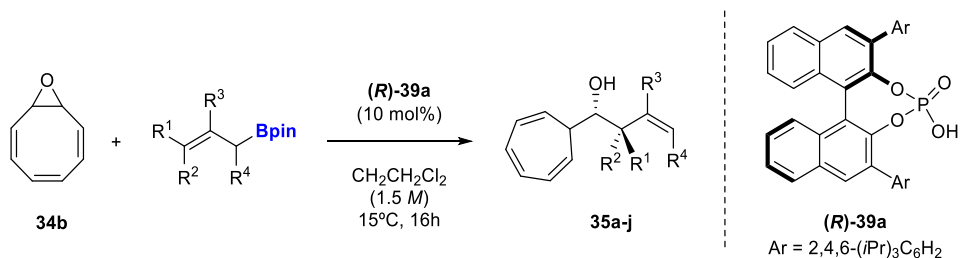
Scheme 6.9. General overview of the synthesis of starting materials.

Compounds **34a** and **34b** were synthesized according to procedure previously described in the literature. Spectroscopic data of **34a** and **34b** were consistent with the reported data.¹⁴ Allylboronic acid pinacol esters were commercially available and used without further purification or prepared following the procedures previously reported in the literature.¹⁵

¹⁴ (a) Del Moro, F.; Crotti, P.; Di Bussolo, V.; Macchia, F.; Pineschi, M. *Org. Lett.* **2003**, *5*, 1971. (b) Nanteuil, F.; Waser, J. *Angew. Chem. Int. Ed.* **2011**, *50*, 12075. (c) Racine, S.; Hegedüs, B.; Scopelliti, R.; Waser, J. *Chem. Eur. J.* **2016**, *22*, 11997. (d) Patel, H. D.; Fallon, T. *Org. Lett.* **2022**, *24*, 2276.

¹⁵ (a) Zhang, P.; Roundtree, I. A.; Morken, J. P. *Org. Lett.* **2012**, *14*, 6, 1416. (b) Semba, K.; Shinomiya, M.; Fujihara, T.; Terao, J.; Tsuji, Y. *Chem. Eur. J.* **2013**, *19*, 7125. (c) Unsworth, P. J.; Leonori, D.; Aggarwal, V. K. *Angew. Chem. Int. Ed.* **2014**, *53*, 9846. (d) Wu, J.; Lorenzo, P.; Zhong, S.; Ali, M.; Butts, C. P.; Myers, E. L.; Aggarwal, V. K. *Nature* **2017**, *547*, 436. (e) Wang, W.-F.; Peng, J.-B.; Qui, X.; Ying, J.; Wu, X.-F. *Chem. Eur. J.* **2019**, *25*, 3521. (f) Maza, R. J.; Davenport, E.; Miralles, N.; Carbó, J. J.; Fernández, E. *Org. Lett.* **2019**, *21*, 2251. (g) Su, W.; Wang, T.-T.; Tian, X.; Han, J.-R.; Zhen, X.-L.; Fan, S.-M.; You, Y.-X.; Zhang, Y.-K.; Qiao, R.-X.; Cheng, Q.; Liu, S. *Org. Lett.* **2021**, *23*, 9094.

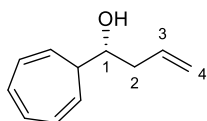
4.2. Enantioselective ring contraction/allylation reaction



Scheme 6.10. General procedure for the synthesis of enantioenriched homoallylic alcohols **35a-j**.

General Procedure A for the synthesis of **35a-j**: To an oven-dried screw-top vial, equipped with a magnetic stirring bar, catalyst **(R)-39a** (10 mol%, 0.02 mmol) was added under Ar atmosphere. Then, epoxide **34b** (1 equiv, 0.20 mmol) was added as a solution in CH₂CH₂Cl₂ (0.13 mL), followed by the dropwise addition of the corresponding allyl boronic ester (1.1 equiv, 0.22 mmol). The reaction was left stirring at 15 °C until consumption of the starting material was observed by TLC. The solvent was evaporated under reduced pressure and purification by column chromatography afforded the desired products. Racemic standards for HPLC separation were prepared under the same reaction conditions, using diphenylphosphoric acid (DPP) (0.02 mmol) as catalyst.

(R)-1-(cyclohepta-2,4,6-trien-1-yl)but-3-en-1-ol (35a). Following the *General*



Procedure A, **35a** (32.40 mg, 0.20 mmol) was isolated after 16h

at 15 °C by flash chromatography (petroleum ether/EtOAc 8:2) in 99% yield as a colourless oil starting from **34b** (24 mg, 0.20

mmol), 2-allyl-4,4,5,5-tetramethyl-1,3,2-dioxaborolane (41 μL,

0.22 mmol), **(R)-39a** (15 mg, 0.02 mmol) and CH₂CH₂Cl₂ (0.13 mL, 1.5 M). ¹H-NMR

(δ, ppm) (300 MHz, CDCl₃): 6.72-6.58 (m, 2H, 2 x CH=CH), 6.26 (dddd, *J* = 21.4,

9.5, 4.4, 1.3 Hz, 2H, 2 x CH=CH), 5.85 (dddd, *J* = 16.8, 10.2, 8.0, 6.3 Hz, 1H, **H-3**),

5.48 (dd, *J* = 9.5, 5.8 Hz, 1H, CH=CH), 5.28 (dd, *J* = 9.5, 5.9 Hz, 1H, CH=CH),

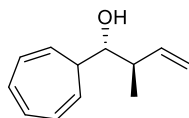
5.22-5.09 (m, 2H, **H-4**), 3.92 (ddd, *J* = 8.5, 7.2, 3.5 Hz, 1H, **H-1**), 2.56-2.39 (m, 1H,

H-2_a), 2.32-2.17 (m, 1H, **H-2_b**), 1.81-1.73 (m, 2H, **H-3** and CH-CH=CH). ¹³C-NMR

(δ, ppm) (75.5 MHz, CDCl₃): 134.4 (**C-3**), 131.0 (CH=CH), 130.7 (CH=CH), 125.6

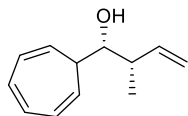
(CH=CH), 125.4 (CH=CH), 122.5 (CH=CH), 122.4 (CH=CH), 118.5 (C-4), 70.8 (C-1), 44.9 (CH-CH=CH), 39.7 (C-2). The enantiomeric excess (e.e.) was determined by HPLC using a CHIRALPAK® AD-3 column (hexane/*i*-PrOH 90:10, 1 mL/min, 251 nm, 25°C); t_r (major) = 5.67 min, t_r (minor) = 6.00 min (89% ee). $[\alpha]_D^{20}$: -44.8 ($c = 1.0$, CH₂Cl₂). IR (ATR) cm⁻¹: 3390, 3012, 1275, 1260, 994, 916, 749, 701. MS (EI, 70 eV) m/z (%): 129 (2), 128 (2), 121 (2), 120 (1), 119 (1), 115 (2), 104 (1), 103 (10), 102 (1), 93 (2), 92 (25), 91 (100), 90 (1), 89 (3), 79 (2), 78 (3), 77 (10), 66 (2), 65 (12), 64 (1), 63 (4), 62 (1), 55 (1), 53 (1), 52 (1), 51 (3), 50 (1). HRMS (ESI) m/z : [M-H₂O+H]⁺ Calcd for C₁₁H₁₃ 145.1012; Found 145.1015.

(1*R*,2*R*)-1-(cyclohepta-2,4,6-trien-1-yl)-2-methylbut-3-en-1-ol (35b). Following



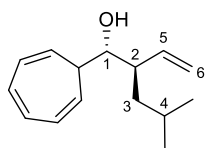
the *General Procedure A*, **35b** (34.89 mg, 0.19 mmol) was isolated after 16h at 15 °C by flash chromatography (petroleum ether/EtOAc 8:2) in 99% yield as a colorless oil starting from **34b** (24 mg, 0.20 mmol), *trans*-crotylboronic acid pinacol ester (45

μL, 0.22 mmol), (**R**)-**39a** (15 mg, 0.02 mmol) and CH₂CH₂Cl₂ (0.13 mL, 1.5 M). ¹H-NMR (δ, ppm) (300 MHz, CDCl₃): 6.73-6.52 (m, 2H, 2 x CH=CH), 6.40-6.13 (m, 2H, 2 x CH=CH), 5.75 (ddd, $J = 17.8, 10.3, 8.4$ Hz, 1H, H-3), 5.48 (dd, $J = 9.5, 5.9$ Hz, 1H, CH=CH), 5.34 (dd, $J = 9.5, 5.9$ Hz, 1H, CH=CH), 5.22-5.15 (m, 1H, H-4_a), 5.13 (s, 1H, H-4_b), 3.67 (t, $J = 6.1$ Hz, 1H, H-1), 2.63-2.46 (m, 1H, CH-CH=CH), 1.82 (q, $J = 6.1$ Hz, 1H, H-2), 1.61 (br s, 1H, OH), 1.02 (d, $J = 6.9$ Hz, 3H, CH₃). ¹³C-NMR (δ, ppm) (75.5 MHz, CDCl₃): 139.6 (C-3), 130.8 (CH=CH), 130.6 (CH=CH), 125.4 (CH=CH), 125.1 (CH=CH), 123.0 (CH=CH), 122.0 (CH=CH), 116.9 (C-4), 74.8 (C-1), 42.5 (C-2), 41.7 (CH-CH=CH), 16.7 (CH₃). The enantiomeric excess (e.e.) was determined by HPLC using a CHIRALPAK® AD-H column (hexane/*i*-PrOH 95:05, 1 mL/min, 251 nm, 25°C); t_r (major) = 7.22 min, t_r (minor) = 7.73 min (93% ee). $[\alpha]_D^{20}$: -23.2 ($c = 1.0$, CH₂Cl₂). IR (ATR) cm⁻¹: 3445, 3010, 1275, 1260, 763, 750. MS (EI, 70 eV) m/z (%): 158 (1), 143 (3), 141 (1), 129 (2), 128 (4), 127 (1), 121 (2), 120 (1), 119 (1), 116 (1), 115 (3), 104 (2), 103 (15), 102 (1), 93 (3), 92 (34), 91 (100), 90 (1), 89 (3), 80 (1), 79 (2), 78 (5), 77 (13), 76 (1), 75 (1), 66 (1), 65 (12), 64 (1), 63 (4), 62 (1), 57 (1), 56 (1), 55 (5), 53 (2), 52 (1), 51 (4). HRMS (ESI) m/z : [M-H₂O+H]⁺ Calcd for C₁₂H₁₅ 159.1168; Found 159.1172.

(1*R*,2*S*)-1-(cyclohepta-2,4,6-trien-1-yl)-2-methylbut-3-en-1-ol (35c).

Following the *General Procedure A*, **35c** (31.80 mg, 0.18 mmol) was isolated after 16h at 15 °C by flash chromatography (petroleum ether/EtOAc 8:2) in 90% yield as a colorless oil starting from **34b** (24 mg, 0.20 mmol), *cis*-crotylboronic acid pinacol ester (45 μ L,

0.22 mmol), (**R**)-**39a** (15 mg, 0.02 mmol) and $\text{CH}_2\text{CH}_2\text{Cl}_2$ (0.13 mL, 1.5 *M*). $^1\text{H-NMR}$ (δ , ppm) (300 MHz, CDCl_3): 6.73-6.52 (m, 2H, 2 x $\text{CH}=\text{CH}$), 6.45-6.10 (m, 2H, 2 x $\text{CH}=\text{CH}$), 5.82 (ddd, $J = 17.3, 10.4, 7.0$ Hz, 1H, **H-3**), 5.47 (dd, $J = 9.5, 5.8$ Hz, 1H, $\text{CH}=\text{CH}$), 5.26 (dd, $J = 9.4, 6.0$ Hz, 1H, $\text{CH}=\text{CH}$), 5.18-4.96 (m, 2H, **H-4**), 3.82 (dd, $J = 7.3, 4.8$ Hz, 1H, **H-1**), 2.59 (dtd, $J = 8.3, 6.6, 1.4$ Hz, 1H, $\text{CH}-\text{CH}=\text{CH}$), 1.85 (tdd, $J = 7.2, 5.2, 1.2$ Hz, 1H, **H-2**), 1.67 (br s, 1H, **OH**), 1.01 (d, $J = 6.8$ Hz, 3H, CH_3). $^{13}\text{C-NMR}$ (δ , ppm) (75.5 MHz, CDCl_3): 141.1 (**C-3**), 131.0 ($\text{CH}=\text{CH}$), 130.5 ($\text{CH}=\text{CH}$), 125.3 ($\text{CH}=\text{CH}$), 125.2 ($\text{CH}=\text{CH}$), 122.6 ($\text{CH}=\text{CH}$), 122.2 ($\text{CH}=\text{CH}$), 115.2 (**C-4**), 74.8 (**C-1**), 42.7 (**C-2**), 40.8 ($\text{CH}-\text{CH}=\text{CH}$), 12.9 (CH_3). The enantiomeric excess (e.e.) was determined by HPLC using a CHIRALPAK® AD-H column (hexane/*i*-PrOH 95:05, 1 mL/min, 251 nm, 25°C); t_r (major) = 9.02 min, t_r (minor) = 10.44 min (98% ee). $[\alpha]_D^{20}$: -15.0 ($c = 1.0, \text{CH}_2\text{Cl}_2$). IR (ATR) cm^{-1} : 3419, 3012, 2973, 2875, 2359, 1275, 1260, 915, 763, 749, 704. MS (EI, 70 eV) m/z (%): 158 (1), 143 (3), 141 (1), 129 (2), 128 (4), 127 (1), 121 (2), 120 (1), 116 (1), 115 (2), 104 (1), 103 (13), 102 (1), 93 (4), 92 (43), 91 (100), 90 (1), 89 (2), 80 (1), 79 (2), 78 (3), 77 (10), 66 (1), 65 (9), 64 (1), 63 (2), 62 (1), 57 (1), 56 (1), 55 (3), 53 (2), 52 (1), 51 (3). HRMS (ESI) m/z : $[\text{M}-\text{H}_2\text{O}+\text{H}]^+$ Calcd for $\text{C}_{12}\text{H}_{15}$ 159.1168; Found 159.1172.

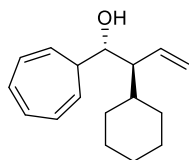
(1*R*,2*R*)-1-(cyclohepta-2,4,6-trien-1-yl)-4-methyl-2-vinylpentan-1-ol (35d).

Following the *General Procedure A*, **35d** (40.1 mg, 0.18 mmol) was isolated after 16h at 15 °C by flash chromatography (petroleum ether/EtOAc 8:2) in 92% yield as a colorless oil starting from **34b** (24 mg, 0.20 mmol), (*E*)-4,4,5,5-tetramethyl-

2-(5-methylhex-2-en-1-yl)-1,3,2-dioxaborolane (49 mg, 0.22 mmol), (**R**)-**39a** (30 mg, 0.04 mmol) and $\text{CH}_2\text{CH}_2\text{Cl}_2$ (0.10 mL, 2.0 *M*). $^1\text{H-NMR}$ (δ , ppm) (300 MHz, CDCl_3): 6.75-6.49 (m, 2H, 2 x $\text{CH}=\text{CH}$), 6.26 (td, $J = 10.7, 10.5, 4.4$ Hz, 2H, 2 x

CH=CH), 5.63 (dt, $J = 17.1, 9.8$ Hz, 1H, **H-5**), 5.47 (dd, $J = 9.5, 6.0$ Hz, 1H, CH=CH), 5.37-5.27 (m, 1H, CH=CH), 5.21-5.05 (m, 2H, **H-6**), 3.71-3.62 (m, 1H, **H-1**), 2.45 (tt, $J = 9.7, 4.9$ Hz, 1H, CH-CH=CH), 1.89 (q, $J = 6.4$ Hz, 1H, **H-2**), 1.37-1.20 (m, 3H, **H-3** and **OH**), 1.12 (ddd, $J = 13.7, 9.3, 4.9$ Hz, 1H, **H-4**), 0.86 (dd, $J = 9.5, 6.5$ Hz, 6H, 2 x **CH₃**). $^{13}\text{C-NMR}$ (δ , ppm) (75.5 MHz, CDCl_3): 137.3 (**C-5**), 129.8 (CH=CH), 129.6 (CH=CH), 124.5 (CH=CH), 124.1 (CH=CH), 121.9 (CH=CH), 121.3 (CH=CH), 117.1 (**C-6**), 72.6 (**C-1**), 44.5 (**C-2**), 41.7 (**C-3**), 39.0 (CH-CH=CH), 24.2 (**C-4**), 22.5 (**CH₃**), 20.4 (**CH₃**). The enantiomeric excess (e.e.) was determined by HPLC using a CHIRALPAK[®] AD-H column (hexane/*i*-PrOH 95:05, 1 mL/min, 251 nm, 25°C); t_r (major) = 5.82 min, t_r (minor) = 6.47 min (78% ee). $[\alpha]_D^{20}$: -28.0 ($c = 2.0, \text{CH}_2\text{Cl}_2$). IR (ATR) cm^{-1} : 3445, 3007, 2360, 2342, 1275, 1260, 763, 750. MS (EI, 70 eV) m/z (%): 144 (1), 143 (6), 142 (1), 141 (2), 129 (3), 128 (7), 127 (2), 122 (1), 121 (5), 120 (2), 119 (1), 117 (1), 116 (1), 115 (4), 109 (2), 105 (1), 104 (2), 103 (16), 102 (1), 93 (6), 92 (56), 91 (100), 90 (1), 89 (3), 85 (1), 83 (1), 81 (1), 79 (3), 78 (4), 77 (13), 71 (1), 70 (2), 69 (3), 67 (3), 66 (1), 65 (11), 64 (1), 63 (2), 57 (5), 56 (1), 55 (7), 54 (1), 53 (2), 52 (1), 51 (3), 50 (1). HRMS (ESI) m/z : $[\text{M-H}_2\text{O}+\text{H}]^+$ Calcd for $\text{C}_{15}\text{H}_{21}$ 201.1638; Found 201.1643.

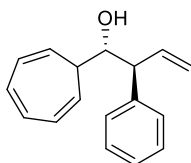
(1*R*,2*S*)-1-(cyclohepta-2,4,6-trien-1-yl)-2-cyclohexylbut-3-en-1-ol (35e).



Following the *General Procedure A*, **35e** (43.3 mg, 0.18 mmol) was isolated after 16h at 15 °C by flash chromatography (petroleum ether/EtOAc 8:2) in 89% yield as a colorless oil starting from **34b** (24 mg, 0.20 mmol), (*E*)-2-(3-cyclohexylallyl)-4,4,5,5-tetramethyl-1,3,2-dioxaborolane (55 mg, 0.22 mmol), (**R**)-**39a** (30 mg, 0.04 mmol) and $\text{CH}_2\text{CH}_2\text{Cl}_2$ (0.10 mL, 2.0 *M*). $^1\text{H-NMR}$ (δ , ppm) (300 MHz, CDCl_3): 6.69-6.52 (m, 2H, 2 x CH=CH), 6.33-6.16 (m, 2H, 2 x CH=CH), 5.71 (dt, $J = 17.1, 10.0$ Hz, 1H, **H-3**), 5.46 (dd, $J = 9.5, 6.1$ Hz, 1H, CH=CH), 5.25 (dd, $J = 9.5, 6.1$ Hz, 1H, CH=CH), 5.16 (dd, $J = 10.2, 2.2$ Hz, 1H, **H-4_a**), 5.03 (dd, $J = 17.1, 2.2$ Hz, 1H, **H-4_b**), 3.95 (dd, $J = 8.0, 4.2$ Hz, 1H, **H-1**), 2.07 (ddd, $J = 9.8, 7.2, 4.1$ Hz, 1H, CH-CH=CH), 1.95 (q, $J = 6.6$ Hz, 1H, **H-2**), 1.80-1.61 (m, 5H, **CH_{2,a}** and 2 x **CH₂**), 1.46-1.37 (m, 1H, **CH₂-CH-CH₂**), 1.29-1.07 (m, 3H, **CH_{2,b}** and **CH₂**), 1.06-0.79 (m, 2H, **CH₂**). $^{13}\text{C-NMR}$ (δ , ppm) (75.5 MHz, CDCl_3): 136.4 (**C-3**), 130.8

(CH=CH), 130.7 (CH=CH), 125.7 (CH=CH), 125.2 (CH=CH), 122.9 (CH=CH), 122.8 (CH=CH), 118.6 (C-4), 70.3 (C-1), 53.3 (C-2), 43.1 (CH₂-CH-CH₂), 37.5 (CH-CH=CH), 31.5 (CH₂), 30.5 (CH₂), 26.5 (CH₂), 26.4 (CH₂), 26.3 (CH₂). The enantiomeric excess (e.e.) was determined by HPLC using a CHIRALPAK® AD-3 column (hexane/*i*-PrOH 90:10, 1 mL/min, 251 nm, 25°C); *t_r* (major) = 5.14 min, *t_r* (minor) = 6.78 min (66% ee). $[\alpha]_{\text{D}}^{20}$: -11.6 (*c* = 2.0, CH₂Cl₂). IR (ATR) cm⁻¹: 3445, 3008, 2921, 2360, 2341, 1275, 1260, 763, 750. MS (EI, 70 eV) *m/z* (%): 153 (3), 152 (1), 144 (1), 143 (3), 142 (1), 141 (1), 136 (1), 135 (7), 134 (1), 131 (1), 130 (1); 129 (5), 128 (4), 127 (1), 125 (6), 124 (57), 123 (2), 122 (6), 121 (60), 120 (8), 119 (2), 117 (1), 116 (1), 115 (3), 111 (2), 110 (1), 109 (8), 108 (1), 107 (3), 105 (2), 104 (4), 103 (36), 102 (1), 97 (2); 96 (6), 95 (12), 94 (2), 93 (17), 92 (100), 91 (77), 90 (1), 89 (3), 84 (2), 83 (26), 82 (43), 81 (36), 80 (5), 79 (18), 78 (5), 77 (20), 71 (6), 70 (15), 69 (12), 68 (8), 67 (25), 66 (5), 65 (17), 64 (1), 63 (3), 57 (4), 56 (2), 55 (41), 54 (4), 53 (7), 52 (2), 51 (4). HRMS (ESI) *m/z*: [M-H₂O+H]⁺ Calcd for C₁₇H₂₃ 227.1794; Found 227.1793.

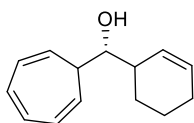
(1*S*,2*S*)-1-(cyclohepta-2,4,6-trien-1-yl)-2-phenylbut-3-en-1-ol (35f). Following



the *General Procedure A*, **35f** (47.20 mg, 0.20 mmol) was isolated after 16h at 15 °C by flash chromatography (petroleum ether/EtOAc 8:2) in 99% yield as a yellow oil starting from **34b** (24 mg, 0.20 mmol), 2-*trans*-cinnamyl-4,4,5,5-tetramethyl-1,3,2-dioxaborolane (54 mg, 0.22 mmol), (**R**)-**39a** (15 mg, 0.02 mmol) and CH₂CH₂Cl₂ (0.13 mL, 1.5 *M*). ¹H-NMR (δ, ppm) (300 MHz, CDCl₃): 7.34-7.27 (m, 2H, 2 x CH_{arom}), 7.26-7.17 (m, 3H, 3 x CH_{arom}), 6.63-6.55 (m, 2H, 2 x CH=CH), 6.37-6.24 (m, 1H, H-3), 6.24-6.14 (m, 2H, 2 x CH=CH), 5.46-5.63 (m, 1H, CH=CH), 5.37 (dd, *J* = 9.5, 5.9 Hz, 1H, CH=CH), 5.30-5.20 (m, 2H, H-4), 4.10 (t, *J* = 6.2 Hz, 1H, H-1), 3.66 (dd, *J* = 9.2, 6.6 Hz, 1H, H-2), 1.96 (br s, 1H, OH), 1.73 (q, *J* = 5.8 Hz, 1H, CH-CH=CH). ¹³C-NMR (δ, ppm) (75.5 MHz, CDCl₃): 141.2 (C_{arom}), 137.3 (C-3), 130.8 (CH=CH), 130.5 (CH=CH), 128.6 (CH=CH), 127.9 (CH=CH), 126.7 (CH_{arom}), 125.4 (CH=CH), 125.1 (CH=CH), 123.0 (CH_{arom}), 121.6 (CH_{arom}), 118.5 (C-4), 74.2 (C-1), 54.3 (C-2), 42.2 (CH-CH=CH). The enantiomeric excess (e.e.) was determined by HPLC using a CHIRALPAK® OD-3 column (hexane/*i*-PrOH

90:10, 1 mL/min, 251 nm, 25°C); t_r (major) = 5.82 min, t_r (minor) = 7.72 min (55% ee). $[\alpha]_D^{20}$: -13.1 (c = 1.0, CH_2Cl_2). IR (ATR) cm^{-1} : 3445, 3008, 2361, 2342, 1275, 1260, 763, 750. MS (EI, 70 eV) m/z (%): 238 (M^+ , 1), 220 (1), 219 (1), 205 (1), 204 (1), 203 (1), 202 (1), 191 (1), 190 (1), 189 (1), 179 (1), 178 (1), 165 (2), 152 (1), 143 (1), 142 (1), 141 (1), 139 (1), 130 (1), 129 (6), 128 (4), 127 (1), 122 (4), 121 (45), 120 (5), 119 (7), 118 (36), 117 (28), 116 (7), 115 (31), 105 (4), 104 (5), 103 (47), 102 (3), 101 (1), 94 (1), 93 (12), 92 (33), 91 (100), 90 (2), 89 (7), 87 (1), 79 (8), 78 (7), 77 (31), 76 (1), 75 (1), 74 (1), 66 (2), 65 (15), 64 (1), 63 (5), 62 (1), 55 (2), 53 (2), 52 (1), 51 (5), 50 (1). HRMS (ESI) m/z : $[\text{M}-\text{H}_2\text{O}+\text{H}]^+$ Calcd for $\text{C}_{17}\text{H}_{17}$ 221.1325; Found 221.1324.

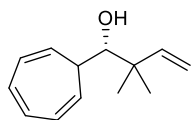
(1*R*)-cyclohepta-2,4,6-trien-1-yl(cyclohex-2-en-1-yl)methanol (35g). Following



the *General Procedure A*, **35g** (23.6 mg, 0.12 mmol) was isolated after 16h at 15 °C by flash chromatography (petroleum ether/EtOAc 8:2) in 58% yield as a colourless oil starting from **34b** (24 mg, 0.20 mmol), 2-(cyclohex-2-en-1-yl)-4,4,5,5-tetramethyl-1,3,2-dioxaborolane (46 mg, 0.22 mmol), (**R**)-**39a** (15 mg, 0.02 mmol) and $\text{CH}_2\text{CH}_2\text{Cl}_2$ (0.13 mL, 1.5 *M*). $^1\text{H-NMR}$ (δ , ppm) (300 MHz, CDCl_3): 6.67 (t, J = 4.4 Hz, 2H, 2 x $\text{CH}=\text{CH}$), 6.26 (ddd, J = 15.2, 9.4, 4.9 Hz, 2H, 2 x $\text{CH}=\text{CH}$), 5.96-5.81 (m, 1H, **H-3**), 5.51 (dd, J = 9.4, 4.9 Hz, 2H, 2 x $\text{CH}=\text{CH}$), 5.24 (dd, J = 9.4, 6.0 Hz, 1H, **H-4**), 3.89 (dd, J = 8.2, 4.2 Hz, 1H, **H-1**), 2.55 (br s, 1H, OH), 2.16-1.90 (m, 2H, CH_2), 1.89-1.69 (m, 2H, **H-2** and $\text{CH}-\text{CH}=\text{CH}$), 1.62-1.46 (m, 4H, 2 x CH_2). $^{13}\text{C-NMR}$ (δ , ppm) (75.5 MHz, CDCl_3): 131.2 ($\text{CH}=\text{CH}$), 131.1 ($\text{CH}=\text{CH}$), 130.6 ($\text{CH}=\text{CH}$), 128.6 ($\text{CH}=\text{CH}$), 125.3 (**C-4**), 123.3 (**C-3**), 121.8 ($\text{CH}=\text{CH}$), 74.8 (**C-1**), 42.3 (**C-2**), 39.0 ($\text{CH}-\text{CH}=\text{CH}$), 25.1 (CH_2), 21.8 (CH_2), 21.2 (CH_2). The enantiomeric excess (e.e.) was determined by HPLC using a CHIRALPAK® OD-3 column (hexane/*i*-PrOH 90:10, 1 mL/min, 210 nm, 25°C); t_r (major) = 5.02 min, t_r (minor) = 6.05 min (88% ee). $[\alpha]_D^{20}$: -53.6 (c = 1.0, CH_2Cl_2). IR (ATR) cm^{-1} : 3445, 3008, 2360, 1275, 1260, 763, 750. MS (EI, 70 eV) m/z (%): 184 (2), 169 (1), 165 (1), 156 (1), 155 (2), 154 (1), 153 (1), 152 (1), 143 (1), 142 (2), 141 (6), 130 (1), 129 (2), 128 (4), 127 (1), 122 (3), 121 (36), 120 (2), 119 (2), 117 (1), 116 (1), 115 (5), 111 (1), 110 (1), 105 (2), 104 (4), 103 (35), 102 (2), 95 (1), 94 (1), 93 (16), 92 (53),

91 (100), 90 (1), 89 (4), 82 (1), 81 (9), 80 (3), 79 (18), 78 (7), 77 (33), 76 (1), 75 (1), 67 (4), 66 (3), 65 (15), 64 (1), 63 (4), 62 (1), 57 (1), 55 (6), 54 (1), 53 (8), 52 (2), 51 (6). HRMS (ESI) m/z : $[M-H_2O+H]^+$ Calcd for $C_{14}H_{17}$ 185.1325; Found 185.1327.

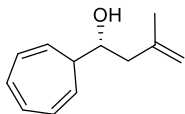
(S)-1-(cyclohepta-2,4,6-trien-1-yl)-2,2-dimethylbut-3-en-1-ol (35h). Following



the *General Procedure A*, **35h** (32.80 mg, 0.17 mmol) was isolated after 16h at 15 °C by flash chromatography (petroleum ether/EtOAc 8:2) in 86% yield as a colorless oil starting from **34b** (24 mg, 0.20 mmol), 4,4,5,5-tetramethyl-2-(3-methylbut-2-en-1-

yl)-1,3,2-dioxaborolane (49 μ L, 0.22 mmol), **(R)-39a** (15 mg, 0.02 mmol) and $CH_2CH_2Cl_2$ (0.13 mL, 1.5 M). 1H -NMR (δ , ppm) (300 MHz, $CDCl_3$): 6.78-6.50 (m, 2H, 2 x $CH=CH$), 6.37-6.08 (m, 2H, 2 x $CH=CH$), 5.87 (dd, $J = 17.4, 10.8$ Hz, 1H, **H-3**), 5.49 (dd, $J = 9.4, 5.9$ Hz, 1H, $CH=CH$), 5.29 (dd, $J = 9.3, 5.9$ Hz, 1H, $CH=CH$), 5.20-4.90 (m, 2H, **H-4**), 3.68 (d, $J = 4.0$ Hz, 1H, **H-1**), 2.22-1.57 (m, 2H, **OH** and $CH-CH=CH$), 1.06 (d, $J = 2.7$ Hz, 6H, 2 x CH_3). ^{13}C -NMR (δ , ppm) (75.5 MHz, $CDCl_3$): 145.5 (**C-3**), 130.9 ($CH=CH$), 130.3 ($CH=CH$), 123.9 ($CH=CH$), 123.7 ($CH=CH$), 123.4 ($CH=CH$), 120.5 ($CH=CH$), 113.7 (**C-4**), 78.4 (**C-1**), 42.2 (**C-2**), 40.8 ($CH-CH=CH$), 24.1 (CH_3), 22.9 (CH_3). The enantiomeric excess (e.e.) was determined by HPLC using a CHIRALPAK® AD-H column (hexane/*i*-PrOH 98:02, 1 mL/min, 251 nm, 25°C); t_r (major) = 10.90 min, t_r (minor) = 11.83 min (86% ee). $[\alpha]_D^{20}$: +3.6 ($c = 1.0, CH_2Cl_2$). IR (ATR) cm^{-1} : 3452, 2966, 2362, 2342, 1275, 1260, 763, 750. MS (EI, 70 eV) m/z (%): 172 (1), 157 (3), 143 (1), 142 (2), 141 (1), 130 (1), 129 (5), 128 (2), 127 (1), 121 (4), 120 (2), 119 (1), 117 (1), 116 (1), 115 (2), 105 (1), 104 (3), 103 (24), 102 (1), 97 (1), 93 (5), 92 (56), 91 (100), 90 (1), 89 (3), 81 (1), 79 (4), 78 (5), 77 (15), 76 (1), 70 (2), 69 (4), 67 (1), 66 (1), 65 (11), 64 (1), 63 (3), 62 (1), 57 (1), 55 (4), 53 (3), 52 (1), 51 (4), 50 (1). HRMS (ESI) m/z : $[M+CH_3OH-H]^-$ Calcd for $C_{14}H_{21}O_2$ 221.1547; Found 221.1550.

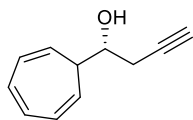
(R)-1-(cyclohepta-2,4,6-trien-1-yl)-3-methylbut-3-en-1-ol (35i). Following the



General Procedure A, **35i** (34.80 mg, 0.20 mmol) was isolated after 16h at 15 °C by flash chromatography (petroleum ether/EtOAc 8:2) in 99% yield as a colourless oil starting from **34b** (24 mg, 0.20 mmol), 4,4,5,5-tetramethyl-2-(2-methylallyl)-

1,3,2-dioxaborolane (41 μ L, 0.22 mmol), **(R)-39a** (15 mg, 0.02 mmol) and $\text{CH}_2\text{CH}_2\text{Cl}_2$ (0.13 mL, 1.5 M). $^1\text{H-NMR}$ (δ , ppm) (300 MHz, CDCl_3): 6.78-6.51 (m, 2H, 2 x $\text{CH}=\text{CH}$), 6.37-6.11 (m, 2H, 2 x $\text{CH}=\text{CH}$), 5.51 (dd, $J = 9.6, 5.7$ Hz, 1H, $\text{CH}=\text{CH}$), 5.30 (dd, $J = 9.5, 5.9$ Hz, 1H, $\text{CH}=\text{CH}$), 4.90 (d, $J = 21.9$ Hz, 2H, **H-4**), 4.02 (ddd, $J = 9.8, 6.8, 3.1$ Hz, 1H, **H-1**), 2.45-2.31 (m, 1H, **H-2a**), 2.23 (dd, $J = 13.9, 9.8$ Hz, 1H, $\text{CH}-\text{CH}=\text{CH}$), 1.85 (br s, 1H, **OH**), 1.79 (s, 3H, CH_3), 1.73 (dt, $J = 7.0, 5.6$ Hz, 1H, **H-2b**). $^{13}\text{C-NMR}$ (δ , ppm) (75.5 MHz, CDCl_3): 142.4 (**C-3**), 131.1 ($\text{CH}=\text{CH}$), 130.6 ($\text{CH}=\text{CH}$), 125.4 ($\text{CH}=\text{CH}$), 125.3 ($\text{CH}=\text{CH}$), 122.6 ($\text{CH}=\text{CH}$), 122.5 ($\text{CH}=\text{CH}$), 113.8 (**C-4**), 69.0 (**C-1**), 45.1 (**C-2**), 43.9 ($\text{CH}-\text{CH}=\text{CH}$), 22.4 (CH_3). The enantiomeric excess (e.e.) was determined by HPLC using a CHIRALPAK® AD-3 column (hexane/*i*-PrOH 98:02, 1 mL/min, 251 nm, 25°C); t_r (major) = 13.31 min, t_r (minor) = 14.29 min (28% ee). $[\alpha]_D^{20}$: -47.9 ($c = 1.0, \text{CH}_2\text{Cl}_2$). IR (ATR) cm^{-1} : 3422, 3011, 1275, 1260, 763, 749. MS (EI, 70 eV) m/z (%): 158 (2), 144 (1), 143 (5), 142 (1), 141 (1), 130 (1), 129 (3), 128 (4), 127 (1), 121 (3), 120 (3), 119 (1); 117 (1), 116 (1), 115 (4), 105 (1), 104 (2), 103 (14), 102 (1), 98 (1), 93 (4), 92 (50), 91 (100), 90 (1), 89 (4), 85 (1), 83 (1), 80 (1), 79 (2), 78 (3), 77 (11), 70 (1), 69 (1), 67 (1), 66 (1), 65 (13), 64 (1), 63 (3), 62 (1), 57 (2), 56 (1), 55 (2), 53 (2), 52 (1), 51 (3), 50 (1). HRMS (ESI) m/z : $[\text{M}-\text{H}_2\text{O}+\text{H}]^+$ Calcd for $\text{C}_{12}\text{H}_{15}$ 159.1168; Found 159.1171.

(R)-1-(cyclohepta-2,4,6-trien-1-yl)but-3-yn-1-ol (35j). Following the *General*



Procedure A, **35j** (30.40 mg, 0.19 mmol) was isolated after 16h at 15 °C by flash chromatography (petroleum ether/EtOAc 8:2) in 95% yield as a colorless oil starting from **34b** (24 mg, 0.20 mmol),

4,4,5,5-tetramethyl-2-(propa-1,2-dien-1-yl)-1,3,2-dioxaborolane (40 μ L, 0.22 mmol), **(R)-39a** (30 mg, 0.04 mmol) and $\text{CH}_2\text{CH}_2\text{Cl}_2$ (0.10 mL, 2.0 M). $^1\text{H-NMR}$ (δ , ppm) (300 MHz, CDCl_3): 6.66 (t, $J = 3.9$ Hz, 2H, 2 x **CH=CH**), 6.27 (ddd, $J = 14.4, 9.5, 4.8$ Hz, 2H, 2 x **CH=CH**), 5.49 (dd, $J = 9.5, 5.9$ Hz, 1H, **CH=CH**), 5.25 (dd, $J = 9.4, 6.1$ Hz, 1H, **CH=CH**), 4.00 (td, $J = 7.4, 4.1$ Hz, 1H, **H-1**), 2.75-2.35 (m, 2H, **H-2**), 2.06 (t, $J = 2.6$ Hz, 1H, **H-4**), 1.94 (q, $J = 6.5$ Hz, 1H, **CH-CH=CH**), 1.57 (br s, 1H, **OH**). $^{13}\text{C-NMR}$ (δ , ppm) (75.5 MHz, CDCl_3): 131.1 (**CH=CH**), 130.7 (**CH=CH**), 125.9 (**CH=CH**), 125.8 (**CH=CH**), 122.2 (**CH=CH**), 121.8 (**CH=CH**), 80.5 (**C-3**), 71.1 (**C-1**), 69.9 (**C-4**), 44.4 (**CH-CH=CH**), 25.4 (**C-2**). The enantiomeric excess (e.e.) was determined by HPLC using a CHIRALPAK® AD-H column (hexane/*i*-PrOH 95:05, 1 mL/min, 251 nm, 25°C); t_r (major) = 11.09 min, t_r (minor) = 12.23 min (80% ee). $[\alpha]_{\text{D}}^{20}$: +7.9 ($c = 1.0, \text{CH}_2\text{Cl}_2$). IR (ATR) cm^{-1} : 3293, 3010, 2360, 2342, 1275, 1260, 763, 750. MS (EI, 70 eV) m/z (%): 142 (1), 141 (3), 121 (3), 120 (1), 115 (2), 104 (1), 103 (7), 102 (1), 93 (1), 92 (12), 91 (100), 90 (1), 89 (3), 79 (1), 78 (3), 77 (8), 66 (1), 65 (11), 64 (1), 63 (3), 62 (1), 53 (1), 52 (1), 51 (3). HRMS (ESI) m/z : $[\text{M}-\text{H}_2\text{O}+\text{H}]^+$ Calcd for $\text{C}_{11}\text{H}_{11}$ 143.0855; Found 143.0858.

7

7

Scientific Collaborations

1. PROJECTS IN COLLABORATION	259
1.1. Transition-metal-free stereoselective borylation of allenamides	259
1.2. Synthesis of carbocyclic boronic esters <i>via</i> intramolecular lithiation-borylation and ring contraction	263

1. PROJECTS IN COLLABORATION

The present chapter includes contributions to other projects and publications in which I have participated during the development of the present doctoral thesis and in parallel to the main line of research of this work.

1.1. Transition-metal-free stereoselective borylation of allenamides

(*Chem. Eur. J.* **2018**, *24*, 14059.)



DOI: 10.1002/chem.201803004

CHEMISTRY
A European Journal
Communication

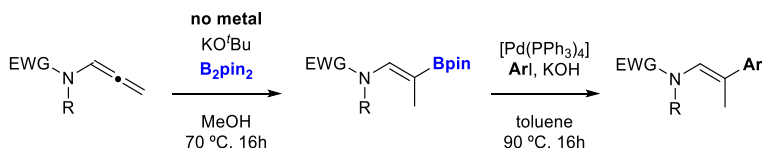
Borylation

Transition-Metal-Free Stereoselective Borylation of Allenamides

Lorena García,^[b] Jana Sendra,^[a] Núria Miralles,^[a] Efraim Reyes,^[b] Jorge J. Carbó,^{*,[a]}
Jose L. Vicario,^{*,[b]} and Elena Fernández^{*,[a]}

Dedicated to Professor Ernesto Carmona on the occasion of his 70th birthday

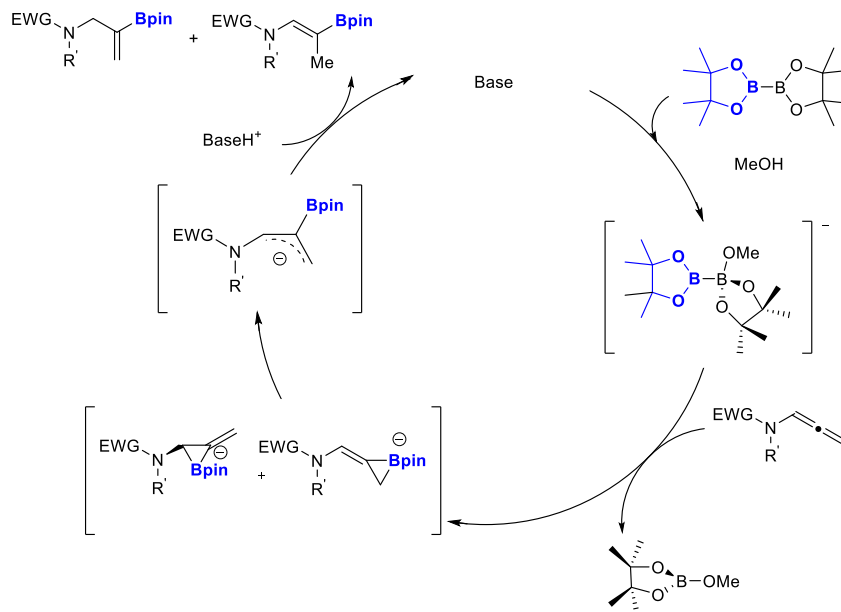
This article was published on Chemistry: A European Journal, and it describes a stereocontrolled methodology for the transition-metal-free hydroboration of different substituted allenamides, providing exclusively the *Z*-isomer from the borylation of the distal double bond. A consecutive Pd-catalyzed Suzuki-Miyaura cross-coupling reaction allowed the preparation of trisubstituted enamides with total control of the stereoselectivity (Scheme 7.1).



Scheme 7.1. Transition-metal-free stereoselective borylation of allenamides.

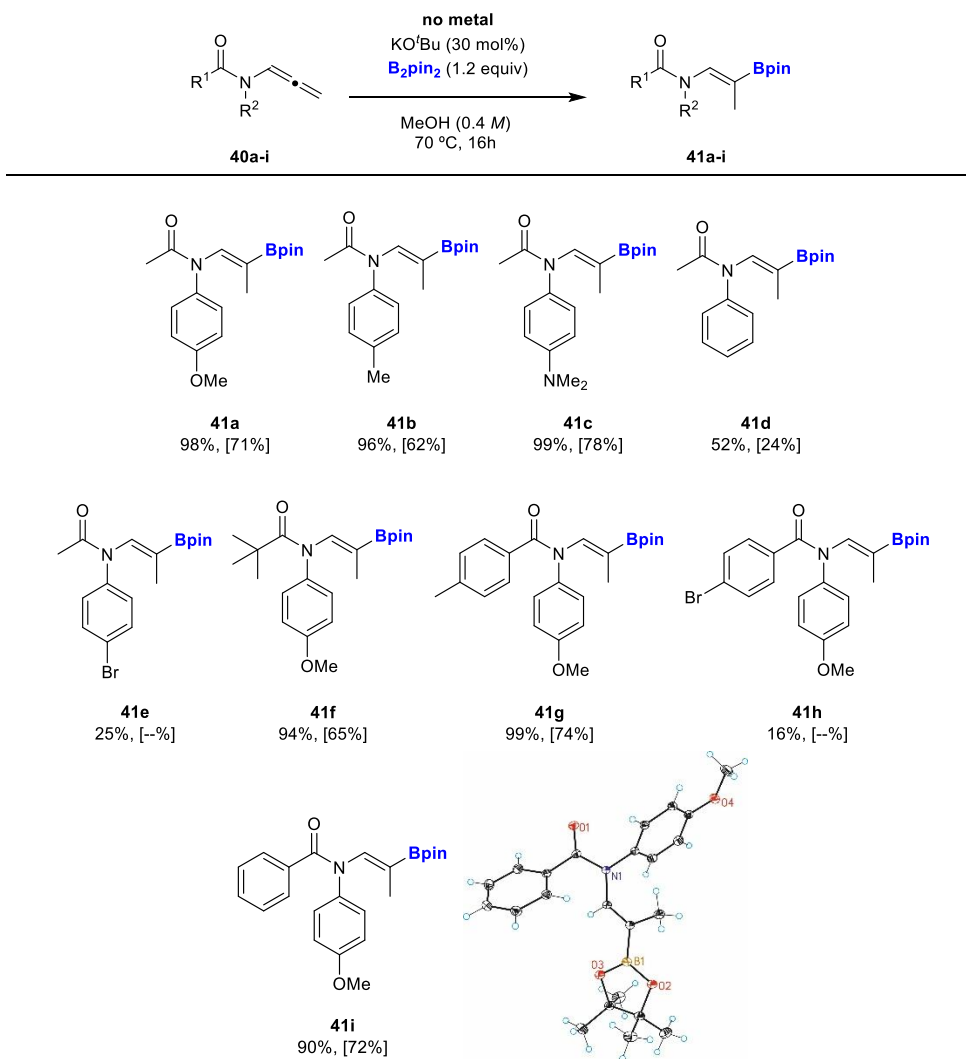
The observed reactivity showed an umpolung on the reactivity trend of the allenamides due to the *in situ* generation of the nucleophilic boryl moiety that can exert a nucleophilic attack to the allene system. Moreover, the nature of the electron

withdrawing substituent turned out to be crucial in order to obtain the exclusive regioselectivity. Computational studies, performed by Dr. Jordi J. Carbó, suggested a possible reaction mechanism and determined that the selectivity of the transformation mainly depends on the protonation step of the stable allylic anion intermediate, formed after ring opening of the two possible boracyclic intermediates as illustrated in Scheme 7.2.



Scheme 7.2. Suggested mechanism for the stereoselective borylation of allenamides.

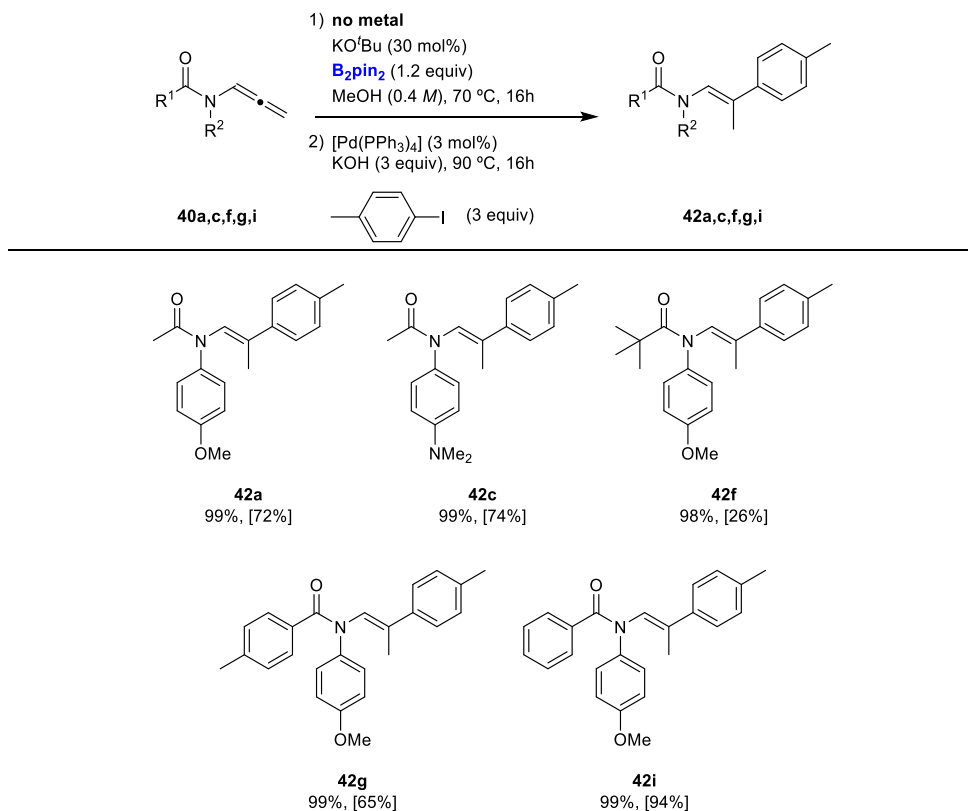
My personal contribution to this project was mainly focused on establishing the substrate scope of the reaction after Dr. Núria Miralles and Dr. Lorena García determined that acyl substituted allenamides were the optimal substrates for the projected transformation. In that sense, different acyl derivatives, prepared in the group of Prof. Jose Luis Vicario, were tested under the optimized reaction conditions in order to obtain the corresponding stereodefined alkenyl boronates showed below in Table 7.1.

Table 7.1. Scope of transition-metal-free borylation of acyl substituted allenamides.^[a]

[a] Reactions were performed with 0.2 mmol of **40a-i**, KO^tBu (30 mol%), B₂pin₂ (1.2 equiv) and MeOH (0.4 M) at 70 °C for 16h. NMR yields calculated from ¹H-NMR spectra with naphthalene as internal standard and isolated yields after flash chromatography purification.

Finally, I conducted an *in situ* functionalization of the obtained 2-pinacolboryl prope-1-en-1-amide intermediates via the development of a *one-pot* transition-metal-free hydroboration of the corresponding allenamides and subsequent Pd-catalyzed Suzuki-Miyaura cross-coupling reaction with 1-iodo-4-methylbenzene (Table 7.2).

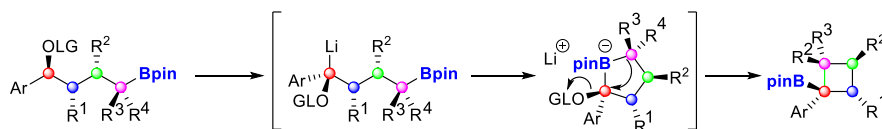
Table 7.2. Scope of transition-metal-free hydroboration/Suzuki-Miyaura cross-coupling reaction. ^[a]



[a] Reactions were performed with: (1) 0.5 mmol of **40a,c,f,g,i**, KO^tBu (30 mol%), B₂pin₂ (1.2 equiv) and MeOH (0.4 M) at 70 °C for 16h. Then evaporation of MeOH and (2) [Pd(PPh₃)₄] (3 mol%), **ArI** (3 equiv), KOH 3 M (6 equiv) and toluene (0.4 M) at 90 °C for 16h. NMR yields calculated from ¹H-NMR spectra with naphthalene as internal standard and isolated yields after flash chromatography purification.

1.2. Synthesis of carbocyclic boronic esters *via* intramolecular lithiation-borylation and ring contraction

During the three months research stay carried out in the group of Prof. Varinder K Aggarwal, at the University of Bristol, I had the opportunity to join an ongoing project focused on the application of intramolecular lithiation-borylation chemistry for the stereoselective synthesis of small cyclic molecules, starting from the corresponding acyclic precursors (Scheme 7.3).



Scheme 7.3. Summary of the studied reactivity.

My personal contribution to this project was mainly to work together with Christopher Cope, a second year PhD student, to finish the optimization of the projected reactivity as well as to start establishing the substrate scope of different synthesized acyclic boronic esters.

Appendix

Abbreviations, acronyms and symbols¹

Å	Angstrom
Ac	Acetyl group
Ar	Aryl group or Argon
atm	Atmospheric pressure
ATR	Attenuated total reflectance
BA	Brønsted acid
B₂cat₂	Bis(catecholato)diboron
BDPP	2,4-Bis(diphenylphosphino)pentane
B₂hex₂	Bis(hexylene glycolato)diboron
BINAP	2,2'-Bis(diphenylphosphino)-1,1'-binaphthalene
BINOL	2,2'-Dihydroxy-1,1'-binaphthyl
Bn	Benzyl group
B₂neop₂	Bis(neopentyl glycolato)diboron
B₂pin₂	Bis(pinacolato)diboron
BpinBdan	2-(4,4,5,5-tetramethyl-1,3,2-dioxaborolan-2-yl)-2,3-dihydro-1 <i>H</i> -naphtho[1,8-de][1,3,2]diazaborinine
br	Broad
Bz	Benzoyl group
c	Concentration
C_{arom}	Aromatic carbon
cat	Catechol
Cat	Catalyst
CHT	Cycloheptatrienyl group
Conv.	Conversion
COSY	Correlated spectroscopy
COT	Cyclooctatetraene

¹ For Standard Abbreviations and Acronyms, see: "Guidelines for Authors" *J. Org. Chem.* **2017**.

Cryst.	Crystallization
Cy	Cyclohexyl group
δ	Chemical shift
d	Doublet
DCC	<i>N,N</i> -Dicyclohexylcarbodiimide
DFT	Density-functional theory
DMAP	4-(Dimethylamino)pyridine
DMF	Dimethylformamide
DMSO	Dimethyl sulfoxide
DPP	Diphenylphosphoric acid
dppe	1,2-Bis(diphenylphosphino)ethane
dppf	1,1'-Bis(diphenylphosphino)ferrocene
d.r.	Diastereomeric ratio
e.e.	Enantiomeric excess
EI	Electron ionization
ent.	Enantiomer
equiv.	Equivalent
ELF	Electron localization function
ESI	Electrospray ionization
Et	Ethyl group
EWG	Electron-withdrawing group
FC	Flash chromatography
FT	Fourier transform
gen.	Generation
HA	Acid
HIV	Human immunodeficiency virus
HOMO	Highest occupied molecular orbital
HPLC	High performance liquid chromatography
HSQC	Heteronuclear single quantum coherence spectroscopy
IBX	2-Iodobenzoic acid
IMDA	Intramolecular Diels-Alder reaction

IR	Infrared spectroscopy
IRC	Intrinsic reaction coordinate
IY	Isolated yield
J	Coupling constant
L	Ligand
LG	Leaving group
LUMO	Lowest unoccupied molecular orbital
m	multiplet
M	Metal, molarity or molecular weight
mCPBA	<i>meta</i> -Chloroperoxybenzoic acid
Me	Methyl group
Mes	Mesityl group
MHz	Megahertz
M.p.	Melting point
MS	Mass spectrometry or molecular sieves
MTBE	Methyl <i>tert</i> -butyl ether
Naph	Naphtalene
NCD	Norcaradiene
N.d.	Not determined
NHC	<i>N</i> -Heterocyclic carbene
NMR	Nuclear magnetic resonance
n.O.e	Nuclear Overhauser effect
NOESY	Nuclear overhauser enhancement spectroscopy
Nu	Nucleophile
Ph	Phenyl group
PIDA	(Diacetoxyiodo)benzene
Pin	Pinacol
Piv	Pivaloyl group
pK_a	Acid dissociation constant
ppm	Parts per million
<i>i</i>Pr	<i>iso</i> -Propyl group

PTC	Phase-Transfer catalysis
<i>p</i>-TsOH	<i>para</i> -Toluenesulfonic acid
q	Quadruplet
QTOF	Quadrupole time of flight
QuinoxP*	Chiral 2,3-Bis(tert-butylmethylphosphino)quinoxaline
R	Alkyl group or substituent
RCM	Ring-closing metathesis
rt	Room temperature
S_N	Nucleophilic substitution reaction
SPINOL	1,1'-Spirobiindane-7,7'-diol
t	Time
T	Temperature
TADA	Transannular Diels-Alder reaction
TBDPS	<i>tert</i> -Butyldiphenylsilyl
TBS	<i>tert</i> -Butyldimethylsilyl
<i>t</i>Bu	<i>tert</i> -Butyl group
Tf	Trifluoromethanesulfonate group
THF	Tetrahydrofuran
TLC	Thin layer chromatography
TMS	Trimethylsilyl
TRIP	3,3'-Bis(2,4,6-triisopropylphenyl)-1,1'-binaphthyl-2,2'-diyl hydrogenphosphate
Ts	Tosyl group
TS	Transition state
UPLC	Ultra performance liquid chromatography
VAPOL	2,2'-Diphenyl-(4-biphenanthrol)
X	Halogen or heteroatom
T₁	Retention time for the first enantiomer
T₂	Retention time for the second enantiomer

Resumen Extendido

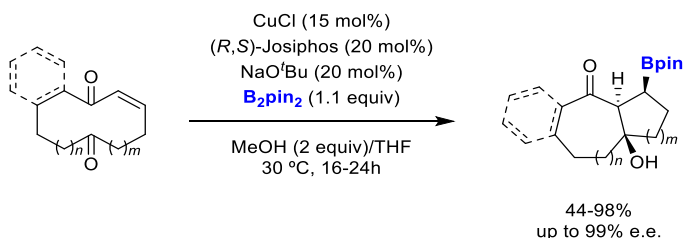
Las reacciones transanulares, por definición, son procesos químicos que tienen lugar entre dos puntos reactivos, que se encuentran en un mismo precursor cíclico, dando lugar a la formación de un nuevo enlace. En los últimos años, esta clase de reacciones han captado el interés de numerosos grupos de investigación, dentro del ámbito de la química sintética, ya que han demostrado ser una herramienta sintética eficiente para la preparación de estructuras policíclicas complejas de una forma sencilla, concisa y con un alto grado de economía de átomos.

Por lo que respecta al control de la estereoquímica en esta clase de transformaciones, la mayoría de los ejemplos desarrollados hasta ahora se basan en el uso de sustratos enantiopuros dando lugar a procesos diastereoselectivos mientras que el número de transformaciones enantioselectivas sigue siendo escaso. En este sentido, el grupo de investigación del Prof. José L. Vicario se ha centrado recientemente en el desarrollo de reacciones transanulares enantioselectivas mediante el uso de la organocatálisis. En línea con los trabajos de investigación realizados y dada la co-dirección de la presente tesis doctoral con la Prof. Elena Fernández, el objetivo principal de este trabajo se basa en encontrar sinergias entre los conocimientos de ambos grupos, combinando la reactividad transanular con la catálisis con boro. En la presente memoria se recogen los resultados más relevantes obtenidos durante el desarrollo de nuevas transformaciones transanulares catalíticas asimétricas para la síntesis estereoselectiva de estructuras complejas.

En un primer capítulo, se muestra un resumen de la revisión bibliográfica realizada acerca de las características más relevantes y el empleo de reacciones transanulares como estrategia sintética para la preparación de arquitecturas moleculares policíclicas como, por ejemplo, productos naturales o compuestos de interés biológico. A fin de tener una mejor contextualización del trabajo

desarrollado en esta tesis, se han detallado diversos ejemplos de reacciones transanulares clasificados en función de la metodología usada para el control de la estereoquímica y haciendo especial mención a los ejemplos de transformaciones catalíticas enantioselectivas desarrolladas con éxito hasta la fecha.

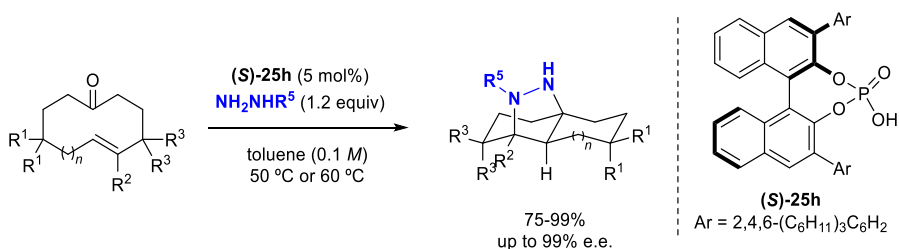
En un segundo capítulo, se describen los resultados obtenidos durante la investigación dirigida a estudiar la viabilidad de la secuencia de reacción de **borilación conjugada/aldólica transanular** en ceto-enonas cíclicas de tamaño medio. Para ello se ha evaluado el uso de un sistema catalítico basado en cobre, un ligando ferroceno y una base para promover la activación del B_2pin_2 , generando así una especie nucleófila Cu-Bpin susceptible de dar la adición conjugada sobre la enona. El paso clave para conseguir la transformación deseada es la formación de un enolato de cobre, favoreciendo la subsiguiente condensación aldólica transanular con la cetona electrófila presente en el sustrato de partida. Además, se ha estudiado la posibilidad de incorporar un ligando quiral en el sistema catalítico para el desarrollo de la versión enantioselectiva, obteniendo los correspondientes productos policíclicos con buenos rendimientos y enantioselectividades (Esquema 1).



Esquema 1. Secuencia de reacción de borilación conjugada/aldólica transannular desarrollada.

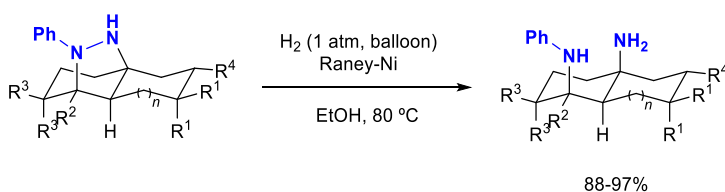
En un tercer capítulo, se recogen los principales resultados obtenidos durante el desarrollo de la primera reacción de **cicloadición (3+2) transanular enantioselectiva** de alquenonas cíclicas catalizada por ácidos fosfóricos quirales. Inicialmente se ha demostrado la capacidad de los sustratos para dar lugar a la reacción de cicloadición proyectada mediante la formación *in situ* de la hidrazona, permitiendo la posterior generación del correspondiente 1,3-dipolo que, en

presencia de un catalizador ácido de Brønsted quiral, reaccionará transanularmente con el alqueno presente en el sustrato de partida. Un análisis sistemático de los parámetros experimentales (hidracina, disolvente, concentración, temperatura...) así como la optimización de las características estructurales del catalizador, han permitido seleccionar el catalizador **(S)-25h** para la síntesis de compuestos policíclicos enantioenriquecidos con un esqueleto compuesto por un puente de pirazolidina (Esquema 2).



Esquema 2. Reacción de cicloadición (3+2) transanular desarrollada.

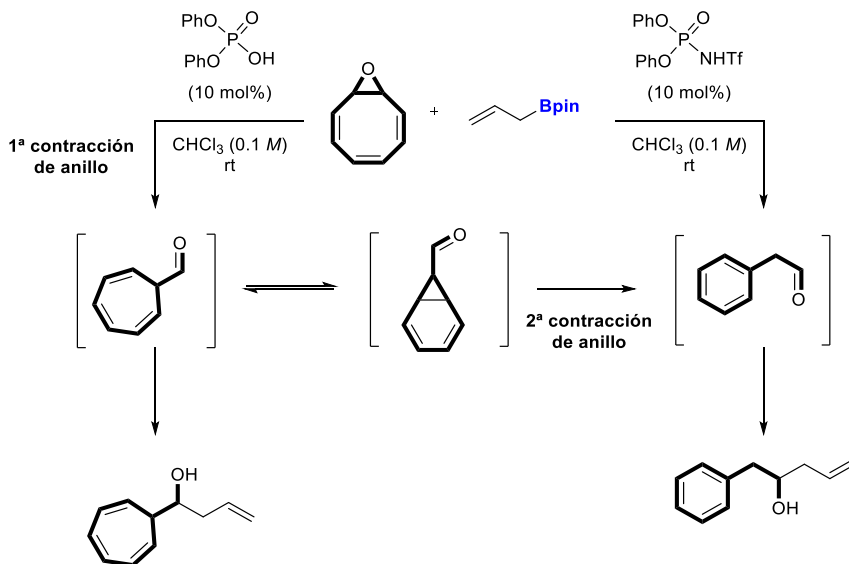
Los productos obtenidos como consecuencia de la reacción organocatalítica han sido transformados mediante la ruptura reductora del enlace N-N, para dar lugar a la síntesis de diversas 1,3-diaminas, con un control total de la estereoquímica y cuya estructura molecular es más difícil de obtener mediante metodologías más convencionales (Esquema 3).



Esquema 3. Funcionalización de los productos obtenidos.

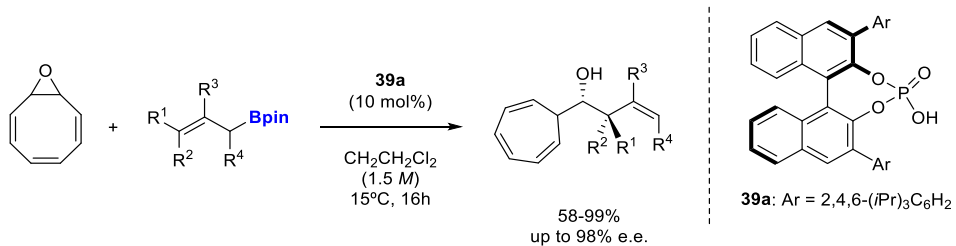
En un cuarto capítulo, se ha estudiado la reactividad del óxido de ciclooctatetraeno catalizada por ácidos de Brønsted. En la fase inicial del proyecto, se ha llevado a cabo el estudio del mecanismo del comportamiento conmutable observado para este sustrato específico, frente a la secuencia de reacción de

contracción de anillo/alilación catalizada por ácidos de distinta naturaleza. Para ello se ha establecido una colaboración con el grupo de investigación del Prof. Pedro Merino, en la Universidad de Zaragoza, para estudiar la influencia de la acidez en la transformación, mediante cálculos y experimentos, así como obtener una comprensión más profunda del mecanismo y los parámetros que determinan la selectividad del proceso resumido en el siguiente Esquema 4.



Esquema 4. Secuencia de reacción conmutable de contracción de anillo/alilación.

Asimismo, una vez adquiridos los conocimientos necesarios sobre la reacción proyectada, se ha desarrollado la versión asimétrica de la secuencia de contracción de anillo/alilación para la preparación enantioselectiva de alcoholes homoalílicos sustituidos con un cicloheptatrieno. Una extensa optimización de los parámetros de la reacción ha permitido seleccionar el ácido fosfórico (**R**)-**39a** como el catalizador idóneo para dar lugar al proceso de forma selectiva para la primera contracción de anillo, cuyo intermedio ha demostrado reaccionar eficientemente con diversos alilboranos mediante la reactividad descrita de alilación de aldehídos.



Esquema 5. Secuencia de reacción de contracción de anillo/alilación enantioselectiva.

Finalmente, en un último capítulo, se destacan las contribuciones científicas realizadas en otros proyectos, así como un breve resumen del trabajo desarrollado durante la estancia predoctoral de 3 meses en el grupo de investigación del Prof. Varinder K Aggarwal en la Universidad de Bristol (UK).

Papers

From part of the work presented in this manuscript the following publications have emerged:

1. “*Catalytic Stereoselective Borylative Transannular Reactions*”

Jana Sendra, Ruben Manzano, Efraim Reyes, Jose L. Vicario and Elena Fernández

Angew. Chem. Int. Ed. **2020**, 59, 2100.

2. “*Transannular Enantioselective (3+2) Cycloaddition of Cycloalkenone Hydrazones under Brønsted Acid Catalysis*”

Jana Sendra, Efraim Reyes, Liher Prieto, Elena Fernández and Jose L. Vicario

Org. Lett. **2021**, 23, 8738.

3. “*Switchable Brønsted Acid-Catalyzed Ring Contraction of Cyclooctatetraene Oxide towards the Enantioselective Synthesis of Cycloheptatrienyl-Substituted Homoallylic Alcohols and Oxaborinanes*”

Jana Sendra, Oriol Salvado, Manuel Pedrón, Efraim Reyes, Tomás Tejero, Elena Fernández, Pedro Merino and Jose L. Vicario

Manuscript submitted.

From part of the work presented as scientific collaborations the following publication has emerged:

4. “*Transition-Metal-Free Stereoselective Borylation of Allenamides*”

Lorena García, Jana Sendra, Núria Miralles, Efraim Reyes, Jorge J. Carbó,
Jose L. Vicario and Elena Fernández

Chem. Eur. J. **2018**, *24*, 14059.

Catalysis

 International Edition: DOI: 10.1002/anie.201913438
 German Edition: DOI: 10.1002/ange.201913438

Catalytic Stereoselective Borylative Transannular Reactions

Jana Sendra, Ruben Manzano, Efraim Reyes, Jose L. Vicario,* and Elena Fernández*

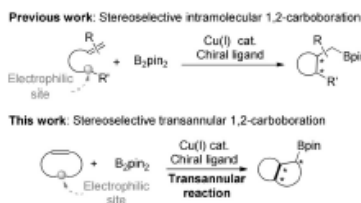
Dedicated to Prof. Sergio Castellón

Abstract: Medium-sized carbocycles containing an α,β -unsaturated ketone moiety as Michael acceptor site and a ketone moiety as internal electrophilic site are ideal substrates to conduct Cu(I)-catalyzed conjugated borylation followed by electrophilic intramolecular trapping that results into a pioneer transannular borylative ring closing reaction. The relative configuration of three adjacent stereocenters is controlled, giving access to a single diastereoisomer for a wide range of substrates tested. Moreover, when a chiral ligand is incorporated, the reaction provides enantioenriched polycyclic products with up to 99% ee.

Generating molecular complexity from simple starting materials is intrinsically associated to the task of organic synthesis. Often, these are a combination of several cyclic structures and, in this sense, chemists typically face the generation of such cyclic molecular scaffolds by using either cyclization or cycloaddition processes. As an alternative, transannular reactions in which the two reacting centers are tethered together as part of a macrocyclic starting material show up as an appealing alternative for the fast and reliable construction of complex polycyclic molecular scaffolds.^[1] In fact, several research groups have demonstrated that transannular reactions can be an excellent strategic decision when designing the synthesis of complex natural products.^[2] However, in almost all cases, the reported examples make use of chiral starting materials, therefore relying on substrate control during the diastereoselective generation of new stereocenters. On the other hand, catalytic and enantioselective variants of transannular reactions are limited to a handful of examples. In particular, and after the seminal report by Jacobsen dealing with an elegant example of a transannular Diels–Alder reaction under chiral oxazaborolidine catalysis,^[3] only four additional transformations have been reported up to date. Jacobsen himself described an enantioselective transannular ketone–ene reaction using a salen–Cr(III) Lewis acid catalyst^[4] and Hierseman has reported the use of Cu(II)-

bis-oxazoline complexes as catalysts in a transannular Claisen rearrangement.^[5] Alternatively, enamine catalysis has been used by List in a transannular aldol reaction,^[6] and some of us have also very recently reported one example of a catalytic and enantioselective transannular Morita–Baylis–Hillman reaction under chiral phosphine catalysis.^[7]

On the other hand, borylative ring closing of functionalized alkenes bearing internal electrophilic sites appears as a very efficient strategy for the strategic construction of carbocycles. There are many literature examples involving borylative cyclization of enynes, enediyne, allenynes, and enallenes under Pd, Au, Rh, or Ni catalysis that show the excellent performance of this approach.^[8] On the contrary, copper-catalyzed borylative ring closing reactions that take place through C–B bond formation with concomitant C–C coupling based on the 1,2-carboration concept has been more scarcely studied (Scheme 1, top). Most of the reactions



Scheme 1. Catalytic enantioselective borylative ring closing reactions.

reported involve borylcupration of the alkene followed by intramolecular nucleophilic substitution,^[9] together with some limited examples in which the internal electrophile reacting with the alkylcuprate intermediate is a carbonyl-based functionality^[10] or an imine.^[11] There are also some examples in which chiral ligands are incorporated to achieve enantiocontrol.^[12] On the contrary, examples of borylative ring closing reactions that involve an initial conjugated borylation process that generates a copper enolate intermediate that is subsequently trapped by the internal electrophile is restricted to just three limited examples in the literature.^[13]

In view of these precedents, we envisaged the possibility of developing transannular reactions initiated by a copper catalyzed borylation/ring closing process on a macrocyclic substrate containing an α,β -unsaturated ketone as suitable moiety for the initial conjugated borylation reaction and

[*] J. Sendra, Dr. E. Fernández
 Department Química Física I Inorgánica, University Rovira i Virgili
 C/ Marcel·lí Domingo s/n (Spain)
 E-mail: mariaelena.fernandez@urv.cat
 J. Sendra, Dr. R. Manzano, Dr. E. Reyes, Dr. J. L. Vicario
 Department of Organic Chemistry II, University of the Basque
 Country (UPV/EHU)
 P.O. Box 644, 48080 Bilbao (Spain)
 E-mail: joseluis.vicario@ehu.es

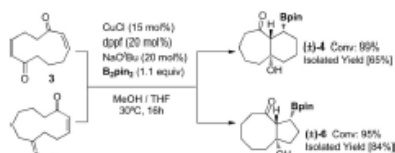
Supporting information and the ORCID identification number(s) for the author(s) of this article can be found under:
<https://doi.org/10.1002/anie.201913438>.

a ketone as internal electrophilic site to promote the transannular process (see Scheme 1, bottom). The addition of a chiral ligand at the Cu(I) catalyst would also provide an opportunity to control the stereochemical outcome of the concomitant C–B and C–C bond forming steps, enabling an overall enantioselective transannular reaction, which would significantly expand the toolbox of chemical synthesis through different manipulations of the stereogenic alkyl boronate.^[14]

We first started our work by evaluating the viability of the envisaged domino conjugated borylation–transannular aldol reaction using (*Z*)-cyclodec-2-ene-1,6-dione (**1**) as a suitable model compound that would lead to the formation of adduct **2** showing an octahydroazulenone-type architecture, which is a general motif present in a variety of natural products and bioactive compounds.^[15] We decided to use the catalytic system based on CuCl/base to promote the activation of B₂pin₂ through α -bond metathesis step.^[16] As it can be seen in Table 1, the projected transannular reaction took place smoothly with NaOtBu or KOtBu as bases (entries 1–2), providing the borylated bicyclo[5.3.0]decane adduct (\pm)-**2** as a single diastereoisomer generating three consecutive stereocenters. Interestingly, no reactivity was observed when NaOMe was the base of choice (entry 3). Since NaOtBu resulted the most efficient base, we next explored the influence of several mono- and diphenylphosphines in the reaction outcome. It was found that PPh₃, P^t(Bu)₃, dppe and dppf, were convenient ligands to achieve high conversions and isolated yields, keeping the formation of the bicyclic product as a single diastereoisomer (entries 4–8). Under optimized reaction conditions, other copper (I) sources were employed without any significant improvement (entries 9, 10), whereas no product formation was detected using a Cu(II) salt or in

the absence of copper catalysts (entries 11, 12). Interestingly, in all the examples, the reaction was fully regioselective, in line with our initial hypothesis that expected an initial β -boration of the enone to generate a copper enolate intermediate.

The precise arrangement of the relative position of the functional groups in undecane macrocyclic architectures also allowed to convert substrate (*Z*)-cycloundec-7-ene-1,6-dione (**3**) and (*Z*)-cycloundec-2-ene-1,6-dione (**5**) into the corresponding adducts with the bicyclo[5.4.0]undecane structure (\pm)-**4** and bicyclo[6.3.0]undecane core (\pm)-**6**, respectively, in both cases as single diastereoisomers (Scheme 2).



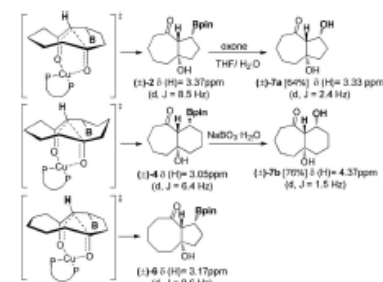
Scheme 2. Cu-catalyzed diastereoselective borylative transannular reaction of substrates **3** and **5**.

The highly diastereoselective aldol reaction might be explained by the preferred formation of a chelated (*Z*)-configured cyclic copper enolate intermediate (Scheme 3). The relative stereochemistry has been assigned by comparison of the ¹H NMR spectra of the three new products. The bicyclo[5.3.0]decane adduct (\pm)-**2** has a characteristic doublet at 3.37 ppm for H_a with a coupling constant value (*J* = 8.5 Hz) indicative of this proton being *cis*-axial/equatorial and to the adjacent proton (confirmed by the X-ray structure of a derivative compound, see Supporting Information). Similarly, the ¹H NMR spectrum for (\pm)-**4** and (\pm)-**6** shows a doublet for H_a at 3.05 ppm and 3.17 ppm, respectively, with similar coupling constant values (*J* = 6.4 Hz and *J* = 8.6 Hz) (Scheme 3). These values are in contrast to the typical *trans*-axial coupling constants for similar products.^[17] When

Table 1. Cu-catalyzed diastereoselective borylative transannular reaction of model substrate **1**.^[a]

Entry	Cu catalyst	Base	Ligand	Conv [%] ^[b]	Y [%] ^[c]
1	CuCl	NaOtBu	–	92	–
2	CuCl	KOtBu	–	63	–
3	CuCl	NaOMe	–	0	–
4	CuCl	NaOtBu	PPh ₃	99	–
5	CuCl	NaOtBu	PCy ₃	82	–
6	CuCl	NaOtBu	P ^t (Bu) ₃ ^[d]	99 [91]	–
7	CuCl	NaOtBu	dppe	99	–
8	CuCl	NaOtBu	dppf	99 [86]	–
9	CuI	NaOtBu	dppf	45	–
10	[Cu(CH ₃ CN) ₂] ⁺ OTf [–]	NaOtBu	dppf	91	–
11	CuO	NaOtBu	dppf	0	–
12	–	NaOtBu	dppf	0	–

[a] Reactions were performed with 0.1 mmol of substrate, with Cu catalyst (15 mol %), base (20 mol %), ligand (20 mol %), B₂pin₂ (1.1 equiv), THF (6 mL), MeOH (2 equiv), at 30°C, 16 h. [b] Conversion calculated by NMR using naphthalene as internal standard. [c] Y: isolated yields of pure product after column chromatography. [d] 15 mol % of ligand was used.



Scheme 3. Proposed stereochemical models and conversion of borylated adducts into diols.

adducts (\pm)-**2** and (\pm)-**4** were oxidized, the corresponding diols (\pm)-**7a** and (\pm)-**7b** show doublets for H_a at 3.33 ppm and 4.37 ppm, respectively, and coupling constants values about $J = 2.4$ Hz and $J = 1.5$ Hz, suggesting a quasi-coplanar disposition of the two adjacent protons probably due to the repulsion of the *cis* diol moieties.

In order to establish the general behavior of the diastereoselective conjugated borylation-transannular aldol reaction, we first focused on macrocycles with cyclodec-2-en-1,6-dione architectures that contain fused aromatic systems with diverse substitution patterns. All these substrates were efficiently converted into the corresponding borylated tricyclic products under optimized conditions as single diastereoisomers (Table 2).

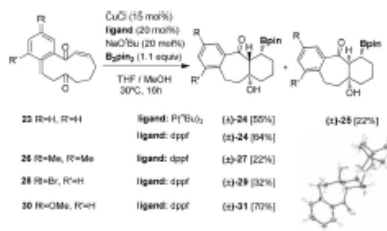
Table 2: Scope of the diastereoselective Cu/dppf diastereoselective borylative transannular reaction.^[a]

Entry	Substrate	Product	Conversion [%] ^[b] [Y %] ^[c]
1			99 [86]
2			90 [31]
3			96 [47]
4			99 [46]
5			95 [60]
6			99 [71]
7			99 [58]

[a] Reactions were performed with 0.2 mmol of substrate, with Cu catalyst (5 mol%), NaOtBu (20 mol%), dppf (20 mol%), B₂pin₂ (1.1 equiv), THF (6 mL), MeOH (2 equiv), at 30 °C, 16 h. [b] Conversion calculated by NMR using naphthalene as internal standard. [c] [Y]: isolated yields of pure product.

For those substrates with a fused arene at the enone moiety the isolated yield of the bicyclic adduct was strongly dependent on the nature of the substituents at the aryl core, although in all cases the reaction proceeded cleanly towards full conversion towards the corresponding borylated transannular product as indicates by NMR analysis (entries 1–4). When this fused aromatic ring was located next to the ketone group, that plays the role of the internal electrophilic site, the expected borylated adducts were obtained with higher isolated yields possibly due to the higher stabilization of the products (entries 5,6). On the other hand, the presence of two fused arene moieties next to both the enone and to the ketone in **20**, provided tetracyclic product (\pm)-**21** with only one stereocenter (entry 7), presumably as a consequence of a dehydration process favoured by the highly conjugated nature of this final product.

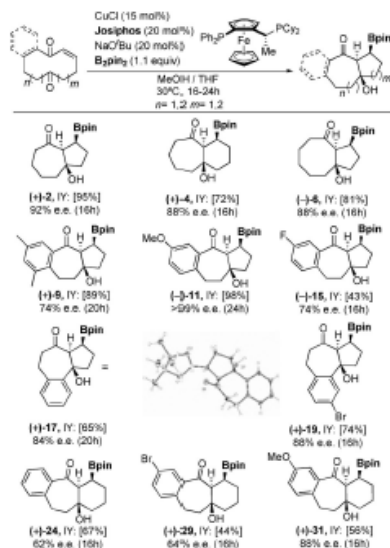
With a view to complete the substrate scope, we conducted the Cu/dppf catalyzed borylative transannular reaction of cycloundec-2-en-1,7-dione macrocyclic substrates toward the diastereoselective formation of bicyclo[5.4.0]undecane scaffolds (Scheme 4). These substrates also



Scheme 4. Cu-catalyzed diastereoselective borylative transannular reaction on cycloundecane substrates.

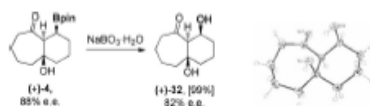
contain a fused aromatic group adjacent to the enone moiety with different substitution patterns. The control on the diastereoselectivity was complete for all substrates explored when dppf was used as ligand, despite the fact that, as it was observed before, isolated yields were dependent on the nature of the substituents at the arene moiety. In the case of substrate **23**, when P(*n*Bu)₃ was used as ligand, the expected product (\pm)-**24** was formed in 55 % together with a minor amount of its diastereoisomer (\pm)-**25** that could be fully characterized by X-ray analysis (Scheme 4).

Finally, to demonstrate the feasibility of developing enantioselective variants of this diastereoselective borylative transannular reaction, macrocycle **1** was subjected to standard reaction conditions using a type of Josiphos chiral ligand (Scheme 5).^[9] Interestingly, in addition to the complete diastereoselectivity observed, high levels of asymmetric induction could be achieved (92 % ee for (+)-**2**). The absolute stereostructure of the enantiomers was established by single-crystal X-ray analysis of an enantiopure sample of (+)-**17** (Scheme 5).



Scheme 5. Cu-catalyzed enantioselective transannular conjugate borylation/aldol cyclization with decane and undecane macrocyclic substrates.

Synthetic manipulations on compound (+)-4 as representative model of the enantio-enriched polycyclic products prepared was also surveyed (Scheme 6). In particular, oxidative protocol was explored which proceeded with complete stereochemical retention from C–B to C–OH bond.



Scheme 6. Stereospecific C–B bond oxidation of (+)-4.

In conclusion, we have shown that copper-catalyzed conjugate borylation can be used to trigger highly diastereoselective transannular reactions that enable the construction of complex bicyclic scaffolds such as the azulene core in a simple and straightforward manner. Furthermore, the reaction can also be carried out in a highly enantioselective fashion through the incorporation of a chiral ligand in the catalytic system. The practical synthetic utility of this transformation is noteworthy considering the possibilities for the alkyl boronate unit to undergo stereospecific transformations.

Acknowledgements

This research was supported by the Spanish Ministerio de Ciencia, Innovación y Universidades (MCIU) through projects FEDER-CTQ2016-80328-P and FEDER-CTQ2017-83633-P and by the Basque Government (IT908-16). J.S. acknowledges the Spanish MCIU for an FPI fellowship and R.M. acknowledges the Basque Government for a postdoctoral contract. We thank AllyChem for the gift of diboranes.

Conflict of interest

The authors declare no conflict of interest.

Keywords: copper catalysts · electrophilic intramolecular trapping · ring closing · stereogenic alkyl boronate · transannular borylation

How to cite: *Angew. Chem. Int. Ed.* 2020, 59, 2100–2104
Angew. Chem. 2020, 132, 2116–2120

- [1] For some reviews, see: a) E. Marsault, A. Toro, P. Nowak, P. Deslongchamps, *Tetrahedron* 2001, 57, 4243; b) S. Handa, G. Pattenden, *Contemp. Org. Synth.* 1997, 4, 196; c) A. M. Montaña, C. Batalla, J. A. Barcia, *Curr. Org. Chem.* 2009, 13, 919; d) A. Rizzo, S. R. Harutyunyan, *Org. Biomol. Chem.* 2014, 12, 6570.
- [2] For a focused review, see: E. Reyes, U. Uria, L. Carrillo, I. L. Vicario, *Tetrahedron* 2014, 70, 9461.
- [3] E. P. Balkus, E. N. Jacobsen, *Science* 2007, 317, 1736.
- [4] N. S. Rajapaksa, E. N. Jacobsen, *Org. Lett.* 2013, 15, 4238.
- [5] T. Jaschinski, M. Hiersemann, *Org. Lett.* 2012, 14, 4114.
- [6] a) C. L. Chandler, B. List, *J. Am. Chem. Soc.* 2008, 130, 6737; There is also one example of an enantioselective transannular aldol reaction using stoichiometric amounts of a chiral metal alkoxide as Brønsted base; b) O. Knopff, J. Kühne, C. Fehr, *Angew. Chem. Int. Ed.* 2007, 46, 1307; *Angew. Chem.* 2007, 119, 1329.
- [7] R. Mako, R. Manzano, E. Reyes, L. Carrillo, U. Uria, I. L. Vicario, *J. Am. Chem. Soc.* 2019, 141, 9495.
- [8] For an excellent review on this concept see: E. Buñuel, D. J. Cárdenas, *Chem. Eur. J.* 2016, 22, 5446.
- [9] For a review, see: a) K. Kubota, H. Iwamoto, H. Ito, *Org. Biomol. Chem.* 2017, 15, 285; For some examples: b) H. Ito, T. Toyoda, M. Sawamura, *J. Am. Chem. Soc.* 2010, 132, 5990; c) K. Kubota, E. Yamamoto, H. Ito, *J. Am. Chem. Soc.* 2013, 135, 2635; d) J. Royes S. Ni, A. Farre, E. La Cascia, J. J. Carbó, A. B. Cuenca, F. Maseras, E. Fernández, *ACS Catal.* 2018, 8, 2833; e) Y.-J. Zuo, X.-T. Chang, Z.-M. Hsu, C.-M. Zhong, *Org. Biomol. Chem.* 2017, 15, 6323.
- [10] a) E. Yamamoto, R. Kojima, K. Kubota, H. Ito, *Synlett* 2015, 26, 272; b) A. Whyte, K. I. Burton, J. Zhang, M. Lautens, *Angew. Chem. Int. Ed.* 2018, 57, 13927; *Angew. Chem.* 2018, 130, 14123; c) A. R. Burns, S. González, H. W. Lam, *Angew. Chem. Int. Ed.* 2012, 51, 10827; *Angew. Chem.* 2012, 124, 10985; d) A. Whyte, B. Mirabi, A. Torelli, L. Prieto, J. Bajohr, M. Lautens, *ACS Catal.* 2019, 9, 9253; e) A. Whyte, A. Torelli, B. Mirabi, M. Lautens, *Org. Lett.* 2019, <https://doi.org/10.1021/acsorglett.9b03144>.
- [11] a) H.-M. Wang, H. Zhou, Q.-S. Xu, T.-S. Liu, C.-L. Zhuang, M.-H. Shen, H.-D. Xu, *Org. Lett.* 2018, 20, 1777; b) G. Zhang, A. Cang, Y. Wang, Y. Li, G. Xu, Q. Zhang, T. Xiong, Q. Zhang, *Org. Lett.* 2018, 20, 1798.



- [12] a) H. Ito, Y. Kosaka, K. Nonoyama, Y. Sasaki, M. Sawamura, *Angew. Chem. Int. Ed.* **2008**, *47*, 7424; *Angew. Chem.* **2008**, *120*, 7534; b) C. Zhong, S. Kunii, Y. Kosaka, M. Sawamura, H. Ito, *J. Am. Chem. Soc.* **2010**, *132*, 11440; c) See also refs. [10b–d] and [11b].
- [13] M. Tobisu, H. Fujihara, K. Koh, N. Chatani, *J. Org. Chem.* **2010**, *75*, 4841. See also refs. [9e] and [10c].
- [14] a) *Boronic Acids: Preparation and Applications in Organic Synthesis, Medicine and Materials*, 2nd ed. (Eds.: D. G. Hall), Wiley-VCH, Weinheim, **2011**; b) *Synthesis and Applications of Organoboron Compounds: Topics in Organometallic Chemistry*, Vol. 49 (Eds.: E. Fernández, A. Whiting), Springer, Berlin, **2015**; c) E. C. Neeve, S. J. Geier, I. A. I. Mkhaliid, S. A. Westcott, T. B. Marder, *Chem. Rev.* **2016**, *116*, 9091.
- [15] a) B. M. Fraga, *Nat. Prod. Rep.* **2004**, *21*, 669; b) G. Rücker, *Angew. Chem. Int. Ed. Engl.* **1973**, *12*, 793; *Angew. Chem.* **1973**, *85*, 895.
- [16] J. Cid, H. Gulyás, I. J. Carbó, E. Fernández, *Chem. Soc. Rev.* **2012**, *41*, 3558.
- [17] K. Agapiou, D. F. Cauble, M. J. Krische, *J. Am. Chem. Soc.* **2004**, *126*, 4528.
- [18] See Supporting Information for screening of chiral ligands.

Manuscript received: October 21, 2019

Accepted manuscript online: November 15, 2019

Version of record online: December 18, 2019

Transannular Enantioselective (3 + 2) Cycloaddition of Cycloalkenone Hydrzones under Brønsted Acid Catalysis

Jana Sendra, Efraim Reyes, Liher Prieto, Elena Fernández,* and Jose L. Vicario*

Cite This: *Org. Lett.* 2021, 23, 8738–8743

Read Online

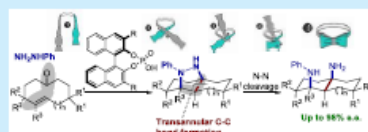
ACCESS |

Metrics & More

Article Recommendations

Supporting Information

ABSTRACT: Hydrzones derived from cycloalkenones undergo an enantioselective transannular formal (3 + 2) cycloaddition catalyzed by a chiral phosphoric acid. The reaction provides high yields and excellent stereoselectivity in the formation of complex adducts with one or two α -tertiary amine moieties at the ring fusion, and these can be converted into very versatile stereodefined decalin- or octahydro-1H-indene-derived 1,3-diamines through simple reductive N–N cleavage.



Downloaded via UNIV DEL PAIS VASCO on January 16, 2023 at 15:09:55 (UTC).
See <https://pubs.acs.org/sharingguidelines> for options on how to legitimately share published articles.

Transannular reactions, in which two reacting sites are connected to each other as part of a medium- or large-size cyclic starting material, represent an unconventional strategic decision in organic synthesis that enables the rapid construction of complex polycyclic molecular scaffolds.¹ In fact, there are many reports of elegant total syntheses that make use of transannular reactions to build up the key structural framework of the final target,² including several examples of biomimetic approaches that show that this type of reactivity is also operating as part of the portfolio of chemical reactions in the secondary metabolism of living cells. Despite all of the advances in the area, the majority of the reports still rely on the use of chiral cyclic substrates as starting materials, therefore involving the diastereoselective generation of new stereogenic centers during the transannular process.³ This implies that the stereochemical outcome of the reaction is strictly under substrate control, and consequently, it is largely conditioned by the innate asymmetric induction profile of the chiral starting material. In contrast, enantioselective versions of transannular reactions have received very little attention, and only a few limited reports can be found in the literature that comprise a couple of examples in which stoichiometric amounts of a chiral ligand or promoter are used in transannular aldol⁴ or Rauhut–Currier reactions.⁵ Catalytic and enantioselective transannular reactions are limited to three cases of transformations under Lewis acid catalysis, such as transannular Diels–Alder,⁶ ketone–ene,⁶ and Claisen rearrangement,⁷ and to one example of a transannular aldol reaction under enamine catalysis.⁸ On the contrary, and very recently, we also demonstrated the excellent performance of catalytic transannular reactions in the enantioselective synthesis of complex polycyclic systems with the development of a transannular Morita–Baylis–Hillman reaction under chiral phosphine catalysis,⁹ a Michael-initiated cascade reaction under bifunctional tertiary amine/squaramide catalysis,¹⁰ and

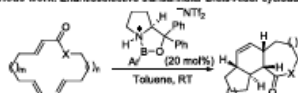
a copper-catalyzed transannular borylative ring-closing process.¹¹

We present herein the use of hydrzones derived from cycloalkenones as substrates that undergo enantioselective transannular (3 + 2) cycloaddition¹² under catalysis by a BINOL-based chiral Brønsted acid (Scheme 1, bottom).

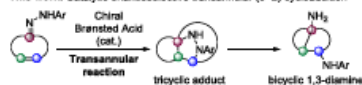
In comparison with the only existing literature precedent of an enantioselective transannular cycloaddition (the transannular Diels–Alder cycloaddition developed by Jacobsen and coworkers shown in Scheme 1, top),⁶ this new reaction leads to tricyclic scaffolds with a bridging hydrazine moiety,

Scheme 1. Enantioselective Transannular Diels–Alder Reaction and the Brønsted-Acid-Catalyzed Transannular (3 + 2) Cycloaddition of Cycloalkenone Hydrzones

Previous work: Enantioselective transannular Diels–Alder cycloaddition



This work: Catalytic enantioselective transannular (3+2) cycloaddition



Received: September 20, 2021

Published: November 2, 2021



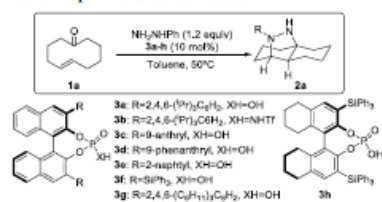
Organic Letters

pubs.acs.org/OrgLet

Letter

therefore providing a direct alternative entry to compounds whose structures resemble the type of adducts that can be accessed through type-II intramolecular cycloadditions.¹³ Remarkably, the adducts obtained through this transannular (3 + 2) cycloaddition are direct precursors to orthogonal and stereodefined bicyclic 1,3-diamines, which are key structural motifs in many natural products and also serve as highly versatile chiral building blocks in synthetic organic chemistry.¹⁴ Finally, it should also be pointed out that the number of examples of catalytic and enantioselective (3 + 2) cycloadditions between hydrazones and alkenes is very scarce, in most cases involving electron-poor *N*-acyl hydrazones together with electronically biased alkenes as dipolarophiles, such as enol ethers and thioethers, styrenes, or cyclopentadiene.¹⁵

We first started our work by evaluating the viability of the reaction using ketone **1a** as a model substrate and phenylhydrazine, envisaging the *in situ* formation of the hydrazone intermediate that would subsequently undergo the transannular (3 + 2) cycloaddition (Table 1).

Table 1. Optimization of the Reaction^a

entry	catalyst	T (°C)	conv. (%) ^b	e.e. (%) ^c
1	(PhO) ₂ P(O)OH	r.t.	<5 ^d	
2	(PhO) ₂ P(O)OH	50	99 (72)	
3	3a	50	99	85
4	3b	50	55	25
5	3c	50	99	33
6	3d	50	99	23
7	3e	50	99	17
8	3f	50	99 (92)	88
9	3g	50	99 (99)	98
10	3h	50	99 (90)	90
11	3g	r.t.	<5 ^d	n.d.
12 ^e	3g	50	99 (99)	96

^aReactions were performed with 0.15 mmol of **1a**, NH₂NHR (1.2 equiv), catalyst (10 mol %), and toluene (0.1 M) as the solvent. ^bConversion was calculated by ¹H NMR using 1,3,5-trimethoxybenzene as the internal standard. Isolated yield after flash column chromatography purification is given in parentheses. ^ce.e. was calculated by HPLC in the chiral stationary phase after derivatization into the corresponding benzoyl hydrazone. (See the Supporting Information.) n.d., not determined. ^dStarting material was recovered as the corresponding hydrazone. ^e5 mol % of catalyst was used.

As can be seen in this table, the reaction using diphenylphosphoric acid as the catalyst at room temperature (r.t.) was unsuccessful (entry 1), but heating the mixture to 50 °C resulted in the complete conversion of the starting material and a good isolated yield of the desired cycloaddition product (entry 2). We next moved to the archetypal chiral BINOL-based phosphoric acid TRIP,¹⁶ which also was demonstrated

to be a good catalyst for the transformation of **1a** into **2a**, the latter being formed with 85% e.e. (entry 3). We also surveyed the corresponding *N*-Tr sulfonamide **3b** as a more acidic and potentially more active catalyst but with poorer results (entry 4). Next, phosphoric acid catalysts with different substituents at the 3- and 3'-positions of the BINOL core were surveyed (entries 5–7).¹⁷ We observed that placing extended aryl moieties led to a significant decrease in the enantioselectivity (entries 5–7), whereas moving to the SiPh₃-containing catalyst **3f** resulted in the formation of adduct **2a** with a high 88% e.e. (entry 8). Improved enantioselectivity was obtained using either the bulkier analogue of TRIP (catalyst **3g**, entry 9) or its partially hydrogenated version (catalyst **3h**, entry 10). We observed the best result with the former. We also tested the reaction with this catalyst at lower temperature, verifying the need for 50 °C for quantitative cycloaddition (entry 11). Finally, we also observed that the reaction performed excellently using a 5 mol % catalyst loading (entry 12).

With a robust experimental protocol in hand, we next focused on studying the scope and limitations of the reaction, starting with the role played by the nature of the hydrazone substituent (Table 2).

Table 2. Scope of the Reaction: Hydrazone Component^a

$\text{1a} \xrightarrow[\text{Toluene, 50}^\circ\text{C}]{\text{NH}_2\text{NHR (1.2 equiv), 3h (5 mol\%)}} \text{2a-h}$

entry	R	yield (%) ^b	e.e. (%) ^c
1	C ₆ H ₅ (2a)	99	96
2	C ₆ F ₅ (2b)	96	90
3	4-CF ₃ C ₆ H ₄ (2c)	95	83
4	4-BzC ₆ H ₄ (2d)	84	96
5	3,5-(CF ₃) ₂ C ₆ H ₃ (2e)	90	72
6	4-MeC ₆ H ₄ (2f)	99	94
7	4-MeOC ₆ H ₄ (2g)	<5 ^d	n.d.
8	C(O)C ₆ H ₅ (2h)	85	0
9 ^e	C(O)C ₆ H ₅ (2h)	40	0
10 ^f	Ts	<5	n.d.
11	Ba	<5 ^d	n.d.

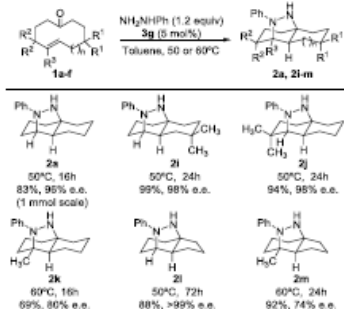
^aReactions were performed with 0.15 mmol of **1a**, NH₂NHR (1.2 equiv), **3g** (5 mol %), and toluene (0.1 M) at 50 °C. ^bIsolated yield after flash column chromatography purification. ^ce.e. was calculated by HPLC in the chiral stationary phase after derivatization into the corresponding benzoyl or acetyl hydrazone. (See the Supporting Information.) ^dStarting material was recovered as the corresponding hydrazone. ^eReaction carried out at r.t.

Arylhydrazines with electron-withdrawing substituents performed excellently, providing the transannular cycloaddition products **2a–e** in excellent yields with excellent enantioselectivities (entries 1–5), with the only exception being the use of *meta*-bis-CF₃-substituted hydrazone (entry 5), which provided adduct **2e** with somewhat lower e.e. When tolylhydrazone was used, the reaction also took place very efficiently (entry 6), but when the more electron-donating *para*-methoxyphenylhydrazone was tested, the reaction was completely suppressed, isolating the hydrazone formed upon condensation of the hydrazide with the starting material (entry 7). *N*-Benzoylhydrazone was also tested, and we observed a remarkably fast reaction and the quantitative conversion to the cycloaddition product **2h**, albeit as a completely racemic

material (entry 8). We tested the reaction at a lower temperature to favor the enantioselective pathway but without any improvement and with a remarkable drop in the yield (entry 9). Alkyl hydrazones were also unreactive under these conditions. (See one example in entry 10.)

Several cycloalkenones were also surveyed in the transformation in combination with phenylhydrazine (Table 3).

Table 3. Scope of the Reaction: Cyclic Ketone Reagent^a



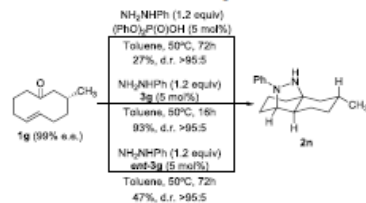
^aReactions were performed with 0.15 mmol of 1a–f, NH_2NHPh (1.2 equiv), **3g** (5 mol %), and toluene (0.1 M) at the indicated temperature. Isolated yields after flash column chromatography purification are given. e.e. was calculated by HPLC in the chiral stationary phase after derivatization into the corresponding benzoyl or acetyl hydrazone. (See the Supporting Information.)

Initially, we tested the reaction on a higher 1.0 mmol scale of model substrate **1a** to guarantee its viability for preparative purposes. As can be seen in Table 3, adduct **2a** was obtained in good yield (83%) and with the same enantioselectivity (96% e.e.) as before. We also evaluated cycloalkenones **1a–f** with different sizes and substitution patterns. As can also be seen in Table 3, in all cases, the reaction provided the corresponding tricyclic adducts in excellent yields with excellent enantioselectivities. This transformation enables the preparation of adducts with an octahydro-2*H*-1,4*a*-epidiazanonaphthalene core, including the possibility of incorporating different substituents at the carbon scaffold (compounds **2a**, **2i**, **2j**, and **2k**). Moreover, the reaction leading to adducts with an octahydro-3*a*,7-epidiazainoindene core (compounds **2l** and **2m**) was also very efficient. Remarkably, this transformation also allows the generation of challenging structures such as **2k** and **2m**, in which two α -tertiary hydrazine stereogenic centers are simultaneously generated in excellent yield with high stereocontrol.

The absolute configuration of **2j** was determined by X-ray analysis of the corresponding *N*-benzoyl derivative (see the Supporting Information for details), and the configurations of all other adducts **2a–m** were established based on mechanistic analogy. This configuration is also in agreement with the reported stereochemical model for the intermolecular addition of activated alkenes to hydrazones under phosphoric acid catalysis.^{15*b*}

We also evaluated the performance of chiral substrate **1g** to get further insight into the natural reactivity trend of this type of cycloalkenones toward the transannular cycloaddition reaction (Scheme 2). In fact, the reaction of **1g** under

Scheme 2. Use of Chiral Ketone **1g** as the Substrate



activation by the achiral catalyst diphenylphosphoric acid cleanly furnished adduct **2n** as a single diastereoisomer, although in a rather low yield, even after a prolonged reaction time. On the contrary, the reaction catalyzed by **3g** proceeded smoothly to form the same compound in a much higher yield, whereas the reaction performed using its enantiomer (*R*)-**3g** as a catalyst also provided the same diastereoisomer but, again, in a much lower yield. These experiments indicate a strong stereochemical bias exerted by the chiral information of the starting material, although with a very important matched/mismatched situation when incorporating a chiral Brønsted acid to promote the reaction.

Finally, we decided to unmask the latent 1,3-diamine functionality present on adducts **2**, which are obtained through the enantioselective transannular cycloaddition process (Table 4). The particular arrangement of nitrogen atoms in these adducts would lead to the formation of compounds with a decaline or octahydro-1*H*-indene molecular architecture that would contain two amine substituents located in pseudoaxial positions, which is a molecular arrangement that is difficult to obtain through conventional approaches. This was accomplished by carrying out the hydrogenolytic cleavage of the *N–N* bond by reacting these adducts with hydrogen under Raney nickel catalysis. We initially optimized the reaction conditions using compound **2a** as a model substrate and obtained diamine **4a** in excellent yield when the reaction was carried out in ethanol at 80 °C (entry 1). We also verified that there was no loss of optical purity during the process by measuring the enantiomeric excess of the final product **4a** by high-performance liquid chromatography (HPLC) on a chiral stationary phase under conditions optimized for a racemic standard. With the optimized reductive cleavage conditions in hand, we generalized this reaction to the other adducts **2i–j**, obtaining in all cases the expected bicyclic 1,3-diamines **4b–g** in almost quantitative yields in most cases. As can be seen in Table 4, this approach enables the synthesis of octahydro-naphthalene-1,4*a*(2*H*)-diamines (entries 1–4 and 7) or octahydro-3*a**H*-indene-3*a*,7-diamines (entries 5 and 6) in excellent overall yields and as highly enantioenriched materials. This also includes the possibility of generating scaffolds containing two α -tertiary amine moieties that are challenging structures that cannot be accessed through conventional methodologies.¹⁸ In this case, these types of compounds were cleanly

Table 4. Reductive Cleavage of the Hydrazine Moiety: Synthesis of Enantioenriched 1,3-Diamines

Entry	Substrate	Product	Yield (%) ^a
1			98 ^b
2			92
3			91
4			88
5			93
6			97
7			90

^aIsolated yield after flash column chromatography. ^be.e. 92%

obtained from adducts **2k** and **2m** with high enantio- and diastereoselectivity. (See entries 4 and 6.)

In conclusion, we have demonstrated the ability of hydrazones derived from cycloalkenones to undergo enantioselective transannular formal (3 + 2) cycloaddition under catalysis by a chiral Brønsted acid derived from BINOL. This simple reaction provides stereodefined tricyclic adducts in high yields with high enantioselectivities, and these can be used as an ideal platform for the preparation of decaline- or octalhydro-1*H*-indene- derived 1,3-diamines with great potential to be used as synthetic intermediates or chiral ligands and that are otherwise challenging compounds to access through conventional methodologies. This type of enantioselective transannular reactivity can be established as an alternative and less conventional disconnection when planning the total synthesis of complex molecules.

■ ASSOCIATED CONTENT

Supporting Information

The Supporting Information is available free of charge at <https://pubs.acs.org/doi/10.1021/acs.orglett.1c03190>.

Experimental procedures, characterization of all new compounds, and copies of ¹H and ¹³C NMR spectra. HPLC traces of all adducts prepared and crystallographic data (PDF)

Accession Codes

CCDC 2091628 contains the supplementary crystallographic data for this paper. These data can be obtained free of charge via www.ccdc.cam.ac.uk/data_request/cif, or by emailing data_request@ccdc.cam.ac.uk, or by contacting The Cambridge Crystallographic Data Centre, 12 Union Road, Cambridge CB2 1EZ, UK; fax: +44 1223 336033.

■ AUTHOR INFORMATION

Corresponding Authors

Elena Fernández – *Departament Química Física i Inorgànica, Universitat Rovira i Virgili, 50009 Tarragona, Spain;*
orcid.org/0000-0001-9025-1791;
 Email: mariaelena.fernandez@urv.cat

Jose L. Vicario – *Department of Organic and Inorganic Chemistry, University of the Basque Country (UPV/EHU), 48080 Bilbao, Spain;*
orcid.org/0000-0001-6557-1777;
 Email: joselu.vicario@ehu.es

Authors

Jana Sendra – *Department of Organic and Inorganic Chemistry, University of the Basque Country (UPV/EHU), 48080 Bilbao, Spain;*
 Departament Química Física i Inorgànica, Universitat Rovira i Virgili, 50009 Tarragona, Spain

Efraim Reyes – *Department of Organic and Inorganic Chemistry, University of the Basque Country (UPV/EHU), 48080 Bilbao, Spain;*
orcid.org/0000-0003-2038-9925

Lihér Prieto – *Department of Organic and Inorganic Chemistry, University of the Basque Country (UPV/EHU), 48080 Bilbao, Spain;*
orcid.org/0000-0001-7965-7168

Complete contact information is available at:
<https://pubs.acs.org/doi/10.1021/acs.orglett.1c03190>

Notes

The authors declare no competing financial interest.

■ ACKNOWLEDGMENTS

This research was supported by the Spanish Ministerio de Ciencia, Innovación y Universidades (MCIU) through projects FEDER-PIID2020-118422-GB-I00, FEDER-PIID2019-109674-GB-I00 and FPI fellowship to J.S. and by the Basque Government (IT908-16). J.S. acknowledges the Spanish MCIU for an FPI fellowship.

■ DEDICATION

This work is dedicated to the memory of our colleague and friend Prof. Gilian Muñiz.

■ REFERENCES

(1) For some reviews, see: (a) Marsault, E.; Toro, A.; Nowak, P.; Deslongchamps, P. The transannular Diels–Alder strategy: applica-

- tions to total synthesis. *Tetrahedron* 2001, 57, 4243. (b) Handa, S.; Patzden, G. Free radical-mediated macrocyclizations and transannular cyclizations in synthesis. *Contemp. Contemp. Org. Synth.* 1997, 4, 196. (c) Montana, A. M.; Batalla, C.; Bacia, J. A. Intramolecular Haloetherification and Transannular Hydrocycloaddition of Alkenes. A Synthetic Methodology to Obtain Polycyclic Ethers and Amines. *Curr. Org. Chem.* 2009, 13, 919. (d) Rizzo, A.; Harutyunyan, S. R. Azabicycles construction: the transannular ring contraction with N-protected nucleophiles. *Org. Biomol. Chem.* 2014, 12, 6570.
- (2) For focused reviews, see (a) Reyes, E.; Uria, U.; Carrillo, L.; Vicario, J. L. Transannular reactions in asymmetric total synthesis. *Tetrahedron* 2014, 70, 9461. (b) Clarke, P. A.; Reeder, A. T.; Winn, J. Transannulation Reactions in the Synthesis of Natural Products. *Synthesis* 2009, 2009, 691.
- (3) Knopf, O.; Kühne, J.; Fehr, C. Enantioselective intramolecular aldol addition/dehydration reaction of a macrocyclic diketone: Synthesis of the musk odorants (R)-muscone and (R,Z)-5-Musconone. *Angew. Chem., Int. Ed.* 2007, 46, 1307.
- (4) Desmeci, A.; Selig, P. S.; Dornaal, R. A.; Spasov, K. A.; Anderson, K. S.; Miller, S. J. Quasi-biomimetic ring contraction promoted by a cysteine-based nucleophile: Total synthesis of Sch-642305, some analogs and their putative anti-HIV activities. *Chem. Sci.* 2011, 2, 1568.
- (5) Bálskus, E. P.; Jacobsen, E. N. Asymmetric catalysis of the transannular Diels-Alder reaction. *Science* 2007, 317, 1736.
- (6) Rajapaksa, N. S.; Jacobsen, E. N. Enantioselective catalytic transannular ketone-one reactions. *Org. Lett.* 2013, 15, 4238.
- (7) Jäschinski, T.; Hienemann, M. [1,6]-Transannular Catalytic Asymmetric Gostli-Claisen Rearrangement. *Org. Lett.* 2012, 14, 4114.
- (8) Chandler, C. L.; List, B. Catalytic asymmetric transannular aldolizations: Total synthesis of (+)-Himutene. *J. Am. Chem. Soc.* 2008, 130, 6737.
- (9) Mato, R.; Manzano, R.; Reyes, E.; Carrillo, L.; Uria, U.; Vicario, J. L. Catalytic Enantioselective Transannular Morita-Baylis-Hillman Reaction. *J. Am. Chem. Soc.* 2019, 141, 9495.
- (10) Mato, R.; Reyes, E.; Carrillo, L.; Uria, U.; Prieto, L.; Manzano, R.; Vicario, J. L. Catalytic enantioselective domino Michael/transannular aldol reaction under bifunctional catalysis. *Chem. Commun.* 2020, 56, 13149.
- (11) Sendra, J.; Manzano, R.; Reyes, E.; Vicario, J. L.; Fernández, E. Catalytic stereoselective borylative transannular reactions. *Angew. Chem., Int. Ed.* 2020, 59, 2100.
- (12) For selected reviews on enantioselective (3 + 2) cycloaddition reactions, see: (a) Trost, B. M.; Mata, G. Forging Odd-Membered Rings: Palladium-Catalyzed Asymmetric Cycloadditions of Trimethylenemethane. *Acc. Chem. Res.* 2020, 53, 1293. (b) Adrio, J.; Carreiro, J. C. Stereochemical diversity in pyrrolidine synthesis by catalytic asymmetric 1,3-dipolar cycloaddition of azomethine ylides. *Chem. Commun.* 2019, 55, 11979. (c) Mariché, K. O.; Doyle, M. P. Catalytic asymmetric cycloaddition reactions of enolizable compounds. *Org. Biomol. Chem.* 2019, 17, 4183. (d) Donda, H.; de Gracia Retamosa, M.; Sansano, J. Current trends towards the synthesis of bioactive heterocycles and natural products using 1,3-dipolar cycloadditions (1,3-DC) with azomethine ylides. *Synthesis* 2017, 49, 2819. (e) Brittain, W. D. G.; Buckley, B. R.; Fosey, J. S. Asymmetric copper-catalyzed azide-alkyne cycloadditions. *ACS Catal.* 2016, 6, 3629. (f) Narayan, R.; Potowski, M.; Ju, Z.-J.; Antonchick, A. P.; Wáldmann, H. Catalytic enantioselective 1,3-dipolar cycloadditions of azomethine ylides for biology-oriented synthesis. *Acc. Chem. Res.* 2014, 47, 1296. (g) Xing, Y.; Wang, N.-X. Organocatalytic and metal-mediated asymmetric [3 + 2] cycloaddition reactions. *Coord. Chem. Rev.* 2012, 256, 938. (h) Stanley, L. N.; Sibi, M. P. Enantioselective copper-catalyzed 1,3-dipolar cycloadditions. *Chem. Rev.* 2008, 108, 2887. (i) Le Manqand, P.; Tam, W. Enantioselective Palladium-Catalyzed Trimethylenemethane [3 + 2] Cycloadditions. *Angew. Chem., Int. Ed.* 2008, 47, 2926.
- (13) For some reviews on type-II intramolecular cycloadditions, see: (a) Min, L.; Hu, Y.-J.; Fan, J.-H.; Zhang, W.; Li, C.-C. Synthetic applications of type II intramolecular cycloadditions. *Chem. Soc. Rev.* 2020, 49, 7015. (b) Bear, B. R.; Sparks, S. M.; Shea, K. J. The type 2 intramolecular diels-alder reaction: synthesis and chemistry of bridgehead alkenes. *Angew. Chem., Int. Ed.* 2001, 40, 820.
- (14) (a) Fleurisson, C.; Benedetti, E.; Micouin, L. Cyclic cis-1,3-Diamines Derived from Bicyclic Hydrazines: Synthesis and Applications. *Synlett* 2021, 32, 858. (b) Ju, X.; Hwang, H. Synthetic methods for 1,3-diamines. *Org. Biomol. Chem.* 2016, 14, 10557. (c) Kizirian, J.-C. Chiral tertiary diamines in asymmetric synthesis. *Chem. Rev.* 2008, 108, 140.
- (15) (a) Hong, X.; Küçük, H. B.; Maji, M. S.; Yang, Y.-F.; Rueping, M.; Houk, K. N. Mechanism and Selectivity of N-Triflylphosphoramidate Catalyzed (3 + 2) Cycloaddition between Hydrazones and Alkenes. *J. Am. Chem. Soc.* 2014, 136, 13769. (b) Rueping, M.; Maji, M. S.; Küçük, H. B.; Andreoli, I. Asymmetric Brønsted Acid Catalyzed Cycloadditions—Efficient Enantioselective Synthesis of Pyrrolidines, Pyrrolones, and 1,3-Diamines from N-Acyl Hydrazones and Alkenes. *Angew. Chem., Int. Ed.* 2012, 51, 12864. (c) Kobayashi, S.; Shimizu, H.; Yamashita, Y.; Ishitani, H.; Kobayashi, J. Asymmetric intramolecular [3 + 2] cycloaddition reactions of acylhydrazones/olefins using a chiral zirconium catalyst. *J. Am. Chem. Soc.* 2002, 124, 13678. (d) Yamashita, Y.; Kobayashi, S. Zirconium-catalyzed enantioselective [3 + 2] cycloaddition of hydrazones to olefins leading to optically active pyrrolidines, pyrrolones, and 1,3-diamine derivatives. *J. Am. Chem. Soc.* 2004, 126, 11279. (e) Shinokawa, S.; Lombardi, P. J.; Leighton, J. L. A Simple and General Chiral Silicon Lewis Acid for Asymmetric Synthesis: Highly Enantioselective [3 + 2] Acylhydrazone—Enol Ether Cycloadditions. *J. Am. Chem. Soc.* 2005, 127, 9974. (f) Zamfir, A.; Tsogova, S. B. Towards a Catalytic Asymmetric Version of the [3 + 2] Cycloaddition between Hydrazones and Cyclopropenylidene. *Synthesis* 2011, 2011, 1988. (g) Serdyuk, O. V.; Zamfir, A.; Hampel, F.; Tsogova, S. B. Combining in situ Generated Chiral Silicon Lewis Acid and Chiral Brønsted Acid Catalysts for [3 + 2] Cycloadditions: Cooperative Catalysis as a Convenient Enantioselective Route to Pyrrolidines. *Adv. Synth. Catal.* 2012, 354, 3115. Conjugated aldehyde hydrazones have also been reported to undergo enantioselective 6 π electrocyclicization under Brønsted acid catalysis to provide 2-pyrrolidones: (h) Müller, S.; List, B. A Catalytic Asymmetric 6 π Electrocyclization: Enantioselective Synthesis of 2-Pyrrolidones. *Angew. Chem., Int. Ed.* 2009, 48, 9975.
- (16) For some selected reviews on chiral BINOL-based phosphoric acid catalysis, see: (a) Maji, R.; Mallojola, S. C.; Wheeler, S. E. Chiral phosphoric acid catalysis: from numbers to insights. *Chem. Soc. Rev.* 2018, 47, 1142. (b) Akiyama, T.; Mori, K. Stronger Brønsted acids: recent progress. *Chem. Rev.* 2015, 115, 9277. (c) Parmar, D.; Sugiono, E.; Raja, S.; Rueping, M. Complete field guide to asymmetric BINOL-phosphate derived Brønsted acid and metal catalysis: history and classification by mode of activation; Brønsted Acidity; Hydrogen Bonding; Ion Pairing; and Metal Phosphates. *Chem. Rev.* 2014, 114, 9047. (d) Terada, M. Chiral phosphoric acids as versatile catalysts for enantioselective transformations. *Synthesis* 2010, 2010, 1929. (e) Terada, M. Enantioselective carbon-carbon bond forming reactions catalyzed by chiral phosphoric acid catalysts. *Curr. Org. Chem.* 2011, 15, 2227. (f) Terada, M. Chiral phosphoric acids as versatile catalysts for enantioselective carbon-carbon bond forming reactions. *Bull. Chem. Soc. Jpn.* 2010, 83, 101. (g) Kampen, D.; Rösinger, C. M.; List, B. Chiral Brønsted acids for asymmetric organocatalysis. *Top. Curr. Chem.* 2009, 291, 395. (h) Zamfir, A.; Schenker, S.; Freund, M.; Tsogova, S. B. Chiral BINOL-derived phosphoric acids: privileged Brønsted acid organocatalysts for C—C bond formation reactions. *Org. Biomol. Chem.* 2010, 8, 5362. (i) Terada, M. Binaphthol-derived phosphoric acid as a versatile catalyst for enantioselective carbon-carbon bond forming reactions. *Chem. Commun.* 2008, 35, 4097. (j) Adair, G.; Mulhverjee, S.; List, B. TRIP-A powerful Brønsted acid catalyst for asymmetric synthesis.

Aldrichimica Acta 2008, 41, 31. (k) Akiyama, T. Stronger Brønsted acids. *Chem. Rev.* 2007, 107, 5744.

(17) Melikian, M.; Gramüller, J.; Hise, J.; Gröndl, J.; Gschwind, R. M. Brønsted acid catalysis—the effect of 3, 3'-substituents on the structural space and the stabilization of imine/phosphoric acid complexes. *Chem. Sci.* 2019, 10, 5226. See also ref 16c.

(18) See, for example: (a) Vasu, D.; Puentes de Arriba, A. L.; Leitch, J. A.; de Gombert, A.; Dixon, D. J. Primary α -tertiary amine synthesis via α -C–H functionalization. *Chem. Sci.* 2019, 10, 3401. (b) Ryder, A. S. H.; Cunningham, W. B.; Ballantyne, G.; Mules, T.; Kinsella, A. G.; Turner-Dore, J.; Alder, C. M.; Edwards, E. L. J.; McKay, B. S. J.; Grayson, M. N.; Cresswell, A. J. Photocatalytic α -Tertiary Amine Synthesis via C–H Alkylation of Unmasked Primary Amines. *Angew. Chem., Int. Ed.* 2020, 59, 14986. (c) Jackl, M. K.; Schümacher, A.; Shiro, T.; Bode, J. W. Synthesis of N,N-Alkylated α -Tertiary Amines by Coupling of α -Aminoallyltrifluoroborates and Grignard Reagents. *Org. Lett.* 2018, 20, 4044. (d) Kano, T.; Aota, Y.; Maruoka, K. Asymmetric Synthesis of Less Accessible α -Tertiary Amines from Alkynyl Z-Ketimines. *Angew. Chem., Int. Ed.* 2017, 56, 16293.

Borylation

Transition-Metal-Free Stereoselective Borylation of Allenamides

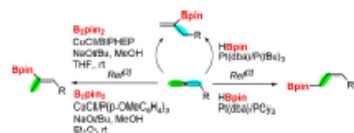
Lorena García,^[a] Jana Sendra,^[a] Núria Miralles,^[a] Efraim Reyes,^[b] Jorge J. Carbó,^{*[a]}
Jose L. Vicario,^{*[b]} and Elena Fernández^{*[a]}

Dedicated to Professor Ernesto Carmona on the occasion of his 70th birthday

Abstract: Complete stereocontrol on the transition-metal-free hydroboration of the distal double bond of allenamides could be achieved when allenamides contained acetyl substituents, which provided exclusively the *Z*-isomer. The consecutive Pd-catalyzed cross-coupling reaction allowed the straightforward formation of trisubstituted enamides, with total control of the stereoselectivity.

Hydroboration of alkenes to afford stereodefined alkenyl boronates represents an efficient synthetic strategy to prepare poly-substituted olefins with total control on the stereoselectivity.^[1] The first challenge is the regiocontrol of the C–B and C–H formation along the alkene system, which depends on the transition-metal catalyst used, the ligands involved and the substrate itself.

From the original proof of concept by Miyaura and co-workers,^[2] the hydroboration of alkoxyallenes with HBpin catalyzed by Pt(dba)₂/PCy₃ generated exclusively allylboranes, whereas the hydroboration of alkyl- and aryl-substituted allenes with HBpin catalyzed by Pt(dba)₂/P(tBu)₃ occurred at the internal double bond to selectively provide 1-alken-2-yl boronates (Scheme 1).^[2] The copper-catalyzed hydroboration of allenes



Scheme 1. Synthetic approaches towards divergent transition metal-catalyzed hydroboration of allenes with HBpin and B₂pin₂.

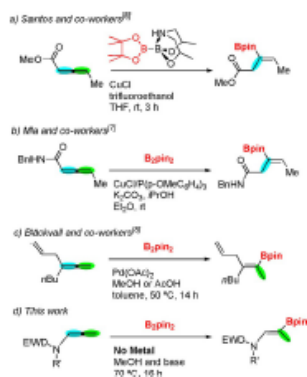
[a] J. Sendra, Dr. N. Miralles, Dr. J. J. Carbó, Dr. E. Fernández
Department Química Física I Inorgánica, University Rovira i Virgili
C/ Marcel·lí Domingo s/n, 43007 Tarragona (Spain)
E-mail: mariaelena.fernandez@urv.cat
j.carbo@urv.cat

[b] E. Reyes, Dr. E. Reyes, Dr. J. L. Vicario
Department of Organic Chemistry II
University of the Basque Country (UPV/EHU)
RD. Box 644, 48960 Leioa (Spain)
E-mail: joseluis.vicario@ehu.es

Supporting information and the ORCID number(s) for the author(s) of this article can be found under <https://doi.org/10.1002/chem.201803004>.

with bis(pinacolato) diboron (B₂pin₂) formed 2-alken-2-yl or 1-alken-2-yl boronates also by applying a ligand effect.^[3–5]

Alternatively a substrate-directing effect to control the regioselective hydroboration has been pursued by electrophilic allenates that react with pinacolato diisopropanolamino diboron (PDIPA diboron) in the presence of a copper(I) catalyst to install a boron moiety on the β-position through hydroboration of the internal double bond (Scheme 2 a).^[6] Similarly, the effect of the amide group in 2,3-disubstituted allenamides influenced the copper-catalyzed hydroboration with B₂pin₂ to take place regioselectively, thus producing β-borylated β,γ-unsaturated enamides through a plausible intramolecular interaction between the carbonyl group and the organocopper intermediates (Scheme 2 b).^[7] In contrast, an efficient olefin-directed palladium-catalyzed hydroboration of allenes, containing an allyl moiety promoted the hydroboration and subsequent borylation to hydroborate the terminal double bond with B₂pin₂.^[8] Now, we have planned to conduct the borylation of the unexplored allenamides to identify the influence of the amine group on the chemo- and regioselective addition of the boryl moiety (Scheme 2 d), and to give access to stereodefined trisubstituted alkenes.



Scheme 2. Substrate-directed transition metal-catalyzed hydroboration of allenes with B₂pin₂ (a, b, c) and transition metal-free hydroboration of allenamides in this work (d).

To explore this new piece of chemistry, we avoided the use of any transition-metal complexes as catalysts and instead we selected the alkoxide activation of B₂pin₂ to form the nucleophilic boryl moiety in the acid-base Lewis adduct [MeO-Bpin-Bpin]⁺[Hbase]⁻.¹⁰ This system has already proven to be efficient in the borylation of C=C bonds,^{10a} C=N bonds,¹¹ electron-deficient C=C bonds¹² and tertiary allylic or propargylic alcohols.¹³ The addition of the acid-base Lewis adduct [MeO-Bpin-Bpin]⁺[Hbase]⁻ to aliphatic allenes was previously explored giving access to the 1,2-diboration of the terminal double bond.¹⁴ Considering that the replacement of the aliphatic group in allenes by the amine group renders the allenamide more electronically enriched and, consequently, very reactive and sensitive towards hydrolysis and polymerization, we focussed the study on the electron-deficient variants of allenamides, therefore diminishing the electron-donating ability of the nitrogen atom and providing superior stability as substrates.¹⁴ Consequently, we prepared *N*-(4-methoxyphenyl)-4-methyl-*N*-(propa-1,2-dien-1-yl)benzenesulfonamide (**1**)¹⁵ as the model substrate to test the transition-metal-free borylation with B₂pin₂ and MeOH/base. We selected KOtBu as the most efficient base versus Cs₂CO₃ and NaOtBu, with an optimized 30 mol% loading. The reaction temperature was explored in a range from 70 to 110 °C, and we found that the highest temperature favoured the major conversion towards a mixture of two hydroborated products. In both of these products, the boryl moiety is located at the central carbon of the allenamide but with a 2:1 (A:B) ratio in favour of the hydroboration along the terminal double bond (Table 1, entry 1). A similar effect was observed for a series of *N*-Ts-substituted amines, with electron-donating or electron-withdrawing aryl substituents, but no significant differences were detected in the reaction outcome or in the regioselectivity (Table 1, entries 1–3). When the aryl substituent was replaced by a methyl group in the amine moiety (allenamide **4**), the reaction was less efficient (60% NMR yield) but the ratio of 2-pinacolboryl prop-1-en-1-amine (A) to 2-pinacolboryl prop-2-en-1-amine (B) was still 2:1 (Table 1, entry 4). The replacement of Ts by Boc in the amine functional group showed that the borylation reaction might be favoured with electron-withdrawing substituents on the phenyl group of the substrate (90% NMR yield, Table 1, entry 6) rather than electron-donating substituents on substrate **5** (75% NMR yield, Table 1, entry 5). However, the regioselectivity was again a mixture of the two hydroborated products with a 2:1 ratio in favour of the hydroboration along the terminal double bond. Interestingly, when the acetyl group was introduced as the electron-withdrawing group in the allenamide substrate **7**, we were able to perform the reaction with total conversion and exclusive formation of the 2-pinacolboryl prop-1-en-1-amine **7A**, even at 70 °C (Table 1, entry 7).

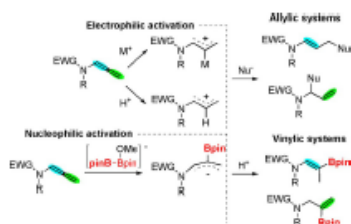
The complete regioselectivity observed requires a deep understanding of the factors that might control it, particularly because no transition-metal catalysts or ligands are involved in such control. But also, in terms of chemical behaviour, we observe an upturning on the natural reactivity trend of the allenamide reagent. Allenamides with electron-withdrawing groups are known to conduct electrophilic activation¹⁶ assisted by

Table 1. Transition metal free borylation of electronic deficient variants of allenamides.^[a]

Entry	Substrate	T [°C]	NMR yield ^[b] [%] (ratio A:B)	A, isolated yield [%]	B, isolated yield [%]
1		70	16	nd	nd
		90	53 (2:1)	1A, 34	1B, 22
		110	82 (2:1)	1A, 53	1B, 26 ^[c]
2		110	86 (2:1)	2A, 48	2B, 9 ^[c]
			110	84 (2:1)	3A, 47 ^[c]
4		110	60 (2:1)	4A, 20 ^[c]	4B, 11 ^[c]
			110	75 (2:1)	5A, 41
6		110	90 (2:1)	6A, 51	6B, 25 ^[c]
			70	98 (1:0)	7A, 71

[a] Conditions: allenamide (0.2 mmol), KOtBu (30 mol%), B₂pin₂ (1.2 equiv), MeOH (0.4 M), 70–110 °C, 16 h. [b] NMR yields calculated from ¹H NMR spectra with naphthalene as internal standard based on the consumption of substrate. [c] Isolated yield of pure material after flash column chromatography purification.

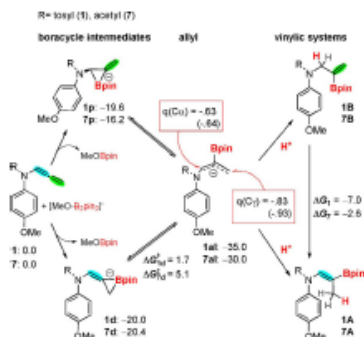
transition-metal complexes or Brønsted acids, to generate a stabilized carbocation that eventually reacts with nucleophilic reagents either at the α or γ position, involving the proximal or distal C=C bond, respectively (Scheme 3, top).¹⁷ Interestingly, the products formed in all these cases are allylic systems. However, in our transition-metal-free hydroboration of the same allenamides, we realized that the in situ generated nucleophilic Bpin moiety exerts a nucleophilic attack on the C=C=C π system forming the C–B bond on the central carbon and generating the corresponding carbanion with a relative stabilized energy (Scheme 3, bottom). Furthermore, the carbanion



Scheme 3. Umpolung reactivity of allenamides through electrophilic or nucleophilic activation.

can be protonated both at the α or γ position, and therefore, to control the regioselective outcome of the reaction, a systematic study on the influence of the *N*-substituents is required.

Previous DFT studies had characterized the mechanisms for transition-metal-free diboration and borylation of alkenes by diboron reagents activated with Lewis bases.^{70, 80} Those studies proposed that the nucleophilic attack of the adduct (MeO-Bpin-Bpin)⁻ to a C=C double bond yields an anionic, 3-membered boracycle intermediate (see Scheme 4, top) and the release of Bpin-OMe. Subsequent protonation leads to the hydroborated product. For allenamides, we propose that the formation of this anionic intermediate is favoured because conjugation with the exocyclic C=C bond stabilizes the negative charge. However, in these allenamides, the boracycle intermediate can open to form a more stable allylic anion that can be then protonated to give the final product. To evaluate this mechanistic proposal and to rationalize the observed stereoselectivity we have performed DFT calculations⁷⁹ on the key intermediates, using substrates **1** and **7** as representative examples.



Scheme 4. Proposed mechanism for the hydroboration of allenamides **1** and **7**. Relative Gibbs free energies (ΔG^\ddagger) in kcalmol⁻¹. Electrostatic-based atomic charges for the α and γ carbons of allylic species in a.u.

Scheme 4 summarizes the results of our computational study for allenamides **1** and **7**. Initially we characterized the formation of the two boracycle intermediates corresponding to the borylation of the proximal (**1p** and **7p**) and distal (**1d** and **7d**) double bonds. The functionalization of the distal C=C bond is thermodynamically preferred, although in the case of the tosyl substituent (**1**), both regioisomers are almost isoenergetic. Nevertheless, for both substituents, the open allylic species **1a** and **7a**, with the Bpin moiety attached to the central carbon in both cases, are thermodynamically favoured and the overall process for boryl addition to allene is highly exergonic, that is, -35.0 and -30.0 kcal mol⁻¹ for **1a** and **7a**, respectively. In addition, the formation of the allylic intermediate from the boracycle has a low free-energy barrier (1.7 and 5.1 kcal mol⁻¹, respectively from the lowest energy distal isomers **1d** and **7d**), indicating that the process is a very fast transformation at the high reaction temperature. Thus, it is likely that protonation to yield the hydroborated product occurs at the allylic intermediate and that this irreversible reaction step determines the selectivity of the process. Moreover, in the structures of the more stable allylic anion, the amine substituent has an *anti*-configuration (see Scheme 4) that should yield a *trans*-configuration between the amine and the Bpin substituents in the major alkene product **A**.

To understand the difference in reactivity between the C α and C γ , we performed an analysis of charge distribution in the allylic intermediates **1a** and **7a** (Scheme 4). Our calculations show that the C γ is more negatively charged than the C α , and consequently, more reactive towards electrophiles, which is in full agreement with experimental selectivity. The protonation at the C γ results in products (**1A** and **7A**), which are more stable than those resulting from protonation at C α (**1B** and **7B**) by 7.0 and 2.6 kcalmol⁻¹, respectively. Nevertheless, we assume that the selectivity is not thermodynamically but rather kinetically controlled in the irreversible protonation step. Accordingly, in the allylic intermediate **7a**, the difference in atomic charges is larger than that computed for **1a**, which could explain the higher selectivity observed in the hydroboration of allenamide **7**.

Taking advantage of the exclusive regioselectivity observed by the acetyl-substituted allenamide **7**, we conducted a series of reactivity experiments to establish the substrate scope but also the limitations in the methodology. By changing the electron properties of the *para*-substituents of the aryl group in the allenamide substrates, it was proved that electron-donating *para*-substituents contributed to quantitative conversions with complete stereoselectivity towards the formation of the *Z*-isomer (Table 2, entries 1–3). However, a trend that diminished conversions was observed when electron-withdrawing *para*-substituents on the aryl group were involved, (Table 1, entries 4 and 5), but fortunately, this did not affect the exclusive regioselective product formation. Replacement of the Me group by a *t*Bu group at the acyl moiety did not influence the reaction outcome, and product **12A** was obtained in quantitative yield as a single *Z*-isomer from *N*-(4-methoxyphenyl)-*N*-(propa-1,2-dien-1-yl)picvalamide (**12**, Table 2, entry 6). The reaction was also generalized for *N*-(4-methoxyphenyl)-*N*-(propa-

Table 2. Transition-metal free borylation of acyl-substituted allenamides^[a]

Entry	Substrate	Product	NMR yield ^[b] [%]	Isolated yield [%]
1			98	71
2			96	62
3			99	78
4			52	24
5			25	-
6			94	65
7			99	74
8			90	72
9			16	-

[a] Conditions: allenamide (0.2 mmol), KOBu (30 mol %), B₂pin₂ (1.2 equiv), MeOH (0.4 M), 70 °C, 16 h. [b] NMR yields calculated from ¹H NMR spectra with naphthalene as internal standard.

1,2-dien-1-yl)benzamide (14), demonstrating that the nature of the aryl substituents in the acyl group contributed similarly to the borylation reaction (Table 2, entry 8). The exclusive product 14A, formed from the transition-metal-free borylation of 14, could be fully characterized by means of single-crystal X-ray diffraction. Figure 1 illustrates the *trans*-stereoselectivity of the

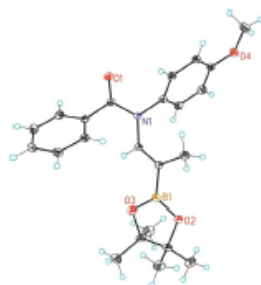
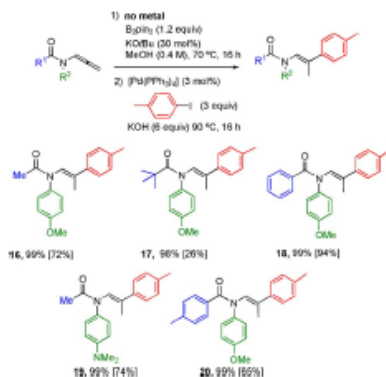


Figure 1. Single-crystal X-ray diffraction structure of stereocontrolled borylated product 14A.

amine and boryl moieties along the trisubstituted alkene. Moreover, the electron-releasing substituents in the phenyl group favoured the reaction in contrast to the electron-withdrawing substituents (see Table 2, entries 8 and 9 for comparison). The reaction, however, showed a limitation for the α - and γ -substituted allenamides [*N*-(buta-2,3-dien-2-yl)-*N*-(4-methoxyphenyl)benzamide and *N*-(4-methoxyphenyl)-*N*-(penta-1,2-dien-1-yl)benzamide, respectively], probably due to the steric hindrance offered by the substrates in the nucleophilic attack of the Bpin moiety.

Next, we explored the "in situ" functionalization of the 2-pi-nacolboryl prop-1-en-1-amine intermediates through a one-pot metal-free borylation of the allenamide followed by a Pd-catalyzed Suzuki-Miyaura cross-coupling reaction with 1-iodo-4-methylbenzene. The consecutive reactions allowed the straightforward formation of the trisubstituted olefin, with total control of the stereoselectivity (Scheme 5). The methodol-



Scheme 5. Sequential transition-metal free borylation of acyl-substituted allenamides and Pd-catalyzed Suzuki-Miyaura cross-coupling.

ogy seems to be general because it is tolerant towards alkyl and aryl substituents on the acyl moiety.

To conclude, we have described a transition-metal-free borylation of electron-deficient variants of allenamides, with high yields and complete stereocontrol of the hydroboration of the distal double bond, providing exclusively the *Z*-isomers. The acetyl groups on the amine moiety are crucial to obtain the complete stereoselectivity, which is a consequence of the formation of a stable allylic anion intermediate that is further regioselectively protonated to give the final product. The transition-metal-free borylation can be followed by Pd-catalyzed cross-coupling with aryl iodides generating trisubstituted olefins in a stereoselective manner.

Acknowledgements

The present research was supported by the Spanish Ministerio de Economía y competitividad (MINECO) through projects FEDER-CTQ2016-80328-P and FEDER-CTQ2017-83633-P and by the Basque Government (Project IT908-16). L.G. and N.M. also acknowledge Spanish MINECO for FPI fellowships. We thank AllyChem for the gift of diboranes.

Conflict of interest

The authors declare no conflict of interest.

Keywords: allenamines · borylation · density functional calculations · stereoselectivity · transition-metal free

- [1] K. Semba, N. Bessho, T. Fujihara, J. Terao, Y. Tsuji, *Angew. Chem. Int. Ed.* **2014**, *53*, 9007; *Angew. Chem.* **2014**, *126*, 9153.

- [2] Y. Yamamoto, R. Fujikawa, A. Yamada, N. Miyaura, *Chem. Lett.* **1999**, *28*, 1069.
 [3] W. Yuan, S. Ma, *Adv. Synth. Catal.* **2012**, *354*, 1867.
 [4] a) F. Meng, B. Jung, F. Hoffner, A. H. Hoveyda, *Org. Lett.* **2013**, *15*, 1414; b) H. Jung, B. Jung, A. H. Hoveyda, *Org. Lett.* **2014**, *16*, 4658.
 [5] K. Semba, M. Shinomiya, T. Fujihara, J. Terao, Y. Tsuji, *Chem. Eur. J.* **2013**, *19*, 7125.
 [6] S. B. Thorpe, X. Guo, W. Santos, *Chem. Commun.* **2011**, *47*, 424.
 [7] W. Yuan, X. Zhang, Y. Yu, S. Ma, *Chem. Eur. J.* **2013**, *19*, 7193.
 [8] C. Zhu, B. Yang, Y. Qiu, J. F. Backwall, *Chem. Eur. J.* **2016**, *22*, 2999.
 [9] a) A. B. Cuenca, R. Shishido, H. Ito, E. Fernández, *Chem. Soc. Rev.* **2017**, *46*, 415; b) E. C. Neeve, S. J. Geier, I. A. I. Khalid, S. A. Westcott, T. B. Mardeš, *Chem. Rev.* **2016**, *116*, 9091; c) J. Cid, H. Gulyás, J. J. Carbó, E. Fernández, *Chem. Soc. Rev.* **2012**, *41*, 3558.
 [10] A. Bonet, C. Pubill-Lludemolins, C. Bio, H. Gulyás, E. Fernández, *Angew. Chem. Int. Ed.* **2011**, *50*, 7158; *Angew. Chem.* **2011**, *123*, 7296.
 [11] C. Solé, H. Gulyás, E. Fernández, *Chem. Commun.* **2012**, *48*, 3769.
 [12] A. Bonet, H. Gulyás, E. Fernández, *Angew. Chem. Int. Ed.* **2010**, *49*, 5130; *Angew. Chem.* **2010**, *122*, 5254.
 [13] N. Miralles, R. Alam, K. Szabó, E. Fernández, *Angew. Chem. Int. Ed.* **2016**, *55*, 4303; *Angew. Chem.* **2016**, *128*, 4375.
 [14] L. L. Wei, J. A. Mulder, H. Xiong, C. A. Zifcak, Ch. J. Douglas, R. P. Hsung, *Tetrahedron* **2001**, *57*, 459.
 [15] For the synthesis of **1**, see a) Y. Yang, F. D. Toste, *Chem. Sci.* **2016**, *7*, 2653. See also b) L. Villar, U. Ulla, J. I. Martínez, L. Prieto, E. Reyes, L. Carrillo, J. L. Vicario, *Angew. Chem. Int. Ed.* **2017**, *56*, 10535; *Angew. Chem.* **2017**, *129*, 10671.
 [16] T. Lu, Z. Lu, Z.-X. Ma, Y. Zhang, R. P. Hsung, *Chem. Rev.* **2013**, *113*, 4862.
 [17] a) C. Romano, M. Ja, M. Monari, E. Manori, M. Bandini, *Angew. Chem. Int. Ed.* **2014**, *53*, 13854; *Angew. Chem.* **2014**, *126*, 14074; b) R. R. Liu, J. P. Hui, J.-J. Hong, Ch.-J. Lu, J. R. Gao, Y.-X. Jia, *Chem. Sci.* **2017**, *8*, 2811.
 [18] N. Miralles, J. Cid, A. B. Cuenca, J. J. Carbó, E. Fernández, *Chem. Commun.* **2015**, *51*, 1693.
 [19] Calculations were performed using Gaussian 09 (M06-2X functional) and the 6-311g(d,p) basis set. Energies include free energy corrections and the solvent effect of methanol ($\epsilon = 32.613$) by SMD continuum solvent model. See the Supporting Information for details.

Manuscript received: June 12, 2018

Accepted manuscript online: June 14, 2018

Version of record online: August 24, 2018